

Proceedings of **GSM** 2020

4th Grid Service Markets Symposium

19-20 October, Lucerne, Switzerland

Edited by: Prof. Christoph Imboden (Chair)

Davor Bošnjak
Thomas Kudela
Andreas Svendstrup-Bjerre

Prof. K. Andreas Friedrich
Prof. Carlo Alberto Nucci

Prof. Nikos Hatziargyriou
Dr. Bastian Schwark
Sebastian Ziegler

Co-Edited by: James Hock Fiona Moore Dr. Michael Spirig



Copyright © Hochschule Luzern + European Fuel Cell Forum AG
These proceedings must not be made available for sharing through any other open electronic means.
DOI 10.5281/zenodo.4284325 ISBN 978-3-905592-81-8

Sessions:

G01 OPENING AND WELCOME

G02 Market developments and international collaborations I

G03 Market developments and international collaborations II

G04 POSTER SESSION – ALL TOPICS

G05 Market developments and international collaborations III

G06 Operation and enabling technologies I

G07 Operation and enabling technologies II

G08 VPP and advanced technologies I

G09 VPP and advanced technologies II

G10 POSTER SESSION – ALL TOPICS

G11 Advanced technologies providing flexibility

Copyright © 2020 HSLU + EFCF

Published on:

www.zenodo.org/communities/LORY

LORY Lucerne Open Repository
Universität Luzern
Hochschule Luzern
Pädagogische Hochschule Luzern
Historisches Museum Luzern

www.EFCF.com/LIBRARY

EFCF-Library

by
Hochschule Luzern
Werftstrasse 4
6002 Luzern
Switzerland

by
European Fuel Cell Forum AG
Obgardihalde 2
6043 Luzern-Adligenswil
Switzerland

Tel. +41 - 41 - 228 4242
Info@HSLU.ch, www.HSLU.ch

Tel. +41 - 44 - 586-5644
Forum@EFCF.com, www.EFCF.com

Foreword

In its World Energy Outlook 2020, the International Energy Agency predicts that renewable energy will more than double by 2030 for achieving global net zero emissions by 2050. Renewable energy is about to replace a significant proportion of fossil fuels, which are expected to decline by more than 35% compared to 2019. Under the same scenario, it is expected that 58% of car and light truck sales will be electric- and fuel cell-driven by 2030. Such developments would represent a significant reduction in CO₂ emissions, while at the same time easily stored carriers become replaced with inflexible and geographically as well as temporally unevenly available alternatives. Such a transformation puts the existing electrical energy system under stress and requires an increasing degree of capacity and flexibility, both short-term and seasonal, at regional, national and international levels.

From October 19 to 20 2020, 78 experts from industry, administration and academia discussed for the fourth time the effects, prospects and solutions of grid services for a transforming electricity system. With 15 scientific papers and 17 invited presentations, the symposium dealt with market developments, international cooperation, operation and enabling technologies, virtual power plants and flexibility providing technologies. The European perspective on energy transition and the flexibility roadmap were delved into along with national perspectives for the implementation of harmonized grid services markets, where their orientation and implementation also took account of national circumstances. Expanding flexibility products, digitalization, risk hedging and advanced market design were pointed out as ways of increasing market liquidity. Crucially as important, improved weather and load forecasting algorithms for reducing the balancing gap was covered.

With Corona influencing the way people met, the symposium had to be transferred to a virtual space at short notice. Although questions to the speakers had to be asked in the live chat room, no quality and quantity compared to previous years was lost. The discussions between the participants took place in break-out sessions, where personal contacts could be made. Despite travel restrictions, a very diverse and valuable exchange between experts from industry, administration and science could ultimately still take place.

This gives the base and the motivation to reorganise the growing Grid Service Market symposium. Due to the shift of GSM 2020 in to autumn, the GSM 2021 will be a shorter, attractive reunion of the experts also in autumn. However, GSM 2022 is planned to be a fully physical networking and exchange event in summer in Lucerne again. Naturally the virtual attendance will be one of the new features allowing participating from all over the world, when travelling is restricted due to any reason. Enjoy now the proceedings of GSM 2020 and seek for upcoming releases.

Sincerely
Prof. Christoph Imboden & Dr. Michael Spirig
HSLU EFCF





A specially formed **International Advisory Board (IAB)** assured constant high quality and a strong focus on industry challenges. The members of the IAB are:

- Davor Bošnjak, HEP
- Prof. K. Andreas Friedrich, Deutsches Zentrum für Luft- und Raumfahrt e.V. (DLR)
- Prof. Nikos Hatzigiorgiou, National Technical University of Athens (NTUA)
- Prof. Christoph Imboden, Lucerne University
- Thomas Kudela, Ørsted A/S
- Prof. Carlo Alberto Nucci, Uni Bologna
- Dr. Bastian Schwark, Swissgrid AG
- Andreas Svendstrup-Bjerre, Vestas Wind Systems A/S
- Sebastian Ziegler, 50 Hertz

The following pages contain the paper contributions accepted by the IAB.

The GSM 2020 was again supported by:

- the Swiss State Secretariat for Education, Research and Innovation (SERI) under contract No 17.00009
- the Fuel Cells and Hydrogen 2 Joint Undertaking under agreements No 735485 and 700339
- the Lucerne University of Applied Sciences and Arts UAS HSLU, www.HSLU.ch
- European Fuel Cell Forum AG, www.EFCF.com

 PACE Pathway to a Competitive European Fuel Cell micro-CHP Market	 QualyGridS	 COGEN EUROPE	 Schweizerische Eidgenossenschaft Confédération suisse Confederazione Svizzera Confederaziun svizra State Secretariat for Education, Research and Innovation SERI
PACE-energy.eu FCH JU project Pathway to a Competitive European Fuel Cell micro- Cogeneration Market	QualyGridS.eu FCH JU project Standardized qualifying tests of electrolyzers for grid services	CogenEurope.eu The European Association for the Promotion of Cogeneration	SERI Swiss State Secretariat for Education, Research and Innovation



GSM VPP Panel has received funding from the Fuel Cells and Hydrogen 2 Joint Undertaking under grant agreement No 700339. This Joint Undertaking receives support from the European Union's Horizon 2020 research and innovation programme.



Content

Foreword	3
G05	7
Market developments & international collaborations III	
G0501	8
Balancing markets and DERs in the Italian regulatory framework: Insights on the UVAM Case Study	
A. Rossi (1), F. Bovera (1), G. Rancilio (1), D. Falabretti (1), A. Galliani (2), M. Merlo (1)	
(1) <i>Dept. of Energy, Politecnico di Milano, Milano/Italy</i>	
(2) <i>ARERA, Milano, Italy</i>	
G0504	17
Impact of COVID-19 on the demand curves of Croatia and region	
Igor Vidić, Matija Melnjak, Davor Bošnjak	
<i>HEP Trade LTD, member of HEP group, Zagreb/Croatia</i>	
G0505	39
Integration of voluntary Flexibility at Runtime FlexA a Linear Flexibility Agent for Sector Coupled Energy Systems	
Dr. Philipp Graf, Dr. Jan Jurczyk, Klaus Nagl	
<i>Consolinno Energy GmbH</i>	
<i>Franz-Mayer-Straße 1, 93053 Regensburg/Germany</i>	
G06	45
Operation and enabling technologies I	
G0603	46
Active Distribution Grid Management – a decentralized approach for the management of flexibility options	
Michael Merz	
<i>PONTON GmbH</i>	
<i>Dorotheenstr. 64, 22301 Hamburg/Germany</i>	
G07	54
Operation and enabling technologies II	
G0701	55
Options for the Implementation of Fast Control Reserves in the Continental European Power System	
A. Stimmer, M. Lenz, M. Froschauer, M. Leonhardt (1), W. Gawlik, C. Alacs, C. Corinaldesi, G. Lettner, Y. Guo, J. Marchgraber (2), A. Anta (3), K. Oberhauser (4)	
(1) <i>Austrian Power Grid, Wagramer Straße 19, AT-1220 Vienna</i>	
(2) <i>Technical University Vienna, Gusshausstraße 25, AT-1040 Vienna</i>	
(3) <i>Austrian Institute of Technology, Giefinggasse 2, AT-1210 Vienna</i>	
(4) <i>Verbund Hydro Power, Europaplatz 2, AT-1150 Vienna</i>	
G0703	67
Benefits of multi-voltage-level grid control in future distribution grids	
Wolfgang Biener (1), Thomas Erge (1), Thomas Kumm (2), Bernhard Wille-Haussmann (1)	
(1) <i>Fraunhofer Institute for Solar Energy Systems ISE</i>	
<i>Heidenhofstrasse 2, D-79110 Freiburg</i>	
(2) <i>EWE NETZ GmbH</i>	
<i>Cloppenburg Strasse 302, D-26133 Oldenburg</i>	
G0704	77
Forecasting and Optimization Approaches Utilized for Simulating a Hybrid District Heating Network	
Lukas Gnam, Christian Pfeiffer, Markus Schindler, Markus Puchegger	

*Forschung Burgenland GmbH
Campus 1, 7000 Eisenstadt/Austria*

G0705	89
Readiness of Short-term Load Forecasting Methods for their Deployment on Company Level		
Thilo Walser (1,2), Martin Reisinger (1,2), Niklas Hartmann (3), Christian Dierolf (1,2), Alexander Sauer (1,2)		
(1) Fraunhofer Institute for Manufacturing Engineering and Automation IPA Nobelstraße 12, 70569 Stuttgart/Germany		
(2) Institute for Energy Efficiency in Production EEP Nobelstraße 12, 70569 Stuttgart/Germany		
(3) Offenburg University of Applied Sciences Badstraße 24, 77652 Offenburg/Germany		
G08	104
VPP and advanced technologies I		
G0802	105
Enhancing Power-to-Gas operations with a Virtual Power Plant to improve renewable grid integration		
Aleksandra Radwanska, Felix Jedamzik, Joan Recasens		
Next Kraftwerke GmbH Lichtstr. 43g 50825 Cologne/Germany		
G09	115
VPP and advanced technologies II		
G0901	116
Converting wastes efficiently and flexibly for grid-balancing services and sector coupling		
Ligang Wang (1,2), Yumeng Zhang (2), Chengzhou Li (2), Mar Pérez-Fortes (1), Yi Zong (3), Vincenzo Motola (4), Alessandro Agostini (4), Stefan Diethelm (5), Olivier Bucheli (5), Jan Van herle (1)		
(1) Swiss Federal Institute of Technology in Lausanne/Switzerland		
(2) North China Electric Power University, China		
(3) Technical University of Denmark, Denmark		
(4) ENEA, Italy		
(5) SOLIDpower SA, Switzerland		
G0903	126
Opportunities and challenges for Water Electrolysers to participate in grid services		
Stéphanie Crevon (1), Valérie Seguin (1)		
(1) CEA Liten 17, avenue des Martyrs, FR 38 054 Grenoble Cedex 9		
G11	136
Advanced technologies providing flexibility		
G1103	137
Frequency control by run-of-river hydropower: A case study on energetic and economic potentials		
Bastian Hase, Christian Seidel		
Technische Universität Braunschweig, AG Regenerative Energien, Institut für Statik Beethovenstr. 51, D-38106 Braunschweig/Germany		
G1104	155
Hydro Storage as Enabler of Energy Transition		
Peter Bauhofer, Michael Zoglauer		
Abt. Energiestrategie und Energieeffizienz TIWAG-Tiroler Wasserkraft AG, Eduard-Wallnöfer Pl.2, A-6020 Innsbruck		

G05

Market developments & international collaborations III

G0501

Balancing markets and DERs in the Italian regulatory framework: Insights on the UVAM Case Study

**A. Rossi (1), F. Bovera (1), G. Rancilio (1),
D. Falabretti (1), A. Galliani (2), M. Merlo (1)**
(1) Dept. of Energy, Politecnico di Milano, Milano/Italy
(2) ARERA, Milano, Italy
Tel.: +39- 026556 - 5558
arianna.rossi@polimi.it

INTRODUCTION

The renewable energy generation and distributed energy sources rise has led to new challenges on electric system operation to guarantee its reliability and the real-time balance between electricity consumed and supplied. Transmission System Operators (TSOs) are in charge to procure ancillary services; historically, the suppliers of these services were large conventional (hydro and thermoelectric) power plants. However, with the progressive decarbonization, a large part of thermoelectric units risks to be out of the market due to their high marginal costs and environmental impact; hence new flexible resources are required. Moreover, the unpredictability of renewables (mainly wind and solar based) and lack of observability of distributed generators are causing an increasing volume of capacity reserve needs and of the amount of energy moved for balancing purposes, as shown for the Italian case in Figure 1.

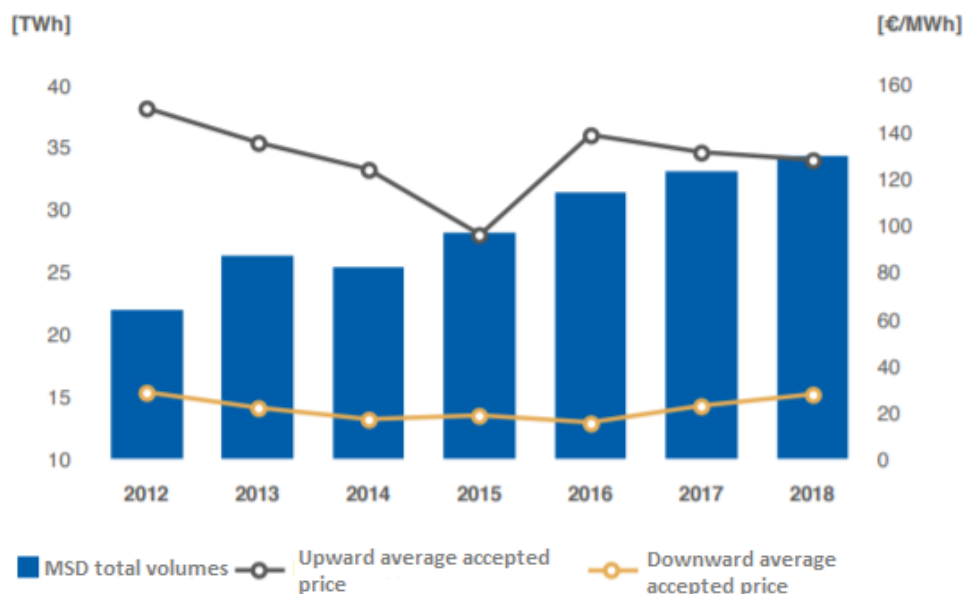


Figure 1: energy (“MSD total volumes”) and prices trends in Italy between 2012 and 2018 [1]

To date, in Italy, only conventional generating units equal or larger than 10 MVA are enabled (and obliged) to provide ancillary services. However, in 2017, the Italian

Regulatory Authority (ARERA) issued the resolution 300/2017/R/eel [2]. This launched a widespread experiment throughout the national territory aimed at innovating dispatching regulation by enabling distributed and not programmable resources to provide ancillary services by means of pilot projects. This experimental and transient regulation aims at leading the evolution of electricity balancing in the direction of integrating Distributed Energy Resources (DERs) and inverter-based systems in network dispatching; this is made in accordance with the European provisions on the access of RES, storage and demand to the energy markets – ancillary services market included (lastly, with the Regulation EU 943/2019 [3] and the Directive EU 2019/944 [4]). The overall integrated dispatching reform, and the corresponding regulation, is currently underway and the first consultation [5] has been published by the Italian Authority in summer 2019.

Pilot projects are gathering useful elements for this dispatching reform to make new resources promptly available, thus opening the market to all network-connected units, applying a principle of technology neutrality.

Actually, the term “pilot project” derives from the goal to test the reliability and affordability of the new dispatching resources and subsequently review the ancillary services market (named MSD in Italy, which is an Integrated Scheduling Process based on a central dispatch system) rules and the Italian Grid Code prescriptions.

The first pilot project, which started in 2017, made it possible to test the voluntary participation to MSD of UVAC (enabled virtual units consisting only of consumption units) [6] [7] and UVAP (enabled virtual units of production, including energy storage systems) [8] [9]. Since November 2018, UVAC and UVAP pilot projects were merged into the UVAM pilot project [10] [11], featuring mixed virtual enabled units, which is still ongoing.

UVAM PILOT PROJECT

A UVAM¹ is composed of one or more among electricity consumption, generation and storage systems (including e-mobility charging stations). These are connected to the grid at any voltage level and fall within the same perimeter of aggregation defined by Italian TSO (Terna): aggregation perimeters cannot exceed the market zone and are defined in order to avoid that the movements of the units included in the UVAM violate network constraints. The minimum bid size to be qualified for the selection process and then offered on the market is 1 MW; a further reduction up to 0.2 MW is actually under discussion [12].

There are two types of UVAM:

1. UVAM-A, characterized by the presence of the so-called “non-significant” generating units (< 10 MVA), significant generating units (≥ 10 MVA) not obliged to participate in the MSD sharing the point of connection to the grid with one or more consumption units (the total measured power input at the connection point shall not exceed 10 MVA), and consumption units;
2. UVAM-B, characterized by the presence of significant production units, not obliged to participate in the MSD, with a power input at the grid connection point equal to or exceeding 10 MVA, and consumption units that share the same connection point.

An UVAM, at the moment, is enabled to provide only certain ancillary services: congestion management, balancing and tertiary reserve. These services can be supplied upward and/or downward independently². Table 1 reports the technical requirements for each service.

¹ Unità Virtuale Abilitata Mista

² Secondary reserve is under evaluation.

Table 1: UVAM pilot project technical requirements

Service	Minimum bid size	Response time	Delivery duration
Congestion management	1 MW	within 15 min	at least 120 min
Tertiary spinning reserve	1 MW	within 15 min	at least 120 min
Tertiary replacement reserve	1 MW	within 120 min	at least 480 min
Balancing	1 MW	within 15 min	at least 120 min

In case of UVAM project, according to EU codes, the Balancing Service Provider (BSP), i.e. the party responsible for trading and supplying balancing services on the MSD, is an independent aggregator. The BSP does not necessarily have to coincide with the Balancing Responsible Party (BRP). In fact, the BSP provides services directly to the TSO, while the BRP is responsible for scheduling and payment of imbalance fees with respect to its scheduled injection/withdrawal program.

In the pilot projects, the UVAM aggregation is relevant only for the participation in the MSD, and not for energy markets (day-ahead and intraday markets). This means that UVAM may be made up by units included in different dispatch points, whereas each traditional significant unit mandatorily enabled to MSD must have each own dispatch point and must participate to energy markets and to MSD without any kind of aggregation. Consequently, for the definition of schedules and for the imbalance settlement, each unit belonging to an UVAM keeps remaining inserted in the existing dispatch points and on day-ahead the BSP has to communicate a baseline for the UVAM, i.e. the overall net power profile expected for the units included within the UVAM for every quarter-hour of the delivery day (baseline is then different from schedules). The baseline is corrected by TSO according to the injections/withdrawals measured in the previous quarter-hour (see Figure 2). The corrected baseline plus the sum of upward or downward quantities accepted on the MSD determines the final program to be respected by UVAM³.

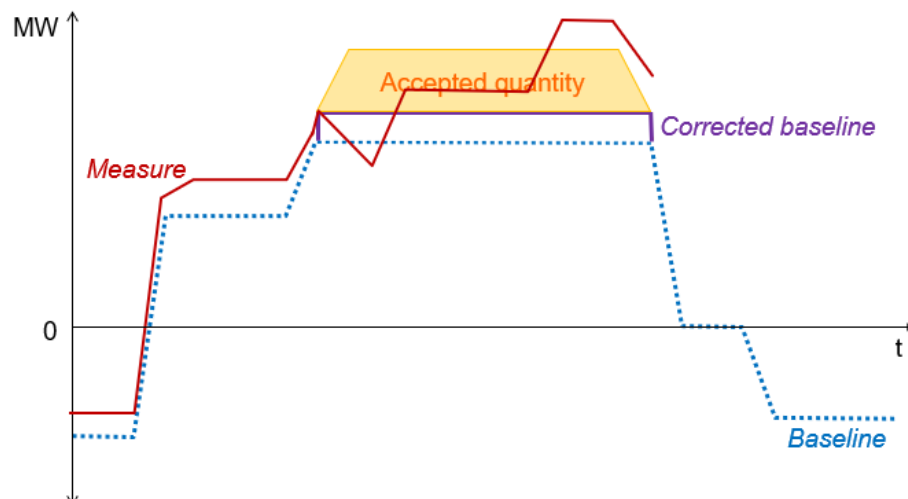


Figure 2: baseline, corrected baseline and accepted quantity (example) [13]

Finally, since the control actions on MSD must not affect imbalances paid by the BRP, the BSP has to communicate to TSO the units belonging to the UVAM and selected in order to

³ Different solutions aimed at defining UVAM aggregations relevant both for the participation in the MSD, and in energy markets are under evaluation [5]. These solutions will probably avoid differences between schedule and baseline and will probably simplify the management of UVAM (but they imply the innovation of the actual dispatch points).

operate the offers accepted on MSD. This enables the Italian TSO to proportionally correct the schedules resulting from the energy markets of the dispatching consumption and/or generation points.

In UVAM projects, for the first time in Italy, remuneration is based on two different mechanisms: the first linked to the energy activated (€/MWh) and a second, started in 2019, linked to the expected availability of the regulation (capacity-based, €/MW/period). In the latter one, Terna procures a certain quota of capacity by means of forward contracts; such capacity is allocated through auctions on a fixed premium varying from 15,000 €/MW/year up to 30,000 €/MW/year, with a pay-as-bid mechanism. Auctions are on yearly, infra-annual and monthly base, up to capacity-quota saturation. The premium is paid by Terna to the BSP upon a commitment to present offers for the overall contracted capacity for upward balancing service during peak hours (from 2 p.m. to 8 p.m., from Monday to Friday); the premium varies from two (15,000 €/MW/year) to four consecutive hours (30,000 €/MW/year) of bids presentation at a price no greater than a strike price, which is set to 400 €/MWh. The introduction (in Italy) of a remuneration in €/MW is strictly related to the experimentation phase: to facilitate the aggregation and the involvement of large costumers, the remuneration of the activated energy only is not sufficient to bear fixed investment costs for installation and calibration of the required equipment and the yearly operational management costs [14].

RESULTS

According to [15], at the end of March 2020, 231 UVAM are enabled (of which 165 with forward contracts with remuneration in €/MW) for a total qualified power of 1348.9 MW for the upward service and 207 MW for the downward service, managed by 34 BSPs. All UVAM are enabled to provide upward services (for power ratings between 1 MW and 62 MW); only 28 of them are also enabled to provide downward services (for power ratings between 1.5 MW and 28 MW). Almost 80% of UVAM are made up of at least one consumption unit, capable of modulating its electricity withdrawals through internal production variation, and programmable (like CHP) or semi-programmable (like run-of-river hydro plants) production units. Regarding not programmable RES, able to provide downward services, there are no UVAM made up only by these resources. In Italy, in fact, PV and wind power plants benefit of incentive schemes linked to the produced or injected energy (in €/MWh): therefore, producers aim to maximize production to obtain the whole incentive. Moreover, 58 UVAM are made up of a single unit (31 of a single production unit, 27 of a consumption unit), whereas only 8 UVAM are made up of at least 10 units. Probably, this is due to the fact that it is easier to manage flexibility of one or a few units.

Regarding the procedure for the forward procurement of dispatching resources through UVAM, in 2020 the maximum quantity that can be contracted is 1,000 MW, divided between Area A (consisting of the North and Centre-North market zones), equal to 800 MW, and Area B (consisting of the remaining market areas: Centre-South, South, Sicily and Sardinia) for the remaining 200 MW. The quota in Area A has been saturated with the yearly auction, at a price of 26,122 €/MW/year, whereas the quota in Area B has been saturated with the infra-annual auction for the period April-December at a price of 9,500 €/MW/year (the average price for the yearly auction in Area B was equal to 28,745 €/MW/year).

The results for the period November 1st 2018 – March 31st 2020 are listed in the following [15]:

- UVAM have been used by Terna exclusively to provide the real-time balancing service, both upward, for a total amount of energy equal to 1043.25 MWh, and downward, for a total amount of energy equal to 234.83 MWh. Figure 3 and Figure 4 report the distribution of the activated energy in the considered period, respectively for the upward and downward services. UVAM aggregated units have been selected for about 221 hours in the considered period for the upward service and for almost 59 h for the downward service. Figure 5 and Figure 6 report the number of quarter-hours per each month, respectively for the upward and downward services;

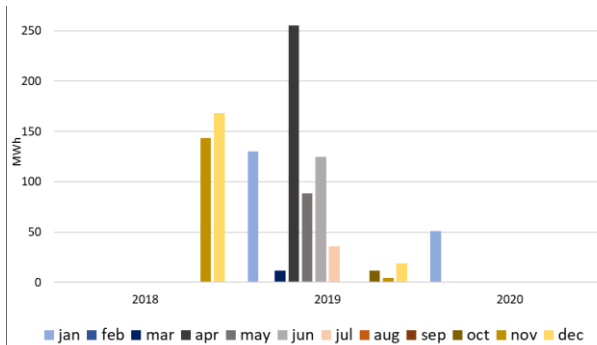


Figure 3: distribution of the activated energy for upward service

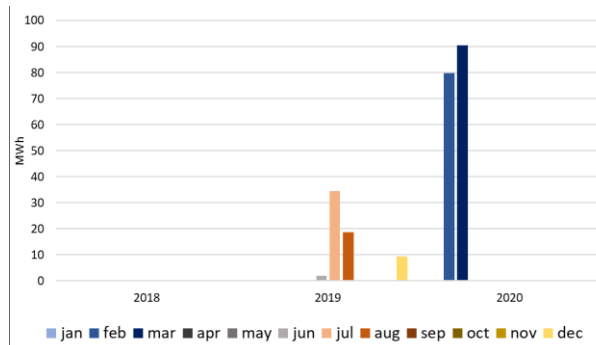


Figure 4: distribution of the activated energy for downward service

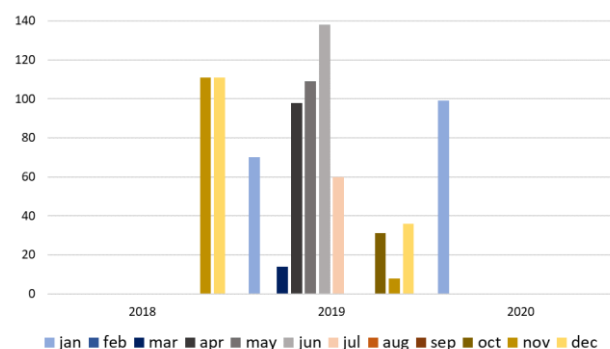


Figure 5: number of quarters of an hour in the considered period in which UVAM have been selected for upward service

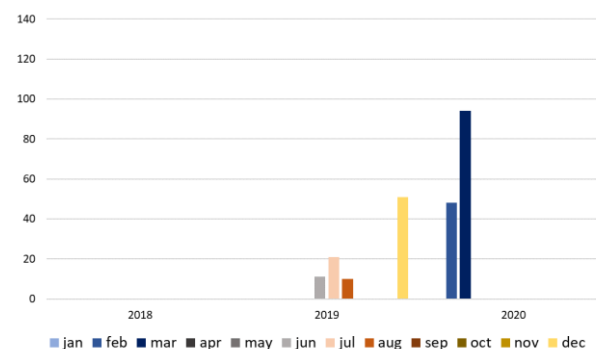


Figure 6: number of quarters of an hour in the considered period in which UVAM have been selected for downward service

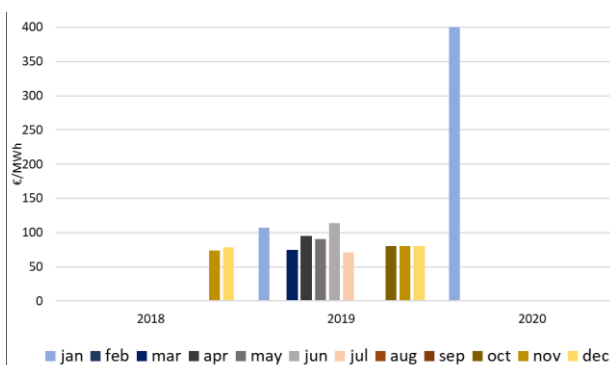


Figure 7: average price of accepted offer for upward service

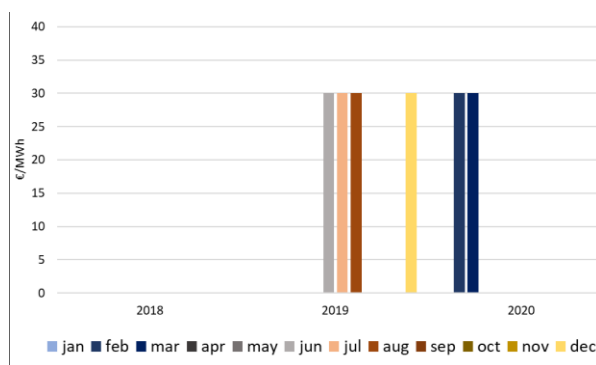


Figure 8: average price of accepted offer for downward service

- the bids submitted for the upward service by the BSPs, especially in the case of UVAM with forward contracts (e.g. for January 2019), are characterized by very high prices, close to the strike price (400 €/MWh), which reduces the probability that they will be selected by Terna, partly frustrating the purpose of the project (in 2018, the upward average price in MSD was about 130 €/MWh, much lower than the bids

presented by BSPs – see Figure 1). In particular, from Figure 9 it can be noted that the price of the offers for the upward service was about 80 €/MWh, in the period 6th November – 31st December 2018, about 351 €/MWh, in the period 1st January – 31st December 2019, and then increased further to about 380 €/MWh in the period 1st January – 31st March 2020. Figure 7 reports the trend of the average price of accepted bids for upward service;

- the accepted bids by Terna for the upward service in numerical terms represent 3.2% of the submitted bids submitted, while the accepted quantities (in MWh) are 0.02% of the quantities offered (in MWh) throughout the entire considered period and are characterized by average prices of about 76 €/MWh in the period November 6th – December 31st 2018, slightly higher than 95 €/MWh in the entire year 2019 and equal to the strike price in the period January - March 2020;
- the bids submitted for the downward service by the BSPs are characterized by prices of about 25 €/MWh in the period November 6th - December 31st 2018, about 22 €/MWh in the period January 1st - December 31st 2019, and about 16 €/MWh in the period January 1st - March 31st 2020 (see Figure 10). Figure 8 reports the trend of the average price of accepted bids for downward service;
- the bids accepted by Terna for the downward service cover 0.5% of the total bids submitted, while the quantities (MWh) accepted by Terna represent 0.04% of the overall quantities offered throughout the entire considered period; moreover, Terna accepted bids with offer price of 30 €/MWh;
- in the case of the accepted offers, UVAM have shown a good degree of reliability, with an average compliance with dispatching orders of 83.5%;
- the UVAM economic regulation (comprehensive of both energy and availability payments, and of non-performance penalties) entailed a total cost of about 26 M€. Despite this, given the role of balancing capacity provision in creating reserve margin during the Integrated Scheduling phase of MSD, the advantages of UVAM introduction into the market have been repeatedly highlighted by the Italian TSO.

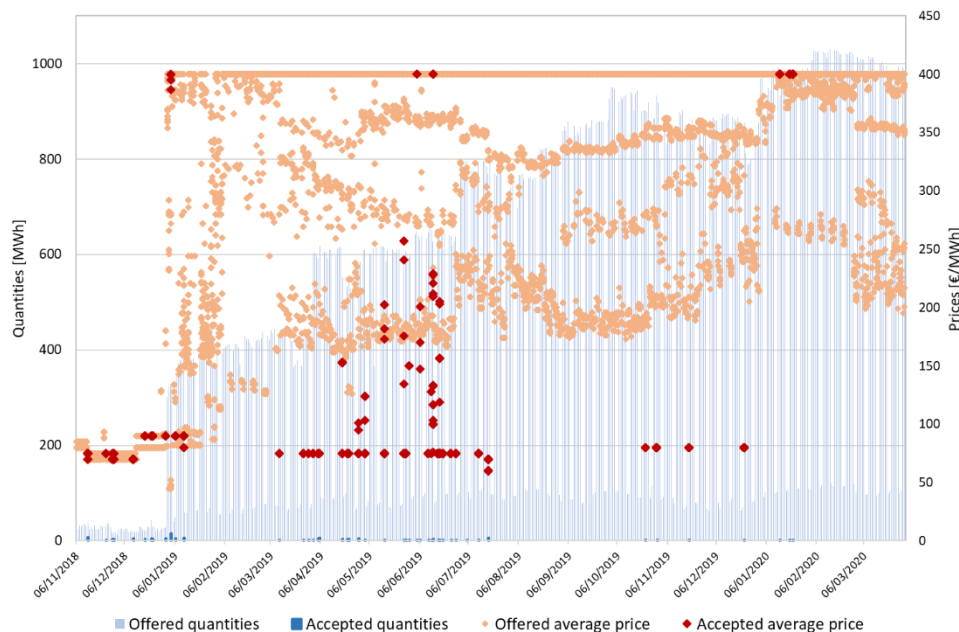


Figure 9: Offered and accepted prices and quantities for upward balancing service [15].

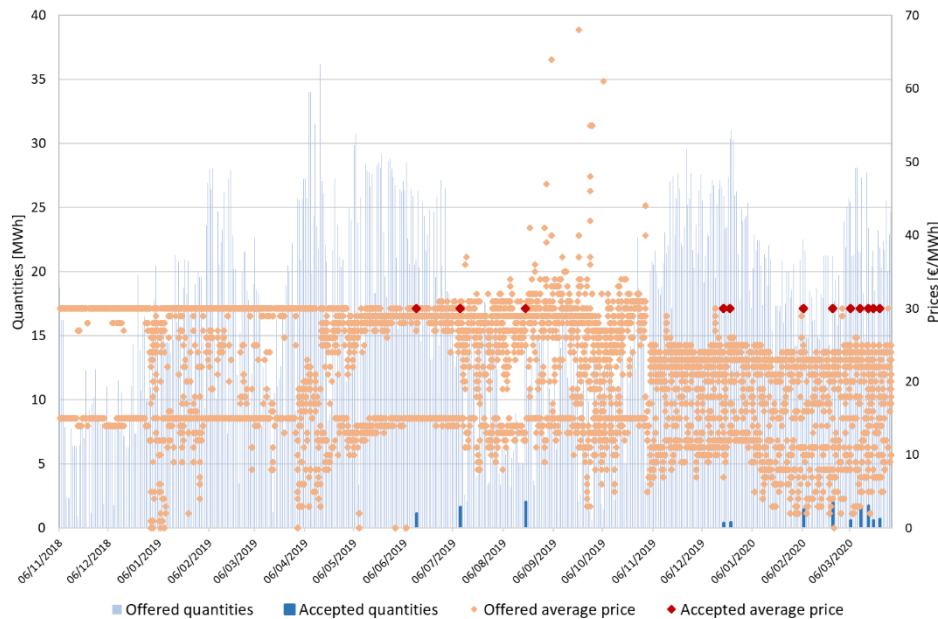


Figure 10: Offered and accepted prices and quantities for downward balancing service [15].

CONCLUSION

The UVAM pilot project, still ongoing, represents the first integration in Italy of distributed energy resources for the provision of ancillary services. The results reported in this work show positive outcomes of the project and give useful elements for next regulatory improvements: several UVAM have been created, mainly constituted by a single consumption or production unit, while lots of BSPs are involved in the project. This is an important innovation for Italy because the active aggregator figure for the provision of ancillary services (essential for the security of the system) did not exist before these pilot projects.

However, Terna has accepted very few of the submitted bids by BSPs. This is probably due to the fact that such bids are characterized by very high prices, much higher than the average price of MSD. In particular, it is interesting to note that in the first few weeks of the pilot project, bids were characterized by prices much lower than the period 1st January 2019 – 31st March 2020. In these first few weeks, in fact, forward contracts – linked to the fixed availability premium upon a commitment to present offers in a certain hours at a price lower than the strike price (400 €/MWh) - had not yet started. This might indicate that BSPs create a UVAM, facing investment and operation costs, only to receive the availability premium. In order to avoid this possible distortion and improve the effectiveness of the project, the regulator could review the strike price downwards. In fact, both the availability premium and the strike price have been introduced due to the experimental nature of this project. The availability premium has been defined to foster the creation of UVAM, covering part of the fixed costs related to the necessary equipment, whereas the strike price has been introduced to allow their effective participation in the MSD, reaching in this way two goals: test the affordability and reliability of UVAMs and limit the system costs. As the first goal has not yet been achieved (probably because of the too high bids), the strike price could be reviewed.

Furthermore, since the capacity quota scheduled in 2020 (1 GW) has been saturated with the first few auctions in both Areas, the Italian Regulator could envisage an increase in the quota.

REFERENCES

- [1] Terna S.p.A. e Gruppo Terna, Contesto ed evoluzione del sistema elettrico, 2019.
- [2] ARERA, resolution 5 May 2017, 300/2017/R/eel, <https://www.arera.it/it/docs/17/300-17.htm>
- [3] Regulation (EU) 2019/943 of the European Parliament and of the Council of 5 June 2019 on the internal market for electricity, https://eur-lex.europa.eu/legal-content/EN/ALL/?uri=uriserv:OJ.L_.2019.158.01.0054.01.ENG
- [4] Directive (EU) 2019/944 of the European Parliament and of the Council of 5 June 2019 on common rules for the internal market for electricity, <https://eur-lex.europa.eu/eli/dir/2019/944/oj>
- [5] ARERA, consultation 23 July 2019, 322/2019/R/eel, <https://www.arera.it/it/docs/19/322-19.htm>
- [6] ARERA, resolution 25 May 2017, 372/2017/R/eel, <https://www.arera.it/it/docs/17/372-17.htm>
- [7] Terna S.p.A., Regolamento recante le modalità per la creazione, qualificazione e gestione di unità virtuali di consumo abilitate al mercato dei servizi di dispacciamento – Regolamento MSD, 30 May 2017.
- [8] ARERA, resolution 3 August 2017, 583/2017/R/eel, <https://www.arera.it/it/docs/17/583-17.htm>
- [9] Terna S.p.A., Regolamento recante le modalità per la creazione, qualificazione e gestione di unità virtuali di produzione abilitate al mercato per il servizio di dispacciamento – Regolamento MSD UVAP, 22 September 2017.
- [10] ARERA, resolution 2 August 2018, 422/2018/R/eel, <https://www.arera.it/it/docs/18/422-18.htm>
- [11] Terna S.p.A., Regolamento recante le modalità per la creazione, qualificazione e gestione di unità virtuali abilitate miste al mercato dei servizi di dispacciamento – Regolamento MSD UVAM, 25 September 2018.
- [12] ARERA, consultation 3 June 2020, 201/2020/R/eel, <https://www.arera.it/it/docs/20/201-20.htm>
- [13] Terna S.p.A., Presentazione incontro tecnico progetto pilota – Partecipazione di UVAM al MSD, 10 July 2018.
- [14] L. Marchisio, F. Genoese, F. Raffo, Distributed resources in the Italian Ancillary Services Market: taking stock after two years.
- [15] ARERA, report 4 August 2020, 321/2020/I/efr, <https://www.arera.it/it/docs/20/321-20.htm>

G0504

Impact of COVID-19 on the demand curves of Croatia and region

Igor Vidić, Matija Melnjak, Davor Bošnjak
HEP Trade LTD, member of HEP group, Zagreb/Croatia
www.hep.hr
Tel.: +385-01/6322226
igor.vidic@hep.hr; matija.melnjak@hep.hr; davor.bosnjak@hep.hr

Abstract

Electrical energy plays a vital role in our everyday lives. Modern lives are unimaginable without a reliable and secure power supply. As electricity generation and consumption have to be always in a balance, the task of planning an accurate day-ahead electricity consumption and generation is of the utmost importance. Electricity consumption forecast is a challenging task, especially in countries with a poor industrial development where the households take the majority of share in the total load. This paper analyzes some of these cases with very variable electricity load, due to volatile household behavior, on cases of Croatia and countries in the region. Additionally, results are compared with the electricity load of North Italy whose economy and industry are far better developed. Electricity consumption is an ever changing curve that is very sensitive to a variety of external factors. Thus, even minor change can drastically change its shape and volume. The main part of this paper focuses on the analysis of the COVID-19 impact on the demand curves of Croatia, but a brief overview of the countries in the region was presented as well. A variety of restrictive, governmental, and epidemiological measures have been gradually introduced and this paper attempts to detect how they affected the total load and the shape of the demand curve in each analyzed country. Historical electricity load data has been gathered for Croatia and five other neighboring countries and the analysis of COVID-19 impact has been carried out. External conditions such as weather and social impact have been taken into account for the analysis in the case of Croatia, but since the category of consumers that contribute in total load (industry, households, entrepreneurship, etc.) were unfortunately unavailable, it is hard to find out whose consumption habits have been changed the most during the lockdown. Some unpredictable, stochastic parameters influenced the demand curve, hence, sometimes it's behavior cannot be easily explained. Results have shown the severe impact of the COVID-19 on the demand curves of every analyzed country. The highest electricity load decrease, in all of the examined countries, has been during the lockdown measures. Moreover, analysis shows that the regions with more significant industry share in total load and more developed economies are starting to recover faster (e.g., North Italy) in terms of electricity load, while the countries with a lower share of industry (in the total load) struggle with such a recovery. The results of this paper highlight the sensitivity of electricity consumption, the significance of COVID-19, and any future possible pandemics in electricity consumption forecast as well as the correlation between countries' economic development and their electricity consumption.

1. Introduction

This research aims to investigate the impact of the COVID-19 on the shape of Croatian load curve and the consumption of electricity in general. Furthermore, a brief analysis of a situation in the region was carried out and the results will be presented.

Many people claim that the corona crisis in Italy and Europe escalated after the Champions League match in Milano on 19th of February 2020 where Atalanta hosted Valencia. Suddenly, a few days after that match Italy became, by far the most affected European country and the city of Bergamo one of its worst-hit towns. The first case of COVID-19 infection in Croatia was confirmed in the last week of February, precisely on 25th of February 2020. As the patient number zero was marked a young guy who attended that football match in Milano. As time was passing, the number of people infected by the coronavirus disease was growing daily, but fortunately, the exponential rise of new cases was mitigated [1].

Consequently, the National crisis management was set up to fight the coronavirus and slow down the spreading of the virus among the population [2]. In cooperation with the government some new rules, that completely changed the way most of the citizen's life, have been adopted.

These rules and restrictions incorporated not only the suspension of lessons in all schools and all universities but also temporarily end of work in all kindergartens. Furthermore, employers were forced to enable working from home to most of their employees, if it is anyhow possible. Otherwise, they had to reduce the number of people sitting in the office at the same time. All public meetings, public occasions, sports competitions, trade fairs, and gatherings for the purpose of religion were strictly forbidden. In addition to this, service activities that are not essential for the functioning of the community were also stopped. Hence all museums, theaters, disco clubs, libraries, gyms and fitness centers, bars, hairdressers closed their doors. Permission to work but with strict rules had only supermarkets, bakeries, restaurants with food deliveries, and pharmacies. Furthermore, all kinds of public, city, and intercity transport were suspended.

Living under these lockdown restrictions completely changed our daily routines and past habits, thus we had to forget the life we had before. Therefore, it is likely to expect significant changes in electricity consumption.

This research focuses on gathering and analyzing electricity consumption data for Croatia and neighboring countries during the COVID-19 pandemic.

2. Electricity demand forecasting

Electricity load forecasting is a complex task which incorporates a variety of variables that directly or indirectly affect the demand for an electricity [3]. Electric energy consumption is the actual energy demand in the real time made on existing electricity supply [4].

Electricity consumption is a vital part of economic activity and an irreplaceable part of our daily needs. Thus, electricity load profile ([5], [6], [7]) reflects “an electrical activity of the hearth of a nation, region or individual customer” like an ECG [8]. It surely represents holistic pulse of customers at an observed moment.

Accurate planning of the day-ahead electricity load can also significantly help system operators with less activation of ancillary services in the real time. Thus, it is important to have a reliable method for electricity consumption prediction and consider time decomposition which includes long, medium and short-term framework [9]. A variety of factors mentioned in [10] in long-term and medium-term load pattern forecasting, such as population, economic development, climate, etc. influence the total electricity load of one country. There are plenty of existing load forecasting methods that can be used for a day-ahead consumption planning. An overview and review of such electricity consumption planning methods were given in [11]. Generally, models could be divided into intelligent non-linear models that incorporate advanced technologies such as Artificial Neural Network ([12],[13]), grey prediction models [10], and statistical analysis models. Moreover, there are also a variety of other hybrid models. One of such developed models is presented in this chapter. This model consists of factors divided into three key categories: weather dependent factors related to the load, social factors connected to the load, and stochastic factors that affect load changes [14]. This is presented by the following equation:

$$P(t) = \alpha * P_w(t) + \beta * P_s(t) + \gamma \quad (1)$$

Where:

- $P(t)$ – total electricity load in a certain period
- $P_w(t)$ – weather dependent factor of the total load
- α – coefficient correlated with the weather dependent factor
- $P_s(t)$ – social dependent factor of the total load
- β – coefficient correlated with social dependent factor
- γ – constant for estimating stochastic load changes

Furthermore, each of these variables, which behave like independent or partly dependent functions is then further decomposed and analyzed in individual sub-functions. For example, a weather dependent factor incorporates air temperature, wind speed and direction, cloudiness as well as type and intensity of a precipitation. Furthermore, there is also a humidity (dew point) which affects a load curve in cases of high and low temperatures. This is presented in following equation:

$$P_w(t) = \alpha_1 * T(t) + \alpha_2 * C(t) + \alpha_3 * Ws(t) + \alpha_4 * Wd(t) + \alpha_5 * Rt(t) + \alpha_6 * Ri(t) + \alpha_7 * H(t) \quad (2)$$

Where:

- $P_w(t)$ – weather dependent factor of the total load
- $T(t)$ – external temperature dependent factor
- $C(t)$ – cloudiness dependent factor
- $Ws(t)$ – wind speed dependent factor
- $Wd(t)$ – wind direction dependent factor
- $Rt(t)$ – precipitation type dependent factor
- $Ri(t)$ – precipitation intensity dependent factor
- $H(t)$ – humidity (dew point) dependent factor
- $\alpha_1, \alpha_2, \alpha_3, \alpha_4, \alpha_5, \alpha_6, \alpha_7$ – coefficients for estimating load changes with correspondent weather dependent factors

This example is just one of the multiple ways of forecasting electricity consumption that illustrates its complexity. Such challenge can be described like forecasting both “nature” and “society” during a timeline which affect the shape and values of the forecasted load curve. Naturally, in countries with higher industrial development and lower share of households’ electricity consumption, load forecasting can be considered somewhat easier since a household consumption can be very fluctuating and unpredictable. An example of such a country where a load forecasting is a tremendous challenge is Croatia where the majority of the electricity demand consists of households. Thus, when forecasting the electricity demand curve a special consideration for social factors (holidays, weekends, semi-working days, public events, lockdown restrictions, etc.) has to be taken into account. Even the slightest weather or social changes can significantly impact the total load curve. The main analysis of this paper considers the impact of COVID-19 and corresponding lockdown measures on the electricity demand curve and how to read its data. Such pandemic has significantly affected behavior of demand curves and it has to be taken into account while analyzing realised electricity load curves during such period and forecasting electricity load curves in ever similar period in any stage in the future.

3. Analysis of electricity demand curves

This chapter will describe and analyze gathered data for Croatia and neighboring countries in terms of electricity consumption as well as give an overview of restrictive lockdown measures and how they affect overall electricity consumption. The analysis will be carried out and results compared to the previous historic data in the following subsections. In addition, the analyses was expanded to the case of Sweden which, although is not in the region with others, is an interesting case to compare with due to its complete opposite approach in national strategy of not imposing the restrictive lockdown measures.

Period of analysis is 14 weeks and exact periods of each week are presented in Table 1.

Table 1. Analyzed period

	2019.	2020.
Week 1	25.2.-3.3.	24.2.-1.3.
Week 2	4.3.-10.3.	2.3.-8.3.
Week 3	11.3.-17.3.	9.3.-15.3.
Week 4	18.3.-24.3.	16.3.-22.3.
Week 5	25.3.-31.3.	23.3.-29.3.
Week 6	1.4.-7.4.	30.3.-5.4.
Week 7	8.4.-14.4.	6.4.-12.4.
Week 8	15.4.-21.4.	13.4.-19.4.
Week 9	22.4.-28.4.	20.4.-26.4.
Week 10	29.4.-5.5.	27.4.-3.5.
Week 11	6.5.-12.5.	4.5.-10.5.
Week 12	13.5.-19.5.	11.5.-17.5.
Week 13	20.5.-26.5.	18.5.-24.5.
Week 14	27.5.-2.6.	25.5.-31.5.

Table 2. Total number of new weekly confirmed COVID-19 cases

	Italy	Croatia	Hungary	Slovenia	Bosnia	Serbia	Sweden
Week 1	1557	7	0	0	0	0	13
Week 2	5686	5	8	16	2	1	189
Week 3	16605	36	31	237	19	54	829
Week 4	35158	187	128	189	141	133	874
Week 5	38551	478	280	321	251	553	1794
Week 6	31259	469	297	258	368	1167	3130
Week 7	27415	418	714	191	292	1722	3653
Week 8	22609	271	526	123	267	2688	3902
Week 9	18703	159	599	72	248	1724	4255
Week 10	13042	66	452	38	358	1422	3677
Week 11	8353	91	249	16	212	650	4005
Week 12	6365	39	251	6	161	496	3821
Week 13	4423	18	221	2	97	549	3316
Week 14	3161	2	120	6	118	253	4083

Along with weekly total load data, the number of weekly COVID-19 positive cases has been gathered for each of analyzed region. Table 2 presents data of new weekly confirmed COVID-19 cases for each of the analyzed region.

However, due to a vast difference in sizes of countries, and thus a much higher number of confirmed cases for larger countries, for purpose of this analyses it is better to look at number of cases per 10 000 residents.

New weekly COVID-19 cases per 10 000 residents

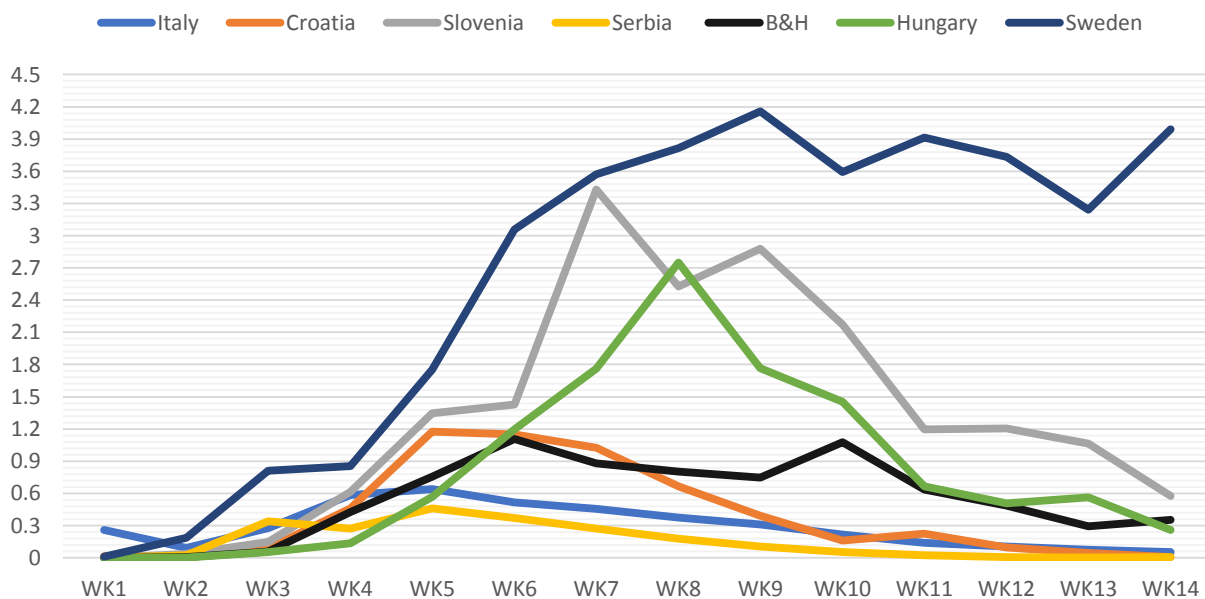


Figure 1. Number of new weekly COVID-19 positive cases per 10 000 residents for each respective region

As seen in **Error! Reference source not found.** Sweden has the highest rate of COVID-19 positive cases per 10 000 residents and their trend from week 7 to week 14 is not declining as it is the case for other countries in this analysis. The main reason for this is that Sweden is the only European country that decided to take a different approach in the battle with the COVID-19 pandemic. They decided against the majority of restrictive measures or a complete lockdown that was introduced in other countries. Instead, they decided to try to overcome the pandemic by acquiring a herd immunity effect. Considering their specific approach, it is very interesting to include Sweden in the total load analyses and comparison with the rest of the countries in the region.

3.1. Electricity demand of Croatia

Forecasting the load curve of Croatia is a challenging task. As there is a significant lack of industry, compared to the leading European countries, the highest share of the load comes from the end-consumers and households. Thus, the forecasting of electricity load curves has a wide range of options due to the stochastic and fluctuating behavior of households' consumption as well as external conditions such as weather and social impact. Observation of Croatian total load was made for 14 weeks starting from the last week of February to the end of May. During the first three observed weeks, there were no signs of the impact of corona virus on the demand curve. Despite the COVID-19's presence in Croatia, there weren't any new rules or restrictions that would change people's lives and daily habits. Life was as usual as before, but things started to change in the week 4 (16.3.2020.-22.3.2020.) when the National crisis management decided to close all schools, universities, and kindergartens to mitigate the spreading of corona virus. From Thursday 19.3.2020., all public events and gatherings were forbidden. Only necessities such as supermarkets, pharmacies, and restaurants with food delivery options have had working permits. All other service activities had temporarily locked their doors. From the Sunday of week 4 (22.3.2020.) all kinds of public transport were stopped. Some of these restrictive rules, such as suspending tram and train traffic, closing the majority of shops and markets, were an obvious cause for the decrease in the electricity consumption. On the other hand, it is hard to estimate how the school closing has affected electricity demand because all pupils and students had to follow the lectures using TV, tablets, and computers.

The demand curve shows that the total load fell off or decrease in regards to the previous week when restrictions haven't been yet adopted. Contrary to what might be expected, the total load of the fifth week has increased. However, it is mostly due to harsh weather conditions that incorporate extreme coldness for this period of the year, snow, and wind during most of the week which can be seen in **Error! Unknown switch argument.** and **Error! Unknown switch argument.** On the demand curve, it can be noticed that even though the temperatures were very low, electricity consumption fell in mornings hours, and increase significantly later, around noon, during afternoon and in the evening. The shape of the demand curve had completely changed and the daily peak was almost as high as the evening peak which is uncharacteristic to previous historic data. In nearly all hours (exception of the morning), consumption was higher than the one in the previous weeks, which can be interpreted by the fact that people woke up later and postponed their usual morning activities and habits since most of them worked from home. In certain hours total load was similar to the period before restrictions. In the sixth observed week, temperatures were also under average, however, the total load has decreased. Summertime calculation (Day-light saving time) led to reaching the evening peak in the twenty-first hour, and more daylight affected consumption too.

During the seventh week, the consumption continued to fall, and it was nearly 32 GWh lower than the previous week. This has marked the highest difference of realized load between two continuous weeks which can be explained by the fact that it was Easter week, and the holiday has significantly impacted total load. Monday of eights' week was a holiday as well, and the total load was also lower than the previous week. However, the demand curve had almost the same shape. It was slightly translated in the downwards direction.

The ninth week was very similar to the previous with an insignificant rise in total consumption. Restrictive rules, adopted during the lockdown, have been cleared starting from week ten. At the beginning of week ten, supermarkets started to reopen, except for the ones in shopping centers. Furthermore, certain services activities, which don't require close contact between people have also started to reopen along with public transport. However, the lowest consumption was achieved in this week, and from that point, the load started to slowly recover in the upcoming weeks. From the eleventh week, it was allowed for all services activities to reopen their doors (hairdressers, barbers, beauticians, etc.). The last phase of restrictions clearing started in week twelve, when shopping centers, bars, and restaurants were reopened. In the last three weeks, the shape of the demand curve changed mostly in the afternoon „gap“ when the total load has risen. In addition, this evening consumption reached a peak in the twenty-second hour.

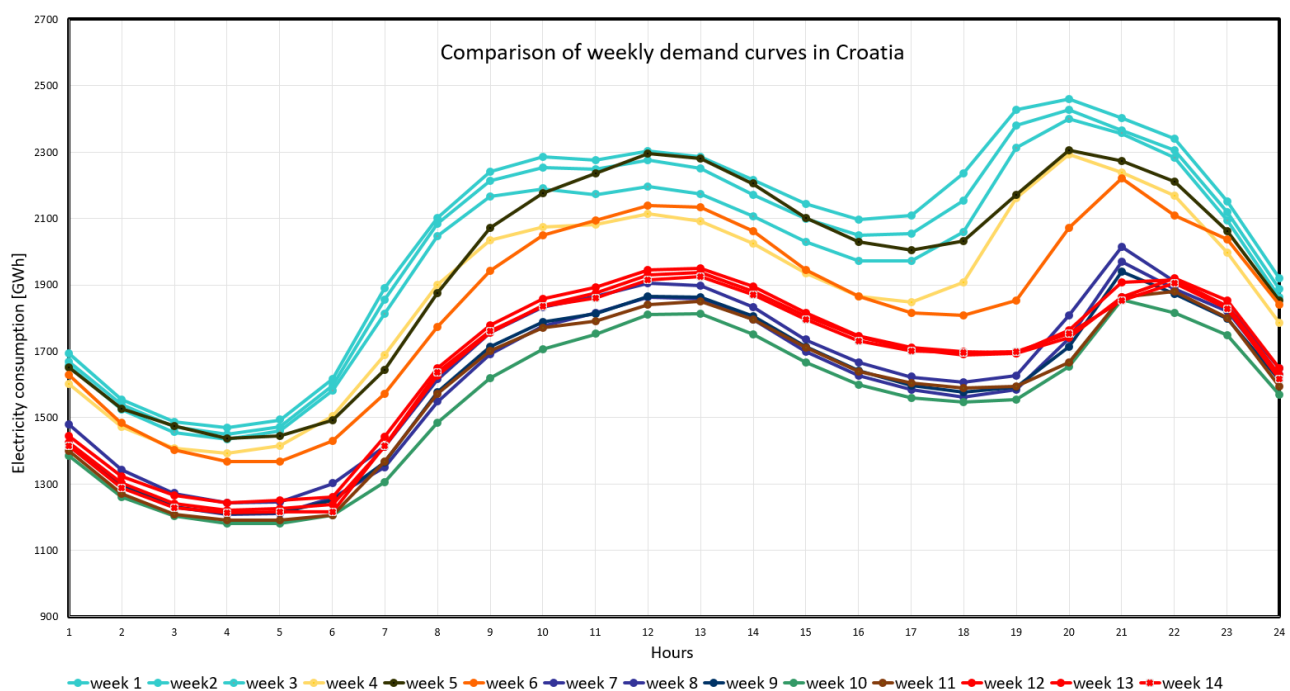


Figure 11. Average weekly demand curves of Croatia

Electricity consumption, in general, is mostly dependent on external conditions such as weather. Some of these parameters are, as already mentioned in the Chapter 2, air temperatures, cloudiness, precipitation, wind speed, wind direction and humidity. A comparison of all of these parameters would be too complicated and nearly impossible, hence, only the air temperature will be taken into consideration in future analysis and comparison with previous historical data.

Following figures (3-6), present average daily temperatures in cities of Zagreb and Split during 14 weeks (98 days) in the year 2019 and 2020.

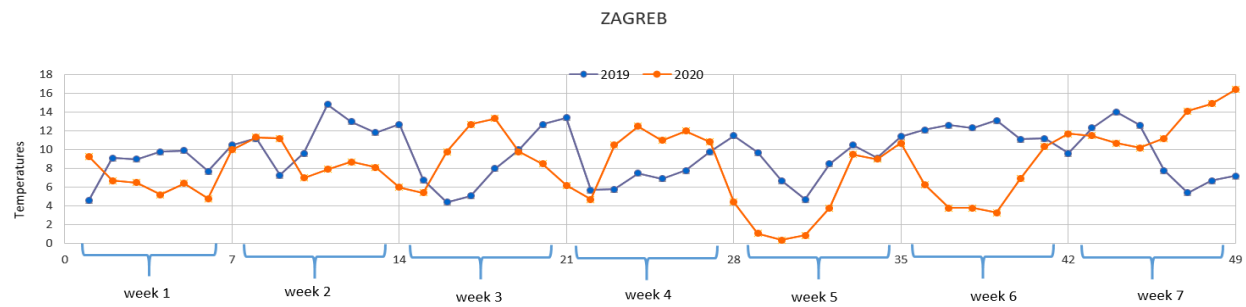


Figure 12. Average air temperature in Zagreb during first seven weeks

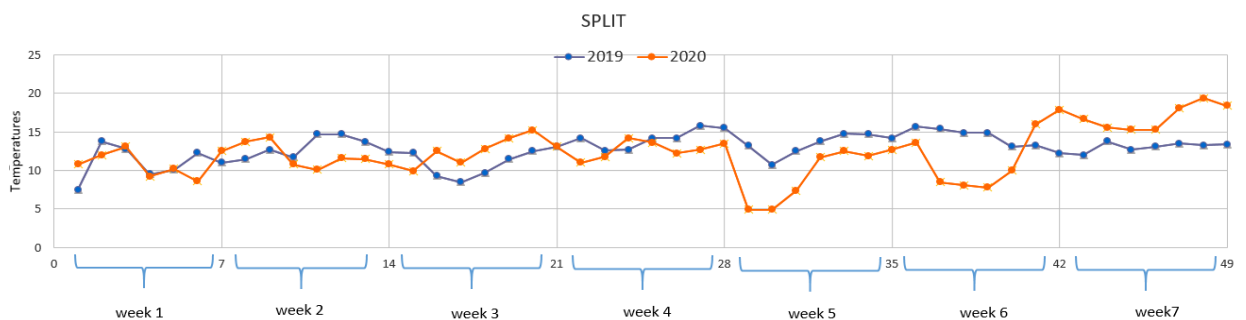


Figure 13. Average air temperature in Split during first seven weeks

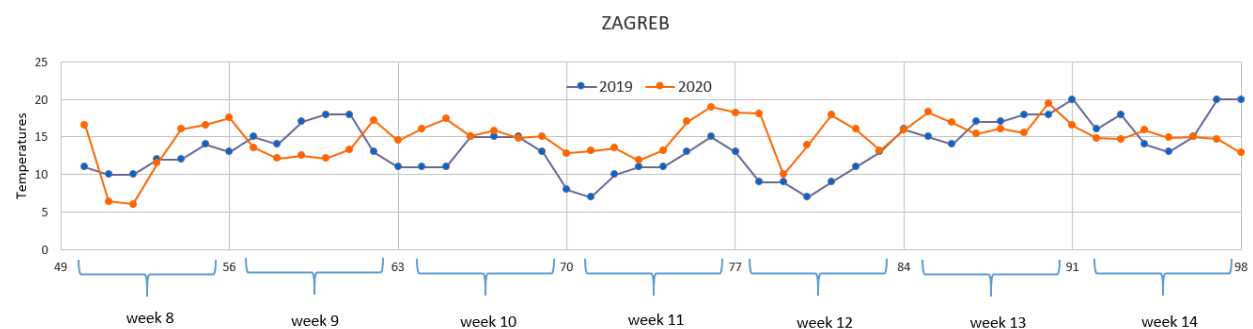


Figure 14. Average air temperature in Zagreb during second seven weeks

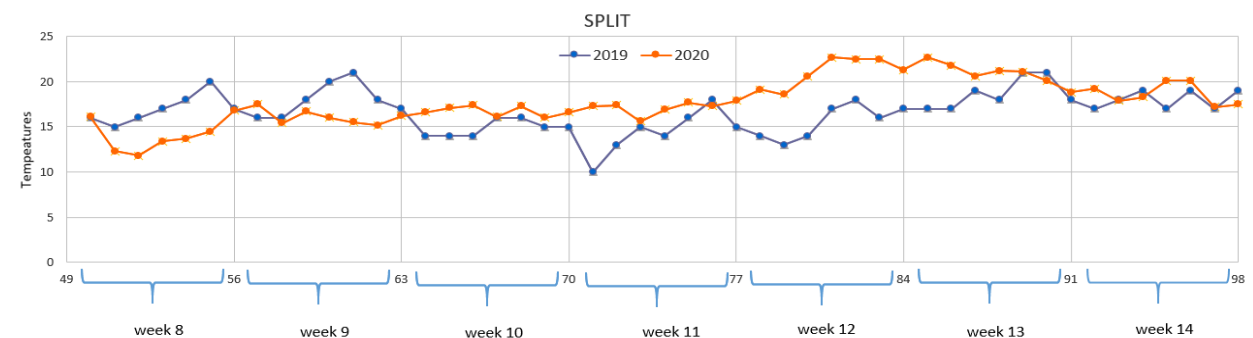


Figure 15. Average air temperature in Split during second seven weeks

Almost in all weeks during the lockdown the total load has decreased in regards to the same period in the previous year which can be seen in **Error! Unknown switch argument.** Only in week five, electricity consumption has risen by 1,57% in comparison with the previous year, even though the new restrictive rules have been adopted. The main reason was certainly weather conditions and very low temperatures as it is shown in **Error! Unknown switch argument.** and **Error! Unknown switch argument.** The impact of new restrictive measures on electricity consumption can be seen in a total load of week six when temperatures were also lower than the ones a year ago, but the total load fell by 2,44%. After the restrictions have been released, the total load started to slowly recover. However, it was almost insignificant. There was still a big difference between the same period of the previous year because previous May has been much colder as it can be seen in **Error! Unknown switch argument.5** and **Error! Unknown switch argument.6**.

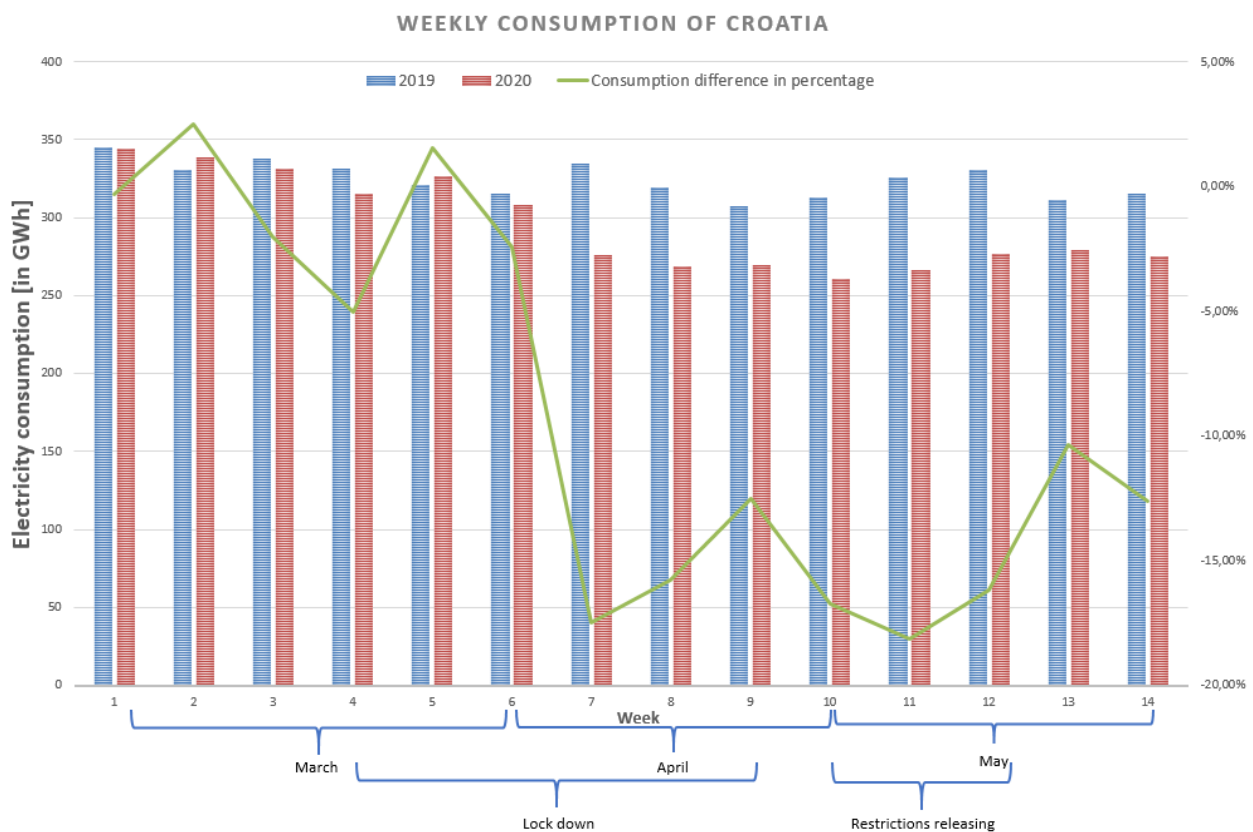


Figure 16. Comparison of weekly total load of Croatia for 2019 and 2020

3.2 Electricity demand of Northern Italy

North Italy was the worst-hit region of the country. Coronavirus spread rapidly after the Champions League match between Atalanta Bergamo and Valencia that was held in Milano, on the 19th of February. It is believed that it is the main reason why Bergamo has become the epicenter of the pandemic. North Italy is the most developed part of the country and it incorporates the following regions: Val D'Aosta, Piemonte, Liguria, Lombardia, Trentino, Veneto, Friuli Venezia Giulia, and Emilia Romagna. A significant contribution to a total load of North Italy is the industry and it is a major reason why electricity consumption decreased significantly during the lockdown. **Error! Unknown switch argument.** shows that the total load has not instantly decreased within the first two weeks of COVID-19 appearance in Northern Italy. However, as the number of confirmed COVID-19 cases grew, restrictive measures were introduced. Moreover, the downwards trend of total load continued from week 3 to week 6 where it reached its minimum with roughly 35% of the total weekly load decrease in comparison with the previous year. Furthermore, week 7 in 2020 includes Good Friday and Easter Sunday holidays, while in 2019 such week was in week 8. These holidays in most of Europe significantly influence the shape of the load curve and Italy especially. As can be seen in , from weeks 7 to 14, the total weekly load has begun to recover reaching roughly 10% of the total load decrease in week 14. However, this assertion has to incorporate influence of different dates and weeks of Eastern holidays when we make conclusions about exact “tipping point” when and why the load curve started to ascend.

According to *Istituto Superiore di Sanita*, almost 80% of the total confirmed cases by 3rd of June 2020 were from the regions listed above. Thus, this paper focuses on North Italy rather than the entirety of Italy. Due to the strong economy and developed industry, the recovery of the total load is significantly faster in comparison with other regions analysed in this paper.

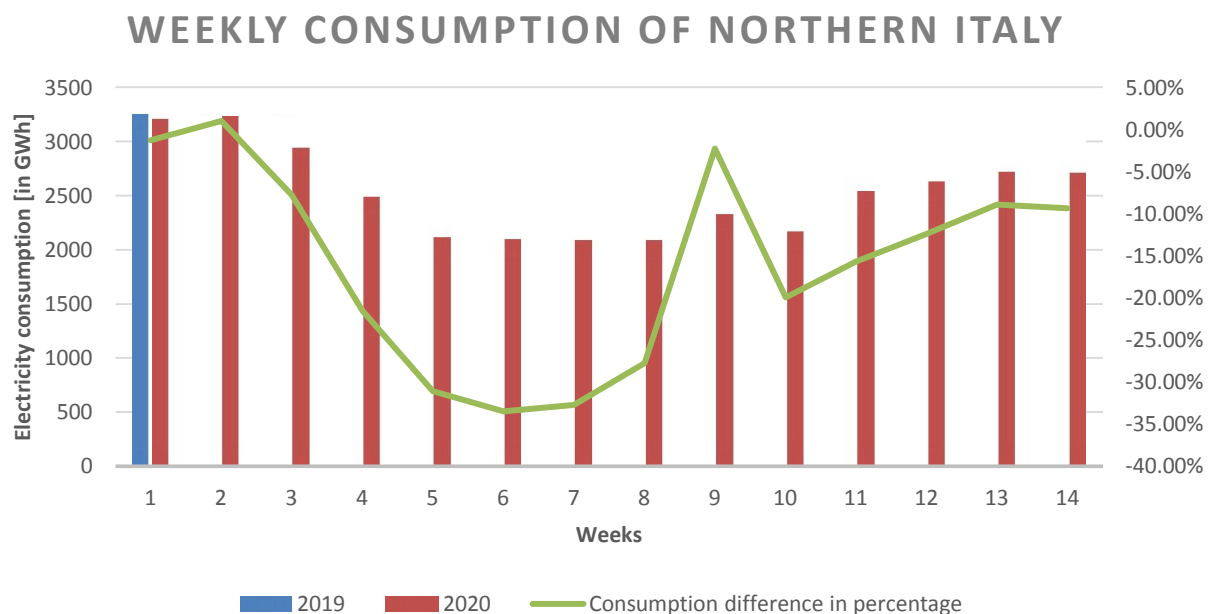


Figure 17. Comparison of weekly total load of North Italy for 2019 and 2020

3.3 Electricity demand of Slovenia

Similar to the case of Croatia, Slovenia decided to tackle the COVID-19 pandemic with strict restrictions and lockdown. The first cases appeared in roughly the same period, and as previously shown in

Figure 11. Slovenia had one of higher rates of COVID-19 infections per 10 000 residents. However, with their governmental measures, they managed to control and stop further growth of cases. From week 7 and on, their measures proved efficient, and the decline in newly infected people started.

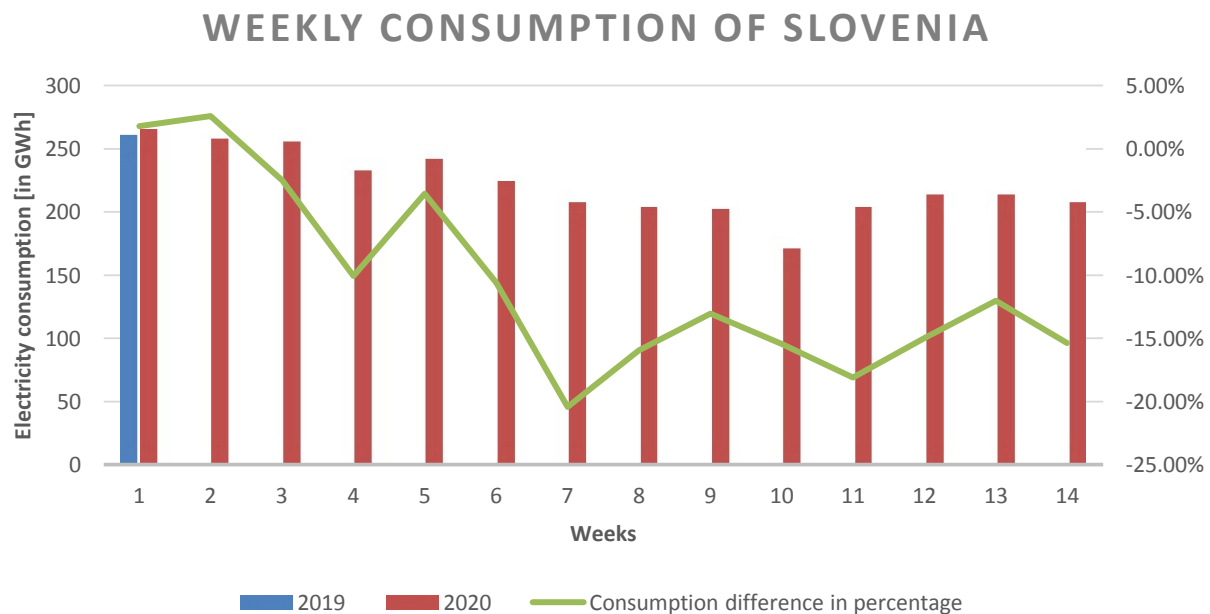


Figure 18. Comparison of weekly total load of Slovenia for 2019 and 2020

Error! Unknown switch argument. presents a comparison of the Slovenian total load in 2019 and 2020. A clear impact of COVID-19 can be seen in the decrease of the total load which has peaked in week 7. A peak difference between these two years is roughly 20% of the total load. This is also the period where the number of new cases has peaked. As the pandemic has been put under control, from week 8 and on, the total load has started to slowly recover. However, their recovery is at a moderate rate and the aftermath of COVID-19 is still present in significantly lower consumption (roughly 15% lower).

3.4 Electricity demand of Serbia

Although the first cases of COVID-19 in Serbia arose in a similar period as the rest of the region, the first 6 weeks marked the total load increase in comparison with the previous year. One of the reasons for this is that their national strategy has decided to wait with restrictive measures and lockdown, and the weather impacted the total load. However, once the number of cases has significantly risen, they introduced strict restrictions and a complete lockdown. Furthermore, a police hour has been enforced during some weekends where people were not allowed to leave their homes unless it was a must. This can be seen in **Error! Unknown switch argument.** where their total load has decreased by nearly 10% in week 8. From this point on, their load was slightly lower in comparison with the previous year.

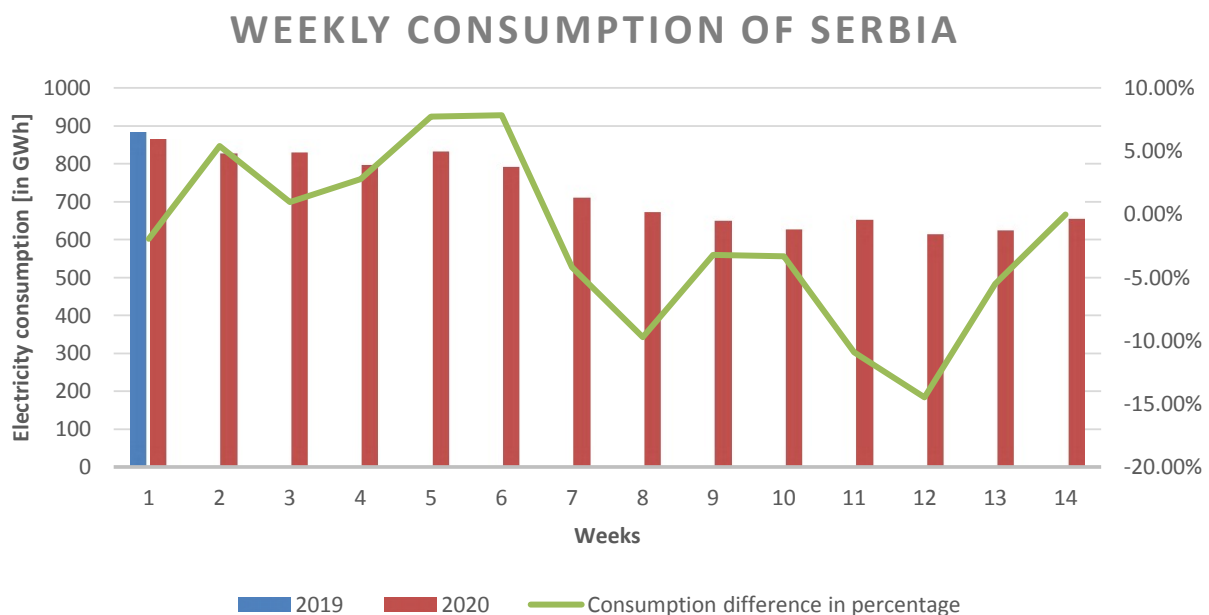


Figure 19. Comparison of weekly total load of Serbia for 2019 and 2020

The case of Serbia shows signs of COVID-19 pandemic consequences on the total load, however, they are not as significant for the total load as the previously analyzed case of North Italy. Moreover, the analysis has not been as in-depth as the case of Croatia as the goal was to present overall total load data comparison.

3.5 Electricity demand of Hungary

The first cases of COVID-19 in Hungary appeared in the second analyzed week. In comparison with other countries in the region, the initial situation in Hungary appeared well as they counted one of the lowest amounts of COVID-19 cases in the first few weeks

Figure 11 graphically shows that they had one of the slowest starts in COVID-19 cases. However, the peak in new cases peak was also later than in other countries. Naturally, the restrictive measures were also implemented in a different time period from other countries. The situation is also translated into the total load curve. In the first three weeks, Hungary marked an increase in the total load in comparison with previous years. Moreover, as the number of cases grew and restrictive measures had been introduced, the decline of the total consumption had begun. Similar to the cases of Croatia and Slovenia, Hungary also experienced the lowest total load in week 7. The total load had decreased by nearly 15% in comparison with the previous year. From this point on, the difference has been fluctuating but it has never recovered above the 7% decrease in the total load.

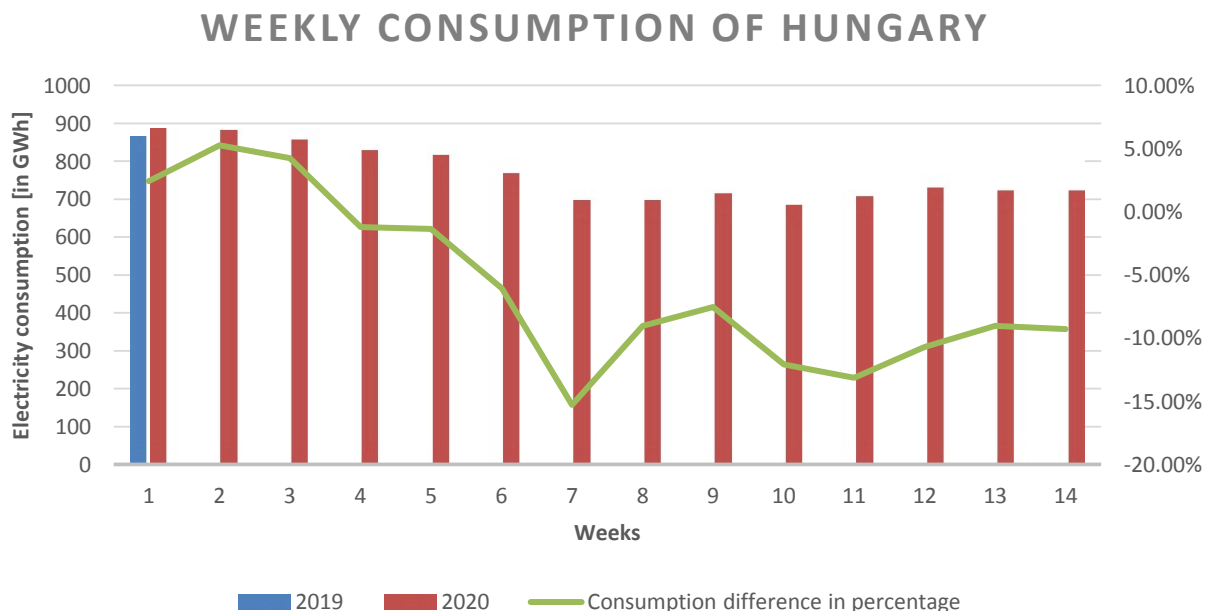


Figure 20. Weekly total load comparison of North Italy for 2019 and 2020.

The case of Hungary is similar to other analysed cases where the COVID-19 pandemic significantly decreased countries' total load due to restrictions.

3.6 Electricity demand of Bosnia and Herzegovina

The case of Bosnia and Herzegovina is challenging to analyze. Despite other countries in the region marking economic and electricity consumption increase, Bosnia and Herzegovina marked a total load decrease even in weeks before the COVID-19 pandemic. Considering their total load decrease before the pandemic, it is hard to judge exactly how huge is the impact of COVID-19.

Data presented in Table 2. shows a similar trend between the number of cases in Bosnia and Herzegovina as in Croatia and Hungary. Interestingly, the number of weekly cases has not gone above 1.25 per 10 000 residents which is the lowest in the region, besides Italy.

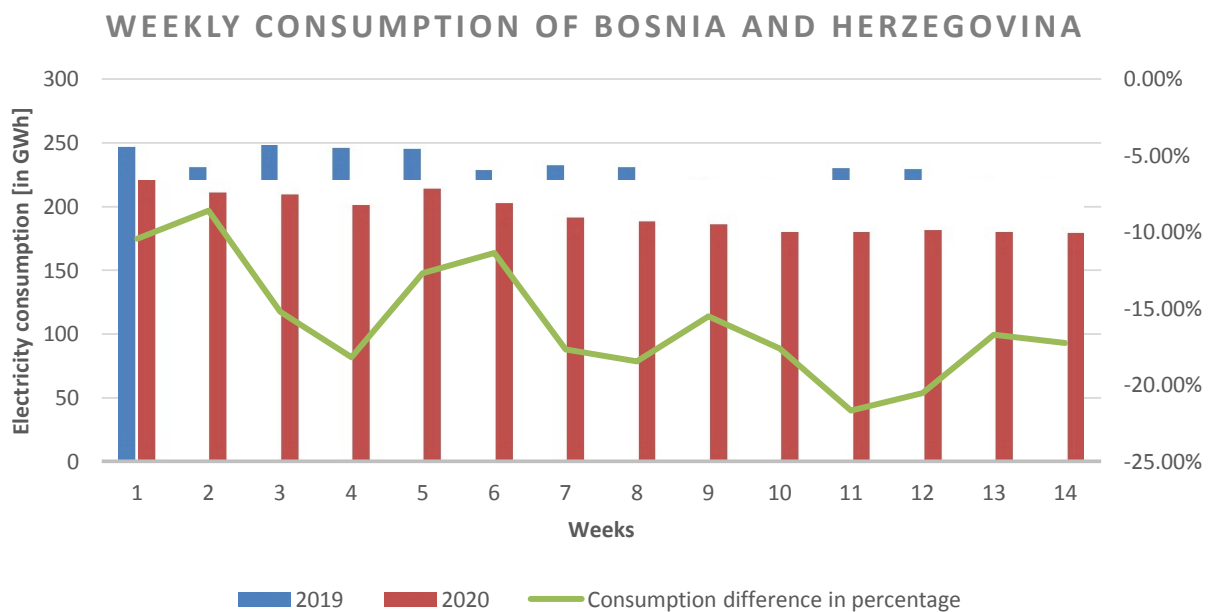


Figure 21. Weekly total load comparison of Bosnia and Herzegovina for 2019 and 2020.

Error! Unknown switch argument. shows a total load decrease in all of the 14 analyzed weeks which is not the case for any other country analyzed in this paper. The COVID-19 pandemic peaked between weeks 4 and 11, and the highest decrease in the total load was in week 11 (20% decrease in relation to the previous year). Generally, their load is very fluctuation and there are no signs of its recovery in this analyzed period.

3.7 Electricity demand of Sweden

As previously mentioned at the beginning of Chapter 3, Sweden decided to take a different approach in battle with this pandemic. Rather than introducing serious restrictive measures and enforcing a lockdown, it was decided that the national strategy was to try to acquire the herd immunity effect. Naturally, this meant that the number of COVID-19 positive patients was much higher in comparison with other countries which can be seen in Figure 11. Contrary to other observed countries, the number of infected people has not declined in upcoming weeks either which is an expected outcome due to the lack of restrictive measures.

However, this strategy meant that the Swedish economy and industry would not take such a hit as other countries observed in this paper. Thus, it is expected that the total load should not massively decline either.

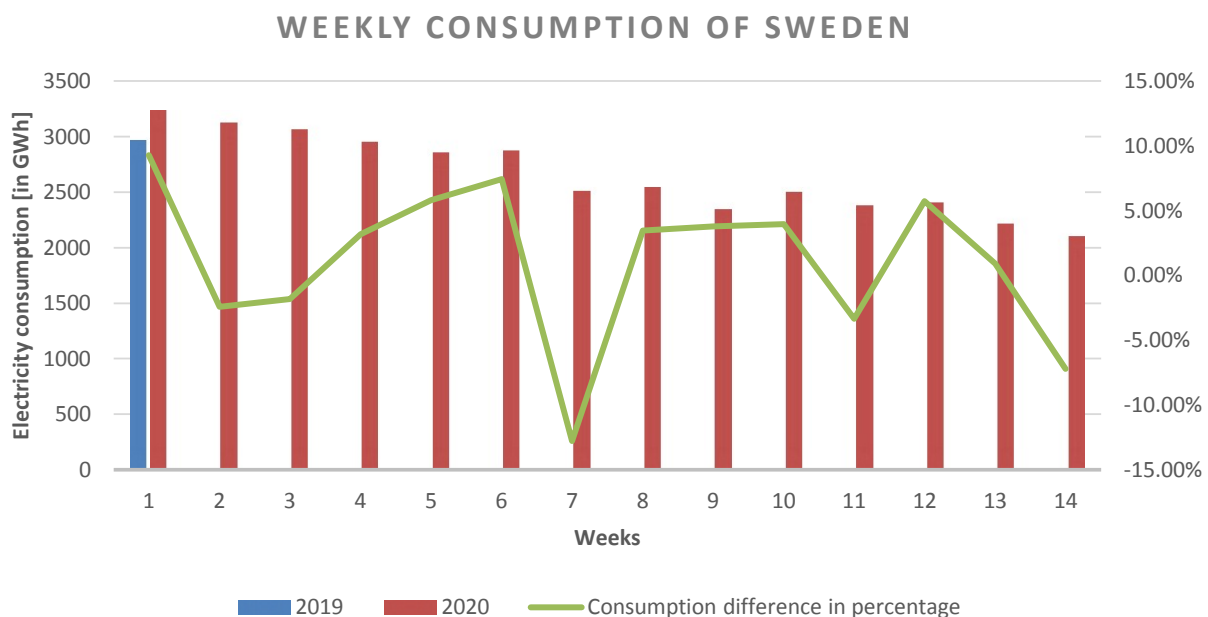


Figure 22. Weekly total load comparison of Sweden for 2019. and 2020.

As seen in **Error! Unknown switch argument.** the total load of Sweden was very similar in the majority of weeks for the years 2019 and in 2020. Undoubtedly, some differences in the total load are always going to exist due to a vast variety of external factors. However, when compared to other analyzed countries in this paper, there is no significant decline besides week 7. The main reason for this are the temperatures which were extremely low in that period in 2019. Temperature data is presented in **Error! Unknown switch argument.** where the average weekly temperature in 2019 was around 1 Celsius degree while the temperature in 2020 was around 8 Celsius degree which is more standard for that period of the year. Consequently, a total load of week 7 in 2019 was significantly higher than it would have been with regular temperatures. Thus, the conclusion is that the main reason for the decline was not COVID-19 pandemic but the extreme weather conditions in the previous year.

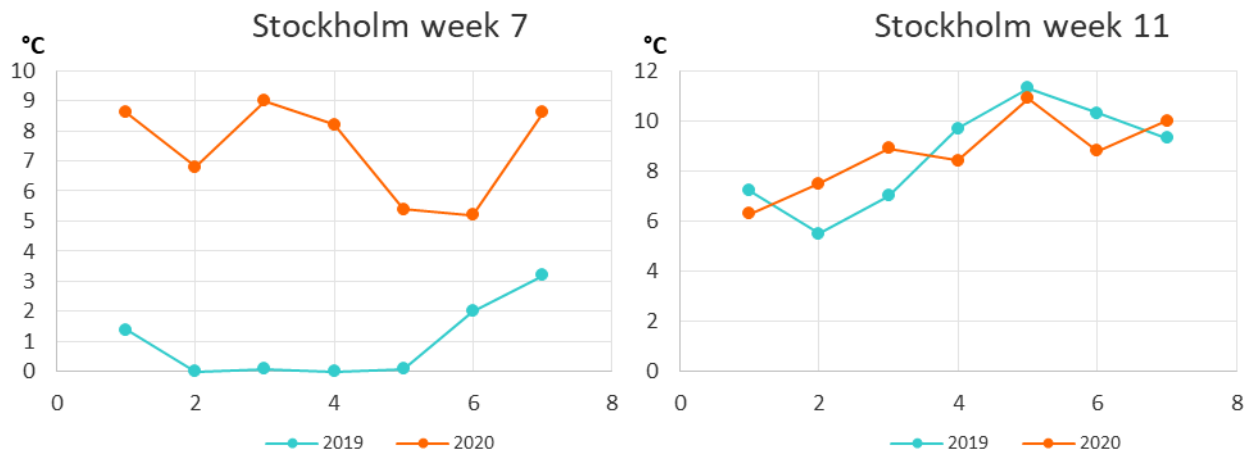


Figure 23 Temperature differences in week 7 and week 11 for Stockholm, Sweden.

Moreover, the total consumption has even increased in weeks almost two-thirds of the weeks.

With Sweden's different approach, it can be seen that the total load has not been as affected during the pandemic as much as it was in other analyzed countries. Furthermore, judging from the total load, their economy and industry have not suffered either.

4. RESULTS AND DISCUSSION

Analysis and data provided in chapter 3 indicate how sensitive a total load of a country is. A variety of external factors significantly affects the consumers' behavior, and thus, the electrical energy consumption. This paper focuses on the social dependent factor connected to the load – COVID-19 pandemic.

The most in-depth analysis was provided for the case of Croatia which is characterized by a very volatile total load. Although the weather-dependent factor is important and cannot be completely neglected, a detailed analysis of it was not provided for cases besides Croatia.

Initially, this paper was meant to include only Croatia and its region (surrounding countries). However, the case of Sweden is extremely interesting and useful for comparison and evaluation of what affects the load the most.

Results indicate that the COVID-19 pandemic caused significant load decrease throughout Europe which was foremost in the period of harsh working restrictions or lockdowns. Cases of Croatia, North Italy, Slovenia, Hungary, and Serbia all suffered a significant load decrease in comparison with previous years. The period of first COVID-19 appearance was similar and each of these countries started to introduce restrictive measures.

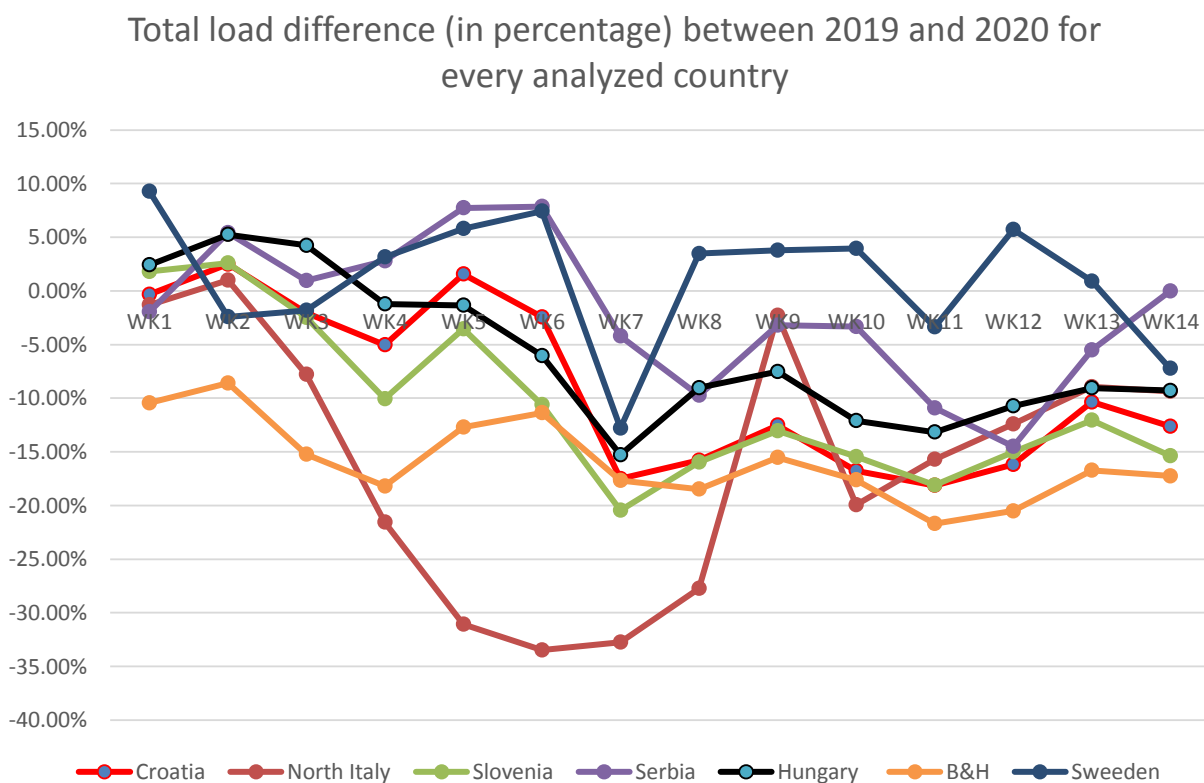


Figure 24. Comparison of total load differences between 2019. and 2020. for analyzed countries

A graphical display of the load difference of the three most interesting cases (Croatia, North Italy and Sweden) is provided in **Error! Unknown switch argument.** The highest load decrease was present in North Italy (up to 35% decrease in comparison with previous years), while Croatia, Slovenia, Hungary, and Serbia all experienced load decrease up to 15%. This only further confirms how strong the industry of North Italy is in terms of the load consumption as it drastically decreased in the period of harsh restrictions and lockdown. On the other hand, it can also be seen that a load of North Italy also has started recover significantly faster than the load of any other analyzed country which once again supports the premise that the industry has a significant share in the total load. Nevertheless, it must not be forgotten the influence of different dates and weeks 7 and 8 in 2019 and 2020 which partly contribute to such steep decline and rise while comparing those two years.

The rest of the countries in the region have also started to recover in terms of load, however, it is at a more moderate rate. For the case of Bosnia and Herzegovina it is rather difficult to provide the right judgement. The results of the analysis imply that they have not suffered a significant load decrease in comparison with previous year which can be somewhat expected due to their poor relative industry contribution in total load share and partly due to different holidays during weeks 7 and 8 comparing most of other countries. However, there are also uncertainties regarding the data.

Contrary to all of the 6 cases, Sweden has taken a completely different approach and introduced nearly no strict restrictions or lockdowns. Their total load is slightly fluctuating, and even increasing in some weeks. They had the highest number of COVID-19 positive cases (per 10 000 residents) of all 7 analyzed countries, and their numbers have not been declining either. This indicates that it is not the number of COVID-19 positive cases that directly and significantly affect the load, but the governmental measures that affect it the most.

Generally speaking, it is expected that the higher number of positive cases would force countries in such restrictive measures and lockdowns which will result in a significant load decrease. However, the case of Sweden proved to us that there are exceptions and that some countries deploy different national strategies. Hence, it is of the utmost importance to keep in track with all national decisions regarding the restrictions, strategies, or lockdowns measures when planning a day-ahead (or further) load.

Moreover, the analysis shows that there are a lot of similarities between countries in the region, especially the ones with similar industrial development. It can be useful to observe their overall situation regarding the load trend, however, it is dangerous to blindly replicate their strategies as it was shown that load is extremely sensitive to all external factors.

5. CONCLUSIONS

This paper clearly shows the complexity of load forecasting and how the stochastic behavior of many influential factors can significantly contribute to the shape of realized load curve. Although there are usually many more examples of a weather influence on the load shape, this particular example teaches us all how social influence can also be important. Its significance is even more influential due to several reasons:

- Such events like sudden pandemic spread and adequate lockdown measures like in those several weeks usually cannot be foreseen in a year ahead, a quarter ahead, or even a month ahead load forecasting process and as a such could be marked as “Black Swan” effect [15].
- Nevertheless, such rare cases with significant impact, no matter how rare they are, must never be underestimated, especially if they have already occurred several times in the history [16] and when contemporary power systems, economic systems, and the whole globalized society are vulnerable [17], [18] to such outbreaks and potential lock-down measures
- Consequences of such measures jeopardize lives and livelihoods [19] of most of the electricity customers and if the statement that “*emotion = energy in motion*” [20] is applied to all customers in a portfolio or a country, an electricity demand response can be significant, sudden and sometimes even long-lasting, usually depending on the economic strength of the observed country [21] or customer’s portfolio
- Such sudden electricity demand response has directly affected electricity prices [22] and the whole electricity sector [23] as well as the entire power sector [24].

Therefore, this case can be very useful for understanding the sensitivity of the load curve, its importance in vital technical and economic processes in the globalized world, and necessary adjustments to the “new normal” conditions [25] which might last for some time in the forthcoming future and affect most of the electricity customers.

6. REFERENCES

- [1] R. Čiviljak, A. Markotić, and I. Kuzman, "The third coronavirus epidemic in the third millennium: What's next?," *Croat. Med. J.*, vol. 61, no. 1, pp. 1–4, 2020, doi: 10.3325/cmj.2020.61.1.
- [2] S. Dodig, I. Čepelak, and I. Pavić, "AGE AND SARS-COV2 INFECTION," *Acta Med Croat*, vol. 74, pp. 135–144, 2020.
- [3] H. Cho, Y. Goude, X. Brossat, and Q. Yao, "Modeling and forecasting daily electricity load curves: A hybrid approach," *J. Am. Stat. Assoc.*, vol. 108, no. 501, pp. 7–21, 2013, doi: 10.1080/01621459.2012.722900.
- [4] Wikipedia, "Electric energy consumption." 2020, Accessed: Sep. 10, 2020. [Online]. Available: https://en.wikipedia.org/wiki/Electric_energy_consumption.
- [5] Wikipedia, "Load profile." 2020, [Online]. Available: https://en.wikipedia.org/wiki/Load_profile.
- [6] HOPS, "Daily Load," 2020. <https://www.hops.hr/en/daily-load> (accessed Sep. 10, 2020).
- [7] Entsoe, "Load data," 2020. <https://transparency.entsoe.eu/> (accessed Sep. 10, 2020).
- [8] Wikipedia, "Electrocardiography." Accessed: Sep. 10, 2020. [Online]. Available: https://en.wikipedia.org/wiki/Electrocardiography#cite_note-4.
- [9] E. Almehaie and H. Soltan, "A methodology for Electric Power Load Forecasting," *Alexandria Eng. J.*, vol. 50, no. 2, pp. 137–144, 2011, doi: 10.1016/j.aej.2011.01.015.
- [10] S. Ding, K. W. Hipel, and Y. guo Dang, "Forecasting China's electricity consumption using a new grey prediction model," *Energy*, vol. 149, pp. 314–328, 2018, doi: 10.1016/j.energy.2018.01.169.
- [11] A. Khosravi, S. Nahavandi, D. Creighton, and D. Srinivasan, "Interval type-2 fuzzy logic systems for load forecasting: A comparative study," *IEEE Trans. Power Syst.*, vol. 27, no. 3, pp. 1274–1282, 2012, doi: 10.1109/TPWRS.2011.2181981.
- [12] A. Khan *et al.*, "Forecasting electricity consumption based on machine learning to improve performance: A case study for the organization of petroleum exporting countries (OPEC)," *Comput. Electr. Eng.*, vol. 86, 2020, doi: 10.1016/j.compeleceng.2020.106737.
- [13] F. Kaytez, "A hybrid approach based on autoregressive integrated moving average and least-square support vector machine for long-term forecasting of net electricity consumption," *Energy*, vol. 197, p. 117200, 2020, doi: 10.1016/j.energy.2020.117200.
- [14] Vitec Software Group, "Model theory." Vitec, 2014, [Online]. Available: <http://viteceducandi.com/>.
- [15] Wikipedia, "Black swan theory." 2020, [Online]. Available: https://en.wikipedia.org/wiki/Black_swan_theory.
- [16] G. McGillivray, "Coronavirus is significant, but is it a true black swan event," 2020. <https://theconversation.com/coronavirus-is-significant-but-is-it-a-true-black-swan-event-136675> (accessed Sep. 20, 2020).
- [17] B. Gates, "The next outbreak? We're not ready," 2015. https://www.youtube.com/watch?v=6Af6b_wyiwl (accessed Sep. 20, 2020).
- [18] T. D. S. D. Show, "Bill Gates on Fighting Coronavirus." <https://www.youtube.com/watch?v=iyFT8qXcOrM>.
- [19] U. N. D. Programme, "Socio-economic impact of COVID-19." <https://www.undp.org/content/undp/en/home/coronavirus/socio-economic-impact-of-covid-19.html>.

- [20] authenticityassociates, “Emotions Are Energy : The bodymind connection and emotion.” <https://www.authenticityassociates.com/emotions-are-energy/>.
- [21] UNIDO, “Coronavirus: the economic impact,” 2020.
<https://www.unido.org/stories/coronavirus-economic-impact-10-july-2020>.
- [22] E. Ghiani, M. Galici, M. Mureddu, and F. Pilo, “Impact on Electricity Consumption and Market Pricing of Energy and Ancillary Services during Pandemic of COVID-19 in Italy,” *Energies*, vol. 13, no. 13, p. 3357, 2020, doi: 10.3390/en13133357.
- [23] IEA, “Covid-19 impact on electricity,” 2020. [Online]. Available:
<https://www.iea.org/reports/covid-19-impact-on-electricity>.
- [24] T. Bakovic, “The Impact of COVID-19 on the Power Sector,” 2020.
- [25] WHO, “COVID-19: ‘new normal,’” 2020.
<https://www.who.int/westernpacific/emergencies/covid-19/information/covid-19-new-normal>.

G0505

Integration of voluntary Flexibility at Runtime FlexA a Linear Flexibility Agent for Sector Coupled Energy Systems

Dr. Philipp Graf, Dr. Jan Jurczyk, Klaus Nagl

Consolinno Energy GmbH

Franz-Mayer-Straße 1, 93053 Regensburg/Germany

Tel.: +49(0)94146297-521

p.graf@consolinno.de, j.jurczyk@consolinno.de, k.nagl@consolinno.de

Abstract

Making flexibility of power plants on distribution grids available for resolution of congestions is one of the future challenges for smart grids. There is a development of understanding flexibility as a prognosis-based quantity ([1] 4.2). In Germany redispatch 2.0 (see novella of NABEG [2]) is a first step to integrate this concept in distribution grid operation. NABEG demands that forecasting and control for CHPs (KWK-Anlagen) and RESs (EEG-Anlagen) of installed electric power bigger than 100 kW is provided to the distribution system operator (DSO). In this non voluntary sense, the knowledge about future flexibility is of highly statistical nature. This seems to be a controllable problem with big powerplant portfolios. Nevertheless, flexibility on distribution grids is of highly local nature. In many cases only a small number of power plants can provide flexibility and the accuracy of forecasted values underlies a higher uncertainty.

The *FlexA process* suggested by the Consolinno Energy GmbH directly addresses this challenge. FlexA uses not only read and write access to current power generation or consumption, but also a minimal number of states needed to provide a linearized model of the actual energy system. It continuously provides schedules, which may be used as forecasts by the DSO and as set points for the energy system. In this manner the process *serves as a bridge between system automation of the power plant and the DSO*. It therefore maximizes the certainty of flexibility provided to the DSO. FlexA takes the role of the operational manager (Einsatzverantwortlicher) known from large scale power plants on the transmission grid and brings it as a fully automated software agent to the distribution grid.

FlexA models sector coupled energy systems based on electric, thermal and fuel energy flows connected to controllable and statistical prosumers and storage systems. There are two ways to integrate flexibility in the FlexA runtime process: *Contracts* and *price signals*. Runtime contracts ensure that FlexA keeps schedules stable in near future. This mechanism considers that energy suppliers may only sell energy at certain times of the day and therefore must assume schedules being stable in the meantime. External contracts allow partners to post preferred schedules and price signals allow for example spot price optimization or own consumption maximization.

FlexA continuously provides flexibility tables for external partners containing schedules together with positive and negative power and energy, which describe how much the system may deviate from the schedule at each time and for how long. In this way voluntary flexibility can be offered on platforms ([1] 4.2.2, [3] 1.2.2, [4] p.38/39). As a service for DSOs and TSOs these platforms aggregate flexibility and call the demands from system operators. Such calls are integrated by FlexA as external contracts. FlexA enables a fully automated communication between system operators and platforms. A similar approach could be realized with energy suppliers trading flexibility intra-day.

Architecture

Besides the separation of cloud and field level, the main principle of the FlexA architecture is the separation in small distinct services. This follows the software architecture paradigm of microservices. The microservices to be defined shall reflect different fields of expertise necessary to implement a FlexA service and guarantee maximum independence between the components.

Message Broker

The message broker is the central communication bus for life data. Typical IoT-communication protocols are for example mqtt or amqp. From the perspective of field devices, the message broker is “the cloud”, as it represents the data-end-point for their communication: The field devices send their metrics to the message broker and receive possible set point values from there. More precisely, the broker provides topics, in which messages may be queued. Services may publish messages to these topics or subscribe to these topics. In the sense of FlexA these topics must reflect all the telemetry- and control-data-end-points necessary to control an energy system. A tenant management must be implemented on the topics to control which services may publish or subscribe to which topics. The topics of the energy systems reflect then the current state of the energy systems.

Forecast services

The Forecast services provide prognosis for all statistical, this means not controllable data, in the energy system. FlexA needs forecasts for thermal and electric energies for all statistical producers and consumers. Then it matches demand and production using the controllable energies in an optimal way. The forecast services must provide forecasted data in predefined time windows and resolution.

Contract service

The contract service serves as an interface, where external partners may, after registration, publish their preferred schedules, which the energy system should try to realize on certain sensors. Requests for contracts are posted as time series. The contract service also must decide priority if competing request of different partners occur.

Price services

Price services may provide price forecasts, such as forecasts for epex prices, or integrate external pricing signals in runtime via an interface as time series. Nevertheless, the price services must transform or scale the price signals in such a way that the optimization service may understand them. This means that it must be possible to transform price signals to time series which may be put on flows to price each kWh of energy being transported at a certain time step.

Optimization service

The optimization service provides optimized schedules for energy systems, i.e. proposals for set point values. To do so, the optimization service processes an abstract configuration of the energy system as input considering pricing, contracts, forecasts, and initial energy

values. The optimization service unfolds the abstract configuration and parses it into an optimization problem understandable by a solver. The optimization may be done by linear optimization. The schedule optimization tries to fulfill contracts first and follows the price signals second.

Flexibility service

Like the optimization service, the flexibility service uses the abstract configuration of the energy system together with a schedule at the electric network transfer point, which FlexA *currently* tries to fulfil. The flexibility service calculates then at each time step the maximal positive and negative deviation from the schedule, the energy system may provide. More precisely, the flexibility service returns a table with columns: “schedule”, “power_plus”, “energy_plus”, “price_plus”, “power_minus”, “energy_minus”, “price_minus”. “power_plus” gives the power in kW the system may deviate in positive direction from the schedule at a timestep, whereas “energy_plus” gives the corresponding energy, which may be provided by schedule deviation. “price_plus” is the price in say €/kWh. In other words, the table gives the information how much and how long the system may deviate from the schedule at given time steps. The flexibility table may be communicated to external partners, who may then request the offered flexibility from the contract service.

Digital twin service

The digital twin service is the central service coordinating the optimization of the energy system in runtime. The digital twin service has the task to build up the abstract configuration of the energy system and to publish it. Therefore, the digital twin must collect the current forecasts, prices, and contracts as well as the initial values of the energy system. Moreover, it has the task to generate runtime contracts for the stabilization of schedules in the nearer future. This means for example that a schedule of a chp shall not deviate from the former schedule in the next say two hours. The digital twin service should be configured by an abstract schema file of the energy system. Beside the system configuration, this schema must also contain the necessary configuration of the runtime environment: length of the time window of the schedules, time grid of the schedules, runtime contracts, frequency of optimization. In this way the whole stack of the FlexA service may be generated by a script for each individual energy system.

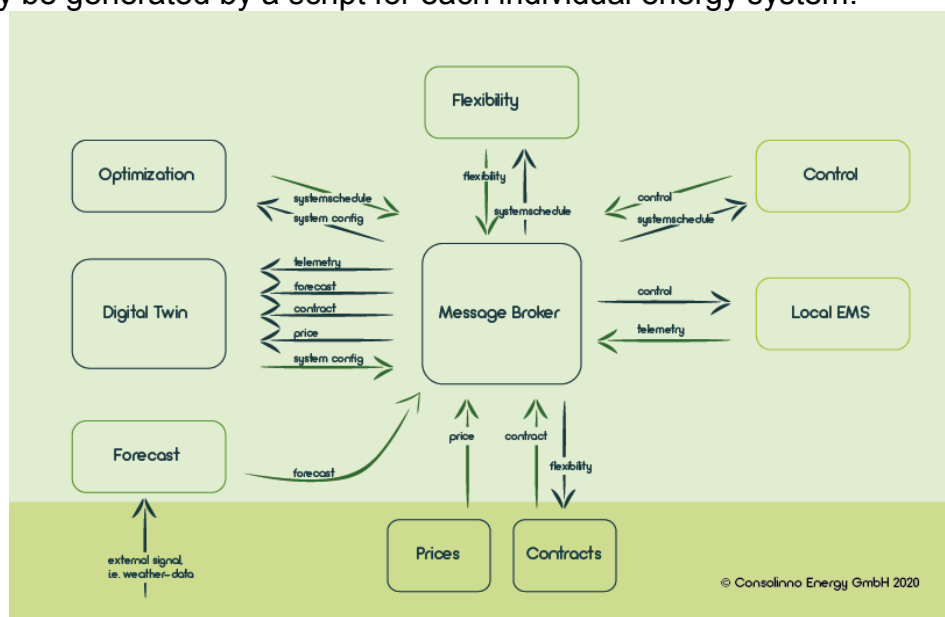


Illustration 1: Microservice communication of FlexA via topics on message broker

Modelling

The modelling describes the implementation of the optimization service as well as the definition of the abstract configuration of the energy system. There are several object-oriented frameworks for linear optimization of energy systems available, such as OEMOF for python [6]. OEMOF is based on modelling optimization problems of energy systems by means of energy flows. It is therefore very suitable for the modelling of the optimization service as described above.

Abstract Configuration of the energy system

The abstract configuration of the energy system contains all devices and flows, which are necessary to model the energy system. On flows variable prices may be put as time series as well as maximal power flow constraints. Devices are defined by their parameters, such as maximum power and electrical efficiency for a combined heat and power plant (chp) or current energy and maximum energy for storage systems. Moreover, devices representing statistical producers or consumers are defined by power forecast in the form of time series. Contracts are put on devices as time series.

Flow and energy conservation modelling

Energy conservation is defined on each device. This means, that on each device and on each time step the sum of energies flowing to the device must equal the energies flowing away from the device. In this manner flow constraints may be considered and via putting prices on flows optimization may find the optimal power flow. The optimal power flow gives than the optimized schedules.

Constraint modelling

Devices are modelled as linear energy transformers. This means, that a chp transforms on each time step according to its parameters a certain amount of fuel provided by an energy flow to a certain amount of thermal and electric energies, which must be consumed by flows. Devices, even if controllable, may often be modulated in a certain power range. The linear model must take this into account by using binary variables. Statistical producers provide a fixed energy value at each time step, which must be consumed by a flow, similarly for consumers. These energy conservations are modelled as hard constraints and may therefore yield unsolvable optimization problems. Therefore, artificial sources and sinks need to be added to the systems providing energy flows at very high costs to ensure solvability. Similarly, external and runtime contracts are modelled as soft constraints on the electric production of devices. This means that deviation from a contract in L1-Norm is punished with high costs. "High" means that these cost terms are set significantly higher than "real" flow costs.

Flexibility modelling

Flexibility is modelled on the electric flows at the electric network transfer point. At a given time step the optimization tries to maximize the deviation and to hold it constantly as long as possible. This means, that the flexibility service will maximize deviated energy as an "energy block".

IoT-Connection to the local EMS

The system architecture interprets FlexA as a cloud service. This means that FlexA is not a replacement of the energy management system (EMS) on field level. FlexA offers forecast based optimization with help of a simple model and a minimal number of data-endpoints to be implemented. The communication with the EMS of the actual energy system on field level works is implemented via the messaging broker.

Data normalization service

In the ideal case the local EMS already talks to the cloud with the corresponding cloud protocol (for example mqtt) and uses the topics and payloads as explained above. But most of the time this will not be the case and there will be the need to integrate energy systems in the sense that a data normalization service has to be implemented translating the communication to a cloud protocol as exemplary defined above.

Requirements for the local EMS

For the FlexA service to work the local EMS must provide the described telemetry data in order to build up a linear model. This must be done by a cloud integration as described above. The EMS must then integrate external set point values for devices to be scheduled optimally. This integration of set point values is not meant in a sense, that the FlexA service may just override the set point value of the local EMS. This may cause a disturbance of the operation by conflicting signals. The local EMS should be able decide whether it executes an external schedule with respect to internal constraints (minimal runtimes and downtimes etc.) to ensure a smooth operation. On the other hand, FlexA already should try to respect such constraints by modelling them as runtime contracts or hard constraints for the devices.

Conclusion

The FlexA service as described above is a modular software stack to realize optimization and to provide flexibility of complex energy systems in a scalable way. FlexA has been deployed on chps by the authors optimizing day-ahead scheduling. The FlexA service is running reliably and operational corrections by the local EMS are only necessary on connection loss to the FlexA service due to rolling updates of schedules. The integration of contracts in runtime has been tested within CsellS [4],[5]. Nevertheless, there are several obstacles to efficiently stabilize electric grids with FlexA services. The integration of existing energy systems is a major task, as the implementation of data normalization services and the compatibility with the local EMS must be considered. The streamlining of this integration process seems to be the most important task for those to offer flexibility services. Moreover, interfaces for offering and requesting flexibility as well as the corresponding processes must be standardized. In Germany, this problem is tackled in the project Connect+ [7]. Connect+ tries to standardize the communication of schedules and flexibility between DSO, TSO, and the operational manager of the system. Connect+ tries to provide a modern framework where redispatch may be performed on the distribution grid level in a fully automated manner. FlexA can then be used as the service enabling the operational manager to provide fully automated redispatch transactions. But this only considers integration of voluntary flexibilities with respect to a fixed given schedule. FlexA still may optimize the initial scheduling process offering the possibility to adjust production and demand. This potential is still free for the market to be used.

Bibliography

- [1] Flexibility in the electricity system, Bundesnetzagentur,
https://www.bundesnetzagentur.de/SharedDocs/Downloads/EN/Areas/ElectricityGas/FlexibilityPaper_EN.pdf
- [2] Netzausbaubeschleunigungsgesetz Übertragungsnetz, www.gesetze-im-internet.de/nabeg
- [3] Dank Schwarmintelligenz und einer smarten Servicewelt in der Energiewirtschaft zum Stromnetz der Zukunft, K. Nagl u. P. Graf, published in Realisierung Utility 4.0 Band 2, Hrsg. Oliver Doleski, Springer Vieweg 2020
- [4] C/sells-Community das Magazin, Ausgabe 2019,
https://www.sinteg.de/fileadmin/media/Publikationen/Schaufenster-Publikationen/csells_magazin_2019.pdf
- [5] <https://www.tennet.eu/de/news/news/intelligenztest-fuer-das-stromnetz-der-zukunft/>
- [6] <https://oemof.org/>
- [7] <https://netz-connectplus.de>

G06

Operation and enabling technologies I

G0603

Active Distribution Grid Management – a decentralized approach for the management of flexibility options

Michael Merz

PONTON GmbH

Dorotheenstr. 64, 22301 Hamburg/Germany

Tel.: +49 40 866 275 341

merz@ponton.de

Abstract

Facing the energy transition, decentralized renewable sources of energy as well as decentralized consumers can lead to congestion situations both horizontally at the transmission grid level and vertically within the areas of distribution grids.

Grid-supportive flexibility is a solution to mitigate such congestions. In order to roll-out a standardized process for congestion management, Austrian DSOs (distribution system operators) conducted the project Active Distribution Grid Management (ADGM) in early 2020 in order to test if the existing data communication infrastructure can be re-used to offer and activate flexibility, to simulate typical congestion scenarios, and finally to visualize the impact on involved asset managers and grid operators.

This paper presents the ADGM project results and how it is applied to a distribution grid congestion scenario. It specifically shows how a distributed flexibility management process is implemented.

Introduction

Facing the energy transition, decentralized renewable sources of energy as well as decentralized consumers will lead to congestion situations both horizontally at the transmission grid level and vertically within distribution grids.

Grid-supportive flexibility is a solution to mitigate such congestions. In order to roll-out a standardized process for congestion management, Austrian DSOs (distribution system operators) conducted the project Active Distribution Grid Management (ADGM) in early 2020 in order to test if the existing data communication infrastructure can be re-used to offer and activate flexibility, to simulate typical congestion scenarios, and finally to visualize the impact on involved asset managers and grid operators.

There are various ways to organize the allocation of flexibility – many are market-based such as Enera [1], GOPACS [2] or NEW 4.0 [3], using a central or decentral platform to match orders between producers and consumers of flexibility. Others are based on bilaterally offering flexibility to the local DSO as being currently implemented in Germany, following the Redispatch 2.0 model, which is, in turn, based on the NABEG legislation [4] (Grid Expansion Acceleration Act, German: Netzausbaubeschleunigungsgesetz).

From an Austrian perspective, it is important to address the requirement for a market-driven allocation of flexibility as 100% of the energy production will be renewable by the year 2030, at least balance-wise (this is the target of the Austrian “Mission 2030”). The Austrian way, as it is foreseeable today, follows first a decentralized approach, similarly to Redispatch 2.0, but allows, secondly, also the trading of flexibility on a market platform.

The rationale for the ADGM project is to explore the process, data formats, data exchange protocols, and scenarios for the interaction between asset operators (also called FSP – Flexibility Service Providers), DSOs and the TSO.

This paper reports on the results of the project and is organized as follows: In section 1, the ADGM process is described. Section 2 focuses on the technical set-up for the project itself plus the existing EDA data communication infrastructure [5], which is re-used by ADGM. Section 3 introduces a simplified grid modelling language while Section 4 finally presents a simulation scenario together with the visualization of the data exchange and activation of flexibility.

1. Flexibility Offering and Activation Process

The offering and activation of flexibility is performed in the following way: On the day prior to delivery (D-1) FSPs from the production and consumption side submit their asset production schedules to their respective DSO. At the same time, the simulation sets the demand for flexibility for both DSOs and TSO, expressed by a demand schedule. This is created on D-1 as well for each grid operator.

For the processing of the offered flexibility, a cycle may be defined for data processing, e.g., 2 or 4 hours. On the delivery day, this cycle is used to process submitted data in order to calculate the activation for the ahead period. As an example, using a 2-hour cycle, the target period 14:00 – 16:00 is calculated at 12:00h. Flexibility that is offered intraday prior to this cut-off time can still be used for the target period.

Whenever a DSO calculates the target period, the own flexibility demand, grid restrictions and available flexibility from FSPs is used to determine the volume required per 15 minute

period within the grid area of the DSO. Any further volume that is not required by a DSO is forwarded to the next-higher grid operator as an anonymized merit order list (MOL).

The TSO, as the operator of the highest level in the grid hierarchy, calculates the own demand for flexibility, also based on the own grid restrictions, and maps it against the MOLs received from underlying DSOs. As a result, the TSO sends an activation message back to each DSO from which flexibility is requested. The latter aggregate demand for flexibility of the TSO and of their own and finally send an activation message to the selected FSP.

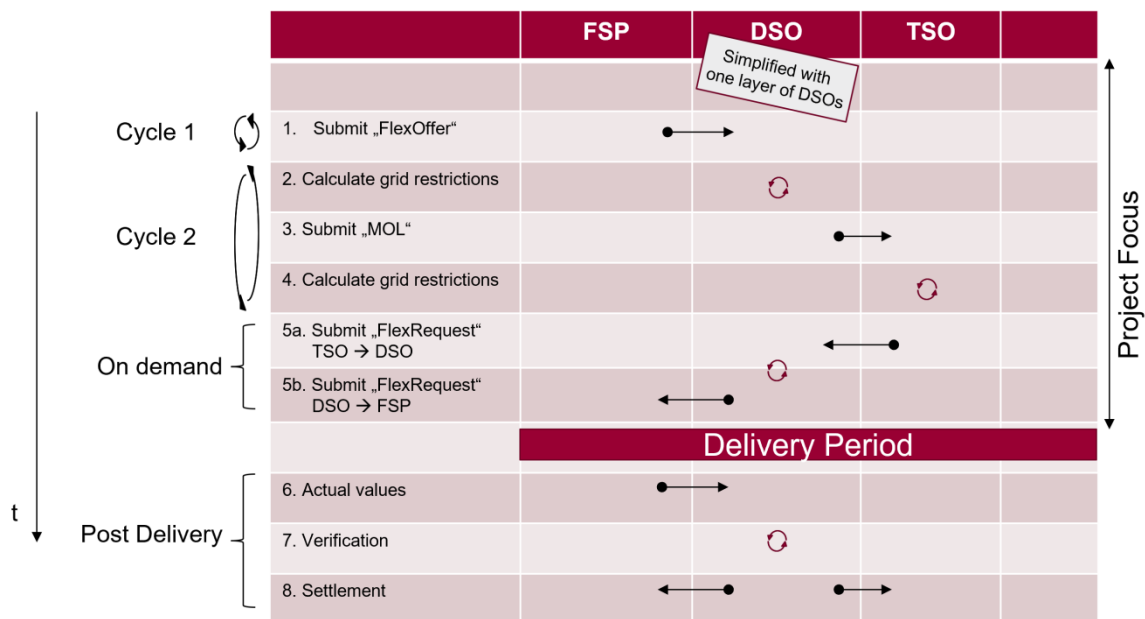


Figure 1: Process Model

2. Technical Setup

The ADGM project builds upon the existing EDA infrastructure. EDA stands for “Energy Data exchange in Austria” which represents the general interoperability layer for a range of Austrian market processes. Originally, EDA was established in the year 2012 to provide a unified, standardized, and decentralized data communication infrastructure for the supplier switching process. As the regulator demanded, a switching process had to be accomplished within 12 business days, while the individual message transfer between process participants had to be accomplished within 5 seconds. So a reliable data communication service was introduced that allows for interoperability between a large number of participants and processes.

In turn, this required a standardized end-to-end communication with full digitalization and process automation. EDA has addressed this by using exactly the same communication endpoints for all participants in the entire energy sector, including TSO, DSOs, suppliers, customers, and many other market roles. Thanks to the high level of standardization, EDA allows for over 99 percent of the switching processes to be accomplished within seconds.

In case of EDA, there is no tight link between a given functional process layer (such as “supplier switching”) and the communication layer. I.e., the EDA communication infrastructure can be re-used for any other business process. This helps minimizing the implementation cost for new processes such as, e.g., the management of flexibility.

For this reason, EDA could easily be utilized for any data exchanged in the ADGM process model described above: Each simulated player uses an EDA communication endpoint as

illustrated in Figure 2. As part of the ADGM project, only the role-specific, functional logic of the FSP, DSO and TSO needed to be implemented. In addition to interacting through the EDA infrastructure, all participants reported monitoring data to a further participant, the Visualization Server. This is used to collect, synchronize, and illustrate input data from all process participants.

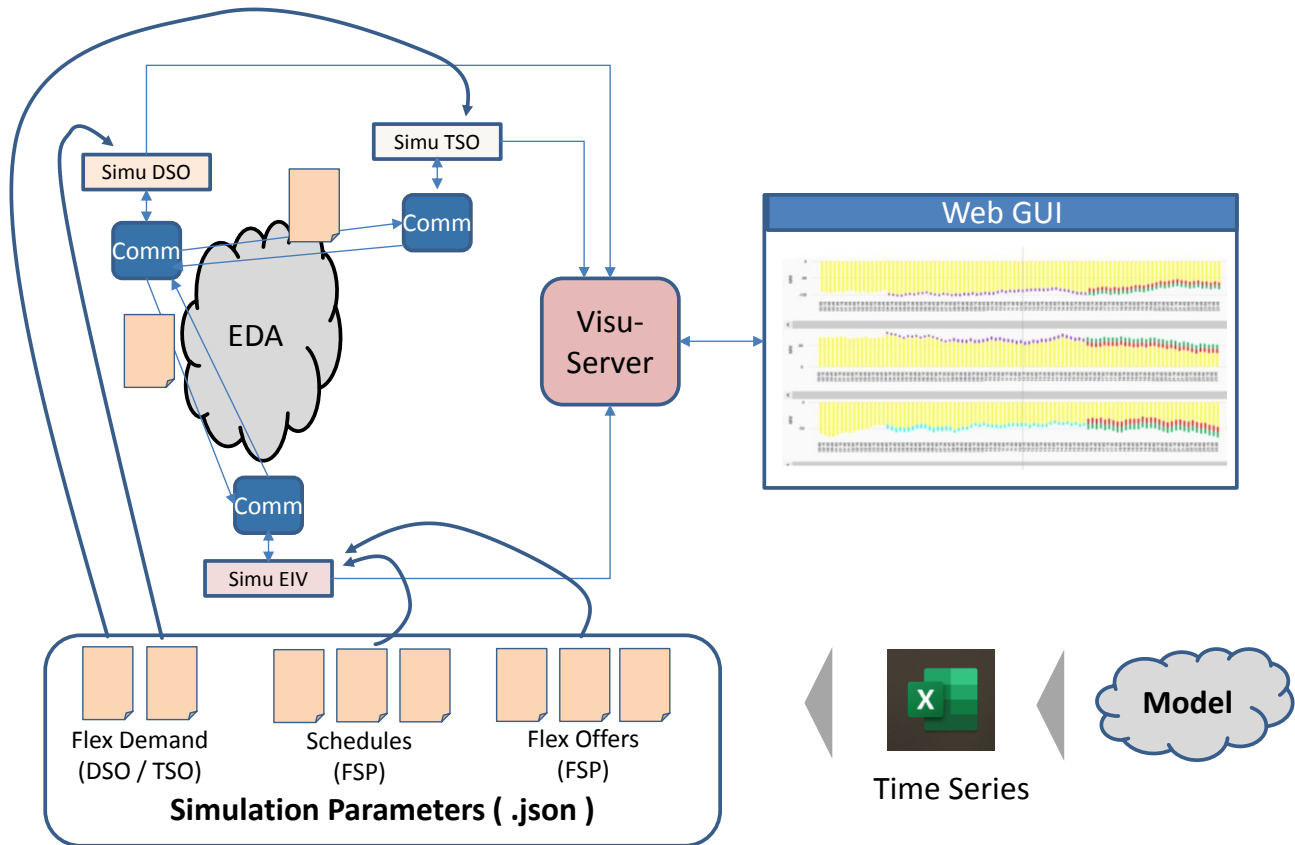


Figure 2: Technical Setup

Whenever a message is exchanged between process participants, it is also copied to the visualization server, leading to an update of the status display for available and demanded flexibility for the given time interval.

The simulation project allows to set parameters for all types of time series involved: Production schedules, flexibility demand and supply curves. With these parameters, any congestion situation can be defined at any location in the simulated grid. Time series are defined using an Excel sheet that is transformed into schedules represented in the JSON format.

3. Simplified Grid Modelling Language

The interconnection of participants is described using a simplified grid modelling language. This language has been developed to model

- the grid hierarchy of the TSO and DOSs with its basic resources,
- the connection of production and consumption assets within the grid topology, and
- the sensitivity of assets. Production / consumption may have a different impact on grids as distribution grids and assets at the 110 kV layer may be connected through redundant lines to the transmission grid – this is called sensitivity.

Usually, a grid modelling language such as GGM (Common Grid Model) and its exchange format CGM-ES (CGM Exchange Standard) [6] could be used for the ADGM project.

However, as the runtime was only four months, we preferred to develop an own, simplified language with still provides enough expressive power so that the modelled grid and its participants could be sufficiently described.

This simplified grid modelling language is used to define the following building blocks:

- “Lines”, representing lines at the different grid layers.
- “CPs”, representing vertical or horizontal connection points that form a grid hierarchy out of individual lines. In order to model congestion flows, the TSO grid is separated into horizontal lines which are also connected through a connection point. Alternatively, a connection point links a lower grid element to a higher one.
- “Assets” (producers and consumers) are linked to a line in the grid hierarchy.
- Should a distribution grid be connected to more than one TSO line, the sensitivity needs to be defined as well per connection point. As can be seen from Figure 3, the impact of the left 110 kV grid towards the left UHVG line is 30% and towards the right is 70%.
- TSO / DSOs. The operator of a grid is attached to a Line element. Naturally, it is the TSO attached to the two UHVG lines, while DSOs are attached to distribution grid lines. If a high-level DSO is attached to a 110 kV line without any further DSOs being attached to subordinated lines, then all subordinated distribution grids are controlled by this DSO. In all (more realistic) other cases, subordinated grid layers may be controlled by second- or third-level DSO. If these exist, they are just attached to the lower grid such that a hierarchy of multiple DSOs can be formed.

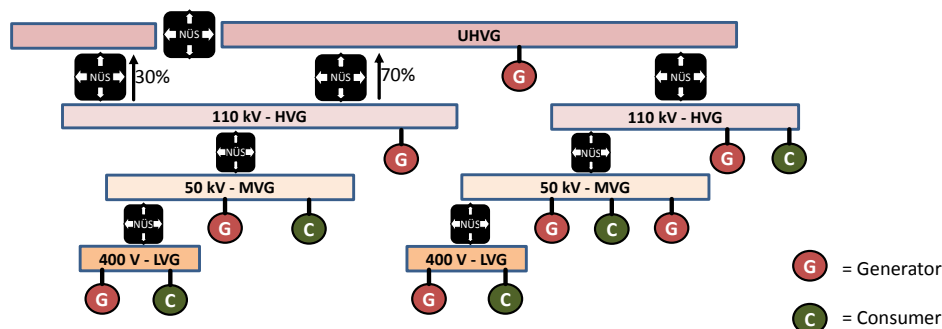


Figure 3: Simplified Grid Model

The grid layout displayed in Figure 3 is constructed from a list of definitions as the following example shows:

```
GridTopology {
  Name = „UpperAustria“;

  Line { Name „APG-East“; Type „UHVG“ }
  Line { Name „APG-West“; Type „UHVG“ }
  Line { Name „Steyr“; Type „HVG“ }
  Line { Name „Gmunden“; Type „HVG“ }
  Line { Name „Kremsland“; Type „MVG“ }
  Line { Name „Donauland“; Type „MVG“ }
  Line { Name „Neuhofen“; Type „LVG“ }
  Line { Name „Hinterhofen“; Type „LVG“ }

  TSO {Name „APG“ Line „APG-East“ }
  TSO {Name „APG“ Line „APG-West“ }
  DSO {Name „Netze OÖ“ Line „Steyr“ }
  DSO {Name „Netze OÖ“ Line „Gmunden“ }
  DSO {Name „Netze NÖ“ Line „NÖ“ }
  DSO {Name „Netze Steiermark“ Line „Steiermark“ }
  DSO {Name „Netze Neuhofen“ Line „Neuhofen“ }
```

```

CP { Name "APG-East-APG-West"; Line "APG-West"; Line "APG-East" }
CP { Name "APG-Steyr-East"; UpperGrid "APG-East"; LowerGrid "Steyr" }
CP { Name "APG-Steyr-West"; UpperGrid "APG-West"; LowerGrid "Steyr" }
CP { Name "APG-Gmünden"; UpperGrid "APG"; LowerGrid "Gmünden" }
CP { Name "Steyr-Kremsland"; UpperGrid "Steyr"; LowerGrid "Kremsland"
Sensitivity { APG-Steyr-West; 0,3 } Sensitivity { APG-Steyr-East; 0,7 } }
CP { Name "Gmünden-Donauland"; UpperGrid "Gmünden"; LowerGrid "Donauland" }
CP { Name "Kremsland-Neuhofen"; UpperGrid "Kremsland"; LowerGrid "Neuhofen" }
CP { Name "Donauland-Hinterhofen"; UpperGrid "Donauland"; LowerGrid "Hinterhofen" }

FlexProvider { Name = "BigCoalPlant"; Line "APG-West" Type „Producer“}
FlexProvider { Name = "Voest Alpine"; Line "APG-East" Type „Consumer“}
FlexProvider { Name = "HydroPlant1"; Line "Kremsland" Type „Producer“}
FlexProvider { Name = "HydroPlant2"; Line "Gmünden" Type „Producer“}
FlexProvider { Name = "GasPlant"; Line "Steyr" Type „Producer“
    Sensitivity {APG-Steyr-West; 0,3 } Sensitivity {APG-Steyr-Ost; 0,7 } }
FlexProvider { Name = "BiogasPlant"; Line "Donauland" Type „Producer“}
FlexProvider { Name = "Battery-1"; Line "Kremsland" Type „Prosumer“}
FlexProvider { Name = "Battery-2"; Line "Neuhofen" Type „Prosumer“}
FlexProvider { Name = "Bäcker Huber"; Line "Neuhofen" Type „Consumer“}
FlexProvider { Name = "Biogas Bauer Bunge"; Line "Hinterhofen" Type „Producer“}
FlexProvider { Name = "Elektrolyseur Erwin Egenhofer"; Line "Kremsland" Type „Consumer“}
}

```

4. Simulation Run

In the course of the ADGM project, a couple of simulations have been performed. Some of them focused on horizontal congestions at the transmission grid level and the possibilities to help mitigate them from a DSO's perspective. The simulation presented falls in the category of a vertical congestion, it is characterized by a high load from decentralized production at the lower grid layers. As means for mitigation there are various possibilities given:

- Increase local consumption close to the affect grid layers,
- Decrease production in the grid layers,
- And/or involve the TSO to support with flexibility activated at locations beyond the distribution grid.

The following Figure shows a vertical grid hierarchy with anonymized identifications:

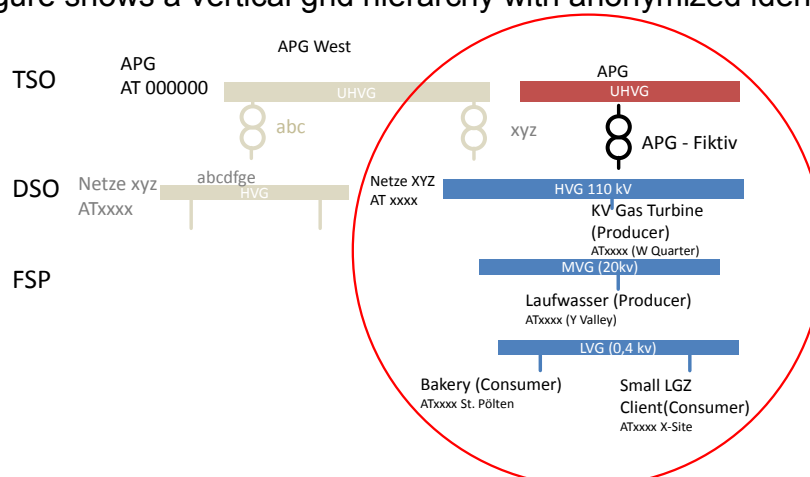


Figure 4: Simulation of a vertical Congestion

The following daily cycle visualizes the congestion situation and measures to mitigate it:

- Early in the morning, there is demand for redispatch to increase production (green DSO curve between 10:00 and 12:00). This leads to the activation of positive flexibility (displayed in violet color), offered by the two FSPs AT002001 and

- AT002002. The offered flexibility has been requested by the DSO at 08:00 in the morning.
- Around noon, there is demand on the TSO side to reduce production. Different offers from FSPs are available as they have been sent from the DSOs to the TSO as a MOL. Consequently, the TSO requests its demand of 1 MW for four 15 minutes intervals from the DSO, which, in turn, activates FSP AT002001 (displayed as reduced production in light blue color).
 - For the afternoon, positive flexibility is requested again by the DSO and activated at both FSPs (violet bars).
 - The time interval after 18:00 is not yet covered by the process as this is still more than one cycle ahead of the simulated time. Flexibility offers are still available here (green for positive and red for negative flexibility).

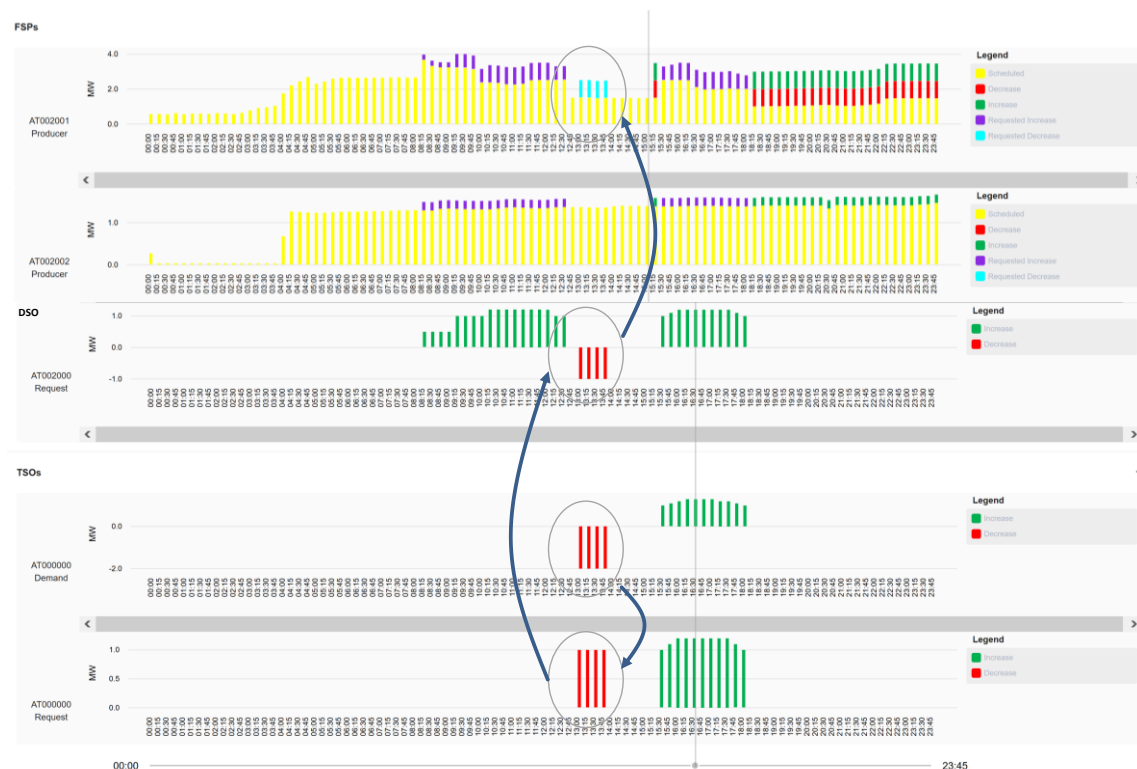


Figure 5: Simulation output

5. Conclusions

The main gain in knowledge of the ADGM project lies for the involved grid operators in the following points:

1. The existing EDA infrastructure can be re-used for the process of flexibility management in a decentralised manner without any severe adaptation effort.
2. The chosen process is capable to let FSPs offer their flexibility for day-ahead or intraday time intervals and to let grid operators decide on the selection and usage of flexibility based on the location, volume and price of the given offers. The cycle interval can be flexibly adjusted.

For PONTON, the project delivered valuable insights in how flexibility offers and activations can be efficiently and securely exchanged between market participants and grid operators. It was also insightful to simulate the activation of flexibility based on a grid model which has a drastically reduced complexity compared with CGMES, but which is sufficiently flexible to model various congestion situations.

As a next step, Austrian grid operators may apply the gained knowledge to advance a common standard process for flexibility management across all grid layers and possibly also with partnering EU member states.

An interesting extension would also be to intensify a market-based redispatch mechanism which applies within the given cycles of two or four hours: As soon as the allocation for a cycle is finalized, market participants may continue to offer and activate the trading of flexibility in a way that is known from the spot market, i.e., on a quarter-hourly basis.

References

- [1] ENERA project website: <https://projekt-enera.de>
- [2] GOPACS project website: <https://gopacs.eu>
- [3] NEW 4.0 project website: <https://www.new4-0.de>
- [4] NABEG (Netzausbaubeschleunigungsgesetz):
<https://www.netzausbau.de/EN/home/en.html>
- [5] EDA project website:
<https://oesterreichsenergie.at/energiewirtschaftlicher-datenaustausch.html>
- [6] CMGES – Common Grid Model Exchange Standard
<https://www.entsoe.eu/digital/cim/cim-for-grid-models-exchange>

G07

Operation and enabling technologies II

G0701

Options for the Implementation of Fast Control Reserves in the Continental European Power System

**A. Stimmer, M. Lenz, M. Froschauer, M. Leonhardt (1),
W. Gawlik, C. Alacs, C. Corinaldesi, G. Lettner, Y. Guo, J. Marchgraber (2),
A. Anta (3), K. Oberhauser (4)**

(1) Austrian Power Grid, Wagramer Straße 19, AT-1220 Vienna

(2) Technical University Vienna, Gusshausstraße 25, AT-1040 Vienna

(3) Austrian Institute of Technology, Giefinggasse 2, AT-1210 Vienna

(4) Verbund Hydro Power, Europaplatz 2, AT-1150 Vienna

alexander.stimmer@apg.at

Abstract

Increasing penetration of power electronics interfaced generation (PEIG) raises several challenges for the operation, control and protection of power systems. Due to the rapid transition towards renewable energy sources (RES) based power systems, conventional generation facilities using synchronous generators (SG) tend to be “out of merit”. The associated reduction of SG based generation leads to a decreasing network time constant (T_A), which corresponds to the overall inertia in the system. Contrary to SG based generation, which provides inertia to the system inherently and therefore effectively counteracts large gradients in the system frequency (rate of change of frequency, RoCoF), PEIG by default do not provide inertia. As a result, power systems will become more prone to frequency instabilities as conventional frequency containment reserves (FCR) will not be able to stabilize the frequency in the event of a sudden power imbalance. In order to address future frequency stability problems different long- and short-term mitigation measures exist.

This paper investigates options for the implementation of fast control reserves in the Continental European (CE) power system, which are being developed and examined within the frame of the R&I project *Advanced Balancing Services for Transmission System Operators* (ABS4TSO).

In the first part of this paper, the fast control reserve concepts *FCR+*, *Enhanced Frequency Response* (EFR), *Synthetic Inertia* (SI) and *Fast Active Power Injection* (FAPI) are described. Furthermore, their impact on the frequency stability is evaluated based on a simulation model of the CE power system, considering a reference incident (imbalance) equal to 3 GW as defined in the System Operation Guideline.

In the second part of this paper, the fast control reserve concepts are evaluated with regard to market and regulatory aspects. The pros and cons of the different implementation options are presented and a possible implementation roadmap is shown, based on current observations, future scenarios and simulation results of the CE power system.

Keywords: Fast Control Reserves, Enhanced Frequency Response, Synthetic Inertia, Fast Active Power Injection, Frequency Containment Reserves, Balancing services

Introduction

Historically, power systems are primarily based on conventional generation facilities, which feed into the grid via synchronous generators (SG). SG possess a rotating mass that helps to limit large gradients in the system frequency (rate of change of frequency, RoCoF) in case of sudden power imbalances in the system. However, recent trends show a decrease of the share of conventional generation facilities and an increasing penetration of power electronics interfaced generation (PEIG) [1] [2]. Unlike SG, PEIG do not inherently provide inertia, unless they are operated under specially designed control schemes. This trend leads to a decrease of the network time constant (T_A), which is a measure for the overall inertia in the system. As a result, power systems will become more prone to frequency instabilities [3] and the question arises, whether the conventional frequency containment reserves (FCR) will be sufficient to adequately stabilize the frequency in the future.

Figure 1 shows simulated frequency curves for a simplified model of the Continental European (CE) power system, considering the “CE Design Hypothesis” [4] and conventional FCR for different values of T_A but not taking into account further emergency functionalities of the power system such as shedding of industrial loads or pumps above 49 Hz. For values of $T_A < 10$ s the frequency drops below the dynamic security limit of 49.2 Hz, if the power imbalance is equal to the reference incident of 3 GW, as defined in the System Operation Guideline [5]. For values of $T_A < 6$ s the frequency drops below 49 Hz, which is the current limit for load shedding in the CE power system. Since such values of the network time constant are likely to occur in the future, different long- and short-term mitigation measures should be considered.

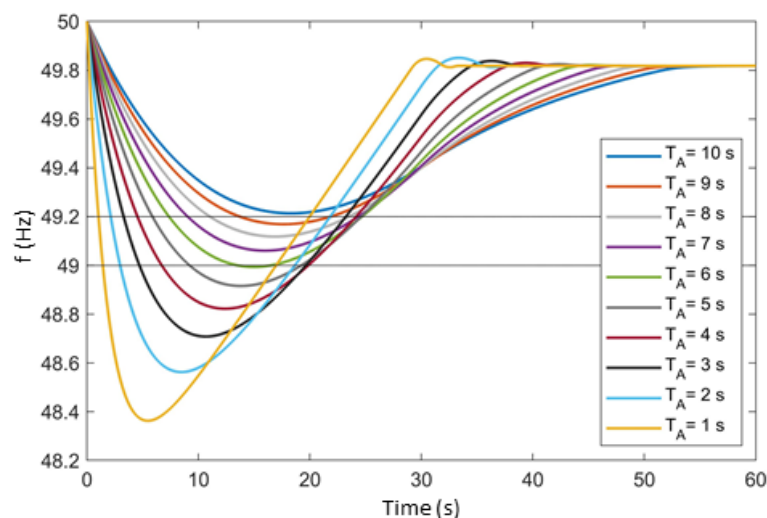


FIGURE 1: SIMULATED FREQUENCY CURVES FOR DIFFERENT NETWORK TIME CONSTANTS (SYSTEM SIZE = 150 GW, SELF-REGULATING EFFECT OF THE LOADS = 1 %/Hz, POWER IMBALANCE = 3 GW)

The aim of this paper is to investigate and summarize options for the implementation of fast control reserves in the CE power system, which are developed and examined within the frame of the R&I project Advanced Balancing Services for Transmission System Operators (ABS4TSO) [6].

1. Development and evaluation of fast control reserve concepts

This section theoretically describes four novel fast control reserve concepts: *FCR+*, *Enhanced Frequency Response* (EFR), *Synthetic Inertia* (SI) and *Fast Active Power*

Injection (FAPI). Firstly, the frequency and time characteristic curves as well as the range of the related parameters are defined. The influence of these parameters is investigated by means of a single-area simulation model (MATLAB/SIMULINK) of the CE power system. A reasonable range for each parameter is selected with regard to technical feasibility considerations and finally a base value is chosen after conducting a sensitivity analysis. In addition, the effectiveness and technical aspects of the different fast control reserve concepts are evaluated.

FCR+ and EFR

FCR+ and EFR are both designed to be activated proportional to the frequency deviation. FCR+ is intended as part of the already existing FCR (3 GW) but is activated significantly faster than conventional FCR, which have to be fully activated within 30 s in the CE power system [5]. Accordingly, the current FCR would be separated into conventional FCR and FCR+. Contrary to FCR+, EFR in this paper is intended as an independent fast control reserve that is only activated at a frequency deviation of more than ± 200 mHz. Accordingly, EFR would be added to the already existing FCR. The corresponding characteristic curves and parameters of FCR+ and EFR are shown in Figure 2 and Figure 3.

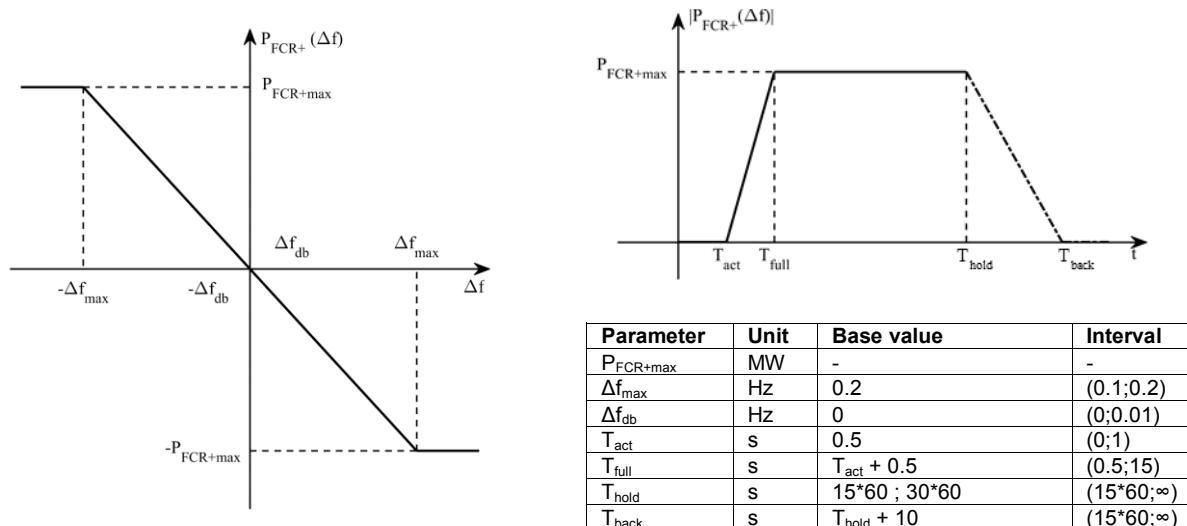


FIGURE 2: CHARACTERISTIC CURVES AND PARAMETERS OF FCR+

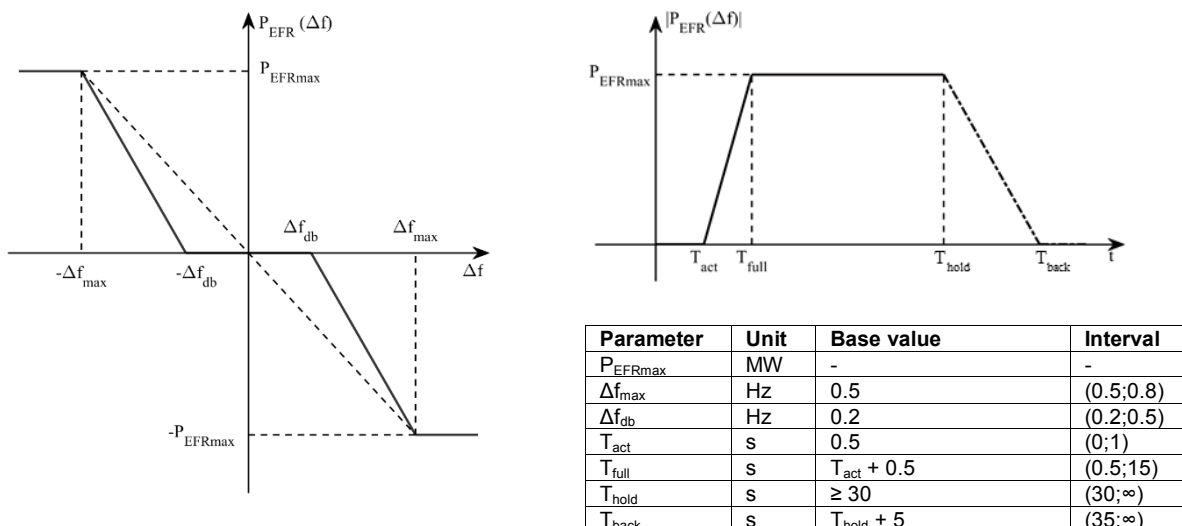


FIGURE 3: CHARACTERISTIC CURVES AND PARAMETERS OF EFR

SI

SI is intended to emulate an inertial response through a change in power, dependent on the RoCoF (passive synthetic inertia [7]). The corresponding characteristic curves and parameters of SI are shown in Figure 4. SI power is activated whenever both the frequency deviation and RoCoF are outside their respective deadbands Δf_{db} and $(\Delta f/\Delta t)_{db}$. The activation dynamics of SI are based on a first order behavior. Since a number of PEIG already try to emulate an inertial response provided by SG, their behavior may be altered by modifying their control scheme in order to improve its effectiveness. One option to achieve this is to implement a zone-selective control of SI, dependent on both the frequency deviation (Δf) and the RoCoF ($\Delta f/\Delta t$) [8].

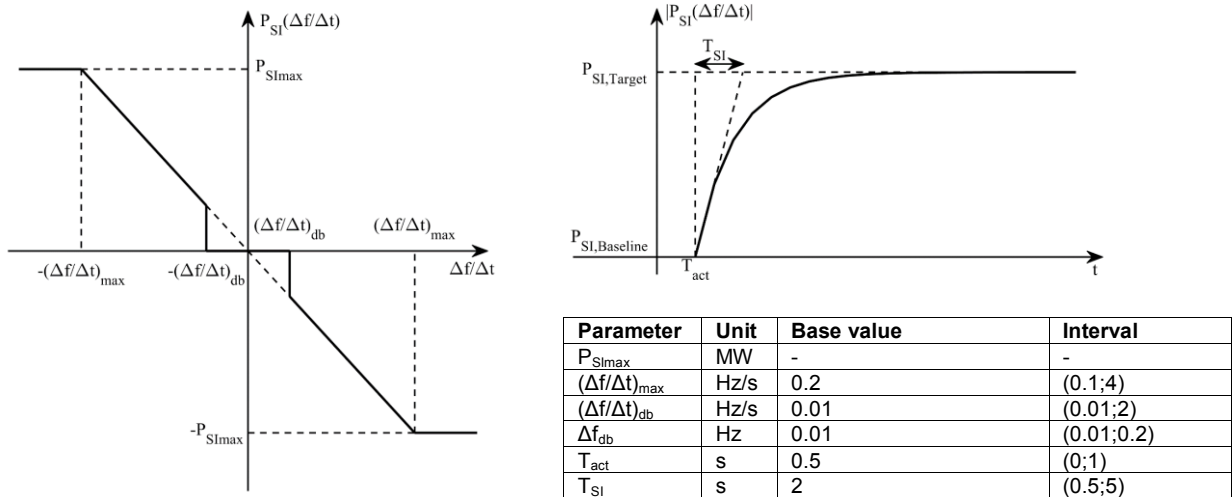


FIGURE 4: CHARACTERISTIC CURVES AND PARAMETERS OF SI

FAP

FAP is intended to support existing control reserves by means of a static power adjustment, which is triggered by exceeding a defined frequency deviation. Since FAP is triggered once the frequency deviation exceeds a certain threshold, it has an activation curve, however no frequency-dependent characteristic curve. The corresponding time response upon activation and parameters of FAP are shown in Figure 5.

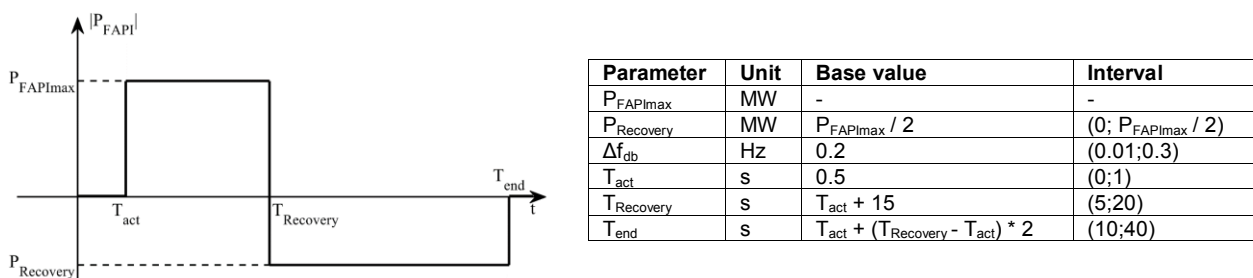


FIGURE 5: TIME RESPONSE AND PARAMETERS OF FAP

Sensitivity analysis and evaluation results based on a CE single-area simulation model

To gain a deeper understanding of the effectiveness of the fast control reserve concepts and assess the impact of their parameters, a sensitivity analysis has been conducted. This section presents only an excerpt of the sensitivity analysis conducted in [9]. The power values $P_{FCR+max}$, P_{EFRmax} , P_{SImax} and $P_{FAPImax}$ have been determined for selected parameter

sets via simulations with the single-area model, by identifying the required power to maintain a frequency above 49.2 Hz. The results are shown in Figure 6.

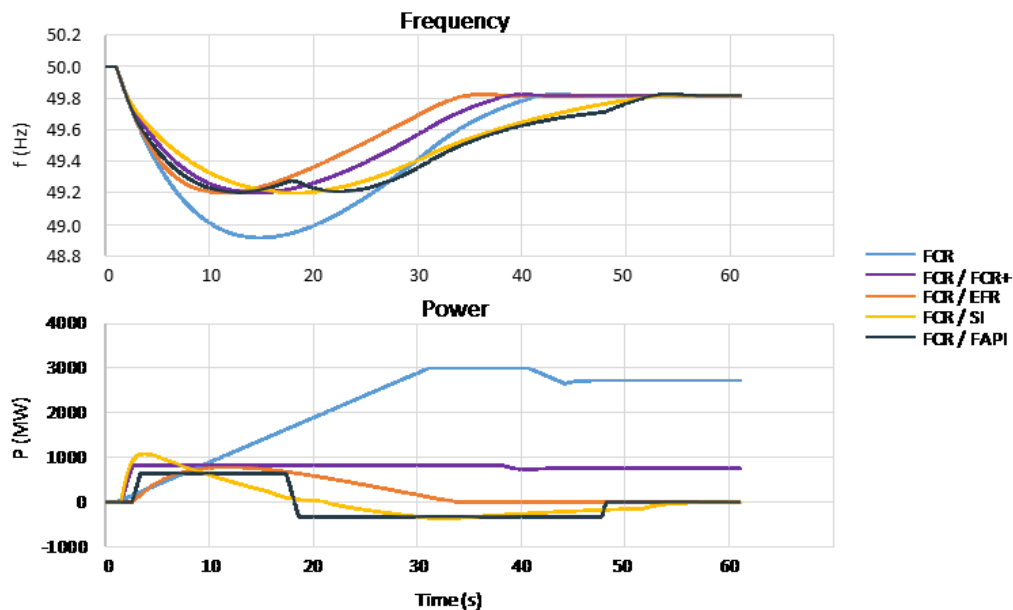


FIGURE 6: FREQUENCY AND POWER CURVES FOR DIFFERENT FAST CONTROL RESERVE CONCEPTS (SYSTEM POWER = 150 GW, SELF-REGULATION EFFECT OF THE LOADS = 1 %/Hz, POWER IMBALANCE = 3 GW, $T_A = 5$ s)

The results of the sensitivity analysis show that both FCR+ and EFR represent robust and fast control reserve concepts, as slight variations of the critical parameters do not have considerable impact on the overall performance. For this reason, FCR+ and EFR would be well suited for use as a fast control reserve. However, it has to be noted that the full activation time of FCR+ and EFR should not be set too high ($T_{full} > 7.5$ s) as this would lead to a significantly higher amount of required control reserves. The same principle applies to the parameters Δf_{db} and Δf_{max} of EFR.

Figure 6 shows that SI can improve the frequency stability and thus can help to keep the frequency above the 49.2 Hz dynamic security limit. Furthermore, it is clearly visible that SI improves the inertial response of the system as it limits the RoCoF and delays the frequency nadir. However, without a zone-selective control, it also delays the frequency recovery after the nadir since it limits the RoCoF during the recovery period. Generally, it can be concluded that the definition of the SI characteristics and the specification of its parameters, especially those regarding the frequency gradient, is not a trivial task and requires thorough research. In addition, SI requires a rather high sampling rate and robust filtering of both frequency and power. Possible measurement delays or outliers could otherwise lead to undesired instabilities [3].

Compared to the other fast control reserve concepts, FAPI shows both the largest dependence on the simulation cases examined and the largest influence of specific parameters on the frequency response. This is due to its static and uncontrolled activation as well as to the recovery period, which causes a second frequency nadir. In particular, the choice of the parameters $P_{FAPImax}$ ($P_{Recovery}$ is given by this) and $T_{Recovery}$ has a strong influence. Too high values of $P_{FAPImax}$ and hence $P_{Recovery}$ could even lead to a critical second frequency nadir, thus counteracting the existing control reserves and endangering the whole power system. These aspects may lead to the conclusion that FAPI tends to be less suitable to be implemented as a fast control reserve in the CE power system.

2. Options for the Implementation in the CE power system

Besides the theoretical development of fast control reserve concepts, the question arises how they should be introduced in a power system. According to Figure 7, two general options exist to achieve the desired system behavior.

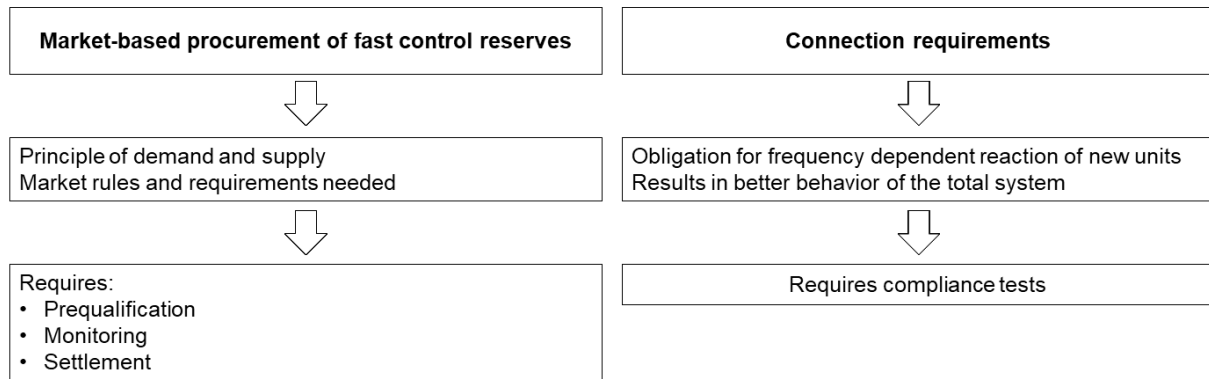


FIGURE 7: OPTIONS FOR THE IMPLEMENTATION OF FAST CONTROL RESERVES IN THE CE POWER SYSTEM

The first option guarantees the desired system behavior via a market-based procurement of fast control reserves – similar to already existing markets (e.g. for FCR). To organize a market, several aspects have to be considered, in particular the product design (maximum/minimum bid size, product period, conditional products, indivisible/divisible products, activation trigger, settlement, penalties, etc.), the prequalification of providers / reserve providing units (RPU) / technical entities (TE) and the monitoring of activation. Apart from that, the necessary regulatory framework (including respective market rules) has to be established. Experiences with existing control reserves have shown that such development processes require adequate time and comprehensive cooperation between the relevant transmission system operators (TSO) and stakeholders. For example, if a new fast control reserve product is intended to be used in an entire synchronous area (SA), TSOs need to compile several aspects, such as common technical requirements, dimensioning rules for the total required amount, allocation keys and possible restrictions for the distribution. Furthermore, market participants would most likely request TSOs to organize a single market for the entire SA, which introduces additional challenges (e.g. establishment of a central tendering/optimization platform, cross-border procurement and settlement, harmonization of boundary conditions, etc.).

While markets have the advantage that TSOs are able to constantly procure and monitor the necessary amount and quality of fast control reserves they may also introduce cost-inefficiencies, if the respective product design and remuneration system are not well suited. In addition, an illiquid market could potentially lead to operational challenges due to missing bids and hence insufficient amounts of fast control reserves.

To address these issues the second option is to mandatory require the necessary system behavior (technical capability) from new and substantially modified RPU/TE. This can be achieved with the introduction of new or extended connection requirements in dedicated Connection Network Codes (CNC) [10] [11]. The implementation of this option might be easier, as it does not require additional market rules. However, an agreement on harmonized connection requirements for the entire SA is also a time-consuming task, which needs to be well organized. Within this context, the scope (size and/or technology of RPU/TE) and a general framework (trigger for activation, parameters for the activation

itself, etc.) has to be first set up on a SA level and then specified in national grid codes. Besides, the current CNC legislation [10] [11] would also require the TSOs to validate the compliance of RPU/TE in the course of the connection process. Contrary to a market where the required behavior may be organized by aggregation (pooling) of individual RPU/TE with different connection points, mandatory connection requirements can only be defined on the level of a single RPU/TE.

Summarizing the mentioned aspects, it is not yet clear which option should be prioritized as a mitigation measure. Probably, a combination of a market-based procurement and new or extended connection requirements could be developed to find the most efficient and technology-neutral solution in the CE power system.

Description of the CE-2030+ implementation scenario

In order to obtain future recommendations for the introduction of fast control reserve concepts, different implementation scenarios have to be developed and evaluated. This section presents an analysis of an exemplary implementation scenario (“CE-2030+”), which is based on parallel developments in other SAs [12] [13] and estimations of the network time constant in the CE power system.

In this paper, the network time constants (T_A), for the CE-2030+ implementation scenario, are estimated with a dedicated electricity market model of the CE power system (Electricity Dispatch Optimization & Balancing Market Model [14]). The input data for the market model is derived from the TYNDP 2020 scenarios “*National Trends*” (NT) and “*Global Ambition*” (GA) [15]. For the purpose of comparison, estimations of T_A for the years 2017 to 2019 have been additionally performed using CE generation data from the ENTSO-E Transparency Platform [16].

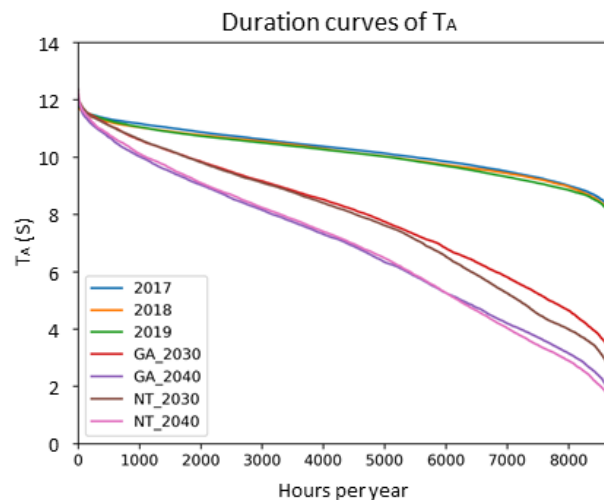


FIGURE 8: ANNUAL DURATION CURVES OF THE CURRENT AND FUTURE NETWORK TIME CONSTANT

Figure 8 shows a comparison of the annual duration curves of T_A for the years 2017 to 2019 and the CE-2030+ implementation scenario, which takes into account the TYNDP 2020 scenarios “*National Trends*” (NT) and “*Global Ambition*” (GA) [15]. As can be seen, the implementation scenario shows a significantly decreasing and more volatile network time constant. The decrease and the greater volatility of T_A is directly linked to the increasing amounts of PEIG/RES. For approximately 30 % of the scenario years NT2030 and GA2030, T_A becomes smaller than 6 s, which could potentially lead to critical frequency drops below 49 Hz (see Figure 1), if no other mitigation measures are active.

Correspondingly, the number of possible critical frequency events increases up to approximately 40 % in the scenario years NT2040 and GA2040.

To gain a deeper understanding of future characteristics in the CE power system, a detailed distribution analysis of the network time constant has been additionally performed with the existing data basis. The distribution of T_A in the year 2019 and in the GA 2030 scenario is shown in Figure 9.

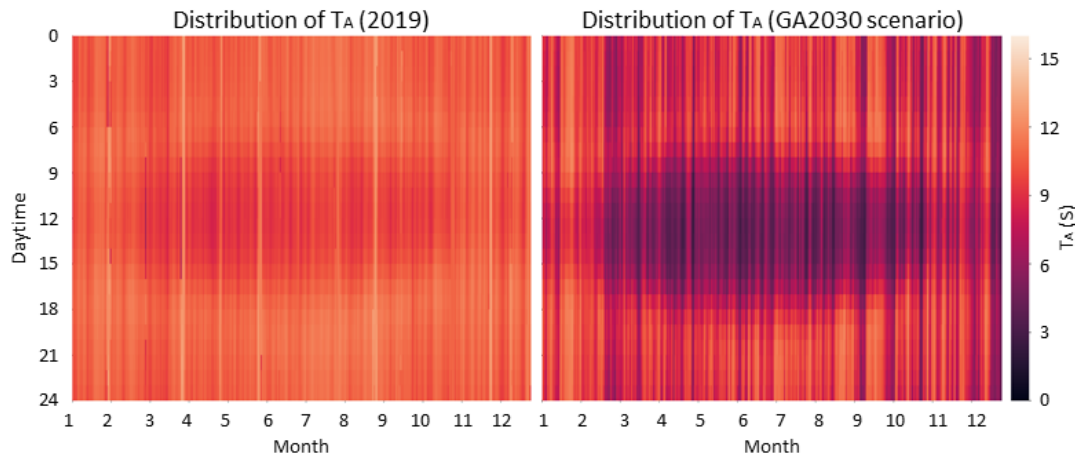


FIGURE 9: DISTRIBUTION OF THE NETWORK TIME CONSTANT IN THE YEARS 2017 TO 2019 AND IN THE GA 2030 SCENARIO

In the year 2019, a decrease of T_A (dark spot in the center of the graph) is already slightly visible, which is mainly caused by the infeed from inverter-based photovoltaic (PV) installations. With the increasing number of inverter-based PV installations in the CE power system, this effect becomes more evident in the scenario year GA2030. Furthermore, the pattern of T_A in the scenario year GA2030 additionally reveals dark vertical lines, which can be characterized by a high infeed from wind power.

The estimations of the future network time constant in the CE power system, shown in Figure 8 and Figure 9, clearly indicate the need of adequate mitigation measures to ensure frequency stability. Similar to [12] [13], the CE-2030+ implementation scenario assumes the introduction of either FCR+ or EFR via a market-based procurement as the most cost-efficient and effective mitigation measure. A detailed sensitivity analysis has shown that SI and FAPI are not necessarily required as long as T_A is greater than approximately 3 s [9]. Therefore, SI and FAPI are not utilized in the CE-2030+ implementation scenario, whereas they may be considered as additional mandatory connection requirements in long-term scenarios. Besides, based on the findings of Figure 9 and similar considerations from other SAs [12] [13], it can be assumed that FCR+ or EFR are more likely to be procured “dynamically” on a seasonal or, where appropriate, weekly or daily basis. However, it has to be noted that a highly dynamic and short-term dimensioning and procurement approach could potentially threaten reliability and planning security.

Evaluation of fast control reserve concepts in the CE-2030+ implementation scenario

The previous chapters and sections have shown that both FCR+ and EFR are technically suitable to be introduced via a market-based procurement in the CE-2030+ implementation scenario. Based on a detailed sensitivity analysis [9] the recommended technical values and necessary maximum amounts for the implementation of FCR+ and EFR are summarized in Table 1.

Parameter	FCR+	EFR
Full activation time	5 - 7.5 s	5 - 7.5 s
Maximum amount of fast control reserves	800 - 1400 MW	650 - 1400 MW
Conventional FCR	2200 - 1600 MW	3000 MW
Total amount of reserves	3000 MW	3650 - 4400 MW

TABLE 1: RECOMMENDED TECHNICAL VALUES AND NECESSARY MAXIMUM AMOUNTS OF FCR+ AND EFR

In this section, the fast control reserve concepts FCR+ and EFR are further evaluated with regard to market and regulatory aspects in the CE-2030+ implementation scenario. The results of the qualitative analysis are summarized in Table 2.

Aspect	FCR+	EFR
Level of implementation	As part of conventional FCR, FCR+ is a product for the entire SA.	Similar to FCR+, EFR can be primarily seen as a product for the entire SA. EFR may also be introduced at national level, if specific operational boundary conditions require faster control reserves (e.g. TSOs at the border of the system with high shares of RES).
Regulatory framework	The introduction of FCR+ at least requires amendments of the System Operation Guideline and the SAFA (Annex A-1 "Dimensioning rules for FCR" and A-2 "Additional properties for FCR").	The introduction of EFR as a product for the entire SA requires similar amendments as in the case of FCR+ and new market rules.
Market rules (terms and conditions)	However, further necessary amendments of legislation (e.g. Balancing Guideline) cannot be excluded. FCR+ can be integrated in the existing FCR market rules.	The introduction of EFR as a national product may only require the establishment of new market rules.
Prequalification	FCR+ can be integrated into the existing FCR prequalification procedure. Existing RPU/TE can be also classified for FCR+ after a proof of the faster full activation time.	As a new separate product, EFR needs a dedicated prequalification procedure (it can, however, be structured similarly to the procedure of FCR).
Dimensioning approach	A dynamic dimensioning approach (based on forecasts) can be applied (this will, however, also have implications on the current FCR dimensioning approach). A too dynamic and short-term dimensioning approach could potentially threaten reliability and planning security.	A dynamic dimensioning approach (based on forecasts) can be applied. A too dynamic and short-term dimensioning approach could potentially threaten reliability and planning security.
Amount of fast reserves	FCR+ replaces a part of conventional FCR, the overall amount of reserves remains the same (3 GW).	EFR is used in addition to conventional FCR, the overall amount of reserves increases accordingly.
Deployment	Similar to conventional FCR, FCR+ is almost continuously active.	With $\Delta f_{db} = \pm 200$ mHz EFR is only activated in usually rare events.
Energy-to-power (E/P)-ratio	FCR+ providers shall ensure to fully activate FCR+ continuously for a predefined time period (15/30 min). The E/P-ratio is determined according to this requirement.	Due to the fact that the frequency will recover and enter the range $50 \pm 0,2$ Hz almost immediately after the activation of EFR, it can be assumed that the E/P-ratio can be low.
Expected costs	The additional costs of FCR+ can be partly compensated with the decreasing costs of conventional FCR.	The introduction of EFR generates additional costs (based on the remuneration system, however, the additional costs may be negligible).
Business Model	Existing FCR providers can alternatively offer FCR+ or participate in the energy market.	EFR may be used as a product for new providers with alternative technologies, due to the low E/P-ratio and less activations. Due to the different product design of EFR, it can be assumed that EFR is not likely to be provided by existing FCR (RPU/TE).

TABLE 2: EVALUATION OF FCR+ AND EFR IN THE FRAME OF MARKET AND REGULATORY ASPECTS

From the findings in Table 2, it can be concluded that both FCR+ and EFR share common aspects and include equivalent advantages and disadvantages. FCR+ could be offered by some existing FCR providers, as different RPU/TE (e.g. battery storage) are capable to act faster than required by conventional FCR, without any or only minor modifications. Accordingly, this could simplify the market access and the prequalification process of FCR+, as only the faster full activation time needs to be adjusted and proved in the frame of an already well-established FCR prequalification process. Contrary, EFR could be a promising product for new providers with alternative technologies (e.g. fast switchable loads or storages with a low E/P-ratio). In this context, it has to be highlighted that this product may be designed asymmetrically to ensure the participation of a sufficient number of providers. Furthermore, EFR would require the establishment of a dedicated prequalification procedure.

3. Conclusions and recommendations

Recent trends show a decrease of the number of conventional generation facilities and an increasing penetration of PEIG. The associated reduction of SG, which inherently provide real inertia, leads to a decreasing network time constant and thus challenges in adequately maintaining the frequency stability in a power system. A possible way to counteract possible frequency stability issues could be the implementation of fast control reserves, which could be also provided by PEIG.

The fast control reserve concepts, developed in the frame of the R&I project ABS4TSO, consider either frequency-proportional (FCR+, EFR), RoCoF-proportional (SI) or static (FAPI) control strategies. As presented in this paper, all of the above-mentioned fast control reserve concepts can improve the frequency stability and can thus help to keep the frequency above the dynamic security limits. Regarding the technical aspects, FCR+ and EFR both represent robust and fast control reserve concepts, as slight variations of the critical parameters do not have a considerable impact on the overall performance.

To ensure the desired system behavior, either a market-based procurement of fast control reserves or the introduction of new or extended connection requirements may be considered.

An exemplary implementation scenario ("CE-2030+"), which is based on parallel developments in other SAs and estimations of the network time constant, shows that the introduction of either FCR+ or EFR via a market-based procurement can possibly be a cost-efficient and effective mitigation measure in the CE power system. The results of a qualitative analysis conclude that both FCR+ and EFR share common aspects and include equivalent advantages and disadvantages with regard to market- and regulatory aspects. FCR+ could be offered instantly by some existing FCR providers, whereas EFR could be a promising product for new providers with alternative technologies.

At this stage, a clear recommendation for a comprehensive implementation scenario in the CE power system cannot be provided. For all possible aspects, there is a need to consider a balance between the system needs, the capability of different technologies, the expectations from market participants and social welfare. Taking this into account, national or regional pilot projects, including TSOs, market participants, manufacturers and regulators, could serve as a promising basis to demonstrate the cost-efficiency and effectiveness of different fast control reserve concepts. Additionally, the outcomes from

such pilot projects could be also used for the development of future regulatory frameworks in the CE power system.

References

- [1] ENTSO-E, “High Penetration of Power Electronic Interfaced Power Sources”, 2017, <https://www.entsoe.eu/Documents/Network%20codes%20documents/Implementation/CNC/170322_IGD25_HPoPEIPS.pdf>.
- [2] ENTSO-E, “High Penetration of Power Electronic Interfaced Power Sources and the Potential Contribution of Grid Forming Converters”, 2019, <https://www.entsoe.eu/Documents/Publications/SOC/High_Penetration_of_Power_Electronic_Interfaced_Power_Sources_and_the_Potential_Contribution_of_Grid_Forming_Converters.pdf>.
- [3] S. Khan, B. Bletterie, A. Anta, W. Gawlik, “On Small Signal Frequency Stability under Virtual Inertia and the Role of PLLs”, *Energies* 2018, vol. 11, 2018.
- [4] ENTSO-E, “Continental Europe Operation Handbook Appendix A1 Load-Frequency Control and Performance”, 2004, <https://www.entsoe.eu/fileadmin/user_upload/_library/publications/entsoe/Operation_Handbook/Policy_1_Appendix%20final.pdf>.
- [5] European Commission, “Commission Regulation (EU) 2017/1485 of 2 August 2017 establishing a guideline on electricity transmission system operation“, *Official Journal of the European Union*, 2017.
- [6] M. Leonhardt, W. Gawlik, “Advanced Balancing Services für Übertragungsnetzbetreiber“, *e&i Elektrotechnik und Informationstechnik*, vol. 136, 2019.
- [7] J. Marchgraber, C. Alács, Y. Guo, W. Gawlik, A. Anta, A. Stimmer, M. Lenz, M. Froschauer, M. Leonhardt, “Comparison of Control Strategies to Realize Synthetic Inertia in Converters”, *Energies* 2020, vol. 13, 2020.
- [8] W. Gawlik, C. Alács, J. Marchgraber, Y. Guo, A. Anta, J. Kathan, B. Weiss, K. Oberhauser, M. Lenz, M. Froschauer, A. Stimmer, M. Leonhardt, “Improving synthetic inertia provision by power electronic interfaced power sources to support future system stability“, *CIGRE session 48*, 2020.
- [9] C. Alács, J. Marchgraber, Y. Guo, W. Gawlik, A. Anta, J. Kathan, B. Weiss, K. Oberhauser, M. Lenz, M. Froschauer, A. Stimmer, M. Leonhardt, “Mögliche Umsetzung von schnellen Regelreserven im kontinentaleuropäischen Verbundsystem“, *16. Symposium Energieinnovation*, Graz, 2020.
- [10] European Commission, “Commission Regulation (EU) 2016/631 of 14 April 2016 establishing a network code on requirements for grid connection of generators“, *Official Journal of the European Union*, 2016.

- [11] European Commission, “Commission Regulation (EU) 2016/631 of 17 August 2016 establishing a Network Code on Demand Connection“, Official Journal of the European Union, 2016.
- [12] ENTSO-E, “Fast Frequency Reserve – Solution to the Nordic inertia challenge“, 2019, <<https://www.epressi.com/media/userfiles/107305/1576157646/fast-frequency-reserve-solution-to-the-nordic-inertia-challenge-1.pdf>>.
- [13] National Grid, “Dynamic Containment – Industry Information“, 2020, <<https://www.nationalgrideso.com/industry-information/balancing-services/frequency-response-services/dynamic-containment>>.
- [14] B. Dallinger, “Model-based Analysis and Design of an improved European Electricity Market with high shares of Renewable Generation Technologies“, Dissertation, Technical University Vienna, 2018, <<http://repositum.tuwien.ac.at/obvutwhs/download/pdf/3381277>>.
- [15] ENTSO-E, “TYNDP 2020 Scenario Report“, 2020, <https://www.entsos-tyndp2020-scenarios.eu/wp-content/uploads/2020/06/TYNDP_2020_Joint_ScenarioReport_final.pdf>.
- [16] ENTSO-E, “Transparency Platform“, 2020, <<https://transparency.entsoe.eu>>.

G0703

Benefits of multi-voltage-level grid control in future distribution grids

Wolfgang Biener (1), Thomas Erge (1), Thomas Kumm (2), Bernhard Wille-Haussmann (1)

(1) Fraunhofer Institute for Solar Energy Systems ISE
Heidenhofstrasse 2, D-79110 Freiburg

(2) EWE NETZ GmbH
Cloppenburg Strasse 302, D-26133 Oldenburg
Tel.: +49-761-4588-5893
wolfgang.biener@ise.fraunhofer.de

Abstract

Operators of distribution grids will be confronted with new challenges caused by a high share of distributed fluctuating generators (PV, wind) together with new load profiles of a fleet of electric vehicles (EV), decentralized storage systems or electricity-heat-converters (like heat-pumps or direct heaters). Conventional grid reinforcement is an expensive and inflexible way to handle upcoming grid problems like the violation of voltage limits or the thermal overloading of operating equipment. By controlling flexible components (like on-load tap changers or reactive power generation from inverters) grid operators can counteract violations of operational limits.

A grid simulation study has been performed to compare benefits of intelligent multi-voltage-level grid control with single-voltage-level control solutions and conventional grid control methods. The starting point for this work was a number of scenarios for the future grid penetration by PV, wind and EV. Representative type grids consisting of interconnected grid segments for rural and municipal distribution grids were modelled within a probabilistic load flow calculation framework. To quantify the probability of voltage violations or thermal overload situations, a probabilistic assignment of grid components (PV, wind, EV) to grid nodes was implemented. Four grid control approaches have been studied by use of the simulation, representing different distributed and centralized control methods.

The results of the investigation show the benefits of multi-voltage-level grid control for distribution grids with a high share of distributed wind, PV and EV. While conventional grid operation solutions might be able to counteract local voltage problems, a combined control algorithm for the LV and MV grid segments is able to prevent the violation of given voltage and current limits in many cases quite effectively. The effectiveness of using transformers with variable on-load tap changers (OLTC) might improve significantly if communication based multi-voltage-level grid control concepts are applied. Overloading of cables resulting from solving local voltage maintenance problems by means of reactive power injection can be avoided. Multi-voltage-level grid control avoids or delays grid extension and increases grid capacity towards the installation of additional PV, wind or EV-charging units.

Keywords: Distribution Grid, Load Flow Analysis, Probabilistic Simulation, Grid Control.

The presented results are part of the project "Green Access", funded by the Federal Ministry of Economics and Energy under the funding code 03ET7534.

Introduction

The ongoing transition of the electricity supply system towards sustainable energy generation accompanied by a partial decentralization of power plants causes serious changes in the geographic and temporal distribution of power flows in the transmission and distribution grids. This trend is amplified by alterations in consumption profiles caused by trends like self-supply via local power generation or the transition of the transport sector towards electric vehicles (EV). Especially distribution grids are increasingly being required to absorb and distribute the decentralized energy volumes and load flows (e.g. resulting from wind and photovoltaic systems). The high volatility and the low full load hours of renewable energies (RES) require rethinking the planning and operation of the distribution networks. A reliable, stable and therefore sustainable integration of renewable energies is only achievable by adapting the distribution network as quickly as possible to the constantly changing conditions.

In a German research project “Green Access” [1] an interdisciplinary research team led by German grid operator EWE NETZ has for four years been testing existing solutions for the automation of medium and low-voltage networks with partners from industry and science - because most wind and solar systems are connected to these two network levels. The project examined how the components of an intelligent network work together efficiently, developed them further and then compared the performance of intelligent and conventional network sections with one another.

Using methods of probabilistic simulation carried out by Fraunhofer ISE, sensitivities regarding the penetration of electric vehicles and renewable energies were simulated for a representative medium-voltage network with subordinate low-voltage networks. On the basis of these simulations and derived key figures, the advantages and disadvantages of cross-voltage network planning processes were assessed.

The remainder of this paper is as follows. After the introduction the investigated electrical grid and scenarios are described. Then control strategies are introduced which shall be evaluated with load flow calculations presented in the following chapter. In the last chapter short conclusions are drawn.

1. Type grids and Scenarios

Based on real distribution grids, EWE NETZ has typified low-voltage and medium-voltage networks and described the corresponding characteristics of these networks. The following five type grids were defined:

- Rural MV type grid,
- Village LV type grid with high feed-in / LV grid with low feed-in,
- Rural LV type grid with high feed-in / LV grid with low feed-in.

The four LV type grids are shown in Figure 1. For the simulation the placement of PV power plants, EV charging stations, heat pumps and small storage systems was determined statistically in probabilistic simulations. Points whose load curve was analyzed in detail are marked by green circles. The green lines mark the lines whose current load was analyzed in detail.

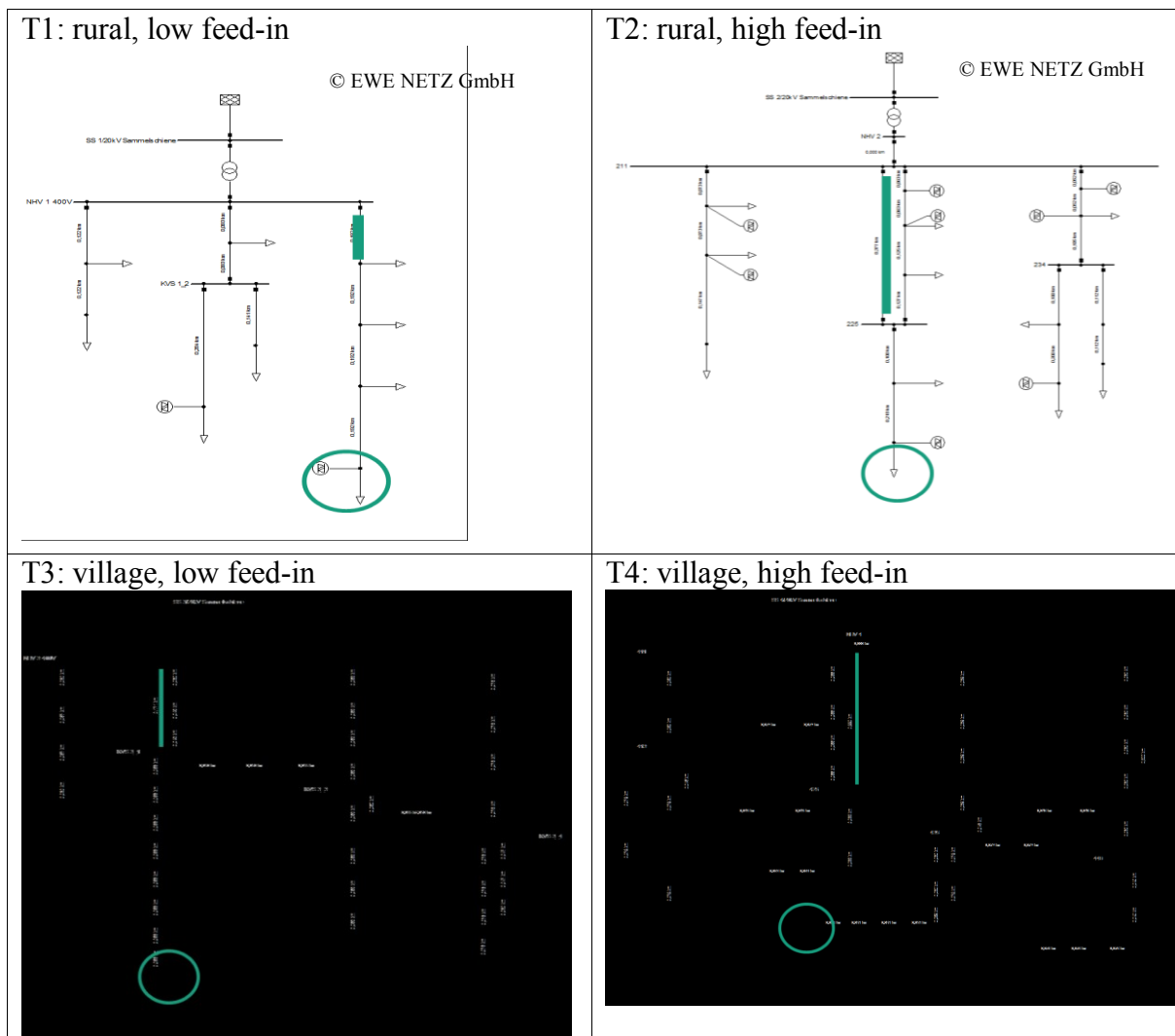


Figure 1: Type grid T1-T4 of EWE NETZ AG.

Figure 2 shows the rural medium voltage grid. This is a medium-voltage grid in normal switching state. Possible redundancies from neighboring grids were not included in the illustration and considered. In the medium-voltage grids, different consumers and generation plants are directly connected. In addition, the low-voltage type networks T1-T4 were assigned to the individual local network stations. The combination of MV and LV grids was realized in accordance to findings in [2].

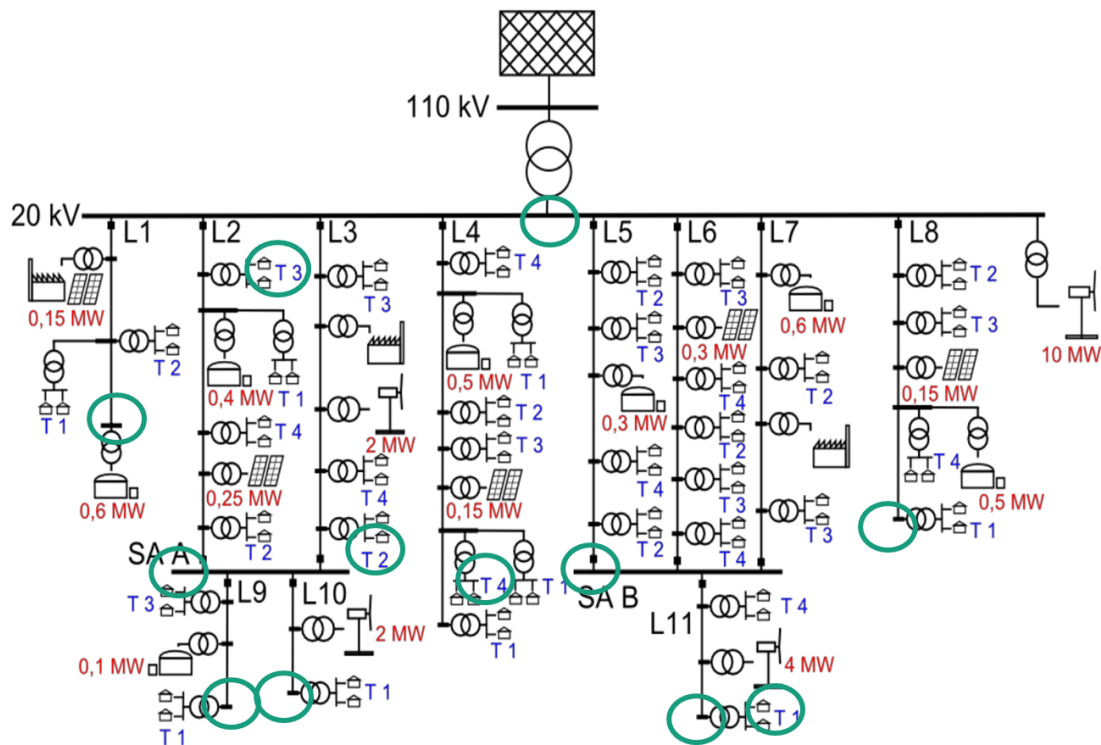


Figure 2: Grid topology of the rural MV grid

Simulated and real time series for loads and generators were integrated into the probabilistic grid simulation framework. A sensitivity analysis regarding the penetration of the grids with PV and wind on the one hand and special types of loads and storage system on the other hand was carried out at the beginning of the project. It started from the status quo in 2015 with 39 GW PV and 39 GW windpower installations and assumed expansion scenarios with an increase of PV capacity by 44%, 88% and 173%, and an increase of wind power capacity by 45%, 90% and 150% (related to type grid specific comparative values).

These scenarios with different RES penetration were combined with a different assumption regarding the perspective EV penetration. Three EV penetration rates (related to connected customers) were evaluated: 1% EV, 17% EV and 50% EV. For all of these combined scenarios load flow simulations of the type grids were carried out for one year in order to determine events violating limit values for the voltage or resource overload of lines and transformers.

2. Grid Control Strategies

In the past there was no classic control system of the kind that exists at the high and extra-high voltage levels, but at the medium and low voltage levels. Access to the field level of medium-voltage grids was provided via proprietary ICT that were limited to one application (e.g., grid protection, monitoring of substations). At the MV level, with the exception of substations and the RES plants connected to the control system in accordance with corresponding laws, there was usually hardly any actuator and sensor technology. With transformers with variable on-load tap changers (OLTC) and controllable generation

plants, new actuator technology was increasingly introduced at the low-voltage level, which had an increased potential for monitoring and control.

A central active power control has already been used by network operators in the course of feed-in management. However, this was limited to the control of large plants, which are mainly located at the medium voltage level. There was no individual control of the plants finely tuned to the current grid situation.

If all components in the distribution network are to be centrally coordinated across voltage levels, this can only be realized at great expense. Decentralized control systems were already used to a limited extent for reactive power control in the past. This was usually limited to the grid connection point of a generating plant (Q(P) or Q(U) control). As a rule, there was no interaction between the control systems of the generation plants that was adapted to the current grid situation or to an entire grid area.

There were already regulators for the active and reactive power control of individual PV systems and wind parks to maintain current and voltage bands and reactive power specifications at grid connection points. Controllers were limited to individual plants or parks and were not part of an adaptive system and thus not interchangeable with other controllers.

The key target of the project Green Access was to design the distribution grid automation to control the power grid across voltage levels (medium and low voltage) in such a way that no violations of current and voltage limits occur under the conditions of a very high penetration of volatile generation facilities and a changing load structure. An important prerequisite for this is a safe and reliable ICT structure, which was also developed, tested and field-tested within the project. The intention of the simulation work reported in this paper was to identify the benefits of across voltage levels control and compare different approaches for more or less centralized control concepts.

Four different control scenarios depending on the position of the “control intelligence” were defined for that purpose:

- **Distributed control (status quo):** the decentralized plants have local measuring sensors and control their reactive power feed-in on the basis of the local grid situation depending on the current feed-in power (PV and wind energy plants) or the voltage ratio (adjustable local grid transformers, OLTC).
- **STATCOM control:** The reactive power actuators are assumed to have STATCOM (static synchronous compensator) properties and systematically regulate the reactive power on the basis of the node voltage measured at the grid connection point, independent of their feed-in power, and there is no limitation by a power factor specification.
- **Hierarchical, autarkic control:** all actuators of a voltage level are connected to a controller for communication purposes. Low-voltage and medium-voltage controllers take measures independently of each other to maintain the voltage band and avoid overload of equipment.
- **Central control:** By means of communication between low and medium-voltage controllers, a central control algorithm of the medium-voltage controller can transmit active and reactive power specifications to the low-voltage controller, so that an overall optimization of both network levels is achieved.

Figure 3 visualizes the concept for the “central control” adaptive control strategy for the multi-voltage level distribution grid.

Centralized medium voltage control(ZMC)

- State estimation
- Coordinated operation

Centralized low voltage control (ZLC)

- Higher level control
- Coordinate operation of LV actors

Local node control (LNC)

- Reactive power control
- On load tap changer

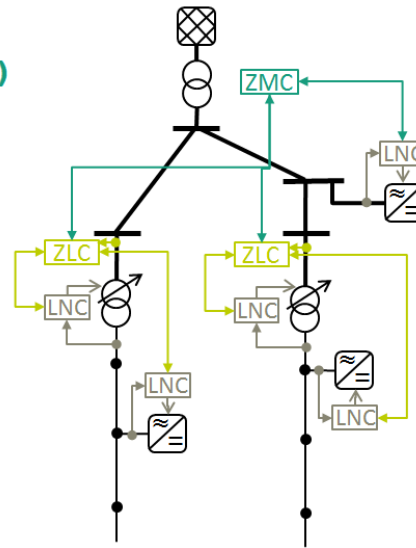


Figure 3: Adaptive control strategies for distribution grids

3. Load Flow Simulation

The results presented in this Chapter are mostly generated by probabilistic load flow calculations. Figure 4 illustrates the basic approach of this method. The intention was to identify situations, where the distribution of loads and generation in the grid leads to critical power flows and voltage levels. Probabilistic load flow analysis is an efficient tool to access the performance of the power system considering the uncertainties of the load demand and generation at the single grid nodes.

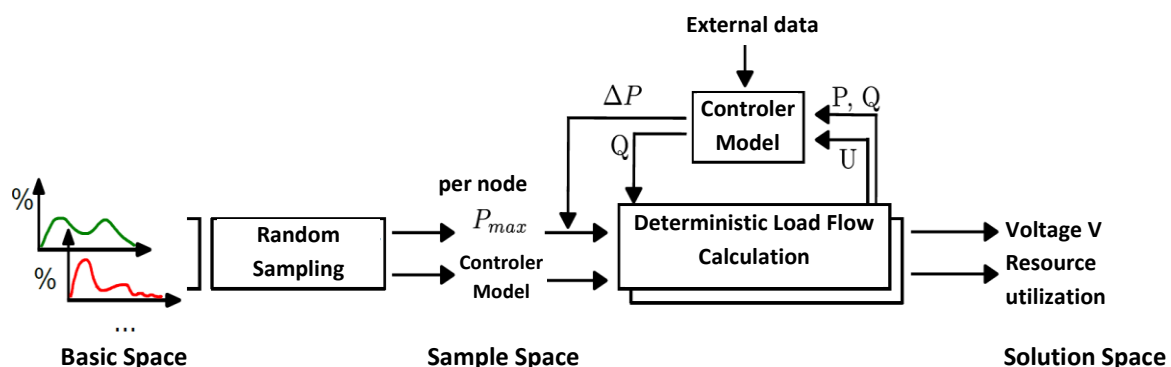


Figure 4: Method of probabilistic load flow calculation

As an example for the simulation results Figure 5 shows the probability for a need of (conventional) grid enforcement because of the violation of limit values (either thermal overload or over-/undervoltages) depending on the different control concepts and with or without the use of a OLTC.

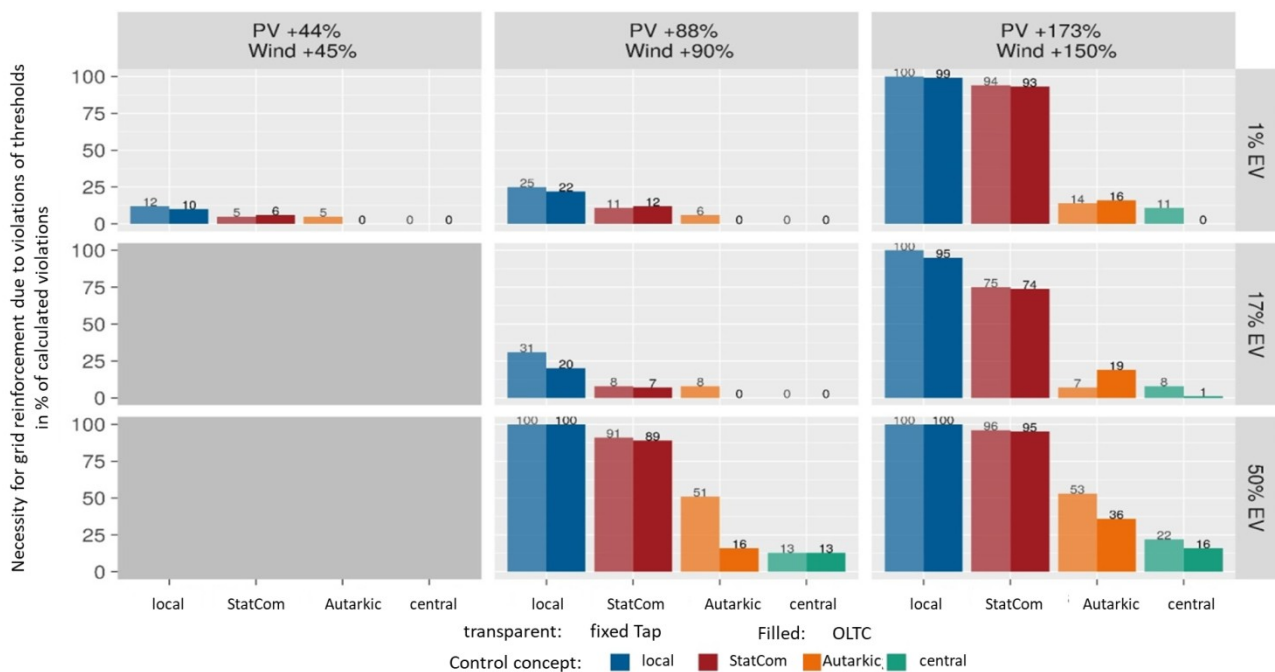


Figure 5: Probability for grid expansion requirement in percent of the probabilistically investigated combinations (left part of the bars: without OLTC control, right part of the bars: with OLTC control). For this simulation, EV charging stations were connected to the LV voltage level only.

The advantage of the central control concept is clearly visible here, as it allows the number of limit value violations to be reduced to a minimum, even with a very high penetration of renewable energy sources and charging stations for electric mobility.

To assess the dependency of the impact of EV charging stations from the voltage level they are connected to, the same simulation had been carried out with MV connection of the EV chargers. The result is shown in Figure 6.

EV connected to MV level

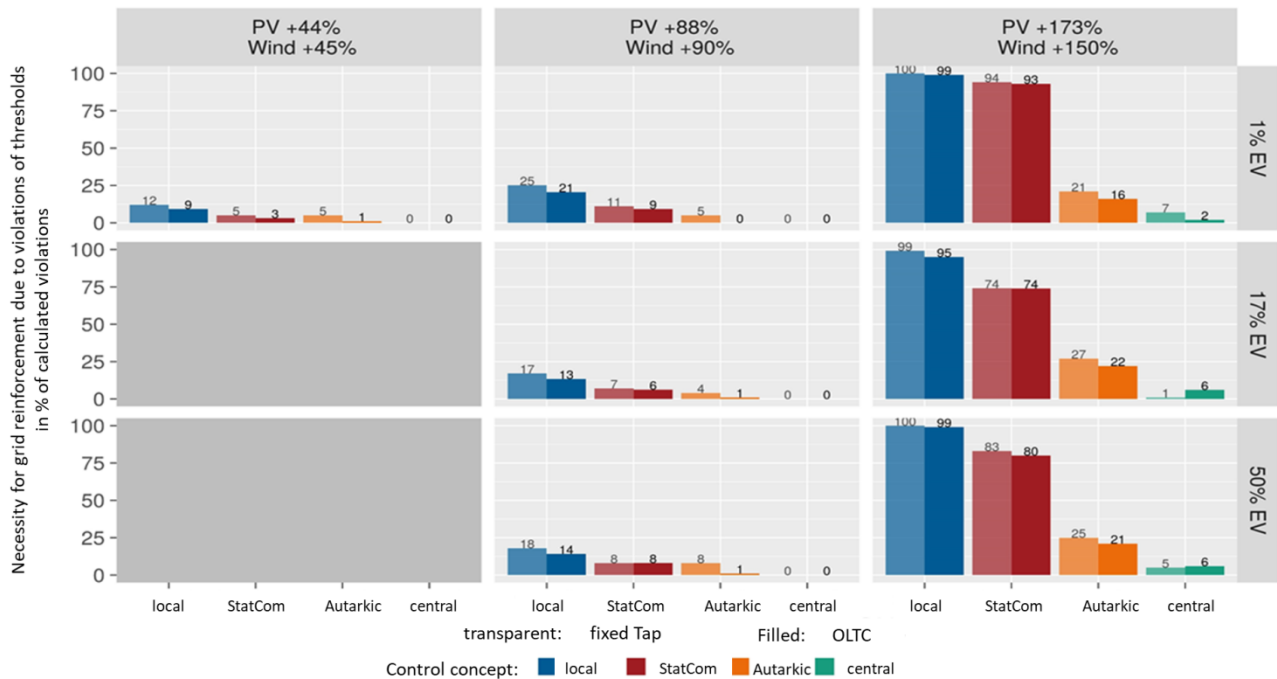


Figure 6: Probability for grid expansion requirement in percent of the probabilistically investigated combinations (left part of the bars: without OLTC control, right part of the bars: with OLTC control). For this simulation, EV charging stations were connected to the MV voltage level only.

It is remarkable to see that even with a very high penetration of EV almost no need for grid expansion was found and almost all problems were generated from PV and wind feed-in.

The detailed evaluations of the simulation investigations have led to a number of core theses which describe the occurrence of or the control strategies for dealing with limit value violations:

- With the current and short-term expected penetration of the distribution networks with PV and wind as well as electric mobility, thermal problems and overvoltages in the network infrastructure are only to be expected selectively, which can be controlled by means of local control (e.g. Q(U) control). The use of OLTC can postpone the need for network expansion, but the installed OLTC are rarely used in operation.
- In case of a high penetration of the distribution networks with renewable energy producers (EE), thermal overloads occur more frequently in the distribution networks, but rather less voltage band violations. A high degree of electromobility penetration also leads to considerable voltage band violations. However, if the penetration of EV and RES is high at the same time, the number of thermal limit value violations can be significantly reduced.
- If the EV charging stations are shifted to medium voltage (and medium RES penetration), hardly any voltage band violations occur and there is no need for network expansion or networked control solutions.

- Communication-based control systems reduce the need for grid expansion with high penetration of renewable energy systems and electric vehicles, and are significantly more effective than control concepts without communication. Locally acting STATCOM controllers (e.g. in charging stations for electric vehicles) can often solve local voltage band problems, but in certain situations they can increase the number of line overloads. The effectiveness of OLTC increases significantly when it is integrated into communication-based control concepts. However, it has to be decided in each individual case whether an OLTC should be installed, since in the vast majority of cases a communication-based control concept avoids overloads even without OLTC.
- With an intelligent communication-based combined control system at low and medium voltage level, network expansion can be avoided completely in some cases, even if there is a high penetration of renewable energies and electric mobility. On the other hand, a self-sufficient control of the medium and low-voltage grids can result in negative effects (especially a higher number of limit value violations at the low-voltage level).

The aim of the additionally performed individual case simulations was to evaluate the effectiveness of individual types of control measures or combinations of measures beyond the extensive simulations. The investigations regarding the input variables were limited to selected critical combinations of loads and generators, whereby complete annual simulations with 10 min time steps were executed. Key figures were determined describing a number of aspects linked to the grid control scenarios.

A number of overall conclusions were drawn from the key figure evaluations:

- By means of a networked central control system, the probability of voltage band violations can be reduced practically to zero, independent of the use of OLTC.
- Beyond the elimination of voltage problems, both autonomous and central control concepts do not lead to any change in the distribution and magnitude of the voltage values at the individual selected network nodes.
- When the charging stations are connected on the medium voltage level, both autonomous and central control concepts can compensate for all operating medium overloads independent of the action of an OLTC. If connected on the low voltage level, however, central control concepts can lead to an increase of the overloads in case of fixed tap position of the transformer.
- An autarkic or networked central control does not lead to a change in the utilization of grid components during normal network operation. In the case of network problems, an increase in resource utilization can occur, which is also possible in the case of distributed control and STATCOM operation.
- By using adaptive networked controllers, there is no increase in annual grid losses.
- The use of adaptive networked controllers does not lead to an increase in inverter losses; compared to STATCOM concepts, the losses are slightly lower.
- By using adaptive networked controllers, there is no significant change in the balance-sheet current flows between the high-voltage level and the subordinate networks.

- When using adaptive networked controllers, the reactive power requirement is slightly lower compared to purely distributed control, but higher compared to STATCOM control (in the order of 10 ... 15%).
- By using adaptive networked controllers, there is no significant change in the maximum positive and negative power flow at the network connection point to the high-voltage level.
- The use of adaptive networked controllers significantly increases the capacity of the distribution grids for including additional renewable energy generation units (multiplication!).
- The use of adaptive networked controllers does not lead to any significant changes in the amount of energy shedding, which is negligible (less than 0.1%) relative to the energy fed into the grid in the scenarios studied.

4. Conclusion

The probabilistic load flow simulations and further investigations of the selected type grids clearly show advantages that can be achieved by multi-voltage-level grid control in situations with grid infrastructure overload or voltage control problems. Somewhat surprising was the result that those type grids (representing the current state-of-the-art for distribution grids) showed a rather high free capacity for the connection of additional RES as well as EV charging points without provoking a high probability for overload problems. Even though the central control concept with communication between the LV and MV controller units clearly is the most efficient means for avoiding grid expansion, local control measures might be sufficient in many cases to avoid voltage problem provided that they do not lead to thermal overload problems themselves. OLTC might be helpful to postpone grid extension but seem to be dispensable in many situations where STATCOM control is applied.

For scenarios with very high RES and EV penetration, multi-voltage-level grid control clearly is the first tool of choice to shift or avoid grid expansion, and probability levels of grid overload could be lowered from 100% to rather small values (that perhaps could be handled by involving decentral flexibilities) for the investigated scenarios.

References

- [1] <https://www.green-access.de/>, Webpage, last access: 28.08.2020
- [2] J. Bömer et al.: „Weiterentwicklung des Verhaltens von Erzeugungsanlagen am Niederspannungsnetz im Fehlerfall“, Internationaler ETG-Kongress 2013, Berlin

G0704

Forecasting and Optimization Approaches Utilized for Simulating a Hybrid District Heating Network

Lukas Gnam, Christian Pfeiffer, Markus Schindler, Markus Puchegger

Forschung Burgenland GmbH
Campus 1, 7000 Eisenstadt/Austria
Tel.: +43-5/7705-5475
lukas.gnam@forschung-burgenland.at

Abstract

The historically grown centralized energy system is undergoing massive changes due to the transformation from centralized energy production with large assets (e.g. fossil-thermal power plants) towards a sustainable, clean and decentralized energy system. This transformation is based on the inclusion of renewable energy sources (RESs) (e.g., wind and solar) into the classical systems. However, as the energy production stemming from RESs is extremely volatile and thus challenging to predict, new approaches have to be found in order to guarantee a successful integration of RESs into the existing infrastructure.

In the Austrian state of Burgenland approximately 1,000 MW of wind capacity is available. As already mentioned above, the high volatility of wind energy together with forecast uncertainties hinders the optimal integration of this RES into the existing energy system. Furthermore, the successful deployment of wind turbines was based on an attractive but timely limited subsidy scheme with a fixed feed-in tariff. As these subsidies now come to an end for more and more wind turbines and future support systems will rely on market premiums and tendering models, new approaches and business models have to be devised in order to sustain the rapid transformation of the classical energy systems.

In the research project HDH Demo in close cooperation with the city of Neusiedl am See, Burgenland, Austria, the aim is to integrate wind energy into the existing district heating grid of the city. This is realized by utilizing power-to-heat technologies, e.g., heat pumps. However, an economically feasible and successful integration is based on accurate forecasts for both, wind production and district heating demand as well as the actual energy prices.

Therefore, this work evaluates the applied data-driven forecasting methods. In particular, ensemble approaches that combine autoregressive models with artificial intelligent techniques are used to exploit the strengths of different methods (e.g. stability, flexibility). To compare the model performance, an overview on the accuracy and efficiency of the ensembles by using appropriate score metrics (e.g. RMSE, MAPE, R^2) is given. Furthermore, a mixed integer linear optimization model is presented for computing optimized schedules for the different components (e.g., heat pumps, energy storage units, biomass boiler) of the district heating grid. Together, these two approaches, forecasting and optimization, are used to investigate and evaluate different business models, which help to ensure the future market integration of wind production.

Keywords: forecasting, optimization, MILP, renewable energy sources.

Introduction

The transformation of the centralized energy system relying mostly on fossil fuels towards decentralized and sustainable systems is based on the rapidly rising amount of production by renewable energy sources (RESs). One of the most prominent RES is wind energy, followed by photovoltaic (PV) systems. Contrary to fossil fuel based power plants, which are available at a moment's notice and can be adjusted accurately following the actual demand, RESs are characterized by totally different and highly volatile production characteristics. For example, wind turbines provide energy only in times of wind and PV systems rely on the incident solar radiation, which can vary highly depending on daytime, weather and cloud conditions. Subsequently, it is rather challenging to accurately predict the energy production stemming from RESs. Furthermore, it is possible that, depending on the weather, the production from RESs exceeds the predictions. In such situations the excess energy has to be sold at a very low or even negative price and/or is causing balancing energy costs directly affecting the economic viability of the specific renewable energy system, for instance, wind turbines.

In Austria the economic viability of wind turbines is heavily dependent on the subsidies (i.e., fixed feed-in tariffs) from the Austrian settlement agency for green energy (OeMAG). However, these subsidies are limited by law to 13 years resulting in economically challenging situations for wind park operators after the subsidy period [1]. Hence, it is economically and environmentally utterly important to develop new business models and thus keeping the wind turbines in operation. Otherwise, the ambitious goals of transforming the energy system is jeopardized due to economically unsuitable legal conditions. A long-term economic perspective for wind turbines affects not only the continuing operation of already existing systems but incentivizes also the construction of new modern wind parks, even for community-based systems.

The presented work focuses on the development of the aforementioned novel business models and their underlying technical and economic requirements, such as forecasting approaches and computational optimization models. These requirements are essential to evaluate prospective business models before testing them in a real-world test bed, i.e., the Austrian city Neusiedl am See. Neusiedl am See is a city in the eastern federal state of Burgenland, located directly at the northern shore of the lake Neusiedl. The city is a perfect test bed as there are numerous wind turbines located in its direct vicinity, which are already at the end of their subsidy period and are already marketed on the liberated electricity market.

Additionally, there is a district heating system in the city providing a test scenario for evaluating sector coupling options for the electric, the heating, and the gas system. The sector coupling allows for an integration of the RES wind into the district heating system of Neusiedl am See, for example, via heat pumps creating already one novel business model.

Hybrid Energy System of Neusiedl am See

The hybrid energy system of the city of Neusiedl am See is comprised of the electric system, consisting of the local wind parks, which are directly connected to an electric storage system (ESS) and four different heat pumps (HPs). The ESS is used as a backup solution for safely shutting down the HPs in cases where abrupt changes in wind power occur and thus insufficient energy for powering the HPs is available and for bridging short term undersupply. Two of the aforementioned HPs are air-to-water HPs (denoted as H_1 and H_2) delivering heat energy to a first thermal storage unit operating at low temperature

(LT) (i.e., 30-40 °C and with a volume of around 14.000 liters). The remaining two HPs are water-to-water devices (H_3 and H_4) transferring energy from the first storage unit to a second thermal storage unit operating at 60-85 °C and containing about 18.000 liters. This second storage is directly linked to a thermal buffer unit, which is providing the heating energy for the district heating grid. If the HPs alone cannot meet the district heating demand, several options exist to provide backup solutions: 1) A biomass boiler (BB) connected to 2) a flue gas condenser (FC), and 3) a gas burner (GB). The aforementioned components of the hybrid energy system operate in two different modes denoted as *summer* and *winter* mode. In summer mode, the air-to-water HPs directly provide energy to the low temperature storage unit, whereas in winter mode they transfer the energy directly to the thermal buffer unit. Furthermore, the BB and GB directly provide heating energy in winter mode for thermal buffer unit and the FC transfers heat to the low temperature storage unit. Additionally, the optimization model utilized in this study is able to include an electrolyzer into the hybrid energy system, extending the sector coupling options to power-to-gas applications. Figure 1 gives an overview of the different components of the hybrid energy system.

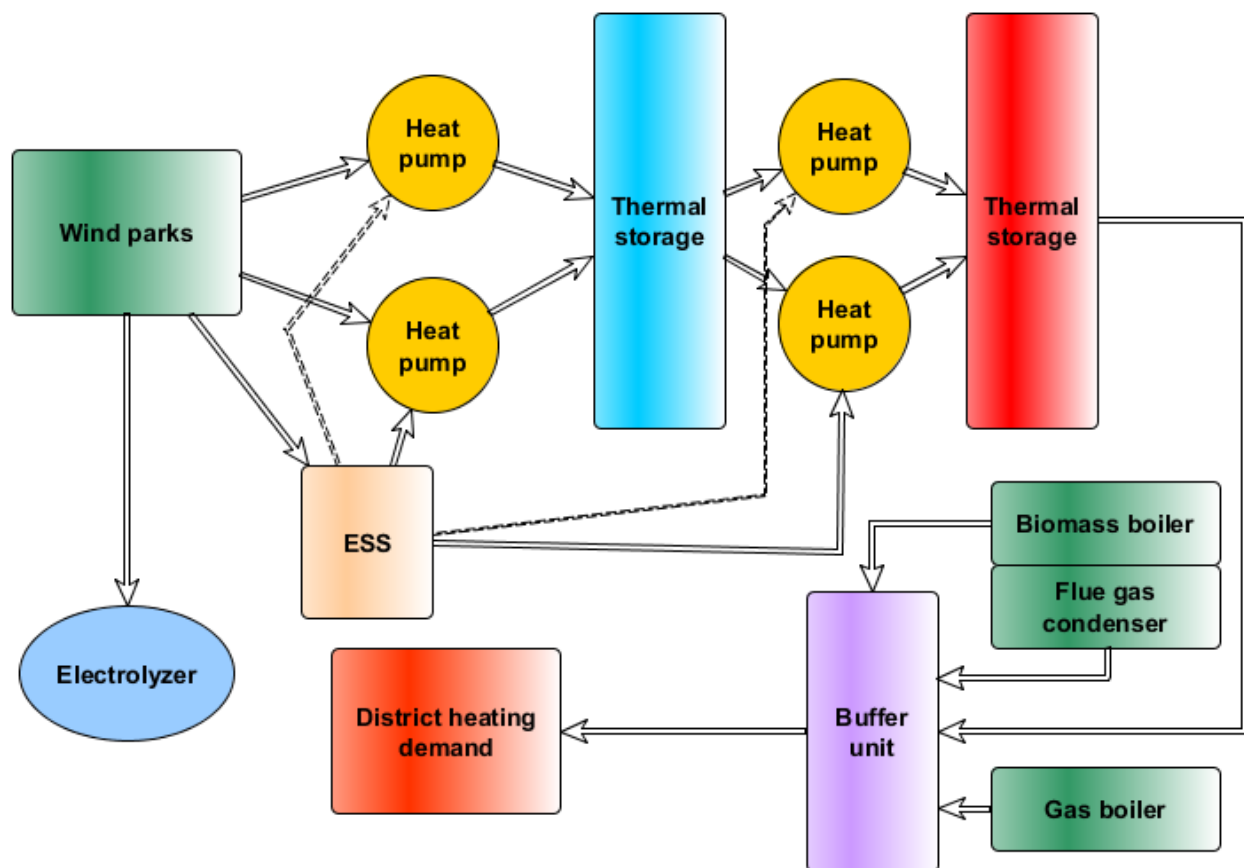


Figure 1 – Overview of the hybrid energy system of Neusiedl am See

Forecasting Approaches

To ensure an economically feasible and successful integration of RESs, accurate forecasts for district heating demand is needed. Research shows that the weather as well as the social behavior has most influence on the heat load in district heating grids [2]. The

outdoor temperature as well as the humidity correlates the most with the heat demand in a district heating grid [3]. Hence, these parameters are chosen as inputs for the investigated models. The social behavior is taken into account implicitly by using the day of the week and the current month as an additional input [4]. To capture the dynamics of the buildings which are connected to the heating grid also past values of outdoor temperature and humidity are used. The similar but different model structures, i.e., AI and NARX models, are summarized in Figure 2.

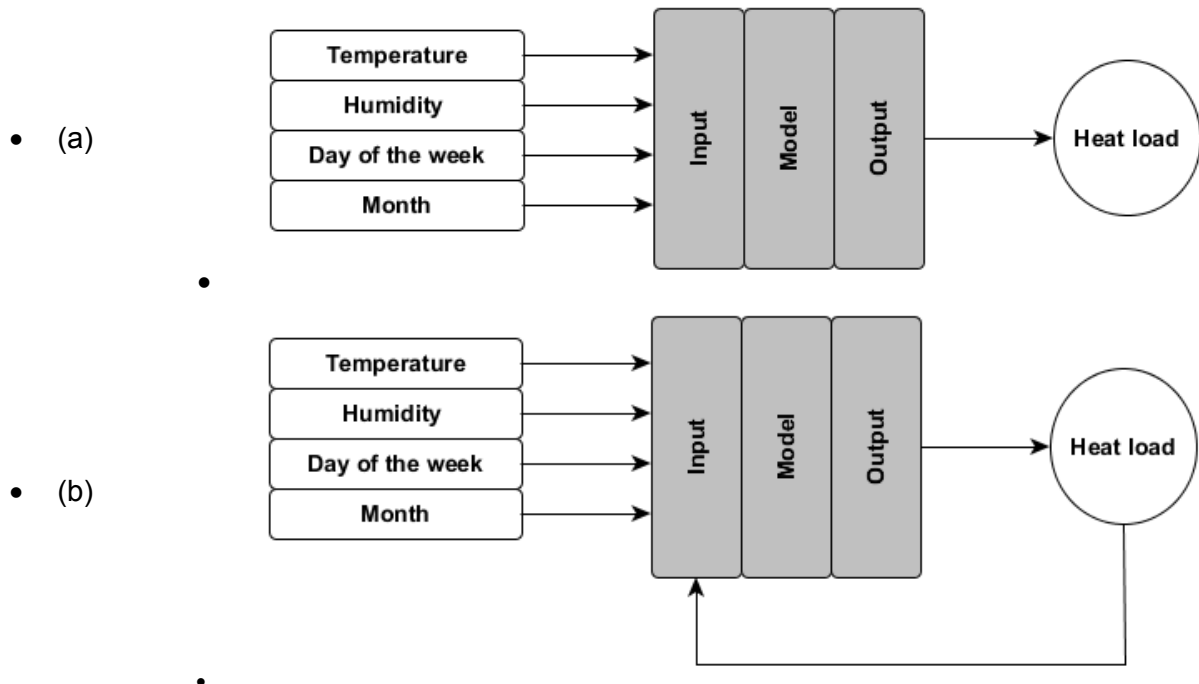


Figure 2 – Model structures of (a) AI and (b) NARX models

These models are used to generate realistic heat load forecasts for a specific time, based on weather data for the project region. In particular, three stationary artificial intelligence (AI) algorithms [5,6] i.e. Random Forest (RF) [7,8], k-Nearest Neighbor (k-NN) [9,10] and Artificial Neural Networks (ANN) [11,12], and a Nonlinear Autoregressive Exogenous (NARX) model [13] are utilized for creating the load models. Details on the models and their evaluation can be found in [14]. In this work, static ensemble approaches that combine these models to exploit their strengths due to flexibility of AI algorithms and stability of autoregressive models, i.e. mean ensemble (MENS), weighted mean ensemble (WENS), and seasonal weighted mean ensemble (SWENS) are used.

Static approaches assign a weight to each model in the ensemble, which is constant for all observations. MENS is the most common static approach, as it is the simple arithmetic mean of the predictions of the available models [15]. Furthermore, ensemble approaches, i.e., WENS and SWENS, which are weighted means and seasonal weighted means of the available models are applied. WENS uses the root mean squared error (see equation (1)) of the available models as weighting factor. SWENS additionally distinguishes between different seasonal errors.

The heat load was measured for a whole year in intervals of 15 minutes. 75% of the data are used as training set, whereas the remaining 25% of test data was split into four seasonal intervals. To compare the ensemble method performance, the metrics root mean squared error (*RMSE*), mean absolute error (*MAE*), and mean absolute percentage error (*MAPE*), as well as the coefficient of determination (R^2) are calculated, given by:

- $RMSE = \sqrt{\frac{1}{n} \sum_{i=1}^n (\hat{y}_i - y_i)^2}$, • (1)
- $MAE = \frac{1}{n} \sum_{i=1}^n |\hat{y}_i - y_i|$, • (2)
- $MAPE = \frac{1}{n} \sum_{i=1}^n \left| \frac{\hat{y}_i - y_i}{y_i} \right|$, • (3)
- $R^2 = 1 - \frac{\sum_{i=1}^n (\hat{y}_i - y_i)^2}{\sum_{i=1}^n (y_i - \bar{y})^2}$, • (4)

where \hat{y}_i is the predicted load, y_i is the observed load, \bar{y} is the mean of the observed loads, and n is the number of samples modeled.

Whilst the maximum heat demand in the district heating system is 785.70 kW, the average heat load of the network measured is 159.76 kW. As expected, the average heat load during summer is lower (68.64 kW) than in winter (409.51 kW).

Table 1 provides a comparison between the introduced ensemble models in terms of four statistical metrics that represent each model performance. In addition, the scores of k-NN as best performing individual model is listed as a baseline to compare the performance of the ensembles.

Table 1 – Evaluation of different approaches

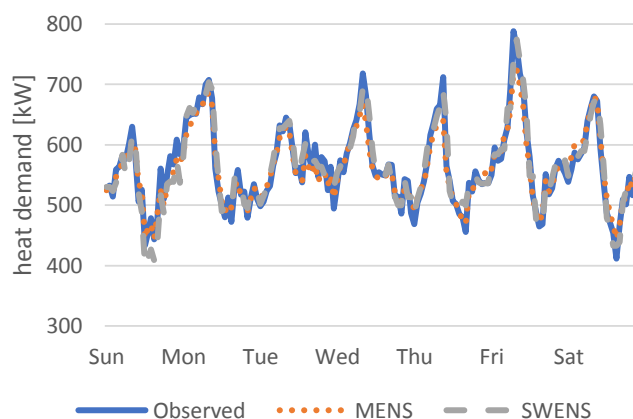
• • Metric	• • Method	• Test season				• • Overall
		• Winter	• Spring	• Summer	• Fall	
• RMSE	• k-NN	• 31.12	• 20.97	• 5.10	• 29.83	• 21.44
• [kW]	• MEN S	• 29.73	• 18.06	• 4.34	• 28.49	• 19.60
•	• WE NS	• 29.52	• 17.87	• 4.19	• 28.38	• 19.33
•	• SWE NS	• 29.62	• 17.90	• 4.08	• 28.40	• 19.34
• MAE	• k-NN	• 17.72	• 10.36	• 3.14	• 17.29	• 11.05
• [kW]	• MEN S	• 16.39	• 8.96	• 2.94	• 15.91	• 9.82
•	• WE NS	• 16.03	• 8.75	• 2.82	• 15.76	• 9.54
•	• SWE NS	• 16.19	• 8.78	• 2.67	• 15.78	• 9.51
• MAPE	• k-NN	• 4.98	• 9.23	• 5.79	• 5.81	• 8.62
• [%]	• MEN S	• 4.17	• 8.40	• 4.51	• 4.65	• 6.91
•	• WE NS	• 4.07	• 8.16	• 4.31	• 4.45	• 6.68

•	• SWE NS	• 4. 12	• 8. 19	• 4.0 9	• 4. 38	• 6.62
• R ²	• k-NN	• .9 6	• .9 5	• .90	• .9 4	• .96
•	• MEN S	• .9 8	• .9 7	• .92	• .9 7	• .98
•	• WE NS	• .9 8	• .9 8	• .92	• .9 7	• .98
•	• SWE NS	• .9 8	• .9 8	• .93	• .9 7	• .98

Table 1 reveals that all ensemble approaches outperform the single k-NN model in terms of each measure. In winter and fall, comparatively high values of MAE are determined while values of MAPE indicate better forecast properties for winter. Due to a reduced heat demand, RMSE and MAE measures in spring and summer are comparatively small. In terms of MAPE, spring measures compared with winter and fall are even worse, indicating a poorer adequacy for prediction. Spring seems to be the most difficult season for predictions regarding heat demand.

Figure 3 indicates the performance of MENS and SWENS models in a one-week-time span in winter and spring. The graph shows that MENS (dotted orange line) yields slightly less accuracy than SWENS (dashed grey line) in both seasons. In winter MENS is not able to reach some of the peaks and tends to underestimate the average heat load. In comparison to the other models, the most precise model regarding the error measures appears to be SWENS as it catches the observed values in winter quite well. However, problems can be detected in cases of daily peaks in winter. On the one hand, viewing the accuracy on Saturday in the test week, heat demand is rather underestimated. On the other hand SWENS ignores lower heat load peaks on Wednesday and Thursday. The test week in spring shows that MENS rather underestimates the daily peaks. In contrast, SWENS shows more accuracy in spring. However, some predictions still remain different from the observed values, confirming the reported error rates.

• (a)



• (b)

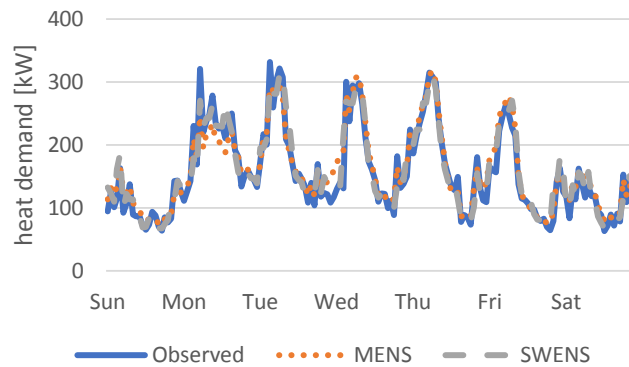


Figure 3 – Exemplary heat load values for a week in (a) winter and (b) spring.

Optimization Model

In order to model and simulate energy systems, various different approaches and methods exist. These range from using simple spreadsheet programs for small scale problems up to specifically designed modelling languages (e.g., GAMS [16], AMPL [17]) utilized to describe larger or more detailed systems. At the very core of each of these methods is the mathematical description of the system components. As the computational complexity is often directly affected by the number of components, it is of utmost importance to either keep the total number of modelled technical components as small as possible or to find simple but accurate mathematical descriptions of their behavior. The first approach is, however, not always possible as, for example, some systems of interest consist of numerous different components where their interaction is of major interest. Hence, different approaches for modelling the components are pursued in most of the scientific investigations

One prominent representative of these mathematical optimization or mathematical programming approaches is the so-called mixed integer linear programming method (MILP) [18]. Generally, a MILP optimization problem consists of an objective function and various constraints. The former is either minimized or maximized, whereas the latter define the value ranges for the variables. In a MILP formulation both, the objective function and the constraints, are linear with the particularity that some variables can only take integer values. For example, a variable denoting the status of a power plant can either be 0 or 1 for on and off, respectively. However, despite their often relatively straightforward formulation, MILP optimization problems are NP-hard [18] and thus potentially require enormous computational resources for optimally solving the mathematical optimization problem, depending on the actual problem formulation.

In order to evaluate the hybrid energy system in the city of Neusiedl am See, a MILP optimization model [19] has been developed to include various different sector coupling approaches, e.g., HPs and electrolyzers. At the core of the model in the research project is the objective function [19]

$$\sum_{t=0}^T C(t) = \sum_{t=0}^T \left(\frac{p_f}{\eta_{BB}} \cdot P_{th,BB}(t) + p_{v,BB} \cdot \sigma_{BMP}(t) + c_{start,BB} \delta_{BMP}(t) + p_g \cdot P_{th,GB}(t) - p_{el} \varepsilon(t) - p_{h2} \dot{m}_{pem}(t) + (p_{el} + p_{el,spread}) \cdot (P_{H1,el,grid}(t) + P_{H2,el,grid}(t) + P_{H3,el,grid}(t) + P_{H4,el,grid}(t)) \right) \quad (1).$$

Here, the first three terms describe the cost of the BB (biomass costs, variable costs and ramp up costs). The fourth term models the costs of the GB, and the following two terms reduce the overall system costs (i.e., selling excess energy and hydrogen). The last two terms model the electricity costs for the four different HPs.

As already mentioned above, the linear formulation of the objective function and constraints in a MILP optimization model is critical. Nevertheless, in reality there are numerous different examples of non-linear relationships. For example, the coefficient of performance (COP) value of a HP is denoted as

$$Q_{th} = COP(T) \cdot P_{el} \quad (2),$$

where $Q_{th}(t)$ is the thermal energy, $COP(T)$ the temperature dependent COP, and P_{el} the consumed electrical energy. Equation (2) is obviously a non-linear relationship and, thus, cannot be used as constraint in a MILP problem. Fortunately, utilizing a piecewise linear approximation, for example, as implemented in the *pyomo* framework [20], circumvents this particular issue. Although linearization is an approximation that comes with a certain error, choosing a suitable number of pieces for the piecewise approach proved to be a feasible option in preventing non-linearities in the MILP formulation of the hybrid energy system. For example, in Figure 4 two different linearization strategies are depicted for the summer and winter operation mode of one of the HPs in the hybrid energy system in Neusiedl am See. As the figure depicts, minor deviations between a simple linear approximation and the piecewise linear approach exist. Hence, for the given HP data the choice of the linearization method has negligible effect on the optimization outcome.

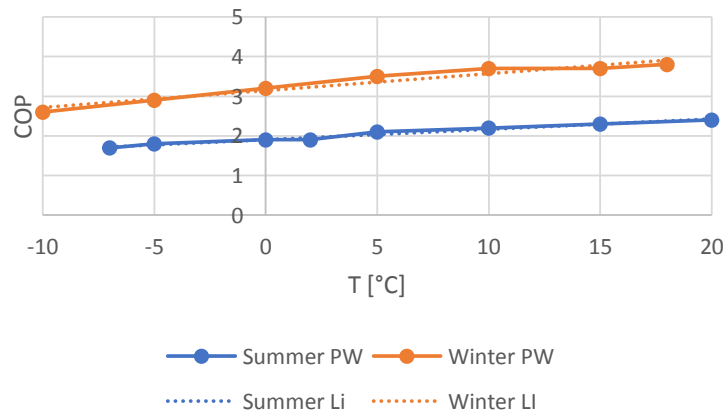


Figure 4 – Piecewise linearization (PW) and approximation using a linear function (LI) for an exemplary heat pump.

Another challenge occurring often while modelling energy systems is the description of minimal up- and down-times, for example, as it is the case for a BB. To formulate these constraints with linear equations the so-called Big-M method is utilized [18]. This formulation yields several inequalities given in equations (2)-(7).

- $switch_{BB}(t) = on_off_{BB}(t) \mid t = 0,$ • (2)
- $switch_{BB}(t) = on_off_{BB}(t) - on_off_{BB}(t - 1),$ • (3)

- $0 \leq -switch_{BB}(t) + M \cdot switch_{onBB}(t),$ • (4)
- $M \geq -switch_{BB}(t) + M \cdot switch_{onBB}(t)$ • (5)
- $0 \leq switch_{BB}(t) + M \cdot switch_{offBB}(t),$ • (6)
- $M \geq switch_{BB}(t) + M \cdot switch_{offBB}(t),$ • (7)

$switch_{BP}$ denotes the status of the switching operation at timestep t (i.e., -1 for switching off, 0 for no action and 1 for switching on) and the binary variable on_off_{BP} gives the status of the BB at a specific timestep. Furthermore, $switch_{onBB}$ and $switch_{offBB}$ are binary variables stating if a switching-on or -off operation is conducted at timestep t . Eventually, the minimum up- and down-times can now be formulated as constraints using sums over the binary variables $switch_{onBB}$ and $switch_{offBB}$.

Evaluation

In order to show the applicability of the forecasting and optimization approaches to the real-world test bed of Neusiedl am See, several different scenarios and business models for the hybrid district heating system of Neusiedl am See were set up. The first scenario utilizes only the HPs as consumers of the electric power provided by the regional wind parks. In the second scenario a 1.75 MW ESS is applied, whereas in the third scenario the ESS is replaced by a 17 MW electrolyzer as consumer. Finally, a fourth scenario with both, ESS and electrolyzer, is analyzed.

As first evaluation metric of the different scenarios the amount of excess energy is analyzed. This is the surplus energy from the regional wind parks around Neusiedl am See, which cannot be consumed in the hybrid district heating system. Figure 5 depicts the total excess energy over the course of a year. As the data indicates, the energy system extended with a 1.75 MW ESS experiences similar excess energy amounts as without an ESS. This is due to the fact that the capacity of the ESS is small compared to the amount of exceeding wind energy, particularly in times of high wind production. Additionally, for a real-world application the limited amount of charging cycles has to be taken into account. This particular property of ESSs is not reflected in the mathematical optimization model. Regarding the electrolyzer, the computational study shows that operation such a power-to-gas device reduces the amount of excess energy by a factor of about two. This seems quite promising, as the produced green hydrogen (i.e., production consuming electrical power originating only from renewable sources) can be used, for example, for regional public transport systems or sold to commercial customers. This alleviates the negative effects of dealing with unpredicted or enormously high excess energy on the balancing market. However, this simple analysis lacks a proper evaluation of the total expenditures for a power-to-gas technology would have to include operational expenditures (OPEX) as well as capital expenditures (CAPEX). As with today, these costs are one of the major obstacles of including hydrogen electrolyzers in existing energy systems. Fortunately, with further research effort and improvements the OPEX are going to decrease in the future. However, the CAPEX can still remain an issue, as high initial investments have to be amortized in a reasonable amount of time, otherwise electrolyzers will suffer from little to no economic attractiveness.

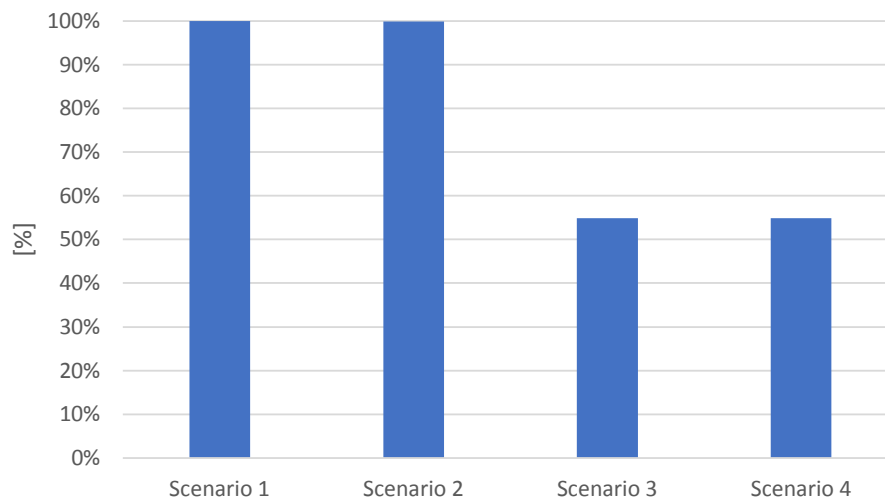


Figure 5 – Excess energy in the different scenarios.

Conclusions

The presented work shows how modern forecasting methods in their various forms together with mathematical optimization methods and techniques form a solid bases for a data-driven evaluation of future-fit energy systems, i.e., the hybrid district heating system of the Austrian city Neusiedl am See. A particular focus was lying on the integration of wind power via power-to-heat technologies, i.e., heat pumps, into the district heating system. However, a major share of wind energy has still to be sold on the regular energy market causing low or negative prices in some cases. Hence, different future technological options are evaluated, including the integration of an electrolyzer and an ESS. A computational analyses shows that utilizing a 17 MW electrolyzer reduces the amount of excess energy by a factor of about two, whereas a 1.75 MW ESS has negligible influence on the excess energy. Nevertheless, ESS are highly important components as they are used for safely shutting down wind power driven HPs when abrupt changes in wind power availability occurs. Furthermore, the work concludes that at the moment investment costs of electrolyzers pose the main challenge for including these power-to-gas technologies in existing energy grids. Therefore, political entities have to design appropriate and attractive subsidies or market structure to guarantee the ongoing transition of our classical energy systems. A successful implementation of funding opportunities helps to overcome the challenges of high initial costs for novel technologies as electrolyzers and, in addition, stimulate further research efforts in these directions. Together with novel business models and marketing strategies for unsubsidized wind energy the goal of a sustainable and fossil fuel free energy system can be successfully pursued.

Acknowledgements

The project “Hybrid DH Demo” is funded by the Austrian Climate and Energy Fund as part of the program “Smart Cities Demo”.

References

- [1] OeMAG. URL: <https://www.oem-ag.at/de/home/>. Accessed on 10 September 2020.
- [2] L. Arvastson. "Stochastic modelling and operational optimization in district-heating systems". PhD Thesis, Sweden, 2001.
- [3] H. Yang, S. Jin, S. Feng, B. Wang, F. Zhang, J. Che. "Heat Load Forecasting of District Heating System Based on Numerical Weather Prediction Model". *Proceedings of the 2nd International Forum on Electrical Engineering and Automation (IFEEA)*. 2015, pp 1-5. DOI: 10.2991/ifeea-15.20161.
- [4] H. Gadd, S. Werner. "Daily heat load variations in Swedish district heating systems". *Applied Energy* 106 (2013), pp 47-55. DOI: 10.1016/j.apenergy.2013.01.030.
- [5] J. Antonanzas, N. Osorio, R. Escobar, R. Urraca, F.J. Martinez-de-Pison, F. Antonanzas-Torres. "Review of photovoltaic power forecasting". *Solar Energy* 136 (2016), pp. 78-111. DOI: 10.1016/j.solener.2016.06.069
- [6] N. Fumo. "A review on the basics of building energy estimation". *Renewable and Sustainable Energy Reviews* 31 (2014), pp. 53-60. DOI: 10.1016/j.rser.2013.11.040.
- [7] L. Breiman. "Random Forests". *Machine Learning* 45 (2001), pp. 5-32. DOI: 10.1023/A:1010933404324.
- [8] G. Dudek. "Short-Term Load Forecasting Using Random Forests". *Proceedings of the 7th IEEE International Conference Intelligent Systems (IS'2014)*. 2014, pp 821-828. DOI: 10.1007/978-3-319-11310-4_71
- [9] S. Yakowitz. "Nearest-Neighbour Methods for Time Series Analysis". *Journal of Time Series Analysis* 8.2 (1987), pp. 235-247. DOI: 10.1111/j.1467-9892.1987.tb00435.x.
- [10] F.H. Al-Qathani, S.F., Crone. "Multivariate k-Nearest Neighbour Regression for Time Series data – a novel Algorithm for Forecasting UK Electricity Demand". *Proceedings of International Joint Conference on Neural Networks (IJCNN)*. 2013, pp. 228-235. DOI: 10.1109/IJCNN.2013.6706742.
- [11] C.M. Bishop. *Neural Networks for Pattern Recognition*. Oxford University Press, 1997. ISBN: 0198538642.
- [12] M. Hayati, Y. Shirvany. "Artificial Neural Network Approach for Short Term Load Forecasting for Illam Region". *International Journal of Electrical, Computer, and Systems Engineering* 1.2 (2007), pp. 121-125. DOI: 10.5281/zenodo.1328642.
- [13] L.G.B. Ruiz, M.P. Cuéllar, M.D. Calvo-Flores, M.D. Jiménez. "An Application of Non-Linear Autoregressive Neural Networks to Predict Energy Consumption in Public Buildings". *Energies* 9.9 (2016), p. 684. DOI: 10.3390/en9090684.
- [14] G. Steindl, C., Pfeiffer. "Comparison of Black Box Models for Load Profile Generation of District Heating Networks". *Proceedings of 12th Conference on Sustainable Development of Energy, Water and Environment Systems (SDEWES)*. 2017.
- [15] R.T., Clemen. "Combining forecasts: A review and annotated bibliography". *International journal of forecasting* 5.4 (1989), pp. 559–583. DOI: 10.1016/0169-2070(89)90012-5.
- [16] GAMS Development Corporation. "General Algebraic Modeling System (GAMS) Release 27.1.0". Fairfax, VA, USA, 2019.
- [17] R. Fourer, D.M. Gay, B.W. Kernighan. *AMPL: A Modeling Language for Mathematical Programming*. 2nd ed. Cengage Learning, 2002. ISBN: 0534388094.
- [18] G. Sierksma, Y. Zwols. *Linear and Integer Optimization*. CRC Press, 2015. ISBN: 9781498743129.
- [19] M. Schindler, L. Gnam, T. Nacht. "A simulation study on the integration of wind in a district heating system". *e-Nova International Conference on Sustainable Technologies (e-Nova)*. 2020. In press.

[20] W.E. Hart, C. D. Laird, J.-P. Watson, D.L. Woodruff, G.A. Hackebeil, B.L. Nicholson, J. D. Sirola. *Pyomo – Optimization Modeling in Python*. Springer International Publishing, 2017. ISBN: 9783319588193.

G0705

Readiness of Short-term Load Forecasting Methods for their Deployment on Company Level

**Thilo Walser (1,2), Martin Reisinger (1,2), Niklas Hartmann (3),
Christian Dierolf (1,2), Alexander Sauer (1,2)**
(1) Fraunhofer Institute for Manufacturing Engineering and Automation IPA
Nobelstraße 12, 70569 Stuttgart/Germany
(2) Institute for Energy Efficiency in Production EEP
Nobelstraße 12, 70569 Stuttgart/Germany
(3) Offenburg University of Applied Sciences
Badstraße 24, 77652 Offenburg/Germany
Tel.: +49 (0)711 /970 1974
thilo.walser@ipa.fraunhofer.de

Abstract

Short-term load forecasting (STLF) has been playing a key role in the electricity sector for several decades, due to the need for aligning energy generation with the demand and the financial risk connected with forecasting errors. Following the top-down approach, forecasts are calculated for aggregated load profiles, meaning the sum of singular loads from consumers belonging to a balancing group. Due to the emerging flexible loads, there is an increasing relevance for STLF of individual factories. These load profiles are typically more stochastic compared to aggregated ones, which imposes new requirements to forecasting methods and tools with a bottom-up approach. The increasing digitalization in industry with enhanced data availability as well as smart metering are enablers for improved load forecasts. There is a need for STLF tools processing live data with a high temporal resolution in the minute range. Furthermore, behind-the-meter (BTM) data from various sources like submetering and production planning data should be integrated in the models. In this case, STLF is becoming a big data problem so that machine learning (ML) methods are required. The research project “GaIN” investigates the improvement of the STLF quality of an energy utility using BTM data and innovative ML models. This paper describes the project scope, proposes a detailed definition for a benchmark and evaluates the readiness of existing STLF methods to fulfil the described requirements as a reviewing paper.

The review highlights that recent STLF investigations focus on ML methods. Especially hybrid models gain more and more importance. ML can outperform classical methods in terms of automation degree and forecasting accuracy. Nevertheless, the potential for improving forecasting accuracy by the use of ML models depends on the underlying data and the types of input variables. The described methods in the analyzed publications only partially fulfil the tool requirements for STLF on company level. There is still a need to develop suitable ML methods to integrate the expanded data base in order to improve load forecasts on company level.

Introduction and Motivation

The German energy market changes in view of the energy policy objectives of a sustainable energy system with guaranteed security of supply at low prices. Top-down organized power plant parks with one-dimensional flow of electricity to the consumer must change to a system of power generating prosumers who consume their own generated electricity and manage their own demand. In an energy system focused on decentral generation, prosumers can now trade energy and charge costs, act in a micro grid connected to the power grid or join together as a self-sufficient community in a closed micro grid [1].

Prosumers, renewable energy and changes in load flow increase the complexity in terms of security of supply. In this context, the balancing group is the central coordination element to ensure the quarter-hourly balancing of electricity load and generation. All electricity consumers and electricity suppliers are organized in balancing groups, for each of which a balancing group manager bears the economic responsibility. In the balancing group, area forecasts are prepared, broken down by profile and measured end customers like industrial companies. Thus, even today, an improved forecast has a direct impact on the security of supply and on the costs of balancing energy. In an energy system focused on prosumers, the demands on the quality of the forecast are growing, due to the different electricity flows. Especially short-term load forecasting including knowledge of behind-the-meter (BTM) data will become more important for improving the load forecasting task of energy providers [2].

Regarding the industrial sector, load forecasts in industrial energy systems will become more important in the future. This is due to upcoming relevance of energy flexibility measures [3], where load forecasts serve as a basis for flexible energy consumption behind the utility meter in the micro grids of the production facilities. Currently, demand side management in Germany mainly focuses on company internal management of single controllable loads, which enables to reduce fees for grid use and, therefore, focuses on the prediction of load peaks. For the offering of flexibility in grid and system flexibility markets each single load must be controllable through external management [4] and, therefore, the focus is currently mainly on large industrial loads. Elements of energy sensitive production planning and control concepts [5] are already implemented by fast movers [6] to enable the use of upcoming variable tariffs offers [7]. This approach needs an integration of energy and production data. Besides demand flexibilities, there is also a growing capacity of distributed generation and storage technologies in these micro grids, where new control strategies on systems [8] are based on short-term load forecasting (STLF) with a need for high accuracy. Beside the described applications of STLF in an industrial company there is also a growing relevance for high quality load forecast on the grid connection point for distribution system operators (DSOs), for enabling the optimal grid integration of these emerging flexible loads into the upstream mid-voltage grid of these DSOs [9].

Our research hypothesis is that energy utility companies can, even today, improve their forecasting accuracy in STLF using the bottom-up approach through integrating BTM data from load measurement systems of individual industrial customers. This would be a first step towards the above listed future needs. Currently, utility companies cannot access BTM data. Though in Germany there would be a significant theoretical rollout potential for this improvements, as there are already up to 70.000 licenses for energy managing software [10] and we assume that these licenses are used to manage BTM data. The potential is even predicted to grow, as on the European level a market forecast estimates a market volume tripling for this product segment until 2025 [11].

The research project “GaIN” develops and benchmarks new forecasting methods to meet future requirements for STLF forecasts in industry. The objective is to improve the accuracy of forecasts on company level by using real-time data with higher temporal resolution than the current standard as well as submetering behind the utility meter and production planning data. Methods which are able to integrate the new data types and sources are required. Further requirements to the methods are an automated implementation and an applicability for a large number of company types.

A wide-ranging review of load forecasting methods was already published in 2010 [12] and in 2020 [13]. In [14], commercial software tools are reviewed including a comparison on forecasting method level. Other than existing reviews, this paper focusses on industrial load forecasts on company level. The objective is to review state-of-the-art methods that totally or partly meet the requirements of the GaIN project mentioned above. The paper is structured as follows: Section 1 describes basics for defining and evaluating forecasting models. Section 2 and 3 review classical and Machine Learning methods, respectively, with regard to the project requirements, in order to assess the readiness. Section 4 concludes the work and gives an outlook regarding future work.

1. Basics of Load Forecasting Models

In none of the analyzed research papers, a detailed definition of load forecasting terms and factors influencing the load of industrial companies is contained. This chapter gives a comprehensive definition of terms and basic load forecasting principles.

1.1 Load forecasting terms and definitions

Relevant forecasting terms are demonstrated in Figure I and explained in this section. In STLF, a load profile is predicted at time t for a forecasting period up to one week ahead [15]. The forecasting period is the time interval between the first forecasted value at time t_0 and the forecasted value furthest in the future at time t_h . Forecasting models require an equidistant temporal resolution Δt meaning a uniform interval between input data points. The model output is a forecasted profile with the same Δt as the input. In case that no real time data exists, a time lag of the last available load measurement results, which is denoted as d . The forecasting horizon h describes the time interval between the last available load measurement and the forecast furthest in the future. Load forecasts are updated with an actualization frequency which depends on the frequency of input data transfer.

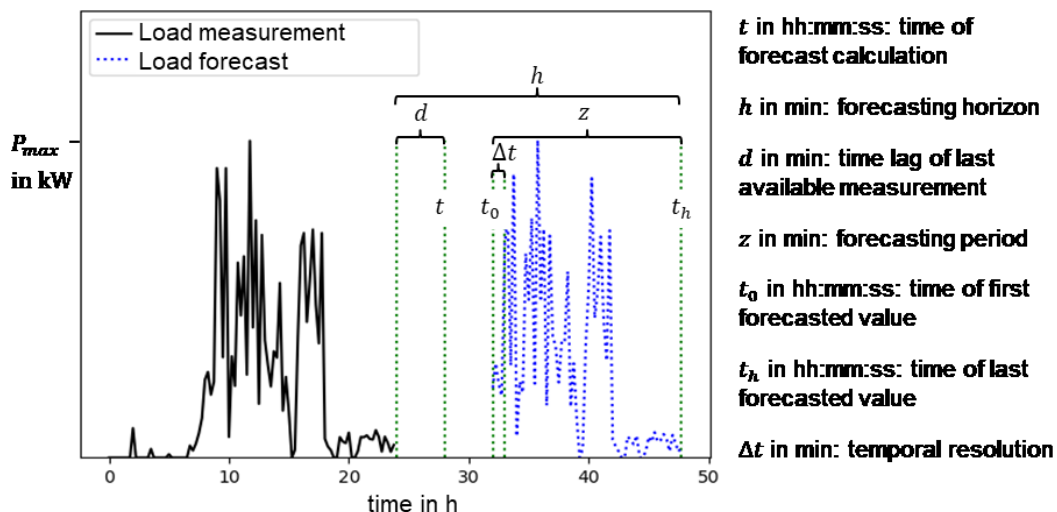


FIGURE I. LOAD FORECASTING TERMS

1.2 Load influencing factors

Factors influencing the load profile of industrial companies can be either static factors or relevant variables [16]. Static factors like the company building size or the number of work shifts in a week are normally not changing routinely [16] and, therefore, they are not considered in STLF models. Relevant variables, in contrast, change by routine [16] and cause daily, weekly and seasonal fluctuations of load profiles. Inputs for forecasting models can be both endogenous inputs which are previous load values, and exogenous inputs which are the relevant variables. The relevant variables for the electric load are dependent on weather, on production or on work shifts. The individual factors are further specified in this section.

Components of the technical building equipment have a mainly weather-dependent load [17]. The load of heating and cooling systems depend on the out- and inside temperature and the solar radiation. For ventilation systems, the load is mainly influenced by the out- and inside temperature and the relative humidity. The electric load of lighting depends on solar radiation. Weather service companies provide both historical weather data and forecasts. The available variables and temporal resolution depend on the provider [14].

In addition to weather influences, the building occupancy and the user behavior as well as the thermal loads through lighting [18] and the production process influence the electric load of technical building equipment.

A further influence on the electric load of industrial companies is the production quantity, which is affected by the economic situation. A typical load profile of a production process is disturbed both by irregularities predictable in the long-term (company holidays, public holidays or extra off days) and by short-term irregularities (short-term change of order situation or machine failure).

In case of self-generation plants for electricity, the purchased electricity depends on the self-produced amount, which is another irregularity. For companies with photovoltaic (PV) plants, the grid load is reduced in case of higher PV power generation, which is mainly influenced by solar radiation. Electricity storages and charging stations for electric cars are additional irregularities on the grid load [19].

The portfolio effect describes that irregularities of individual customers can balance each other out causing a more uniform load profile for balancing groups [20]. Thus, if the load is forecasted with the top-down approach, not all the mentioned influencing factors need to be included in a model in order to get accurate forecasts [21–25]. However, forecasts on company impose new requirements thus STLF models including the relevant variables mentioned above are needed.

1.3 Load measurement, data acquisition and preprocessing

In Germany, metering with a temporal resolution Δt of 15 min is obligatory for companies with an annual electricity consumption exceeding 100.000 kWh [26]. Energy utility companies receive metering data of the preceding day with a delay d . BTM data from load measurement systems of transformers on secondary level or even on machine level are currently not accessible to energy utility companies. They usually cannot access production data and company holidays as standards for transferring the data are not implemented. Furthermore, privacy issues complicate the use of company-specific data.

In forecasting models, data from different sources need to be converted to a uniform format. In data preprocessing, resampling methods like interpolation are applied to achieve equidistant time series. Missing and implausible data need to be identified and replaced with imputation methods [27]. A common source for implausible data are measurements

equal to 0, when the company actually takes electricity from the grid. BTM data can help to identify those. Further model specific preprocessing steps, which are required mainly for ML models, are explained in sections 2 and 3.

1.4 Evaluation metrics and benchmark

While implementing a forecasting model for a use case, metrics serve to compare different model types. Furthermore, metrics are required to monitor and evaluate the forecasting accuracy of a load forecasting service in operation. A wide range of metrics are applied in STLF research papers while no consensus about a standard metric exists [28].

The target quantity for energy utility company is the balancing energy that corresponds to the absolute error of forecasted load integrated over time. As this value is dependent on the observation period, the mean absolute error (MAE) [28] is a more comparative metric. The objective functions of optimization algorithms in regression models generally apply the mean squared error (MSE) [28]. If using the MSE as a metric, the model is evaluated for the optimization criteria. Moreover, the MSE raises importance of the highest errors, thus, it is recommended if high errors are particularly harmful. The root mean squared error (RMSE) converts the MSE to the same unity than the target.

Relative metrics are calculated as an attempt to evaluate the forecasting accuracy more independent of absolute load values. The mean absolute percentage error (MAPE) is the most common relative metric [28]. It is mathematically undefined if the load measurement equals 0 and emphasizes errors on load measurements with low values. This argument gains importance for forecasts of individual customers where the load profile is less uniform than for balancing groups. For forecasts of individual customers, the relative MAE or RMSE are, therefore, recommended as relative metrics rather than the MAPE.

After developing new forecasting models, a benchmark is important, as the forecasting result depends on both the model and the data set. Comparing relative metrics to reference values from literature calculated on different data sets is, therefore, insufficient to evaluate the ability of a model to outperform state-of-the-art models. Furthermore, evaluating a method on data sets from multiple companies can prove its generalization to different use cases.

2. Classical Forecasting Methods

As a first step, STLF models are classified into classical and ML methods based on a literature review. Among the classical approaches presented in this section are reference-based, statistical and analytical methods. Journal publications were systematically reviewed evaluating the readiness of the models to be used as forecasting tool for industrial companies. The temporal resolution of both input and target data as well as the types of input variables serve as evaluation criteria. In addition, the possibility for deployment of the models is evaluated amongst others by online learning methods [29]. Publications with benchmark of their presented method to at least one state-of-the-art model are favored in terms of comparability. As a result, a tabular overview of publications focusing on classical forecasting methods and their accordance with the evaluation criteria is given in Table I.

OVERVIEW OF PUBLICATIONS FOCUSING ON CLASSICAL FORECASTING METHODS WITH REGARD TO PROJECT REQUIREMENTS

Authors	Analyzed object	Industrial load?	Submetering data used?	Production planning data used?	$\Delta t < 15$ min?	Online learning method	Applied methods or models (ML methods in bold)
Bracale et al.	Transformer factory	Yes	No	No	No	No	SN, LR
Bruce-Boye et al.	Aggregated load of households	No	No	No	No	No	Reference-based, ES, ARIMA
Clesle et al.	Only method description	Yes	Yes	No	No	No	Analytical
DIN SPEC 91366	Only method description	Yes	Yes	Yes	No	No	Analytical
Emde et al.	Industrial company	Yes	No	No	No	No	Reference-based
Schmidt et al.	Factory for electricity network components	Yes	Yes	Yes	Yes	No	Analytical

2.1 Reference-based methods

Reference-based methods address the cyclic behavior in load profiles. The load at time t_i is defined by a reference value with similar characteristics.

In a seasonal naive (SN) model, the forecasted value is equal to a measured value of a preceding day, week or year, depending on the historical data and the cyclic behavior. In [30] an SN model with reference value of the preceding week is used as benchmark for a linear regression model. In moving average (MA) models, the reference value is the average load of a predefined number of preceding days, weeks or years. The number of preceding time steps for calculating the average depends on the load fluctuation and the desired smoothness. MA models are used in a commercial forecasting software to roll out load profiles with special considerations of public holidays [31].

Another common reference-based method is to forecast the load of a subsequent day with a comparative profile. This profile can be either a standard load profile or customer-specific. Energy utility companies forecast the load of small-size customers with nine different standard load profiles for each customer type considering differences between weekdays and the weekend and seasonal differences in load. If a load measurement is provided, customer-specific profiles can be calculated and the number of reference profiles can then be adapted to the use case. A case study on aggregated household data demonstrates that with a higher number of reference profiles the forecasting accuracy is improved compared to the standard of nine profiles. Scaling reference profiles with recent load measurements enables to integrate real-time data in the model and reduce the forecasting error by 9 % [20].

In [32] the load of an industrial company is forecasted with a reference-based method including temperature forecasts as exogenous input. In the presented method, the identical day of the week and the lowest mean daily temperature difference to the forecasted day within the preceding weeks is defined as reference day. The forecasts then correspond to the measurements at that reference day. In this use case, the load is rather cyclic and temperature-dependent. The method was not tested yet for use cases with higher irregularities in load profiles.

Reference-based methods find wide-ranging application in industry are reliable if the load behavior is cyclic. The ability to integrate exogenous variables in reference-based models is restricted. Therefore, regression models are more appropriate for load profiles with higher irregularities and unusual influencing factors than reference-based methods.

2.2 Statistical methods

Statistical forecasting methods are classified into univariate and multivariate methods. Applying univariate time series modelling, a time series is forecasted exclusively based on

preceding values of the identic variable. Exponential smoothing (ES) models give more weight to recent compared to earlier values introducing the smoothing parameter α . In [20] it is demonstrated that in ES models the forecasting accuracy drops significantly with the steps ahead predicted. The forecasting error is higher than with the reference-based method for forecasts of more than two steps ahead. ES models are, therefore, not suitable for forecasting load profiles one day ahead with high temporal resolution.

ARIMA usually defines a model family of univariate time-series modelling. The order of autoregression (AR), integration (I) and moving average (MA) are adapted to the data set within model calibration. If the order of a part is equal to 0, the part is left out in the model denotation, so that AR or ARMA models belong to the ARIMA family. For multi-step-ahead forecasts the output calculation is proceeded recursively resulting in a propagation of forecasting errors [12]. Similar to ES models, the ARIMA models are not accurate for multi-step-ahead forecasts, which is evaluated in [33].

Univariate regression models can produce accurate forecasting results if the load depends only on one exogenous variable. Univariate regression models are often applied for heating or cooling load with temperature as relevant variable [32]. Depending on the type of correlation, linear, polynomial or spline regression is appropriate. In [20], an univariate linear regression (LR) model with different regression parameters for every time step at each day type is applied to forecast household data with the top-down approach. No significant accuracy improvement is achieved compared to the reference-based method due to low temperature dependency of the load. In [34], the load of a research factory is forecasted with 47 relevant input variables. A multivariate regression model is not suitable for this application due to the high input vector dimension. In several other papers, linear regression models are used to benchmark Machine Learning methods [22, 35, 36]. If the load has irregularities and if exogenous variables are available, Machine Learning methods are more accurate than regression models.

Time-series modelling and LR is combined in ARIMAX models. In [37] is demonstrated that for forecasting the load of electric cranes, an ARIMAX model with crane movements and moved weights as exogenous inputs outperforms an ARIMA model with a MAE reduced by factor 3,7 as the load is correlated with those two relevant variables.

2.3 Analytical methods

In [38] an analytical method is described comparing control parameters of planned production processes with historical control parameters. The load profile with the smallest deviation in control parameters is used as reference profile for the forecast. Thus, the forecast is based on a comparison of control parameters and without a sophisticated mathematical model.

In [39], an analytical method to assign a factory load to products using resource data is described. A detailed measurement concept is required in order to obtain load series for all relevant manufacturing steps. A product-specific load is identified by matching the load with the resource data. Applying the method for forecasting, production and resource planning data is needed. The load part, which is not assignable to a product but to a machine, is forecasted depending on the operating status of machines. The remaining load is forecasted with reference-based or statistical methods. [40] describes a comparable method with a detailed strategy for measurement and analysis strategy for different machine classes as well as the possibility to use CAD Data for replacing missing production planning data. The application on a factory for electricity network component shows that machines are classified into categories in a non-automated way. Furthermore, the definition of model parameters is not automated and thus require data analytics effort and some degree of expert knowledge.

Due to the mentioned effort for data analytics and required expert knowledge, STLF with analytical methods is discarded in the GaIN project. Machine Learning methods are preferred as the model flexibility and degree of automation is higher, which is further specified in section 3.

3. Machine Learning Methods

Table II gives an overview of publications with ML methods applied for STLF.

When applied for forecasting, the task of Machine Learning (ML) models is to solve a regression problem, like in statistical regression models. The difference is that ML models compute a nonlinear function between the input and output. The model parameters are optimized in an iterative way during model training. ML models are thus characterized by a higher model complexity compared to linear models. The models achieve a higher ability to generalize regression results to new data and, therefore, a higher performance on time series with irregularities. If a single model is applied for regression, high-dimensional input vectors can cause overfitting problems, meaning that the model has a low capability to generalize to unseen data. This can be solved combining multiple regressors either in parallel or in series in an ensemble or hybrid model [41].

OVERVIEW OF PUBLICATIONS FOCUSING ON MACHINE LEARNING METHODS WITH REGARD TO PROJECT REQUIREMENTS

Authors	Analyzed object	Industrial load?	Submetering data used?	Production planning data used?	$\Delta t < 15$ min?	Online learning method	Applied methods or models (ML methods in bold)
Alasali et al.	Electric cranes	Yes	No	Yes	Yes	No	ARIMA, ARIMAX, MLP
Benedetti et al.	Building	No	No	No	No	Yes	MLP
Buch et al.	Only method description	Yes	No	Yes	No	No	MLP
Chahkoutahi et al.	Region	No	No	No	No	No	SARIMA, MLP , ANFIS, Hybrid model
Charytoniuk et al.	Customers of energy utility	No	No	No	Yes	Yes	MLP
Chen et al.	Aggregated load of households	No	No	No	No	No	Ensemble, ANN, Hybrid model
Dietrich et al.	Research factory	Yes	Yes	No	Yes	No	ANN
Fan et al.	Distribution grid	No	No	No	No	No	SVR , Hybrid model
He et al.	Milling and grinding machine	Yes	Yes	No	Yes	No	CNN
Kim et al.	Aggregated load of households	No	No	No	No	No	ARIMA, GPR, SVR , NARX, LSTM, Hybrid model
Li et al.	Region	No	No	No	No	No	Ensemble
Mori et al.	Not named	No	No	No	No	No	MLP , DTR, Ensemble
Petroşanu et al.	Industrial bakery	Yes	No	No	No	No	NARX , LSTM, Hybrid model
Renner et al.	Airport	No	No	No	No	No	LR, Ensemble
Setiawan et al.	Region	No	No	No	No	No	LR, SVR , MLP
Walther et al.	Research factory	Yes	Yes	No	Yes	No	LR, Ensemble

3.1 Single model approaches

In [22], the load of a region is forecasted five minutes ahead comparing a Multilayer Perceptron (MLP) and a Support Vector Regression (SVR) model, both ML models with an LR model and a naïve benchmark. An MLP belongs to Artificial Neural Networks (ANN), which are mathematical models inspired by biological nervous systems with interconnected computational units, the so-called neurons. Multiple ANN types exist differing in architectures. SVR is an ML model using nonlinear kernel functions as decision boundaries. The load is predicted using the four preceding load values and the values

from corresponding times of the previous day as features. Calendar variables as additional features do not improve the forecasting accuracy in this use case. Regression is superior to the naïve approach of setting the forecasted value equal to the last measurement. Neither the SVR nor the MLP outperform the LR model in terms of accuracy, however the training time raises significantly. The hyperparameters which define the model architecture, regularization or the training algorithm, are set as fixed values in [22]. Hyperparameter tuning and evaluation of different combination on a validation data set with data not contained in the training set enables to adjust the values to a use case. With hyperparameter tuning, the ML results could, therefore, be further improved. The proposed method is only valid for a one-step ahead prediction. For multi-step forecasts, recursive predictions would be required leading to a propagation of forecasting errors.

In [37], an MLP is benchmarked to time series models (section 2.2) to forecast the load of an electric crane, which is an industrial application. The MLP architecture is defined by two hidden layers with node numbers optimized with grid search. Compared to an ARIMAX model, the MAE is reduced by 8 % with an MLP. This study proves that ML models can be advantageous compared to statistical model in terms of accuracy. Furthermore, providing context data (crane movements and moved weights) that is correlated with the load, results in significantly lower forecasting errors. However, it is assumed that values for those variables are already certain at the forecasting time for 24 hours ahead. Furthermore, an upscale on industrial company level would enlarge the data amount and, therefore, the input vector dimension. A single model is then likely to cause overfitting problems.

Recurrent neural networks (RNN) are an ANN type with feedback connections which help to capture dynamic behavior of time series. In [33], LSTM and NARX models, which are both types of RNN, are compared to an ARIMA model to forecast the load of a business building. The load is forecasted exclusively on endogenous variables. Seasonal effects and periodicity in the load series are identified using decomposition as feature extraction method. The LSTM outperforms the ARIMA model for different forecasting horizons, while the NARX model achieves no improvement. When combining an LSTM with Virtual Mode Decomposition, the forecasting error is reduced significantly compared to the LSTM without decomposition. The proposed method takes the latest load measurement as initial state, which is the input for the first LSTM that forecasts the load at t_0 . For multi-step ahead forecasts, multiple LSTMs are stacked receiving inputs from upstream LSTMs. This enables a recursive prediction up to 72 hours ahead. For forecasts with multiple input variables, the model would need to be extended to incorporate additional time series.

In [42] the load on machine level for both a milling and a grinding process is predicted using one minute machinery data series as inputs. The local outlier factor (LOF) is applied to determine implausible data. It is demonstrated that a novel feature extraction method based on a Convolutional Neural Network (CNN) outperforms both a statistical method and a principal component analysis. A CNN-based regression model outperforms an Extreme Learning Machine (ELM), which is an ANN with one hidden layer relatively fast to train, on calculating the instantaneous load as function of the features for both the grinding and the milling machine. Furthermore, the CNN outperforms an SVR and a Gaussian Process Regression (GPR) model. The presented approach thus allows to predict a load based on multiple time series of the preceding minute. Using the approach as forecasting method would require the forecasted machinery data in addition to instantaneous and historical data.

3.2 Multi model approaches

Regression models are combined with the idea to profit from the strength of each base regressor to build a more performant model. In ensemble learning, base models are

homogenous, meaning that the model type is the same. The base models differ in architecture or in their initial random model parameters. A third approach is to use different subsamples of the training set for each base model [36].

Base models can be combined by bagging, by stacking or by boosting. In [41] an ensemble learning model is presented where the base models are MLPs with identical architecture trained with different subsamples. The ensemble learning model is constructed in a parallel structure either by bagging the base models, where the output is the mean of the base model outputs, or by stacking them, where the base model outputs are weighted. The daily average load of a household is forecasted one day ahead. The proposed stacking approach leads to a lower forecasting error with a MAPE of 14 %, which is lower than with bagging (15 %) and with one MLP as single model (18 %). All considered ML models have a significantly lower MAPE than the SN model (30 %). The load is mainly influenced by time stamp variables and temperature, which is not the case for industrial applications. A modification of the method in [41] would therefore be required to apply it on company level.

Decision trees are likely to cause an overfitting problem like in [43] where the forecasting error is significantly higher compared to an MLP. The python scikit-learn framework offers ensemble learning models with decision trees as base regressors which are supposed to reduce the overfitting problem of decision trees. Among those are Random Forests (RF) and Extremely Randomized Forests (ERF), which both are bagging methods. Gradient-Boosting Regression Trees (GBRT) is a boosting approach meaning that individual base models are added in series depending on the results of preceding base models. In [34] the load of machines in a research factory is forecasted 15 minutes ahead with a temporal resolution of one minute. The data set consists of measurements from 1670 sensors. The model input are sensor measurements shifted by 15 minutes. With feature selection, the input dimension is reduced to 47 relevant features. The load is forecasted with RF, ERF and GBRT using hyperparameters tuned with randomized search. All models lead to a comparable forecasting accuracy, but the GBRT is favorable in terms of training time. In order to develop the final model, feature engineering is conducted with moving average features. The input dimension is then doubled and hyperparameter tuning is repeated for the GBRT. The general load course is forecasted accurately but the model suffers from recognizing short peaks.

[44] is a further development of [34] by considering multiple forecasting steps between 0 and 100 s and by adapting the proposed method on four different machines. An ANN with one hidden layer is used for prediction as it is superior to RF in terms of accuracy. Besides moving average features, time lag features from multiple step in the past are used. The randomized search is refined with a subsequent grid search in the area of the best hyperparameters proposed by the randomized search. The time when short peaks occur are correctly forecasted, but the peak values are erroneous as the sampling rate is not high enough. The proposed method is able to generalize for multiple machines, but the hyperparameter tuning needs to be repeated for each machine. Especially the test performance declines significantly with an increased forecasting horizon. The authors conclude that including production-planning data in the model could improve the result especially for higher forecasting horizons. For an application in GaIN, the proposed method would need to be adapted for much higher forecasting horizons up to a day and for forecasts on company level.

In contrast to ensemble learning, hybrid models consist of heterogeneous base models. In [45] the daily load of an industrial bakery is forecasted by a NARX with calendar variables as exogenous inputs. An LSTM is trained in a decoupled way using time stamp variables and the daily load as input to forecast the hourly load. The hyperparameters defining the NARX and LSTM architecture are tuned with a grid search, both for three different training algorithms. In test mode, the NARX and LSTM are connected in series to build a hybrid

model where the LSTM receives the NARX forecasts of daily loads. The proposed approach leads to an RMSE reduced by factor 10.3 compared to a NARX as single model for month-ahead hourly forecasts. In reference to an LSTM as single model, the forecasting error reduction factor equals 16.8. This method allows to build a model which is relatively fast to train, as the base models are trained independently of each other. Furthermore, the hybrid model provides accurate multi-step ahead forecasts. In order to apply the method for STLF on company level, further exogenous inputs would need to be included in the model.

The hybrid model proposed in [25] consist of self-organizing maps, which classify days in normal and unusual days, and 24 SVR models for each day type. Each SVR forecasts an hour of the day resulting in an hourly temporal resolution. The model receives endogenous inputs of more than 24 hours before the forecast, meaning that the forecasting horizon is 24 hours. The temperature forecast of the corresponding hour is used as exogenous input. With this approach, the MAPE is reduced by 25 % compared to a single SVR model. The SVR outputs rather uniform daily load profiles while the hybrid model is able to identify days with lower load. With the proposed configuration, no real-time data is included, as the endogenous input are at least 24 hours past for each forecasted time step. Different input configuration for the parallel SVR would enable the method to forecast multi-step ahead with real-time data.

In [24], one ELM is used to forecast the load of a region for each hour of a day. Thus, 24 ELM are stacked to an Ensemble. The load series preprocessed with wavelet decomposition and two exogenous inputs, which are the temperature and the day of the week, are selected as input variables. Due to the parallel structure of the Ensemble model, less training examples per ELM are available. However, the Ensemble has separate regression parameters for each hour of the day. Furthermore, different inputs can be defined for each hour, which enables to forecast 24 hours ahead based on real-time data. The proposed model leads to a MAPE reduced by 20 % compared to a Wavelet-ELM as single model. Moreover, it is demonstrated that stacking is slightly better in terms of accuracy than bagging. The proposed method is evaluated on five data sets from literature. In all cases, it forecasts the load more accurately than state-of-the arts approaches. However, with the proposed input configuration the model is restricted to loads where calendar variables and temperature are the main influences. The model would need to be adapted to include further relevant variables.

3.3 Online learning methods

The presented methods in 3.1 and 3.2 result in static models: While testing the model, no retraining with new data is conducted. Retraining a model during the operation as forecasting service enables to consider changes in the load behavior not contained in the training data. In [15] a method with daily retraining is presented for a model constructed with one MLP for each forecasted time step. The retraining method is growing training: The model is updated using the whole data set. In [46], event-based retraining is presented where the model parameters are updated once the forecasting error exceeded a threshold. Growing training is compared to mobile training where the training set is shifted to have a uniform length for all training periods. For the presented STLF of a business building, growing and mobile training lead to similar forecasting errors.

4. Conclusions and Outlook

There is a wide range of short-term load forecasting methods which are classified in reference-based, statistical, analytical and Machine Learning methods. Reference-based methods provide accurate forecasts if the load behavior is cyclic without bigger irregularities. This is the case for top-down forecasts rather than for load profiles on company level. Statistical methods like univariate time series models are used if no relevant variables are identified or available, but not suitable for multi-step ahead forecasts. Linear regression models lead to accurate results if the load depends on a relatively low number of relevant variables. Analytical methods are non-adaptive and high effort is needed for implementation.

The review shows that selecting the relevant inputs is crucial for obtaining an accurate forecast. Machine Learning methods are suitable for high-dimensional input vectors. Relevant variables can be identified with automated feature selection. Feature extraction methods enable a load forecast of based on multiple time series with measured or forecasted values. Machine learning methods provide high flexibility in choosing a model type for a special use case, especially if base models are combined in ensemble learning or hybrid models.

The reviewed publications are summarized with regard to the GaIN project requirements to assess the readiness of existing STLF methods. To the knowledge of the authors, there is no method which fulfills all the requirements for industrial load forecasts on company level. The most promising approach is presented by Dietrich et al. [44] due to the high number of measurements reduced to an input vector with the most relevant ones applying automated feature selection for a load prediction at multiple forecasting steps. A combination with a CNN-based feature extraction method proposed by He et al. [42] could improve the forecasting results by extracting features not only from single past measurements, but from complete preceding time series. Additionally, a combination with an online learning method as it is proposed by Benedetti et al. [46] would be required and production planning data is not yet considered in the model. Finally, the proposed methods are usually benchmarked on only one company. Therefore, generalization of methods for different companies is not approved. In the GaIN project however, generic methods applicable for multiple industrial companies are required in order to develop generic tools. All the analyzed papers show point forecasts. Recently, in other forecast applications probabilistic forecasts gained importance. Probabilistic forecast methods should also be developed for industrial load in order to evaluate the risk for inaccurate forecasts. Further work focuses on the integration of selected models in an ML-framework in order to benchmark different methods on up to ten industrial use cases and to assess potential adaptations of the state-of-the-art methods. In addition to the listed requirements, the readiness of STLF also requires a reasonable application effort for the life cycle processes [29] from the ramp-up of the models to the operation for different industrial use cases. Therefore, the development goal for the framework is to offer a forecasting service for industrial companies and their energy utility for enabling them to evolve from single load management measures to an active prosumer with a variety of controllable energy flexibility measures.

Acknowledgements

The research has received funding from the German Federal Ministry for Economic Affairs and Energy (Project Number 03EI6019B - Machine learning for power load profile prediction and energy flexibility management strategies).

References

- [1] Yael Parag, Benjamin K. Sovacool (2016). Electricity market design for the prosumer era, *Nature Energy*, Vol. 1, No. 4, doi: 10.1038/nenergy.2016.32.
- [2] Günther Eibl, Kaibin Bao, Philip-William Grassal, Daniel Bernau, Hartmut Schmeck (2018). The influence of differential privacy on short term electric load forecasting, *Energy Informatics*, Vol. 1, S1, doi: 10.1186/s42162-018-0025-3.
- [3] VDI 5207 (2019). *Energy-flexible factory – Fundamentals (Blatt 1) and Identification and technical evaluation (Blatt 2)*, Beuth Verlag GmbH, Berlin.
- [4] SynErgie. Positionspapier zu regulatorischen Änderungen, from https://www.kopernikus-projekte.de/lw_resource/datapool/systemfiles/elements/files/8A7B1981D3AD5C60E0539A695E86C978/live/document/20190123_-_SynErgie_Positionspapier_Regulatorische_Rahmenbedingungen.pdf, accessed July 22, 2020.
- [5] Sebastian Weckmann, Timm Kuhlmann, Alexander Sauer (2017). Decentral Energy Control in a Flexible Production to Balance Energy Supply and Demand, *Procedia CIRP*, Vol. 61, 428–433, doi: 10.1016/j.procir.2016.11.212.
- [6] Thomas Kugle, Olga Meyer, Dirk Oehler, Greg Rauhöft, Daniel Stock. GREEN Factory Cloud-basierte Optimierung des Energieangebots und Prozesssteuerung: Transferdokumentation, from <https://cloud-mall-bw.de/praxispiloten/>, accessed July 22, 2020.
- [7] Next Kraftwerke GmbH. Variable Stromtarife für Industrie & Gewerbe "Best of 96", from <https://www.next-kraftwerke.de/virtuelles-kraftwerk/stromverbraucher/variabler-stromtarif>, accessed July 22, 2020.
- [8] Niklas Panten (2019). *Deep Reinforcement Learning zur Betriebsoptimierung hybrider industrieller Energienetze*, Shaker, Düren.
- [9] Joachim Bagemihl, Gwendolin Wilke, Ramón Christen, Vincent Layec, Holger Wache, Mirjam West, Silvia Ulli-Beer, Juliana Zapata et al. (2019). Power Alliance – Extending Power Grid Capacity on the Medium Voltage Level by Incentivizing a New Class of Emerging Flexible Loads, In: Hochschule Luzern + European Fuel Cell Forum AG (ed.), *Proceedings of GSM 2019: 3rd Grid Service Market Symposium*, Zenodo, 107–116.
- [10] Jürgen Blazejczak, Dietmar Edler, Martin Gornig, Birgit Gehrke, Ulrich Schasse, Christian Kaiser. *Ökonomische Indikatoren von Maßnahmen zur Steigerung der Energieeffizienz - Investitionen, Umsätze und Beschäftigung in ausgewählten Bereichen: Aktualisierte Ausgabe 2020*, Umweltbundesamt, Dessau-Roßlau.
- [11] Klaus Müller, Ralph Büchele, Matei Ciobanu, Patrick Andrae. Energy efficiency services in Europe, from https://www.rolandberger.com/publications/publication_pdf/roland_berger_energy_efficiency_services_in_europe.pdf, accessed July 22, 2020.
- [12] Tao Hong (2010). *Short Term Electric Load Forecasting*.
- [13] Amir Mosavi, Mohsen Salimi, Sina Faizollahzadeh Ardabili, Timon Rabczuk, Shahaboddin Shamshirband, Annamaria Varkonyi-Koczy (2019). State of the Art of

- Machine Learning Models in Energy Systems, a Systematic Review, *Energies*, No. 7, 1301, doi: 10.3390/en12071301.
- [14] Patrick Kronig, Michael Höckel, Urs Wälchli, Stefanie Zürcher (2009). *ELBE; Validierung und Verbesserung von Lastprognosen (Projektphase 1): Schlussbericht Teil 1*. Schweizerische Eidgenossenschaft (Bundesamt für Energie BFE), Bern.
- [15] Wiktor. Charytoniuk, M.-S. Chen (2000). Very short-term load forecasting using artificial neural networks, *IEEE Transactions on Power Systems*, No. 1, 263–268, doi: 10.1109/59.852131.
- [16] DIN EN ISO 50001:2018-12, Energiemanagementsysteme_ - Anforderungen mit Anleitung zur Anwendung (ISO_50001:2018); Deutsche Fassung EN_ISO_50001:2018, Beuth Verlag GmbH, Berlin, doi: 10.31030/2852891.
- [17] Wolfgang Schellong (2016). *Analyse und Optimierung von Energieverbundsystemen*, Springer Berlin Heidelberg, doi: 10.1007/978-3-662-49463-9.
- [18] VDI 2078 (2015). *Calculation of thermal loads and room temperatures (design cooling load and annual simulation)*.
- [19] Thomas Gobmaier, Wolfgang Mauch, Michael Beer, Serafin von Roon, Tobias Schmid, Tomás Mezger, Jochen Habermann, Sebastian Hohlenburger (2012). Forschungsstelle der Energiewirtschaft, KW21 Endbericht: Simulationsgestützte Prognose des elektrischen Lastverhaltens.
- [20] Cecil Bruce-Boye, Joachim Staats, David Watts. Optimierung der Fahrplanprognose für die Beschaffung elektrischer Energie, from https://www.eksh.org/fileadmin/downloads/foerderung/Schlussbericht_Optimierung_der_Fahrplanprognose_FHL_WiE_EKSH.pdf, accessed January 28, 2020.
- [21] Fatemeh Chahkoutahi, Mehdi Khashei (2017). A seasonal direct optimal hybrid model of computational intelligence and soft computing techniques for electricity load forecasting, *Energy*, Vol. 140, 988–1004, doi: 10.1016/j.energy.2017.09.009.
- [22] Anthony Setiawan, Irena Koprinska, Vassilios G. Agelidis. *Very short-term electricity load demand forecasting using support vector regression: Atlanta, International Joint Conference on Neural Networks, 2009*, doi: 10.1109/IJCNN.2009.5179063.
- [23] Helal. M. Al-Hamadi, Abdel hady Soliman (2006). Fuzzy short-term electric load forecasting using Kalman filter, *IEE Proceedings*, Vol. 153, No. 2, 217, doi: 10.1049/ip-gtd:20050088.
- [24] Song Li, Lalit Goel, Peng Wang (2016). An ensemble approach for short-term load forecasting by extreme learning machine, *Applied Energy*, Vol. 170, 22–29, doi: 10.1016/j.apenergy.2016.02.114.
- [25] Shu Fan, Luonan Chen (2006). Short-Term Load Forecasting Based on an Adaptive Hybrid Method, *IEEE Transactions on Power Systems*, No. 1, 392–401, doi: 10.1109/TPWRS.2005.860944.
- [26] Alexander Sauer, Eberhard Abele, Hans Ulrich Buhl (ed.) (2019). *Energieflexibilität in der deutschen Industrie*, Fraunhofer Verlag.
- [27] Arno Wedel (2019). Herausforderung Ersatzwerte - Neue Aufgaben für Messstellenbetreiber, *EMW*, No. 1.
- [28] Frederik Scheidt, Hana Medinová, Nicole Ludwig, Bent Richter, Philipp Staudt, Christof Weinhardt (2020). Data analytics in the electricity sector – A quantitative and qualitative literature review, *Energy and AI*, Vol. 1, 100009, doi: 10.1016/j.egyai.2020.100009.
- [29] DIN Deutsches Institut für Normung e. V. Artificial Intelligence - Life Cycle Processes and Quality Requirements - Part 1: Quality Meta Model, Berlin, Beuth DIN SPEC 92001-1:2019-04.
- [30] Antonio Bracale, Guido Carpinelli, Pasquale De Falco, Tao Hong (2017). *Short-term industrial load forecasting: A case study in an italian factory: Torino, Italy, 26-29 september 2017 Conference proceedings*, doi: 10.1109/ISGTEurope.2017.8260176.

- [31] Robotron Datenbank-Software GmbH. robotron e-predict: Funktionsbeschreibung, from <https://www.robotron.de/produkte/robotronepredict>, accessed November 11, 2019.
- [32] Alexander Emde, Alexander Sauer, Lisa Märkle, Benjamin Kratzer (2020). Ermittlung des zukünftigen Energiebedarfs von Industrieunternehmen: Mithilfe von Lastprognoseverfahren - von der Lastanalyse zur Lastprognose, *ZWF*, doi: 10.3139/104.112194.
- [33] Seon Kim, Gyu Lee, Gu-Young Kwon, Do-In Kim, Yong-June Shin (2018). Deep Learning Based on Multi-Decomposition for Short-Term Load Forecasting, *Energies*, Vol. 11, No. 12, p. 3433, doi: 10.3390/en1123433.
- [34] Jessica Walther, Dario Spanier, Niklas Panten, Eberhard Abele (2019). Very short-term load forecasting on factory level - A machine Learning approach, doi: 10.1016/j.procir.2019.01.060.
- [35] Thomas Renner, Albrecht Reuter, Christoph Schlenzig, Holm Wagner, Siegfried Wagner (2018). *Smart Energy Hub. Fraunhofer IAO, Stuttgart, Germany*.
- [36] Kunlong Chen, Jiuchun Jiang, Fangdan Zheng, Kunjin Chen (2018). A novel data-driven approach for residential electricity consumption prediction based on ensemble learning, *Energy*, Vol 150, p. 49–60, doi: 10.1016/j.energy.2018.02.028.
- [37] Feras Alasali, Stephen Haben, Victor Becarra, William Holderbaum (2018). Day-ahead industrial load forecasting for electric RTG cranes, *Journal of Modern Power Systems and Clean Energy*, Vol. 6, No. 2, 223–234, doi: 10.1007/s40565-018-0394-4.
- [38] Frank-Dieter Clesle, Gerhard Saller (2007) Patent EP 1 748 529 B1.
- [39] DIN Deutsches Institut für Normung e. V. Referenzmodell zur Charakterisierung der Energieflexibilität von Industrieunternehmen, Beuth Verlag, Berlin, DIN SPEC 91366, accessed May 10, 2020.
- [40] Christopher Schmidt, Wen Li, Sebastian Thiede, Sami Kara, Christoph Herrmann (2015). A methodology for customized prediction of energy consumption in manufacturing industries, *International Journal of Precision Engineering and Manufacturing-Green Technology*, Vol. 2, No. 2, 163–172, doi: 10.1007/s40684-015-0021-z.
- [41] Mohammad H. Alobaidi, Fateh Chebana, Mohamed A. Meguid (2018). Robust ensemble learning framework for day-ahead forecasting of household based energy consumption, *Applied Energy*, Vol. 212, 997–1012, doi: 10.1016/j.apenergy.2017.12.054.
- [42] Yan He, Pengcheng Wu, Yufeng Li, Yulin Wang, Fei Tao, Yan Wang (2020). A generic energy prediction model of machine tools using deep learning algorithms, *Applied Energy*, Vol. 275, 115402, doi: 10.1016/j.apenergy.2020.115402.
- [43] Hiroyuki Mori, Noriyuki Kosemura (2002). A data mining method for short-term load forecasting in power systems, *Electrical Engineering in Japan*, Vol. 139, No. 2, 12–22, doi: 10.1002/eej.1150.
- [44] Bastian Dietrich, Jessica Walther, Matthias Weigold, Eberhard Abele (2020). Machine learning based very short term load forecasting of machine tools, *Applied Energy*, Vol. 276, 115440, doi: 10.1016/j.apenergy.2020.115440.
- [45] Dana-Mihaela Petroșanu (2019). Designing, Developing and Validating a Forecasting Method for the Month Ahead Hourly Electricity Consumption in the Case of Medium Industrial Consumers, *Processes*, No. 5, 310, doi: 10.3390/pr7050310.
- [46] Miriam Benedetti, Vittorio Cesarotti, Vito Introna, Jacopo Serranti (2016). Energy consumption control automation using Artificial Neural Networks and adaptive algorithms, *Applied Energy*, 60–71, doi: 10.1016/j.apenergy.2015.12.066.

G08

VPP and advanced technologies I

G0802

Enhancing Power-to-Gas operations with a Virtual Power Plant to improve renewable grid integration

Aleksandra Radwanska, Felix Jedamzik, Joan Recasens

Next Kraftwerke GmbH
Lichtstr. 43g
50825 Cologne/Germany
Tel.: +49 221 820085-754
Radwanska@next-kraftwerke.de

Abstract

The energy sector demands a new way for managing the growing number of distributed power producers of renewable energy. For this purpose, Virtual Power Plants (VPP) and Power-to-Gas (P2G) are two important technologies to ensure the stability of the power grid. On one hand, VPPs can help controlling and monitoring distributed assets to ensure the stabilization of the grid. On the other hand, P2G plants may contribute to enhance the power system's flexibility, to balance generation and consumption in real time. This paper provides a case study that outlines the possibilities and complexity of monitoring and controlling a P2G plant through a VPP. Greenpeace Energy runs the project in collaboration with Next Kraftwerke GmbH and the municipal utility Stadtwerke Haßfurt GmbH of the city of Haßfurt, Germany.

Key Words: Virtual Power Plants, Power-to-Gas, renewable energy

Introduction

The energy sector is undertaking a profound transformation to shift towards cleaner energies. For this reason, there is a growing number of distributed power producers of renewable energy, which results into a more complex energy system. This demands for a new way of managing such distributed energy resources effectively and efficiently.

On one hand, a Virtual Power Plant (VPP) can help controlling and monitoring DER to ensure the correct operation of the grid by keeping the generation and the demand balanced. On the other hand, Power-to-Gas (P2G) is the process of supplying electricity to an electrolysis process in order to convert the energy available into hydrogen. The hydrogen generated can be converted back to electricity, mixed with natural gas [1][2] or used for other purposes. Thus, P2G plants are flexible energy resources that can contribute to enhance the flexibility in the system, when managed properly. Therefore, the combination of VPP and P2G technologies offers several possibilities to ensure the stability of the grid. [3]

To explore such capabilities, this paper provides a case study that outlines the possibilities and complexity of monitoring and controlling a P2G plant through a VPP. The study was conducted in the local distribution grid of the city of Haßfurt, where renewable electricity generation from wind parks surpasses significantly local consumption. The goal of the study was to evaluate the possibility to locally use the excess renewable generation, and reduce exports of this electricity from the distribution system to the transmission system. For this purpose, a P2G plant was implemented to be operated according to the demand and availability of renewable energy fed into the local electricity grid of the municipal utility Stadtwerke Haßfurt GmbH. The hydrogen produced in the P2G plant is either stored in the storage tank, injected into the natural gas pipeline or directly delivered to a malt house. Aside from using the excess renewable energy to produce hydrogen, the electrolyser also provided grid frequency control for the TSO in the region.

1. Background - The electricity and gas sector of the city of Haßfurt

In the Haßfurt distribution network, the local consumption is largely covered by renewables. The electricity consumption of the city of Haßfurt, which is between 4 MW and a maximum of 13 MW, is offset by a supply-dependent, renewables-based generation of almost 50 MW. According to Stadtwerke Haßfurt, this leads to large local surpluses in the distribution network. So far, the surplus electricity has been fed into the upstream transmission grid.

The basic idea behind the project is to use this "green" surplus of electricity in a P2G plant. The P2G plant uses the resulting part of the surplus of electricity to produce synthetic hydrogen. By activating the P2G plant, the local consumption is increased, thus reducing the outflow of electricity into the transmission grid.

The P2G plant in Haßfurt consists of an electrolysis unit, with a maximum power capacity of 1.25 MW; a gas storage facility, with a volumetric capacity for 1750 m³; and two accesses to the local gas piping system, one for the gas network and a direct one for the malting plant. The P2G system is connected to the medium-voltage level of the distribution network. The installed capacity of 1.25 MW peak corresponds to about 10% of the peak load of the total electricity consumption of the city of Haßfurt. The electricity from the medium voltage level is used to split water into hydrogen and oxygen in the electrolysis unit. The resulting hydrogen is fed into the gas storage tank where it is temporarily stored. The hydrogen produced in the P2G plant is to be fed into the gas network of the city of Haßfurt, so that it can be added to the gas supply of the local industry. The gas can be

previously stored in the P2G plant storage tank, with a capacity of 50 m³, to improve the generation flexibility of the P2G plant. The economy in Haßfurt is characterised by small trade and commerce. Household and commercial customers mainly drive the electricity consumption. Moreover, the municipal utility itself consumes electricity to power larger water pumps, which are used in the city's water supply system. There are no large industrial enterprises with distinctive individual power consumption patterns.

On the other hand, ordinary household and commercial customers as well as a big malt house mainly drive the gas demand in the municipality. Household and commercial customers mainly use the purchased natural gas taken from the gas network for normal household applications such as cooking, heating or hot water supply. In the gas network supplying the households, it is possible to add up to 5% hydrogen to natural gas. Under the given circumstances, this is possible because the feed-in point of the P2G plant is located in a different network branch than the natural gas filling station, for which only a hydrogen admixture rate of 2% would be permitted. The household gas consumption varies between 100 m³/h in summer and about 1000 m³/h at peak consumption times in winter.

Moreover, the malting plant requires large amounts of heat to dry the malted grain. The process heat is provided by several cogeneration units, which are operated with natural gas. These cogeneration units are compatible with the hydrogen content in the natural gas up to 10%. The gas consumption of the malt house is very regular and has almost the same structure every day of the year.

Stadtwerke Haßfurt is responsible for the technical management of the P2G plant, the construction, the planning and the implementation. Next Kraftwerke was chosen as the partner for the operation schedule control and power supply of the plant. Next Kraftwerke integrated the plant into their VPP Pool. This makes it possible to optimize the plant operation in a 15-minute basis and provide control energy remotely from Next Kraftwerke's headquarters.

Greenpeace Energy is electricity and gas retailer. They offer to their climate-conscious customers special tariff called 'wind gas' together with a standard contract for sale of natural gas. The clients have an opportunity to support the project via special tariff and can then burn the mixture of natural gas and green hydrogen in their gas heaters without any upgrades in their homes [4].

2. Technical specifications of the P2G plant

The PEM electrolyser for the P2G plant is particularly suitable to take advantage of the surpluses of renewable electricity as the electrolysis can be controlled nimbly and without restrictions. Any operating point can be reached within 20 seconds. Thus, the P2G plant can be ramped up at full capacity, 1.25 MW, within 20 seconds [5]. This results in a load change gradient of 4 - 6 MW/min. The P2G plant is capable of producing 225 m³/h of hydrogen at full capacity. The conversion efficiency from electric energy to chemical energy stored in the Hydrogen goes up to 70%, if the calorific value of the hydrogen is considered 3.54 kWh/m³.

The hydrogen produced has a high purity and is therefore suitable for feeding into the public gas network. The water required for electrolysis is taken from the public water supply of Haßfurt. This water is purified and treated before it is fed to the electrolyser. To produce one cubic meter of hydrogen, 1.5 litres of water are needed. At full load, the electrolyser needs 340 litres per hour [5]. In order to prevent possible failures of the water treatment, a buffer tank between water treatment and electrolyser was also installed. Heat

losses occurring during the operation of the plant, at the efficiency of about 70 % and at a full load of 1250 kW, result in a thermal output of 375 kW [5]. This waste heat is dissipated to the surrounding because practical use of the waste heat is not yet possible due to the low process temperatures.

A buffer storage tank was installed between the electrolyser and the device feeding the hydrogen into the gas network to enable a flexible operation of the plant. The hydrogen produced is first fed into the gas storage tank and from there it is independently fed into the gas injection devices. The gas storage tank has a volume of 50 m³ and can be operated with a pressure of up to 35 bar. Therefore, the storage tank has the capacity of storing 1750 m³ of Hydrogen in gas phase at atmospheric pressure, which approximately corresponds to 1 bar. This means that operating at full capacity the P2G plant could fill the gas tank in less than 8 hours. Once the gas volume reaches the upper limit of the storage tank, the electrolysis process stops automatically. In case of an emergency, such as exceeding the upper storage limit, the pressure relief valve of gas storage tank releases hydrogen.

The gas storage tank of the P2G plant is continuously discharging the stored hydrogen. The gas network and the local industrial consumer, the malting plant, are supplied separately due to the different hydrogen tolerances - 10 % for the malt house, but only 5 % for the public gas network. Since the P2G plant is located in the immediate proximity of the malting plant, it was possible to build a direct gas pipeline from the P2G plant with a reduced budget. The feed-in device continuously measures the natural gas volume flows in the pipelines of the public gas network and the malt house, because it influences the feed-in capacity of the hydrogen from the P2G plant.

3. Input data for optimisation of operation

The operation of the P2G plant aims to maximize the amount of renewable energy consumed at the lowest possible prices. The electricity prices directly relate with the share of renewable generation injected in the power system at every moment. The lowest prices correspond to the largest shares of renewables in the system. It is assumed that renewable generation follows similar production profiles both nationally (Germany) and locally (in the region of Haßfurt). Therefore, maximizing the P2G plant consumption with the lowest electricity prices also entails aligning the consumption when the production of renewable generation is higher, in Germany and in the local wind farms and solar PV parks in the region of Haßfurt. For this purpose, the plant is continuously optimized in a 15-minute basis.

The following routine is carried out: First, the information about the status of the electricity distribution grid in Haßfurt is updated every 15 minutes to verify the amount of available excess electricity. This is calculated by comparing the forecast of local consumption against the local generation forecast of wind and solar PV. These three load curves are used to forecast the electricity surplus in the region for the next 36 hours with a 15-minute resolution, according to following formula:

$$\text{Generation}_{\text{Wind}} + \text{Generation}_{\text{PV}} - \text{Consumption}_{\text{Haßfurt}} = \text{Forecasted surplus}$$

The wind forecast has a special significance for the forecast of the surplus of electricity, as the generation from the wind power plant in the municipality of Haßfurt has the greatest influence on the accessible amount of electricity to power the electrolysis. In fact, as soon as the wind power plant reaches 30% of its maximum capacity production, it exceeds the average consumption of the city. This means that the excess of renewable electricity generated is available for the P2G plant.

To predict precisely the available electricity, Next Kraftwerke uses short and medium-term wind power generation forecasts. On one hand, the short-term forecasts help determine

the wind feed-in for the last tradable product of the intraday. On the other hand, the medium-term forecasts attempt to foresee the wind generation in a time horizon of 3 to 36 hours. The wind forecasts were prepared under the assumption that there is a correlation between the wind feed-in in Germany and the wind feed-in in the distribution grid Haßfurt. The forecasts of solar generation were prepared with data published by Stadtwerke Haßfurt, who provides live values of the current solar feed-in in the entire distribution network. These data include the feed-in from smaller roof systems as well as the feed-in from the four large open space installations in the region. The solar forecast is not as defining to determine the surplus of energy available in the region as the wind forecast. This is motivated by the fact that the solar capacity installed in the region is relatively small in comparison to the wind power installed capacity. Moreover, the generation profile of the PV feed-in corresponds accurately with the consumption load curve, which means that the PV feed-in can be consumed locally more efficiently. For this reason, minor forecasting errors identified during the operation of the system could be neglected, as they would not heavily affect the overall optimization of the P2G plant operation.

The third important parameter to be defined was the electricity consumption in Haßfurt, which could not be directly measured. Therefore, the measured parameter instead was the bidirectional power flow between the transmission grid and the distribution grid. This, combined with the renewable generation, together with the known parameter of the power consumption by the electrolyser was used in the following formula to define the electricity consumption in Haßfurt.

$$\text{Generation}_{\text{Wind}} + \text{Generation}_{\text{PV}} - \text{Consumption}_{\text{Haßfurt}} - \text{Consumption}_{\text{Electrolyser}} = 0$$

Thus, the power consumption can be determined. This method is subject to several inaccuracies and errors that need to be considered. The grid equation is a simplified assumption and was made based on the available data. In addition to household and commercial customers, the distribution network contains several larger, individually controlled consumers, such as groundwater pumps, whose consumption were not reported to the forecast provider. The consumption values considered here were therefore not exclusively standard load profile customers, making the creation of reliable forecasts more complicated.

The forecasts are recalculated iteratively every 15 minutes and they are used to re-evaluate and optimize the operation schedule of the plant. Next Kraftwerke receives the updated forecasts and optimizes the operation of the plant accordingly. Then, the new operation schedule is checked and transmitted to the plant remotely. The reliability and degree of automation were given special consideration when setting up the operation schedule optimisation.

The actual values of hydrogen production of the electrolyser are calculated based on the efficiency characteristic curve. The efficiency of the electrolyser varies depending on the power range, reaching maximum efficiency in the medium power range and the lowest efficiency values in minimum load (125 kW) or maximum load (1250 kW) [5]. Key data points of the efficiency curve were recorded and adjusted to fit a regression function. Thus, it is possible to assign a hydrogen production quantity to each power value. Therefore, the performance schedule of the plant is directly converted into specific quantities of hydrogen production using the transfer function.

Natural gas and hydrogen consumption limits the permitted production of hydrogen in the P2G plant. Therefore, apart from the available energy to power the P2G system, the limits for producing hydrogen are also forecasted. The forecast of gas consumption in the municipality takes into consideration the residential users in the city as well as the malt house.

On one hand, the forecast of gas consumption in the municipality was complex to obtain because historical gas consumption data were only available from the main node in the

gas network, meaning from the entire city of Haßfurt. The gas load curve data show a strong annual seasonality and temperature dependency as the natural gas is mainly used for heating purposes. There is a strong hourly pattern every day. Additionally, slight changes in weekend or holiday patterns can be observed. A regression analysis of the daily mean values of gas consumption with respect to the mean daytime temperature shows that gas consumption is linearly dependent on the outside temperature.

On the other hand, the gas consumption forecast of the CHP unit of the malt house was based on high quality historical data showing a very regular gas consumption. The load profile follows a classic daily pattern. It rises daily from base load between 7:30 and 8:00 a.m. and increases over the course of the day up to midnight. It then drops rapidly and reaches the baseline in the early morning hours. Apart of the distinctive daily pattern, it has a specific weekly pattern, which repeats regularly during the year.

The two natural gas consumption patterns combined with the current filling level of the hydrogen storage tank and the fixed operation schedules of the electrolyser were used to forecast the available level of gas storage capacity. The change in the gas storage level results from the volume flow of hydrogen produced by the electrolyser, minus the outflows of hydrogen to the malting plant and the gas network as shown in the following formula:

$$\Delta V_{gas\ storage} = (\dot{V}_{H_2\ electrolyser} - \dot{V}_{H_2\ gas\ network} - \dot{V}_{H_2\ malt\ house}) * t$$

Then, the current filling level of the gas storage tank is used to calculate the gas storage tank filling level for the next quarter of an hour with the predicted hydrogen flows. Additionally, the forecast respected the limits of the hydrogen absorption in the gas network that were calculated according to the following formulas:

$$\dot{V}_{H_2\ gas\ network,max} = \dot{V}_{CH_4\ gas\ network} * \text{admixture limit}_{gas\ network}$$

$$\dot{V}_{H_2\ malt\ house,max} = \dot{V}_{CH_4\ malt\ house} * \text{admixture limit}_{malt\ house}$$

$$\text{admixture limit}_{gas\ network} = 5\%$$

$$\text{admixture limit}_{malt\ house} = 10\%$$

3. Interaction of the P2G with electricity markets

Electricity in Germany is traded in a liberalised market. The procurement and delivery of electricity therefore takes place under free competition. There are two basic ways of procuring electricity. In direct, bilateral operation schedule deals with electricity producers, the so-called over-the-counter deals, and via an electricity exchange. Various products are available for procurement in the electricity exchange, all of which differ in terms of duration and trading time. There is the futures market, the day-ahead market and the intraday market. The most price-volatile market is the intraday market, as it has the shortest trading times and the electricity is traded just up to 5 minutes before the dispatch. Therefore, the electricity powering the P2G system is procured in the intraday market due to the short-term required activation times of the electrolyser, which needs to take advantage rapidly of the short-duration events in which the excess of electricity is available [6].

With the help of the forecast of excess electricity and the predicted available volume of gas storage, the system was optimized to take advantage of hourly price differences in the intraday market. As explained above, the low electricity prices are directly related with renewable generation in the system. For this reason, concentrating the consumption of the plant during the time slots with lower electricity price also implies consuming the greenest energy. Furthermore, in this case the green electricity is produced locally in the distribution grid by the wind farms and solar parks in the region. For this purpose, it was crucial to

optimise the production operation schedule to adjust the operation profile of the plant as accurately as possible to the available electricity as well as low prices on the wholesale market. The aim of the optimisation is to generate a maximum amount of regenerative gas at the lowest possible cost.

Additionally, the electricity needed to satisfy the base load band is procured in the day-ahead auction. Whenever a quantity has been procured for the system, the corresponding schedule is sent to the Next Box of the P2G system. The Next Box is Next Kraftwerke's hardware-based solution to aggregate power plants in its VPP. The Next Box is a remote technical unit, composed by a programmable logic controller, a modem and an antenna. This guarantees that there are no discrepancies between the plant schedule and the quantities traded.

Another important market in the German energy system is the balancing energy market, which enables electricity generators and consumers to provide flexibility to the transmission system operator (TSO) and thus generate additional revenue [7]. The TSO is obliged at all times to ensure a balance between electricity generation and consumption. For this purpose, the TSO uses control power of different quality, with different call-up duration, call-up principle and time activation duration. The main differentiation criterion is the speed and duration of activation. [8]

The P2G plant is also available to provide balancing services to the TSO. In fact, the P2G plant provides the three main products of the balancing services market: Frequency containment reserve (FCR), automatic frequency restoration reserve (aFRR) and manual frequency restoration reserve (mFRR) [9]. For this reason, apart from gas consumption and the storage capacities in the natural gas network, the production plan of P2G system was based on the predicted periods, during which the installation could be used to provide balancing services to the grid operator. Due to the organisation of the balancing market in Germany, it is required to create forecasts for 13 days ahead, including weather forecasts and forecasts of ambient temperature, which strongly influence the gas consumption of the residential users.

4. P2G operation optimisation logic

The operation optimisation consists of two components: on the one hand, there is a base load consumption and on the other hand, there is a controlled peak consumption in case of surplus scenarios. The achievable production of hydrogen in oversupply scenarios is greater than the consumption capacity of the gas network and the malt house. Therefore, it is necessary to optimize the amount of hydrogen produced with regard to the absorption capacities of the gas network and the malting plant and the filling level of the gas storage tank. To create the operation schedule, a linear optimization problem is solved. The main assumptions are that hydrogen production of the electrolyser increases the filling level of the gas storage tank. Hydrogen intake from the gas network and malt house reduces it.

First, the electricity required to cover the base load is acquired in the day-ahead market for every hour of the next day. The amount of energy acquired refine the base-load operation schedule of the P2G plant for the following day.

A different logic leads the optimisation of the P2G system to provide balancing services. In this case, it is necessary to keep storage capacity free. The free availability of storage capacity is only necessary for the provision of negative balancing energy. In order to provide negative balancing energy, the P2G facility increases its power consumption and produces more hydrogen. According to prequalification criteria, no energy may be wasted for the provision of balancing energy. Therefore, it is necessary to keep sufficient storage capacity available so that all the hydrogen generated can be temporarily stored in the storage tank. On the contrary, no storage capacity is required for the provision of positive

balancing energy. In this case, the electrolyser reduces the output, produces less hydrogen and the storage tank empties. Different storage capacities are required depending on the type of balancing product- for the provision of aFRR, required storage capacity must be available for 4 hours of production [10][8].

The optimization problem has the following structure: The transfer function is used to calculate the amount of hydrogen the electrolyser can generate in each quarter of hour above the base load. The maximum hydrogen production scales up to 56.25 m³ for each quarter. Nevertheless, the absorption capacity of hydrogen of the malting plant and the gas network permits a maximum hydrogen production of the electrolyser of about 60 m³/h in base load operation, which corresponds to a reference power of 330 kW. The absorption capacity of the gas network is therefore not sufficient to store the entire excess flow in the form of hydrogen in the event of a prolonged availability of excess renewable electricity. Therefore, the optimisation problem is solver to choose favourable quarters to produce hydrogen in the case of large surplus quantities. For this purpose, a matrix with the quarter-hour values for the hydrogen absorption capacity of the malting plant and gas network, the amount of hydrogen produced with energy surpluses, the initial gas storage forecast and the forecast electricity prices is created. The optimisation function solves the optimisation problem and returns an operation schedule that provides a maximum of hydrogen production at minimum cost. The optimization tries to produce as much hydrogen as possible within the given optimization horizon, usually all quarter-hours available in the intraday market, and to fill the gas storage as much as possible.

5. Results of the optimization

The successful optimization implemented in the production schedule and control of the P2G system was proved by monthly issued reports verifying the quality of the forecasts and of the operation of the control system. The gas storage tank of the plant was filled during favourable quarter hours. During the entire optimisation period, over 70% of all the quarter-hours, the renewable electricity generation exceeded the consumption of Haßfurt. At first, the system was optimized to make use of excess electricity in all available quarter hours. However, the prices were relatively high with this operation regime. Therefore, the optimisation only selected individual favourable quarter-hours in order to make full use of the absorption capacity of the gas network at the lowest prices. During the favourable night hours, the system worked at full capacity and filled about half of the gas storage tank. On the following day, the PV feed-in in Germany was very high and led to favourable prices in the midday hours. The optimization algorithm made use of them and filled the gas storage in the noon hours at low prices.

Following the initial intraday auction, the operation schedule is further optimised in the continuous intraday operation. For this purpose, the previous schedule of the plant is transferred to the optimization problem. In contrast to the initial optimization, the continuous intraday optimization determines the operation schedule based on supply and demand prices (selling and purchasing bid prices).

6. Conclusions and discussion

Although, the P2G plant in Haßfurt was a pilot project, it can compete on the market under current economic conditions as one of the very first projects of this kind. The practical implementation of its integration into the VPP was successful in terms of both control technology and operation without any major complications. However, some aspect of its operation and the technological process behind the P2G systems require critics and discussion.

Firstly, the efficiency of conversion of electricity to hydrogen in the electrolysis is around 65%. The remaining 35% of waste heat is extracted at relatively low temperatures, can no longer be used for further energetic purposes and must be dissipated to the environment. The hydrogen obtained in the process powers CHP unit of the malt house that generates electricity with an electrical efficiency of 35% and the remaining 65% of energy is used for heat application.

Second, household and commercial customers use the hydrogen injected into the gas network of the city for heat applications. The efficiency of this process is lower than use of gas heaters delivering heat at an efficiency of 90%. In these circumstances, it would have been possible to use more efficient and cheaper power-to-heat plant, which converts electricity directly with an efficiency of 95% into heat at any temperature level. However, the intention of this project was to promote and further develop P2G technology delivering value to more vast set of stakeholders, meaning transmission and distribution network operators, industrial users and residential users.

From this point of view, this project must be seen as a research project that successfully demonstrated the functionality of the technology, its value proposition to an energy industry and provided experience valuable in design of future energy scenarios.

7. Practical implications

The P2G plant is economically successful due to the operational optimization applied remotely by Next Kraftwerke's trading team. This is possible because the P2G plant is aggregated to Next Kraftwerke's VPP. Note that the plant is still controlled and operated according to the customer's wishes as this is a joint collaboration.

Technically, the P2G plant works under almost no restrictions, apart from the limited absorption capacity of the gas network. Therefore, on top of delivering balancing services and contributing to the reduction of local surpluses, it has also proved useful in peak shaving and in the management of balancing groups. These modes of operation could be replicated in other P2G installations.

First, P2G plants can be used to limit power transfer to the transmission network. It would be conceivable to use the plant specifically to cut the peaks in exports of electricity from the distribution network in Haßfurt to the transmission network. This approach reduces costs for the operation of the distribution network, which depends on the maximum capacity requested via a connection point between the distribution network and transmission network.

Another possibility would be to use the P2G plant for balancing group management, using unexpected surpluses of renewable energy. This approach minimizes the risks related with deviations between the forecasts and actual generation of energy. In this case, the P2G plant would activate not to deliver electricity as a balancing service, but to ensure balance in the balancing group.

References

- [1] Weniger, J. et al., 2016. Sektorkopplung durch die Energiewende, Berlin. Available under: <http://dx.doi.org/10.1016/j.jpowsour.2016.06.076>
- [2] Schenuit, C., Heuke, R. & Paschke, J., 2016. Potenzialatlas Power to Gas. Klimaschutz umsetzen, erneuerbare Energien integrieren, regionale Wertschöpfung ermöglichen., Berlin.
- [3] Sterner, M. et al., 2015. Bedeutung und Notwendigkeit von Windgas für die Energiewende in Deutschland. Available under: <https://www.greenpeace->

energy.de/fileadmin/docs/pressematerial/2015_FENES_EBP_GPE_Windgas-Studie.pdf

- [4] Greenpeace Energy eG., 2016. Der innovative Gas-Tarif: proWindgas – Greenpeace Energy. Available under: <https://www.greenpeace-energy.de/privatkunden/windgas.html>
- [5] Siemens AG, 2015b. SILYZER 200 (PEM electrolysis system) driving convergence between energy and industrial markets.
- [6] Bayer, E., Report on the German power system - country profile, Berlin. Available under: http://www.agora-energiawende.org/fileadmin/downloads/publikationen/CountryProfiles/Agora_CP_Germany_web.pdf%5Cnhttps://www.epexspot.com/document/26145/EPEXSPOT_Trading_Brochure.pdf
- [7] Tennet TSO GmbH, 2007. Beschaffung von Regelleistung und -energie in Deutschland. , 6(2), S.2–3. Available under: <http://www.tennetso.de/site/binaries/content/assets/transparency/publications/tender-of-balancing-power/beschaffung-von-regelleistung.pdf>
- [8] VDN, 2013. Mindestanforderungen an die Informationstechnik des Anbieters für die Erbringung von Sekundärregelleistung, Berlin.
- [9] Brückl, O., 2006. Wahrscheinlichkeitstheoretische Bestimmung des Regel- und Reserveleistungsbedarfs in der Elektrizitätswirtschaft. TU München. Available under: http://d-nb.info/991830261/34?origin=publication_detail
- [10] VDN, 2007. TransmissionCode 2007 Anhang D2 Teil 1 Unterlagen zur Präqualifikation von Anbietern zur Erbringung von Sekundärregelleistung für die ÜNB, Berlin. Available under: <https://www.regelleistung.net/ip/action/static/prequal;jsessionid=LhLwTkLQ8CrQwJ87Qp6Hs8t1dgk2C9Tm6ZI7vqLGBNp2M592Tf0z!-1323386705!2134477355>

G09

VPP and advanced technologies II

G0901

Converting wastes efficiently and flexibly for grid-balancing services and sector coupling

Ligang Wang (1,2), Yumeng Zhang (2), Chengzhou Li (2), Mar Pérez-Fortes (1), Yi Zong (3), Vincenzo Motola (4), Alessandro Agostini (4), Stefan Diethelm (5), Olivier Bucheli (5), Jan Van herle (1)

(1) Swiss Federal Institute of Technology in Lausanne/Switzerland

(2) North China Electric Power University, China

(3) Technical University of Denmark, Denmark

(4) ENEA, Italy

(5) SOLIDpower SA, Switzerland

ligang.wang@epfl.ch; ligang.wang@ncepu.edu.cn

Abstract

Biomass-to-electricity or -chemical via power-to-x can be potential flexibility means for future electrical grid with high penetration of variable renewable power in future. However, biomass-to-electricity will not be dispatched frequently due to the high operating costs. The economic benefit of biomass-to-energy might also be limited by low annual operating hours. This issue can be addressed by integrating biomass-to-electricity and -chemical in one single plant with the solid-oxide cell stack, which can work either as fuel cell or electrolyzer with the same stack. Therefore, a triple-mode grid-balancing plant with flexible switch among power generation, power storage and power neutral (with chemical production) modes is proposed to realize high annual operating hours. Its economic potential relies on grid-flexibility needs, biomass supply, and plant design and operation.

In this paper, the potential of this type of grid-balancing plants have been evaluated with an optimization methodology combining flexibility need prediction, biomass potential identification, optimal plant design, optimal grid integration with plant sizing and scheduling, supply chain optimization and CAPEX target calculation. The DK1, DK2, Bornholm island in Denmark and SUD in Italy have been chosen as the renewable energy dominated zones. It is found that the theoretical flexibility needs reach up to several tens of GW for the selected zones and several to tens of TWh in terms of energy. The characteristics of the flexibility needs for different zones vary a lot. Local exploitable wastes are in the same order of magnitude of the theoretical flexibility needs, indicating enough biomass to support the grid balancing. Different optimal plant designs have been obtained with the efficiencies reaching up to 50–60% (PowGen), 72–76% (PowSto) and 47–55% (PowNeu). It can offer different designs according to the flexibility-need characteristics. With more plants installed with optimal sizes, the imbalance can be reduced; however, it becomes less profitable, since more plants are coordinated to operate under less efficient PowNeu mode. The CAPEX target of the W2G plant obtained with the limited case studies is within 1300-2750 €/kWe PowGen power and 550–1000 €/kWe PowSto power.

Introduction

Tuning wastes into a resource is a key factor for a circular economy. However, in EU 28, the wastes recycled or backfilled are still less than half in 2016. Only 10% of the total wastes are recovered as energy, mainly by combustion-based power generation; while the remaining, over 45%, goes to landfill and incineration [1]. In the electricity sector, the fast-growing intermittent renewable power asks for increased grid flexibility, thus more flexibility means [2]. However, when the contribution of intermittent renewable power becomes high enough, biomass power plants with high operating costs (because of the biomass supply chain) will not be dispatched frequently and become even more unprofitable due to low annual operating hours [3]. Thus, there is a strong need for innovative biomass utilization for future energy-system scenarios.

Biomass can be an effective, low carbon alternative for power storage and grid balancing. This could be achieved by gasification based biomass-to-chemicals enhanced by power-to-x capability. By injecting renewable-derived hydrogen into gasification-derived syngas to adapt its composition, the expensive, energy-intensive carbon capture unit equipped in conventional biomass-to-chemicals can be avoided.

Waste-to-electricity and waste-to-fuel can be merged into one single plant with the unique feature of solid-oxide cell stack, i.e., the same stack can work either in fuel cell mode for power generation or electrolyzer mode for power storage. Wastes are gasified first into syngas, which is used in the stack for power generation when electricity is needed by the electrical grid or converted to methane when excess renewable power is available from the grid as shown below. Such plants have the advantages of gaining additional profit of grid-balancing services, enhanced annual operating hours (nonstop over the year), reduced CAPEX, and enhance power storage capability and capacity.

The EU project Waste2GridS (W2G) aims at evaluating the economic feasibility for the large-scale deployment of such plants in 2030 by answering three critical questions, the technical potential, business cases, and bottlenecks at different levels. This paper focuses on the investigation of the technical potential with a newly proposed optimization methodology.

1. The overall deployment methodology

Due to the complexity of the optimization problem, we have proposed a decomposition-based methodology for the overall deployment of the W2G plants, as described in detail in Ref. [4]. The key idea is briefly given in Fig. 1 with the following procedure:

- (1) *Identification of (future) grid flexibility needs.* Based on the multi-timescale data-driven method presented in Ref. [5], for the zone considered, hourly timeseries of the fluctuating discrepancies between variable renewable energy production and electricity consumption are generated for step (4).
- (2) *Identification of (future) biomass availability.* In compliance with the classification schemes and methodology applied in the projects like BEE [6], S2Biom [7] and BIOMASS FUTURE [8], the biomass streams in the zones interested are assessed with further available Directives, Regulations and Reports, to build the geodatabase with their weight, characteristics and location coordinates for step (5).
- (3) *Optimization of conceptual plant design.* The design points of the components, particularly the stacks, strongly affect the thermodynamic performances of the plant and further the economics of the overall application. Therefore, instead of one

- single design, a pool of trade-off designs is generated for each process option for step (4).
- (4) *Optimization of design selection, plant sizing and scheduling to satisfy the flexibility needs.* With hourly flexibility needs from step (1) and multiple plant designs from step (3), the Dispa-SET platform has been modified to determine the number, design, size and scheduling of the W2G plants employed to maximize the gain from grid-balancing services and the sale of SNG by subtracting the costs of auxiliaries to assist the continuous operation of all W2G plants. Note that the capital expenditures (CAPEXs) of the plants are not considered at this step. The input biomass energy needed for each plant is provided to step (5), while the gain is fed to step (6).
 - (5) *Optimization of the biomass supply chain.* With the biomass geodatabase from step (2) and the biomass energy needed for each plant from step (4), the costs of biomass supply chain and pretreatment are minimized with the superstructure-based method presented in Ref. [9–11] and fed to step (6).
 - (6) *Identification of target capital expenditure.* The target CAPEX of the grid-balancing plants employed can be further calculated based on the gain from step (4) and the costs related to biomass collection from step (5).
 - (7) *Identification of the feasibility of the case study.* With the plant details from step (4), the CAPEX of each plant is evaluated at different conditions, e.g., different specific investment costs of the stack, to determine the prerequisites for business cases.

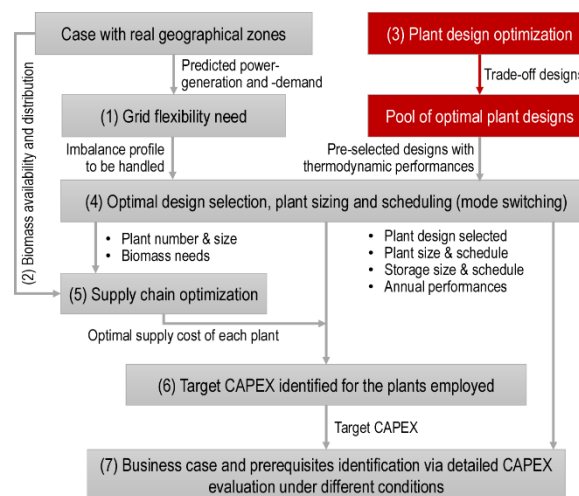


Figure 1 The overall decomposition-based methodology to identify feasible business cases for the grid-balancing plants [4].

2. Grid flexibility needs in 2030 (Step 1)

Denmark and Italy were chosen as representative situations with high wind power and solar power, respectively. The grid flexibility needs in 2030 have been predicted with historical power generation and consumption data, and official energy development plans, etc., according to the methodology given in Ref. [5]. Six potential RES dominated zones were identified as given in Fig. 2. A general approach has also been developed in Ref. [5] to investigate the scenarios of flexibility needs by considering novel ancillary services that could exist in the future, as well as a specification of the data analysis used to match the scenarios and the future situations in the defined RES-dominated zones in Denmark and

Italy. After the quantification of the perspective power balancing needs in 2030, four of these zones (DK1, DK2 and Bornholm in Denmark and SUD in Italy) have shown significant flexibility needs. For each of these four zones, hourly profiles of renewable power generation and demand have been generated, from which statistical analysis has been performed to characterize the flexibility needs, e.g., the Bornholm island (DK) in Fig. 3. The analysis of all zones (Fig. 4) has concluded that **the maximum capacity of UP/DOWN regulations of the flexibility needs in 2030 may reach 4.0/8.0 GW for DK1 (DK), 2.5/2.0 GW for DK2 (DK), 43/114 MW for Bornholm island (DK), 4.0/9.0 GW for SUD (IT), and 3.0/2.0 GW for SICI (IT)**. The flexibility needs (the shapes of the stair curves in Fig. 4) are also quite different between different zones. **Thus, in terms of energy, the flexibility needs become 4.8/17 TWh for DK1, 7.1/1.0 TWh for DK2, 90/110 GWh for Bornholm island, 6.4/14 TWh for SUD and 7.8/1.6 TWh for SICI**. Considering the electricity demand and biomass transportation, the zones, DK1, DK2, Bornholm and SUD, are selected for further investigations in the steps afterward. Note that the flexibility needs do not stand for the real grid balancing needs (market) since part of the flexibility needs will be handled by cross-border transmission and conventional power plants. Their contributions rely on the prediction from local Transmission System Operators (TSOs), e.g., Elia Group report [2] for Belgium and Energinet report [12] for Denmark. The Italian TSO, Terna, has not released any official report, thus the numbers used refer to Refs. [2,12]. When the flexibility needs are scaled to the balancing needs to be handled by the balancing service party, the characteristics of the UP/DOWN regulations are kept the same.



Figure 2 The zones considered in W2G project.

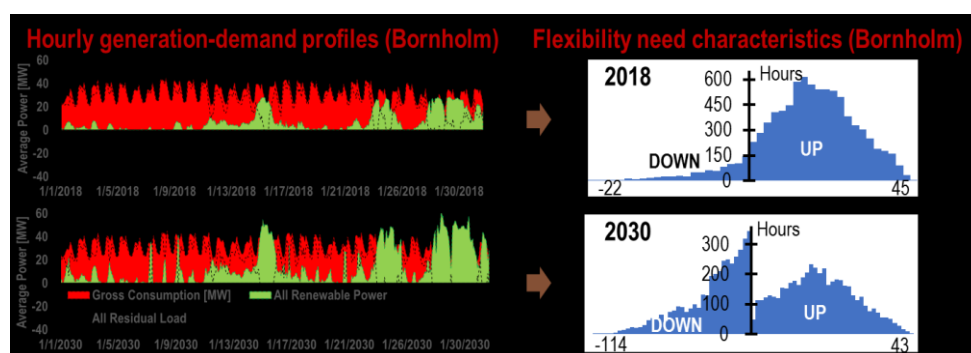


Figure 3 The hourly generation-demand profiles of 2018 and the prediction for 2030 (left), based on which the characteristics shows the regulation needs (right): UP indicates generation needed while DOWN indicates storage needed.

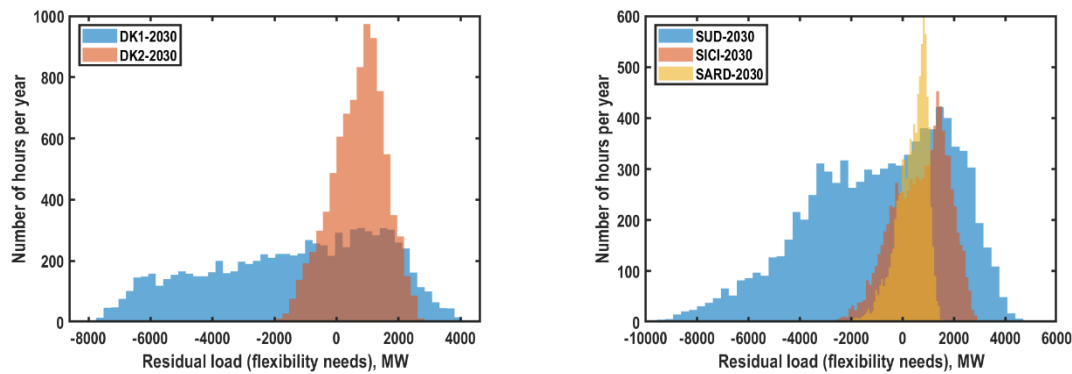


Figure 4 The grid flexibility needs of DK (left) and IT (right) in 2030. The residual load is defined as load (demand) minus renewable power, thus equivalent to the flexibility needs.

3. Waste availability in 2030 (Step 2)

The sustainable potential of organic waste and residual biomass available for zones including and surrounding the selected RES-dominated zones was quantified for 2030. Four different aggregations of Biomass have been evaluated: Agriculture Residues (Straw and Pruning), Forest (net increment and residues), MSW (organic, wood and paper fraction) and Bio-Waste. The data source used is national inventories, satellite-derived data COPERNICUS, EU project S2Biom. Using validated methodologies at the EU level, the Base Potential of the waste stream is derived for 2030 with the consideration of legal restrictions such as constraints from management plans in protected areas and sustainability, restrictions from REDII (Renewable Energy and Climate Directive) and EU-Waste Directive. Denmark is divided into 3 RES-Dominated zones with the 2030 biomass base potential for forest residues of around 1850 k.t. d.m, agriculture residues of 1484 k.t. d.m, biowaste of 1931 k.t. d.m. Italy southern regions ‘in-around’ SUD (the identified zone) have the 2030 annual base potential of 826,384 t.d.m straw, 1,221,102 t.d.m Prunings, 3,317,461 tons of forest increment, an additional stream of 1,287,385 tons of MSW organic fraction. The evaluated Biomass potential is allocated on CORINE land Cover using QGIS software, to obtain a geo dataset with geo reference, shape and raster format, with the aim to have a spatial explicit distribution with geographical cover, the advantages are data interoperability with other software and geo portals, SQL (Standard Query Language) query capabilities, and dynamic maps visualization. For municipal solid waste of Denmark where the detailed distribution is not available, the gross data is assigned according to the publication distribution. All wastes distributions have been provided as visualized in Fig. 5 (with high resolution up to 100 m).

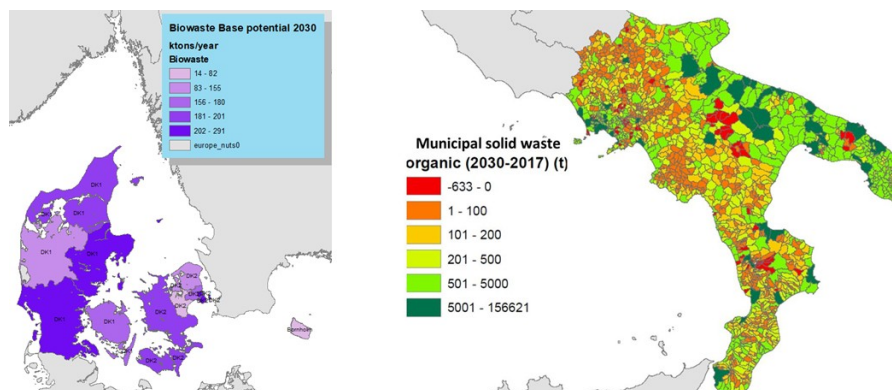


Figure 5 Example of waste availability in 2030 (left – biowaste base potential in Denmark, right – the municipal solid waste organic fraction in South Italy).

The gross wastes excluding forest wastes have been given in Fig. 6 (left). It shows that the local exploitable agri-wastes (straw and prunings) and municipal solid wastes (organic fraction, paper and wood) are in the same order. With the representative lower heating values of each type of wastes, the waste base potentials for each zone in Fig. 6 (right) are in the same order of magnitude of the total energy needed to cope with the flexibility needs obtained in section 2. Considering that the real balancing market is significantly smaller than the theoretical flexibility needs and other flexibility means are also available [2,12], it can be concluded that **local exploitable wastes could be enough to support W2G plants for providing grid balancing services as much as possible.**

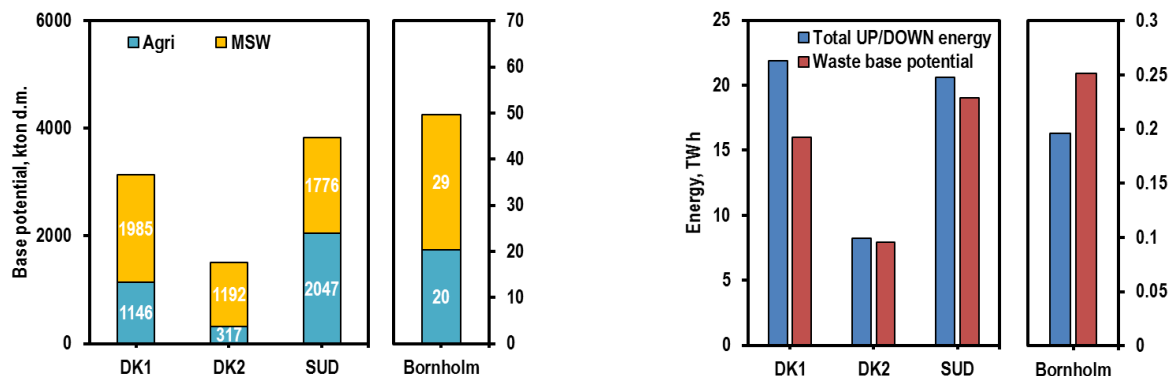


Figure 6 Local exploitable wastes excluding competing use (left) and comparison with the flexibility needs in terms of energy (right).

4. Pool of optimal plant design (Step 3)

4.1. Plant concept

Biomass-to-syngas part is expected to operate without load shifting, while the clean syngas produced is converted in three modes, thanks to the coordination of two RSOC blocks:

- Power generation (PowGen) mode: biomass-to-electricity with both RSOC blocks under the fuel cell (FC) mode.
- Power storage (PowSto) mode: biomass-to-chemical with both RSOC blocks under the electrolyzer (EL) mode to enable the power-to-x capability powered by excess renewable electricity.
- Power Neutral (PowNeu) mode: biomass-to-chemical with one RSOC block under the FC mode to power the other block under the EL mode for chemical production. No external electricity is needed.

4.2. Pool of optimal plant designs

A well-developed optimization method has been employed to investigate the optimal conceptual design of the W2G plants considering (1) various combinations of different types of drying units, gasifiers, syngas cleaning and conditioning, electrolysis mode, etc., (2) key operating variables of the stack and components, and (3) multiple objective functions including PowGen efficiency, PowSto efficiency and specific cell area per kW biomass input (dry basis). Detailed analysis has been given in Ref. [4] with the key results given in Fig. 7:

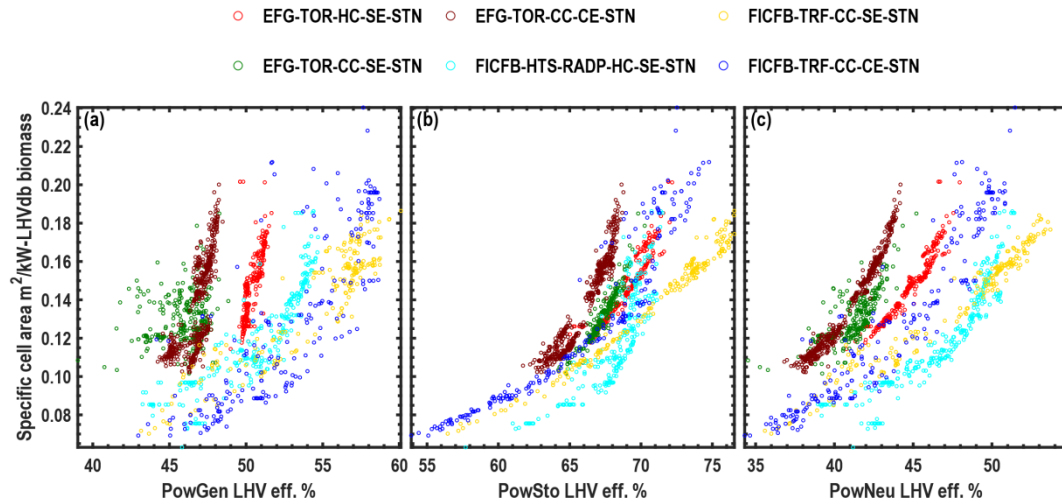


Figure 7 The design pools of different process options illustrating the trade-off between the efficiency and specific cell area needed per kW-LHVdb biomass EFG, TOR, HC, CC, SE, CE, STN, TRF, FICFB standing for entrained flow gasifier, torrefraction, hot gas cleaning, cold gas cleaning, steam electrolysis, co-electrolysis, steam turbine network, tar reformer, twin fluidized-bed gasifier. Each point indicates an optimal plant design with one specific combination of components, design variables.

It is concluded that the increase in efficiency results in an increased cell area for a given biomass feed. There is no big difference (less than 5% points) in efficiency among various process options of the same type of gasifier. The efficiencies reached can be up to 50–60% (PowGen), 72–76% (PowSto) and 47–55% (PowNeu). Those with fluidized bed gasifier can realize higher efficiencies than those with entrained flow gasifier. The design pool in Fig. 7 offers alternatives to best handle different grid balancing scenarios with power generated or needed, methane produced, and oxygen balance per kW-LHVdb biomass.

5. Grid integration with design selection, sizing and scheduling (Step 4)

With the preselected plant designs from Fig. 7, an optimization is performed by varying the number, size and operation of the W2G plants to maximize the profits from energy balancing and capacity reserving with typical constraints implemented in the Dispa-SET platform and W2G specific constraints.

The flexibility needs obtained in section 2 are first characterized in repetitive typical days to reduce computation time. Since the contributions of cross-border transmission and other flexibility means are not available, four scenarios are defined with different balancing needs handled by the W2G plants, referring to Refs. [2,12]: (S0) All flexibility needs, (S1) The flexibility needs excluding interconnections (66% of the total UP regulation, 68% of the total DOWN regulation), (S2) The flexibility needs excluding interconnections, batteries and classic plants (14% of the total UP and 30% of the total DOWN), and (S3) 30% of the S2 (4% of the total UP and 9% of the total DOWN) indicating that the remaining are handled by other competing technologies.

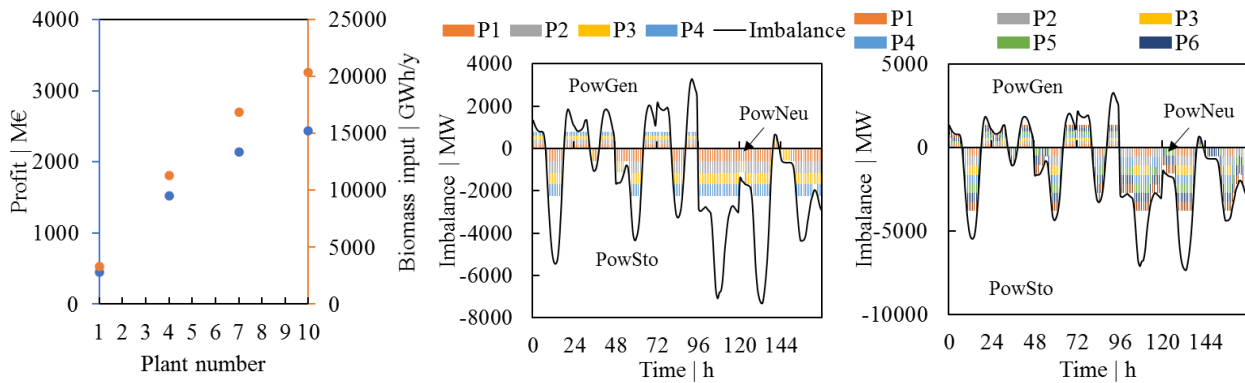


Figure 8 Optimal grid integration of the case (EFG, SUD, S0): (left) balancing profit versus plant number and size, (middle) plant schedules of the case with 4 plants, (right) plant schedules of the case with 6 plants.

The case implementing EFG plant designs for S0 and Italy SUD, represented as (EFG, SUD, S0) is used in Fig. 8 to illustrate the main findings. **By implementing more plants with optimal sizing, the profits obtained from the balancing services increases (Fig. 8 left) due to the decreased imbalance (Fig. 8 middle & right).** When most of the imbalance is taken, further increasing plant numbers does not affect the profit significantly. It is also found that the more the plants used, the longer the PowNeu mode will be operated due to the optimal plant scheduling for specific balancing profile. Similar conclusions have been confirmed with the calculation of all other scenarios S1–S3. For each case study in Fig. 8, the plant sizes and the corresponding biomass needed are fed to the biomass supply chain optimization (Step 5).

6. Supply chain optimization (Step 5)

Due to high computation efforts, biomass supply chain optimization has been performed to minimize supply costs for 8 cases up to now: (FICFB, SUD, S2, (1, 4, 7, 10)) and (EFG, SUD, S0, (1, 4, 7)). The optimization considers the production of agri-wastes and municipal solid wastes, biomass storage & transportation, and superstructure-based biomass pretreatment. The waste distributions were provided from section 3 (Step 2).

Two cases are taken as examples as shown in Fig. 9. The plants tend to locate in the major cities with more municipal solid wastes available. Thus, biomass transportation costs can be minimized.

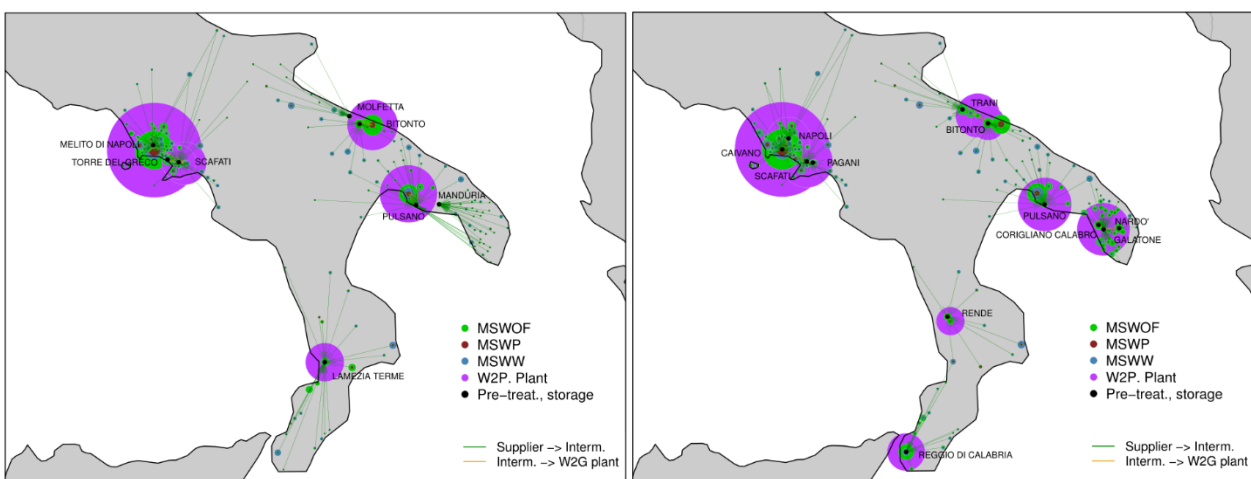


Figure 9 Example of the optimal biomass supply chain for the case studies (FICFB, SUD, S2, 7) and (FICFB, SUD, S2, 10) *considering only municipal solid wastes*. Note that the small dots distributed between different types of biomass are not comparable due to different scaling factors.

7. Target CAPEX calculation (Step 6)

The CAPEX targets have been calculated for the two cases with supply chain optimized. It is given on different bases as shown in Fig. 10. The larger the target, the easier the plants to earn profits. The increase in the number of plants installed to reduce the imbalance reduces the CAPEX targets (Fig. 10 left), which means it becomes less profitable with more plants installed. This is because with more plants installed, the duration of PowNeu operation becomes longer, which is not beneficial due to low efficiency. The difference between the two figures is mainly due to that the S2 case selects the plants with a higher ratio of PowSto power/PowGen power.

The CAPEX targets obtained are within the range of 1300–2750 €/kWe PowGen power. The CAPEX of the conventional biomass power generation with fixed and fluidized bed gasifiers has been reported within 2140–5700 USD/kWe [13], while the state-of-the-art SOFC based small combined heat and power product costs over 4000 €/kWe, which tends to decline to 1000 €/kWe in the future. In general, it is still challenging to further reduce the manufacturing costs of the key components. Detailed CAPEX calculation for the W2G plants with different sizes of each case study will be done in the future to have a better comparison.

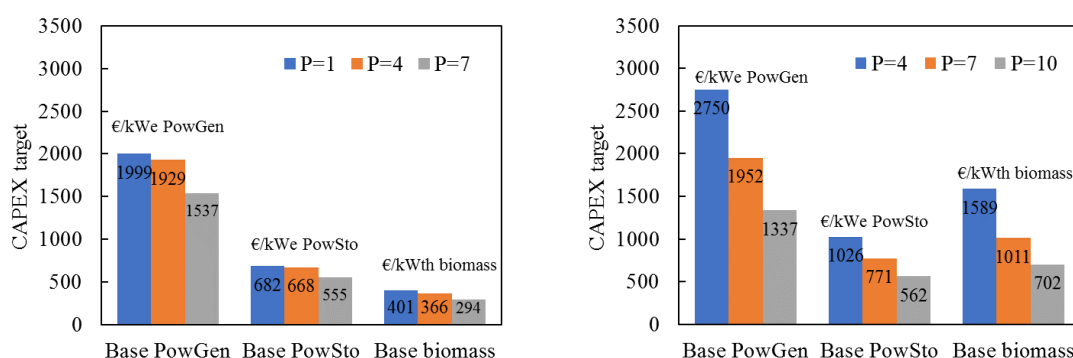


Figure 10 The CAPEX target calculation for the case (EFG, SUD, S0) (left) and (FICFB, SUD, S2) (right).

8. Conclusions

The potential of triple-mode biomass gasifier and reversible solid-oxide cell stack based grid balancing power plants has been evaluated with an optimization methodology combining flexibility need prediction, biomass potential identification, optimal plant design, optimal grid integration with plant sizing and scheduling, supply chain optimization and CAPEX target calculation. The DK1, DK2, Bornholm island in Denmark and SUD in Italy have been chosen as the renewable energy dominated zones. Due to the heavy computation load, the CAPEX target was calculated for several scenarios of SUD. The major findings are

- The theoretical flexibility needs reach up to several tens of GW for the selected zones and several to tens of TWh in terms of energy. The characteristics of the flexibility needs for different zones vary a lot.

- Local exploitable wastes are in the same order of magnitude of the theoretical flexibility needs, indicating enough biomass to support the grid balancing.
- Different optimal plant designs have been obtained with the efficiencies reaching up to 50–60% (PowGen), 72–76% (PowSto) and 47–55% (PowNeu). It can offer different designs according to the flexibility-need characteristics.
- With more plants installed with optimal sizes, the imbalance can be reduced; however, it becomes less profitable, since more plants are coordinated to operate under less efficient PowNeu mode.
- The CAPEX target of the W2G plant obtained with the limited case studies is within 1300-2750 €/kWe PowGen power and 550–1000 €/kWe PowSto power. Detailed CAPEX evaluation of the plants installed in each case study will be performed to have a better comparison.

References

- [1] eurostat, Energy, transport and environment statistics (2019 edition), Tech. rep. (2019).
- [2] Elia Group, Adequacy and flexibility study for belgium 2020–2030, Tech. rep., Elia Group (2019).
- [3] A. Arasto, D. Chiaramonti, J. Kiviluoma, L. Waldheim, K. Maniatis, K. Sipilä, et al., Bioenergy's role in balancing the electricity grid and providing storage options-an eu perspective, Tech. rep., IEA bioenergy (2017).
- [4] L. Wang, Y. Zhang, C. Li, M. Pérez-Fortes, T.-E. Lin, F. Maréchal, J. Van herle, Y. Yang. Triple-mode grid-balancing plants via biomass gasification and reversible solid-oxide cell stack: concept and thermodynamic performance. Revision under review.
- [5] K. P. Olsen, Y. Zong, S. You, H. Bindner, M. Koivisto, J. Gea-Bermúdez, Multi-timescale data-driven method identifying flexibility requirements for scenarios with high penetration of renewables, Applied Energy 264 (2020) 114702.
- [6] Biomass Energy Europe: <http://www.eu-bee.eu/>.
- [7] S2Biom Delivery of sustainable supply of non-food biomass to support a resource-efficient Bioeconomy in Europe: <https://www.s2biom.eu/en/>.
- [8] Biomass Future: <https://ec.europa.eu/energy/intelligent/projects/en/projects/biomass-futures>.
- [9] L. Puigjaner, Syngas from waste: emerging technologies, Springer, 2011.
- [10] J. M. Laínez, M. Pérez-Fortes, A. D. Bojarski, L. Puigjaner, Raw materials supply, in: Syngas from Waste, Springer, 2011, pp. 23–54.
- [11] M. Pérez-Fortes, J. M. Laínez-Aguirre, A. D. Bojarski, L. Puigjaner, Optimization of pre-treatment selection for the use of woody waste in co-combustion plants, Chemical Engineering Research and Design 92 (8) (2014) 1539–1562.
- [12] Energinet, System Perspectives for the 70% target and large-scale offshore wind. 2020.
- [13] Irena, I.R.E.A., 2012. Renewable energy technologies: Cost analysis series. Biomass power generation.

G0903

Opportunities and challenges for Water Electrolysers to participate in grid services

Stéphanie Crevon (1), Valérie Seguin (1)

(1) CEA Liten

17, avenue des Martyrs, FR 38 054 Grenoble Cedex 9

Tel.: +33 4 38 78 95 03

stephanie.crevon@cea.fr ; valerie.seguin@cea.fr

Abstract

This study conducted in the scope of European project QualyGridS analyses the potential economic opportunity for Water Electrolyzers to participate in grid services market. A business case located in Germany considering the possibility to participate in 2 grid services has been modelled and analyzed. A study of potential future evolutions has underlined some important uncertainties WE have to face regarding the interest of this participation.

Introduction

Transmission System Operators (TSOs) have the responsibility to ensure the permanent balance between production and consumption on the electrical grid. In principle, this balance is ensured by the electricity wholesale market: loads contract electricity according to their demand and generators produce only as much electricity as they have sold. But deviations from contracted positions are inevitable, especially for intermittent renewable energy generators.

The resulting imbalances are managed and corrected by the TSOs, which contract for reserve capacity to be called upon in real-time: that is the principle of grid services. Grid services answer instant flexibility need of TSOs. Electricity producers and loads are the providers of these services; more precisely, they offer to the grid to increase and/or decrease their production (resp. their consumption) on demand against a remuneration.

As loads connected to the electrical grid, Water Electrolysers (WE) can be candidate to provide these services. In the framework of this study, we are not considering Power-to-Power solutions (WE producing hydrogen stored in large storage or in the gas network and used later in a Fuel Cell or a gas turbine to produce back electricity), that appear to be a solution much more relevant for the seasonal flexibility need of the electrical grid.

This paper details an economic analysis of a business case involving a WE participating in grid services; this analysis was conducted in the scope of European project QualyGrids. The objective of the study was to better comprehend the potential interest for WE of participating in grid services and to identify which grid service would best fit with the operational constraints.

Literature review indicates that in the current situation installation of a WE cannot be justified only by the participation to electricity grid services (see for example [1]). A remunerating market for the H₂ produced (with H₂ used as feedstock for chemical industry or as a fuel for mobility) should be targeted to reach profitability. These markets represent primary value stream for the WE.

We thus studied a business case where the WE both supply an H₂ load to a customer and participate in grid service.

Description of the business case

The studied business case is located in Germany and represents an installation providing H₂ stored at 200 bars (the stored H₂ can be used for an on-site Hydrogen Refuelling Station (HRS) or can be put on trucks to serve H₂ needs on other sites).

Germany has been chosen notably for the potential of hydrogen market development.

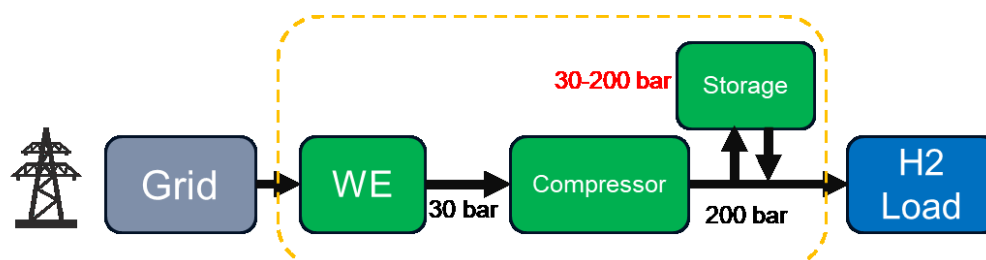


FIGURE 25-ARCHITECTURE OF THE SYSTEM

We modelled a variable load, with a daily constraint on the H₂ to be produced.

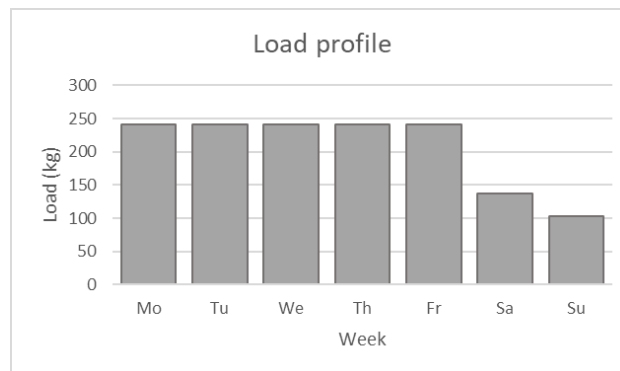


FIGURE 26-HYDROGEN LOAD PROFILE

Grid services are classified into different products. Possible participation in two of these products has been studied in this analysis: FCR (Frequency Containment Reserve) and aFRR (automatic Frequency Restoration Reserve). Participating in FCR product requires a fast time response but activation duration only lasts a few minutes whereas for aFRR product, requirement for time response is less constraining (must be lower than 15 minutes) but activation can last longer.

In this study, the calculations were based on data from years 2016/2017. FCR and aFRR grid services main characteristics at this time in Germany are summarized in the table below:

	Germany	
Product name	FCR	aFRR
(A)Symmetrical ?	Symmetrical	Asymmetrical
Activation time	< 30s	< 5min
Activation duration	< 15min	Can be from minutes to hours
Pmin requested	1 MW	5 MW
Availability window	Week	4 daily products POS_NT/POS_HT and NEG_NT/NEG_HT [Peak=Mon-Frid (8h - 20h) without public holidays, off-peak=residual period]
Frequency of selection	Weekly	Weekly
Commitment period	Tuesday W-1	Wednesday W-1
Price components	Capacity	Capacity + Energy
Remuneration principle	Pay-as-bid (remuneration for capacity reserve)	Pay-as-bid (remuneration for capacity reserve & provided energy when activated)

SUMMARY OF GRID SERVICES CHARACTERISTICS (2016/2017)

	Germany - 2016/2017
Average electricity SPOT price	31,6 €/MWh
FCR remuneration for capacity	14,8 €/MW/h
aFRR+ remuneration for capacity	3,5 €/MW/h
aFRR+ remuneration for energy	50 €/MWh
aFRR- remuneration for capacity	0,9 €/MW/h
aFRR- remuneration for energy	-3,3 €/MWh

Methodology for the study

➤ The economic indicator considered : the levelized cost of hydrogen

The objective set for the study is to minimize the levelized cost of hydrogen (LCOH) produced at the outlet of the defined system (perimeter of the system is defined by the yellow dotted lines on figure [1]).

The LCOH is defined as the sum of the costs generated by the system over its lifetime divided by the quantity of hydrogen produced by the system over its lifetime.

$$LCOH = \frac{\text{Total levelized costs of the system (CAPEX, OPEX, variable costs)}}{\text{Total levelized amount of H2 produced during 20 years}}$$

The costs generated by the system over its lifetime are:

- CAPEX (Investment cost) & OPEX (Fixed maintenance and operation costs) of the installation
- Replacement costs (for the WE stacks)
- Costs of electricity (used by the WE and by the compressor)
- Costs of water (used by the WE)

Costs of water & electricity are variables costs: they depend on the number of hours of operation of the system. When relevant, revenues coming from grid services are taken into account in the calculation of the LCOH. They are deduced from the total levelized costs of the system. Participating to grid services may also impact the optimal number of hours of operation of the system and thus the variable costs (costs of electricity notably).

In the calculation of the LCOH, the costs, revenues and the quantity of hydrogen produced are levelized, using a discount rate. The discount rate includes the perceived risk by the investor, and can be associated to the notion of WACC (Weighted Average Cost of Capital). The discount rate used in this analysis is 8%. The lifetime of the installation is set to 20 years.

The LCOH gives the minimum average hydrogen selling price at the outlet of the system over 20 years to make the installation profitable.

➤ An analysis based on historical data with a time step of one hour

Looking at the situation in more detail, electricity prices are changing every hour on the SPOT market and grid services remunerations are also changing frequently (for example in 2016 & 2017, FCR capacity remuneration was changing every week and data for aFRR average energy activation prices were reported with a time step of 15 minutes).

One can expect that depending on the remuneration level coming from grid services, a WE may or may not have an interest in participating to grid services. There is an interest in refining the level of details of the calculations.

Our calculations were thus based on time series with a time step of 1 hour including historical data from years 2016 & 2017 for the electricity prices and grid services remuneration granted to grid services providers. An EEG tax exemption has been assumed and grid fees have not been considered either.

The time series used for calculation also include the H₂ load time series described on Figure 2.

➤ Optimizing the operating strategy of the system and its sizing with the objective to minimize the LCOH

The key question of the analysis is to determine the best configuration for the studied system, considering economic opportunities coming from electricity and grid services markets and constraints coming from the satisfaction of the H₂ load, with the goal of minimizing the LCOH. By “best configuration”, we both imply the best sizing of the system (size of the WE, size of the storage) and the best operational strategy (electricity purchase and grid services participation strategy).

For this purpose, we defined the problem as a mathematical optimization problem. The variables of the problem are either time dependent:

- The power to be used by the WE at each time step
- The power dedicated to grid services at each time step

Or variables that do not depend on time:

- The size of the storage
- The size of the WE

Solving the optimization problem gives the optimal sizing and the optimal operating strategy of the system.

More precisely, we have defined our problem as a Mixed Integer Linear Programming Problem (MILP Problem). In MILP framework, an objective function to optimize is defined (in our case the LCOH to minimize) as well as constraints that represent the system (modelling of the components and of their relationships). Satisfaction of the load is part of the constraints. In MILP framework, all the constraints must be defined as linear equalities or inequalities, with the possibility to use binary variables to describe nonlinear behavior. That implies some simplifications in the modelling of the system.

The Mixed Integer Linear Programming (MILP) framework is one of the preferred solutions for formulating optimization problems in the energy domain. The first advantage is the close relation of a MILP formulation to the physical equations. The second advantage is the reasonable computational time, especially when using efficient modern MILP solvers.

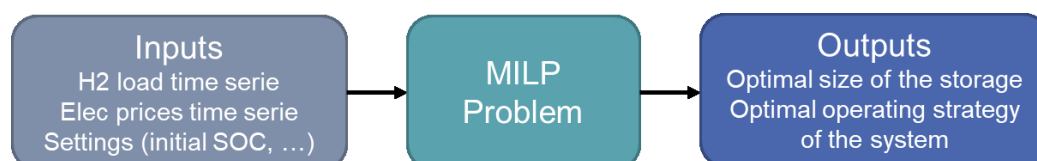


FIGURE 27-MILP MODELLING PRINCIPLE

In our analysis, one single optimization was conducted on the 2 years. That implies that the problem was solved with a perfect knowledge of all the prices. We are thus getting what would have been the best operating strategy knowing all the prices and possible remunerations over these 2 years.

A WE operator that would try to participate to grid services would have to face uncertainties on the future electricity prices and possible grid services remuneration. Thus, the results obtained do not give a fully realistic potential revenue assessment. Though, the

main objective of the analysis was to compare the different grid services and to identify the grid services that would best fit with the operational constraints of the business case we are studying.

Solving the problem on 2 years also implies that an extrapolation is done to calculate the LCOH over 20 years (it is considered that these 2 years repeat 10 times). This choice of performing our optimization over 2 years was done to limit the computation time needed to solve the optimization problem.

➤ Specific modelling difficulties for aFRR

In Germany, the selection process for aFRR is based on Merit-Order-Lists: the bidders are selected for capacity reserve according to a first Merit-Order-List (MOL). The selection is based only on the price offered for capacity reserve. A second MOL is then established among the selected bidders. This MOL is based on the price offered for energy. Then, in real-time, the TSO calls the needed capacity according to this second MOL.

That corresponds to a merit-order activation. In some other countries, aFRR activation is done on pro-rata basis: all the selected bidders for capacity are called to provide a part of the energy needed.

There is an additional difficulty in modelling aFRR linked to the modelling of merit-order energy activation. The duration of activation depends indeed on the effective energy need, on the rank in the MOL and can also depend on the geographic location. The figure extracted from [3] shows the average activation rate (average percentage of time the reserved capacity is effectively activated) depending on the rank in the second MOL.

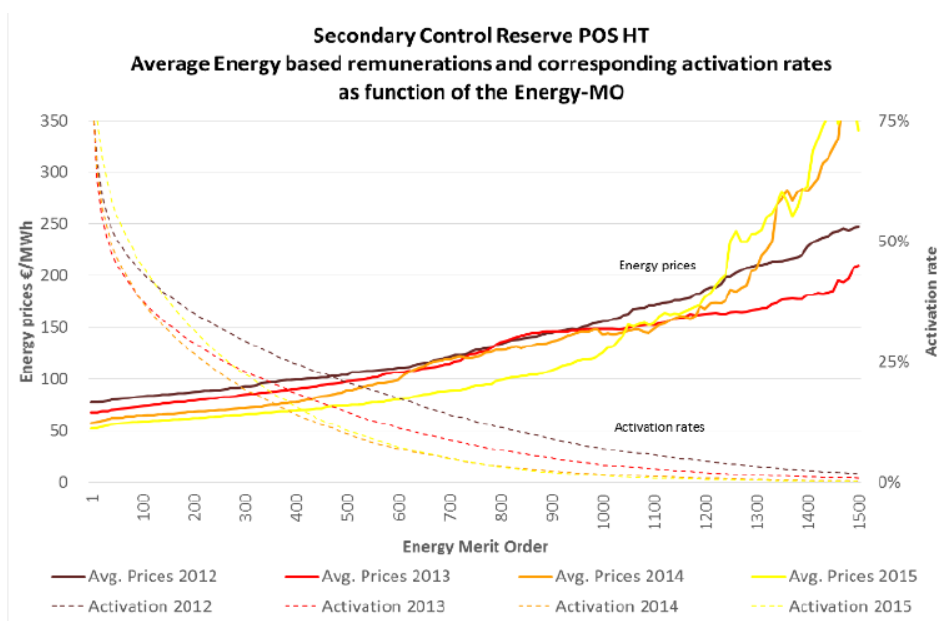


FIGURE 28-ENERGY PAYMENT AND ACTIVATION RATES FOR aFRR+ HT (PEAK PERIOD)

The better the ranking in the MOL is, the higher the probability to be selected is. It appears that the bidder ranked at the first place is activated in average for 75% of time over the bidding period whereas the bidder ranked at the last place is virtually never activated.

We chose again to use simplifying assumptions. For capacity bids, we considered that the WE got the average remuneration (the same assumption done for FCR). For energy bids,

we did not have access to the information linking the average remuneration to the activation duration. We thus decided to model two sub-cases:

- 1st on the MOL case: in this case, we assumed that the WE is always in capacity to place the most competitive bid and can thus always be the first on the MOL; we have access to the time series of the price offer of the bidder ranked at the first place for 2016-2017, so we considered this time series instead of the average remuneration time series. For this case, we considered an average activation duration of 75%.
- Last on the MOL case: for this case, we considered that the WE is never called for energy activation; this could be obtained by always requesting extremely high remuneration for energy.

The first case is probably not completely realistic as a bidder cannot be sure to always place the most competitive offer. Moreover there is no guarantee that this first case corresponds to the best case: there is a potential optimization in the bidding strategy (placing a bid conducting to lower activation time but with a global higher remuneration). However, there were not enough data available to identify this optimal case.

The last on the MOL case can be considered as a case giving a relatively realistic assessment, as it only implies to place average bid for capacity and then requesting very high remuneration in energy bids. This bidding strategy could be reproduced by WE operators.

The results obtained should of course always be looked in light of these considerations.

➤ Technical and economic assumptions for the system

We used FCH-JU report published in June 2017 identifying early business cases for power to H₂ applications ([1]) as a reference for most of the technical and economic assumptions for the parameters linked to the different components of the system.

Economic assumptions		
WE (Alcaline -2017)	Nominal power (MW)	1
	CAPEX (€/kW)	1200
	OPEX (%CAPEX)	4
	CAPEX - Stack replacement (€/kW)	420
	Stack lifetime (hours)	80 000
Storage	CAPEX (k€)	470
	OPEX (%CAPEX)	2
Compressor	CAPEX (k€)	218
	OPEX (%CAPEX)	3
Project overcosts (engineering, commissioning...)	% CAPEX _{components}	60

Technical assumptions		
ALK WE (2017)	Nominal power (MW)	1
	Pmax (%)	100
	Pmin (%)	15
	LHV efficiency (%)	57.5
	Output pressure (bar)	30
Compressor	Input pressure (bar)	30
	Output pressure (bar)	200
	Number of stages	2
	Maximum flow rate (kg/h)	20
Storage	Power consumption (kWhe/kg)	1
	Minimum size (kg) -Corresponding to one-day load	241 kg

TECHNICAL AND ECONOMIC ASSUMPTIONS FOR THE SYSTEMS

Results & analysis

The technical and economic results are detailed below.

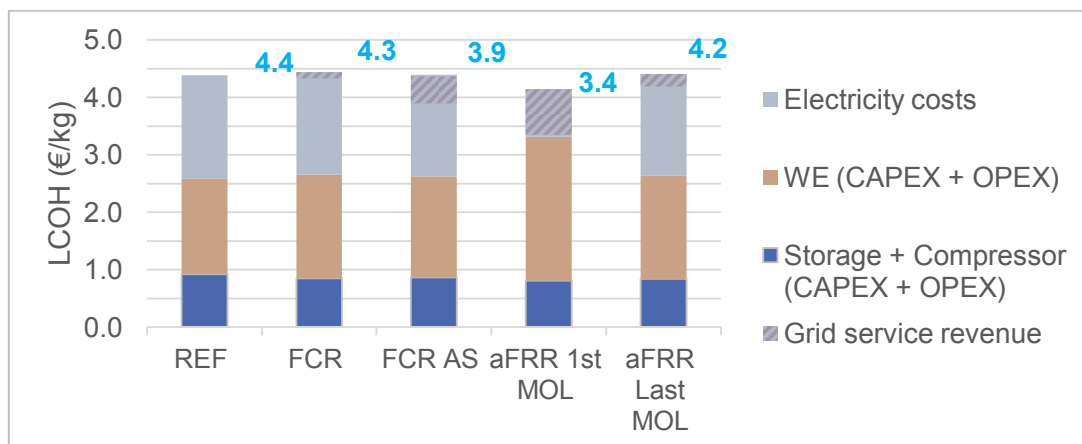


FIGURE 29- LCOH OBTAINED IN THE DIFFERENT SCENARIOS

Technical results	ALK OPTIM				
	REF	FCR	FCR AS	aFRR 1 st MOL	aFRR Last MOL
Storage: Size (kg)	345.25	283.25	299.33	241.52	276.71
WE: Size (MW)	0.515	0.518	0.543	0.777	0.556
WE: Nb of operating hours (h)	8493	8707	8076	8711	7885
Grid: Nb of buying hours (h)	8496	8707	8076	2330	7885
FCR: Nb of hours reserved (h)	-	1736	8076 ⁽⁺⁾ /784 ⁽⁻⁾	-	-
aFRR+: Nb of hours reserved (h)	-	-	-	2011	7885
aFRR+: Nb of hours used (h)	-	-	-	1508.25	0
aFRR-: Nb of hours reserved (h)	-	-	-	6420	786
aFRR-: Nb of hours used (h)	-	-	-	4815	0

EXTRACT OF THE DETAILED RESULTS OF THE OPTIMIZATION

➤ Reference results: without grid services

The minimum size of the WE to satisfy the load is slightly inferior to 0.5 MW. In the context we studied (Germany, current CAPEX level for WE, current electricity prices without taxes & fees), the optimal results globally tend to minimize the size of the WE and to maximize its number of hours of operation. There is though an interest in taking a slightly bigger WE to avoid buying electricity during the most expensive hours. That implies to have a bigger storage.

➤ Impact of the grid services

FCR symmetrical product does not appear very well adapted to the current operation of WE. Without participation in grid services, the optimal number of operating hours is close to 8760 hours. The additional revenue that can be obtained from FCR participation cannot

justify to increase the size of the WE. The possible participation (possible reserved power and number of participation hours) thus remains very limited. The associated gain on the LCOH is limited.

Offering capacity reserve in an asymmetrical way appear to be more adapted to the base operation of the WE today: if it only aims at providing capacity reserve, the WE would operate most of the year and would offer to decrease its electrical consumption if necessary. That is the case for aFRR last on the MOL scenario or that could be the case for FCR if it was possible to participate in an asymmetrical way. Participation in FCR in an asymmetrical way (FCR AS) would bring a higher benefit, due to the potential higher remuneration of the service. The possibility to participate in these services would slightly modify the optimal sizing and operating strategy of the system.

Possibility to use aFRR- cheap energy appears as a potential very interesting opportunity highlighted by aFRR- first on the MOL scenario. Being able to access this cheap electricity would depend on the capacity to place attractive bids on energy prices. Optimal operating strategy in this case will be modified; less electricity is bought on the SPOT market, and the WE is often offering to increase its consumption. The possibility to really benefit on very regular basis of aFRR- cheap energy would need to be tested in real bidding conditions.

Conclusions and perspectives

This study has confirmed a potential economic opportunity for WE in participating in grid services; it has described the opportunity in more detail:

- It thus appears that a **conservative choice** for the WE operator would be to try to **participate in aFRR with the goal to be selected only for capacity reserve**. That corresponds to the aFRR- Last on the MOL scenario. That would require to place competitive bids for capacity reserve and noncompetitive bids for energy.
- **Participating in aFRR with the goal to participate both for capacity reserve and energy is likely to create higher gain but that this possible opportunity would require further analysis**, involving assessment and simulation of possible bidding strategy performed by energy traders.
- In parallel, it would be **interesting to investigate the potential impact of participating in an asymmetrical FCR grid product**, to be prepared for a potential evolution of the grid service product.

Next step after this analysis would be to assess more precisely the possible economic gain; that would require a simulation of grid services participation on a real case and also considering the potential additional costs (such as costs to participate in the reserve markets and remuneration for the aggregator) that have not been taken into account in this study.

This work has already identified several challenges and uncertainties that WE operators would have to face if they want to participate in grid services

- The exact characteristics are different from one country to another and the global context of the country (in particular electricity prices profile) may also influence the results and the level of interest in participating in these grid services.
- A lot of uncertainties around some future evolutions imply uncertainties for WE operators on how they should adjust their systems to seize the opportunity :

- The characteristics of the grid services products are constantly evolving; globally, they tend towards more flexibility as the goal for TSO is to attract more participants on the market. These changes may modify optimal sizing and operating strategy and will also have an influence on balancing prices. The global tendency on these balancing prices are unclear : more “flexible” grid products are likely to attract more competitors to participate in grid services but on the other hand there may be an higher instant flexibility need for electrical grids in the future due notably to higher penetration of intermittent renewable energy sources.
- Evolution of the structure of electricity prices (which is anticipated in electricity production mixes with high renewable energy share) and development of the H₂ market size may also change the optimal sizing and operating strategy of their system.

References

[1] FCH-JU funded study “STUDY ON EARLY BUSINESS CASES FOR H₂ IN ENERGY STORAGE AND MORE BROADLY POWER TO H₂ APPLICATIONS” by Tractebel & Hincio, June 2017

[2]

https://www.smar.de/en/downloadcenter/download_market_data/5730#!?downloadAttributes=%7B%22selectedCategory%22:false,%22selectedSubCategory%22:false,%22selectedRegion%22:false,%22from%22:1581721200000,%22to%22:1582671599999,%22selectedFileType%22:false%7D (Accessed February 2020)

[3] FCH-JU funded study, “Flexibility within the electrical systems through demand side response: Introduction to balancing products and markets in Germany, France and the UK” by Maxime Zeller, June 2017.

[4] <https://www.larevuedelenergie.com/wp-content/uploads/2018/10/Stockage-levier-de-flexibilite.pdf> (Accessed in January 2020)

G11

Advanced technologies providing flexibility

G1103

Frequency control by run-of-river hydropower: A case study on energetic and economic potentials

Bastian Hase, Christian Seidel

Technische Universität Braunschweig,
AG Regenerative Energien, Institut für Statik
Beethovenstr. 51, D-38106 Braunschweig/Germany
Tel.: +49-531-391-3664
b.hase@tu-bs.de

Abstract

With a growing share of fluctuating renewable energies, such as wind and photovoltaics, predictable power generation capacities become more and more important. In parallel, the decarbonization of the energy sector calls for additional renewable balancing energy technologies as substitutes for fossil capacities. We developed an operation strategy that enables run-of-river hydroelectric (ROR) plants to deliver both constant load and balancing energy at the same time. Therefore we made use of the fact that upstream reservoir levels of most plants can, to a certain extent, be flexible, without making further impacts. This reveals significant short term storage potentials.

This operation strategy was successfully validated by simulations on a projected research power plant in northern Germany. When upscaling the balancing energy potentials of this research plant to the whole German non-swelling ROR-capacities, considerable amounts of the yearly national demand for balancing energy can theoretically be covered. These potentials vary with the type of balancing energy produced and the chosen lead value for the upstream water level within the minimum and the maximum possible level. In economic respects investigations for a new plant with feed-in tariff of 2021 producing automatic frequency restoration reserve revealed that despite a lower overall energy production additional income can be generated. This, however, depends on the amount of control power produced and the bidding strategy used in the power auctions.

Introduction

Apart from pumped hydro storage, most countries' production of balancing energy is highly based on fossil technologies. Yet, as reducing carbon footprints in the energy sector becomes more and more important, these capacities are often replaced by fluctuating renewable energies such as wind-power and photovoltaics [1]. This situation calls for additional emission free balancing energy technologies [2].

Run-of-river hydropower (ROR) is a very promising candidate to fill this technological gap. Currently, ROR hydroelectric plants are already used for negative automatic and manual frequency restoration reserve (aFRR and mFRR) [3]. However, when plants are operated at a quasi-constant upstream water level, power reductions due to the delivery of negative frequency restoration reserve almost necessarily lead to additional water losses over the attached weirs and thus to energy losses. Moreover, constant upstream water levels impede the delivery of frequency containment reserve (FCR) and positive frequency restoration reserve. This is because the abrupt increases of output power, coming along with the delivery of positive control power, almost necessarily result in a fall of the upstream reservoir level.

However, on many hydropower sites flexible upstream water levels within a limited band are technically possible and even ecologically desirable [4]. Recent studies showed, that a peak-to-peak amplitude of 30 cm is feasible on most rivers in Germany, including those used as waterways. Where this is impeded by minimum depths or vertical clearances a continuous storage operation using the reservoir of an upper hydroelectric plant as main storage can be implemented [5].

Flexible upstream reservoir levels of ROR-hydroelectric plants create significant short-time storage potentials, allowing a power production that is temporarily independent of the discharge into the reservoir. On the one hand, this enables hydropower stations to schedule their power production before the start of delivery and hold the power exactly constant during the delivery interval. Depending on the maximum lead time and delivery time of energy contracts that can be achieved using these storage capacities, the plant is able to play a similar role in the energy system as a fossil plant. On the other hand, the short time storages can be used to provide positive and negative control energy. Consequently, ROR-plants, making use of these potentials serve the energy system twice: By providing control energy and by exactly complying with the production schedule.

1. Simulation Strategy

A combined operation mode with the supply of constant base power and all three types of control energy was simulated for the years 2015-2017. The simulations were conducted on a model of the hydroelectric plant in Bannetze-Hornbostel that is currently under construction on the Aller-river in northern Germany. The plant is projected to have a maximum power output of 700 kW and a maximum flow rate of $60 \frac{\text{m}^3}{\text{s}}$. Instead of a turbine, it will be equipped with a high-performance waterwheel that is specially designed for high efficiencies on part load and at low heads. With a nominal head of only 1.4 m, this technology allows to generate power down to a minimum head of 30 cm at fair efficiencies. The peak-to-peak amplitude for the flexible upstream reservoir is only 27 cm. The upper and lower limit correspond to the current lead operation levels during summer and winter

of the existing weir were chosen and thus lie in a technically feasible range [6]. For the first investigations in this paper the target upstream water level is set 10 cm below the maximum and 17 cm above the minimum level. Table 1 shows the parameters used for the simulations.

Table 1: Parameters used for modelling the hydroelectric plant in Bannetze-Hornbostel

Simulation parameters		
Parameter	Symbol	Value
maximum power output	P_{max}	700 kW
maximum flow rate	Q_{max}	$60 \frac{m^3}{s}$
efficiency (constant)	η	85%
reservoir area	A_{res}	432,000 m ²
max. upstream water level	h_U^{max}	$h_U^{target} + 0.10 \text{ m}$
min. upstream water level	h_U^{min}	$h_U^{target} - 0.17 \text{ m}$
mean head 2015-2017 at h_U^{max}	H_{nom}	1.79 m
minimum head	H_{min}	0.30 m

In order to keep the influence of the hydro technology on the simulation results as low as possible, the plant's inertia was neglected in the model. In this case, the upstream reservoir level that should be held within the allowed limits is defined by the differential equation

$$\dot{h}_U(t) = \frac{Q(t)}{A_{res}} - \frac{P_{B,i} + P_C(t)}{(h_U(t) - h_D(t))} \cdot \frac{1}{A_{res} \cdot \rho \cdot g \cdot \eta} \quad (1)$$

with

$$P_{B,i} \quad \text{constant base power of delivery interval } i$$

$$\rho = 1000 \frac{kg}{m^3} \quad \text{density of water}$$

$$g = \frac{9,81m}{s^2} \quad \text{earth acceleration.}$$

When interpreting the hydro-plant as a dynamic control system the three time variable values

- produced control energy $P_C(t)$ calculated from the national demand $P_{C,Germany}(t)$
- discharge into the reservoir $Q(t)$
- downstream water level $h_D(t)$

have the function of disturbance inputs, impeding the stabilization of the upstream water level. For the simulations the produced control energy $P_C(t)$ and the discharge $Q(t)$ were available as 15-minute-values, whereas the downstream reservoir level $h_D(t)$ have a daily resolution.

When considering the undisturbed system, these values are constant. In this case, the second derivative of the upstream reservoir level $\ddot{h}_U(t)$ during a delivery interval of constant base power is defined as

$$\ddot{h}_U(t) = \dot{h}_U(t) \cdot \frac{P_{B,i} + P_C}{(h_U(t) - h_D)^2} \cdot \frac{1}{A_{res} \cdot \rho \cdot g \cdot \eta} \quad (2)$$

Since the two right factors $\frac{P_{B,i}+P_C}{(h_U(t)-h_D)^2}$ and $\frac{1}{A_{res} \cdot \rho \cdot g \cdot \eta}$ can never become negative, the condition

$$\text{sgn}(\ddot{h}_U) = \text{sgn}(\dot{h}_U) \quad (3)$$

is always valid. As a consequence, an initial increase/decrease of the upstream water level will keep growing/falling at an ever increasing speed. As soon as the maximum upstream water level is reached, however, the excessive water has to be spilled over the weirs resulting in energy losses. When reaching the minimum water level, the plant's output power has to be reduced in order to prevent the reservoir level from falling any further. As a result, the scheduled power cannot be completely produced reducing the plant's reliability. These undesirable states can be significantly reduced by stabilizing the reservoir level with a controller. Together the controller and the plant model form a closed control loop (see figure 1). Next to the stabilization of the water level, the controller has the task to calculate the maximum deliverable amount of control energy during a tendering interval. Consequently, the controller is responsible for the organization of the entire combined plant operation.

The stabilization of the upstream water level is achieved by adjusting the base power $P_{B,i}$ in regular time intervals i . Therefore the control unit estimates the flow rate through the water wheel necessary to bring the upstream water level back to the target value by the end of the next delivery interval. This flow rate is then used to calculate the scheduled base power for that interval. This base power P_B is scheduled with a lead time t_L and held constant during the length of the delivery interval t_D . Consequently, the time Δt between the calculation of the correcting variable $P_{B,i}$ and it's effect on the system is

$$t_L \leq \Delta t \leq t_L + t_D. \quad (4)$$

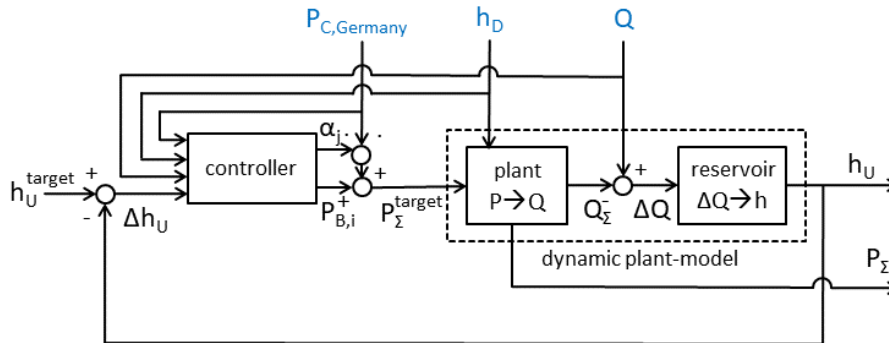


Figure 1: Block diagram of the control loop

This is why a two-step calculation $P_{B,i}$ was implemented (see figure 2). Here the calculation of $P_{B,i}$ is done at t_0 for the next delivery interval 1 (red). In the first step the controller estimates the upstream water level $h_U(t_1)$ at the start of the next delivery interval, based on current discharge and other system parameters. In the second step this water level is used to calculate the output power that is necessary to reach the lead value $h_U(t_2) = h_U^{target}$ by the end of the delivery interval t_2 .

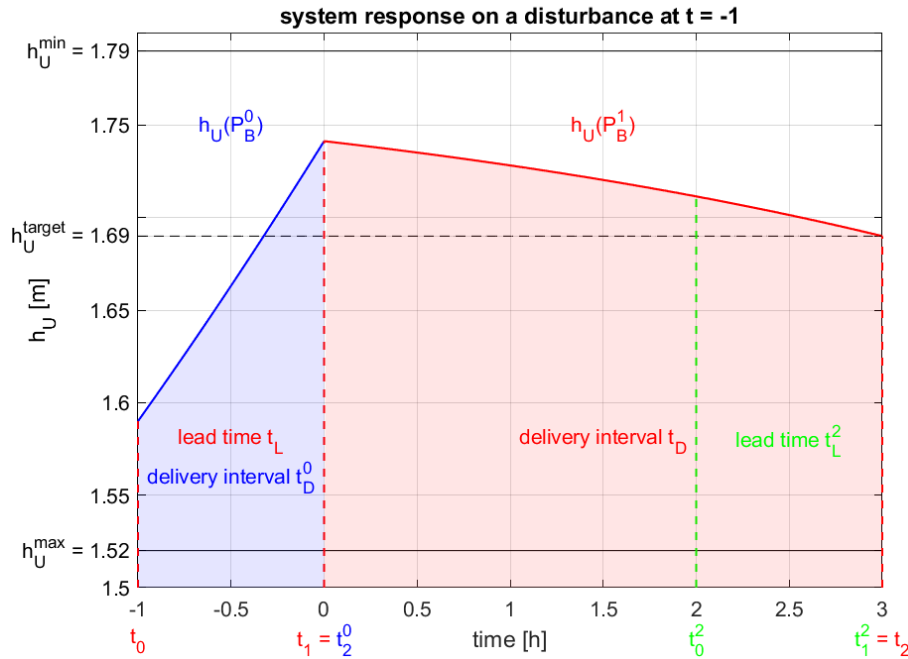


Figure 2: Step response of the undisturbed system with a lead value of $h_U^{target} = 1.69 \text{ m}$ to an initial upstream water level of $h_U(t_0) = 1.59 \text{ m}$ and an insufficient initial base power production.

The second task of the controller is to determine the maximum marketed control power. This is done according to the tender modalities shown in Table 2 that were valid in August 2018. The calculation of the maximum marketed control energy is executed at the time of bidding for each tendering interval. When neglecting special regulations for public holidays etc., this is between 9 and 129 hours before the start of delivery, depending on the type of control energy.

Table 2: Tender modalities of control energy applied to the simulation

Tender modalities for control energy	Type of control energy		
	FCR	aFRR	mFRR
delivery time	weekly	daily	daily
	168 h	24 h	24 h
bidding deadline	Tu. 15:00	15:00	10:00
start of delivery	Mo. 0:00	next day 0:00	next day 0:00
lead time	129 h	9 h	14 h

In order to minimize the influence of the bidding strategy, in the simulation the activation of the control power capacities is not executed in the range of the lowest price offers. Instead it is assumed, that during each tender period j , all ROR-plants deliver the same constant share of α_j of the nationally activated balancing power. This proportion corresponds to the ratio of the control power awarded in the auction $P_{C,plant}^{max}$ and the total amount of control power announced in the tender $P_{C,Germany}^{max}$:

$$\alpha_j = \frac{P_{C,plant}^{max}}{P_{C,Germany}^{max}} = \frac{P_C(t)}{P_{C,Germany}(t)}. \quad (5)$$

Consequently, the control power that has to be delivered by the plant is

$$P_{C,target}(t) = \begin{cases} \alpha_j^+ \cdot P_{C,Germany}(t) & \text{for } P_{C,Germany} > 0 \\ \alpha_j^- \cdot P_{C,Germany}(t) & \text{else} \end{cases} \quad (6)$$

The amount of automatic and manual frequency restoration reserve marketed by the plant in an upcoming tender round is determined by the controller in the form of the delivery factors α_j^+ and α_j^- . These factors represent the share of the national demand of positive and negative control energy that shall be covered by the plant. They are calculated based on the plant's positive and negative power reserves, forecast by the controller. Due to the long delivery periods, the prediction accuracy of these power reserves is very limited. Therefore, the forecast positive and negative power reserves are additionally multiplied by freely selectable marketing factors $0 \leq \kappa^+ \leq 1,5$ and $0 \leq \kappa^- \leq 1,5$.

$$\begin{aligned} \alpha_j^+ &= \kappa^+ \cdot P_{res,i}^+ \\ \alpha_j^- &= \kappa^- \cdot P_{res,i}^- \end{aligned} \quad (7)$$

with

$P_{res,j}^+, P_{res,j}^-$ minimum forecast positive and negative power reserves during coming delivery interval

Hence, this pair of marketing factors $\underline{\kappa} = (\kappa^+ ; \kappa^-)$ determines the share of the predicted power reserves that shall be offered as control power in the upcoming auction. When κ^+ or κ^- are equal to zero, no positive or negative control power is delivered at all. In change, at $\kappa > 1$, the marketed control power gets higher than the predicted power reserve increasing the risk that more capacities are offered than are actually available. Consequently, the marketing can be used to freely adjust of the amount versus the reliability of control energy and allow to investigate the interaction between positive and negative frequency restoration reserve.

In case of frequency containment reserve positive and negative power components are marketed together. As a result a common delivery factor $\alpha_i = \alpha_i^+ = \alpha_i^-$ is used. It is calculated from the minimum of the predicted power reserves in positive and negative direction multiplied by the common marketing factor κ .

$$\alpha_i = \kappa \cdot \min(P_{res,i}^+, P_{res,i}^-) \quad (8)$$

2. Influence of lead time and delivery time of base power

In operation with constant base power the amount and reliability of both, base power and control energy, is significantly influenced by the ability of the controller to stabilize the upstream water levels. Therefore, the lead time and step time between the base power adjustments should not be too high. Figure 3 shows the upstream water levels for different pairs $(t_L; t_D)$ of lead time and delivery time during 4 exemplary days in 2016. In the simulations the downstream water levels were considered as constant and a marketing factor of $\underline{\kappa} = (0 ; 0)$ was chosen, equivalent to no delivery of control power. Consequently, the discharge to the reservoir $Q(t)$ is the only disturbance input in the system. In the figure $Q(t)$ is shown as a green line on the right axis.

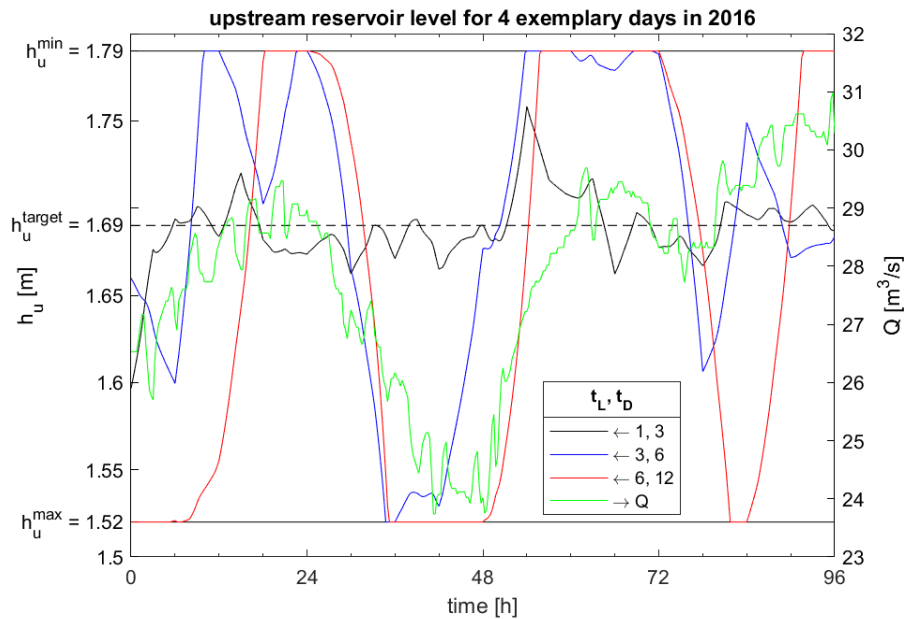


Figure 3: Upstream water levels for different pairs of lead time t_L and delivery time t_D for the base power on the left axis and discharges to the reservoir on the right axis for an exemplary time period of four days in 2016. Other disturbance inputs are neglected.

The different pairs illustrate that the quality of stabilizing the upstream water level clearly depends on the lead time and delivery time, which together sum up to the time between two adjustment steps. In case of the value pair $(t_L, t_D) = (1 \text{ h}, 3 \text{ h})$, represented by the black curve, the upstream water level can be maintained within $\pm 10 \text{ cm}$ of the lead value h_U^{target} . Consequently, neither water must be drained over the weir, nor is the minimum allowed water level reached. If the sum of lead time and delivery time $t_L + t_D = t_2 - t_0$ is further increased the stabilization of the upstream water level becomes more and more difficult. In the extreme case of the red curve with $(t_L, t_D) = (6 \text{ h}, 12 \text{ h})$ the upstream water level permanently oscillates between the upper and lower limit. Reaching the maximum upstream water level results in additional water losses over the weir ΔW_{weir} which should be avoided from an efficiency point of view. However, this does not imply the reliability of scheduled power deliveries. When the lower limit is reached and the plants' total power output must be reduced the delivery of positive control energy and/or base power is directly affected. In this case resulting delivery failures directly reduce the reliability which is defined as the quotient $R = \frac{W}{W_{\text{target}}}$ of actually delivered and projected energy within the time period considered. This reliability factor can be calculated for the base power as well as for the different types of control energy.

In figure 4a the reliability R_B of the base power, kept constant during intervals t_D , is shown as a parameter field of t_L and t_D for 2016. Due to flooding periods water losses over the weir can generally not completely be avoided. However, the comparison with the water losses over the weir in conventional operation (i.e. with a quasi steady upstream water level and no control unit) is a good indicator for an imperfect stabilization of the upstream water level against the upper limit. Figure 4b therefore shows the additional water losses over the weir $w_{\text{weir}} = \frac{\Delta W_{\text{weir}}}{W_{\text{conv}}}$ compared to the energy generation in conventional operation mode W_{conv} . The three value pairs (t_L, t_D) considered in figure 3 are marked in the parameter fields as squares with corresponding color. For the black scenario of $(t_L, t_D) = (1 \text{ h}, 3 \text{ h})$, a base power reliability of almost 100% is achieved. With $w_{\text{weir}} = 0$, the weir losses are not higher than in conventional operation. When the lead time and delivery time

are increased to $(t_L, t_D) = (3 \text{ h}, 6 \text{ h})$, already an additional 0.7% of the energy generated in conventional operation is dissipated over the weir. This value increases to 2.4% at $(t_L, t_D) = (6 \text{ h}, 12 \text{ h})$. At the same time, the reliability of the base power reduces to only 97.8%.

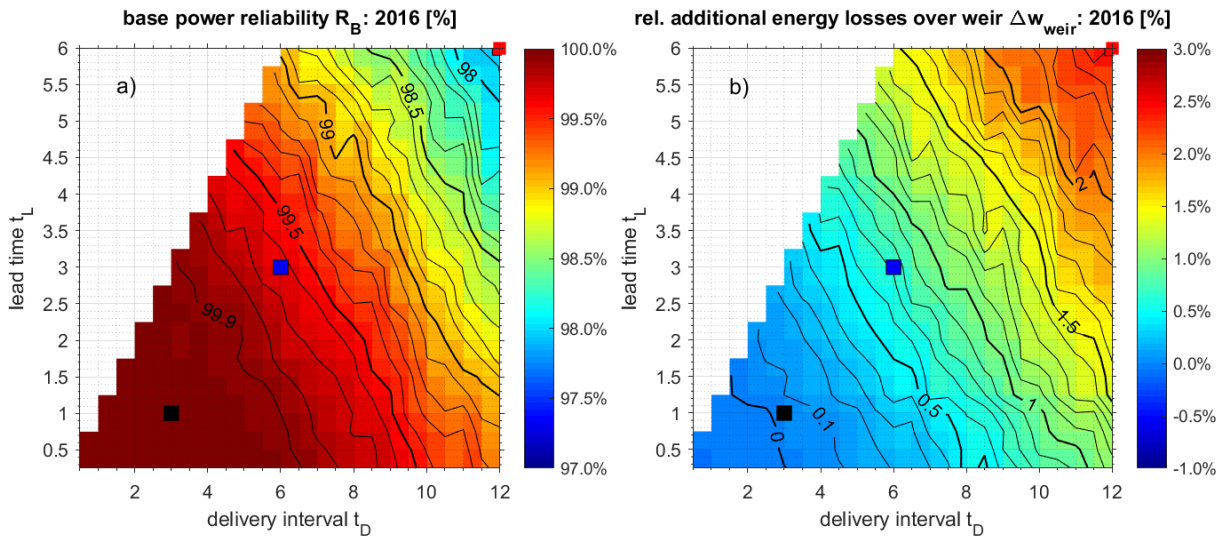


Figure 4a): Reliability of base power depending on lead time and time of constant delivery for a scenario without production of control energy in 2016. b): Energy losses over the weir, caused by the plant operation with constant base power as percentages of the energy production in conventional operation for a scenario without production of control energy in 2016.

Despite the jagged course of the black isolines caused by discrete calculation a dependency of both, the base power reliability R_B and the additional weir losses w_{weir} from the sum of lead and delivery time $t_L + t_D$ is clearly noticeable

$$f \approx f(t_L + t_D) \quad \text{for } f = \{R_B(t_L, t_D); w_{weir}(t_L, t_D)\}. \quad (9)$$

This shows that these important values for the description of the controller quality strongly depend on the time between the calculation of P_B and the end of its effect on the system $t_L + t_D$. The time interval t_D between two consecutive control steps alone, in contrast, has only a minor influence on the control accuracy. Consequently, the duration of a delivery interval of constant base power could be increased/reduced without any change in reliability if the lead time between marketing and start of delivery is reduced/increased by the same time.

A good stabilization of the upstream water level in the system only disturbed by the flow rate $Q(t)$ is necessary, when the production of control energy and the time-variable downstream water level shall also be considered. For this reason, a delivery time of $t_D = 3 \text{ h}$ and a lead time of $t_L = 1 \text{ h}$ are used for the further investigations.

3. Influence of the lead value for the upstream water level

In the previous considerations the lead value of the upstream water level was chosen with $h_U^{max} - h_U^{target} = 10 \text{ cm}$, allowing to store and remove water at any time. This corresponds to a battery that is constantly kept at a charge state of around 60%. The intention behind this approach is to allow the compensation of the disturbance inputs in both directions, namely the demand for control power and fluctuations in the discharge or underwater level. However, reaching the minimum upstream water level h_U^{min} is particularly critical as

the scheduled power cannot be delivered whereas exceeding the upper limit “only” results in a loss of usable energy. Therefore increasing the lead-upstream level and accepting additional water losses over the weir can be useful to increase the reliability of the (positive) control energy.

For an assessment of the influence of the target upstream water level h_U^{target} on the potentials of the plant's different energy products it is necessary to consider both, the amount and reliability of the corresponding product. In order to convey a better understanding of the potentials, instead of total annual work the deliverable balancing energy is expressed as an extrapolated delivery factor α :

$$\alpha = \frac{W_C}{W_{C,Germany}} \cdot \frac{P_{Germany}}{P_{max}} \quad (10)$$

with

$W_{C,Germany}$ national demand of control energy
 $P_{Germany}$ national ROR-capacity

This theoretical value is equivalent to the share of the German control energy demand that can be covered by non-swelling ROR, when upscaling the potentials of the plant in Bannetze-Hornbostel by the total installed power capacity. The extrapolated delivery factor α and the reliability R usually refer to the entire delivery period considered (i.e. generally 1 or 3 years). Therefore, these mean values are sometimes exceeded and sometimes fallen short of. Next to these parameters for the control energy, the annual production of base energy W_B and the total energy produced by the plant W_Σ are also important for judging the potentials. These two values are connected via the balance of generated control energy $W_C^+ + W_C^-$:

$$W_\Sigma = W_B + W_C^+ + W_C^- \quad (11)$$

For a better illustration, these values are related to the energy harvest during conventional operation:

$$w_\Sigma = \frac{W_\Sigma}{W_{conv}} \quad (12)$$

and

$$w_B = \frac{W_B}{W_{conv}}. \quad (13)$$

The influence of the target upstream water level on the base power and control energy potentials can be seen particularly well, when high amounts of control power are produced. Figure 5 shows the most important parameters for the generation of automatic frequency restoration reserve at the maximum marketing factors $\underline{\kappa} = (1.5 ; 1.5)$ during the years 2015-2017. Both the delivery factor α^+ and the reliability R^+ of the positive control energy clearly show an optimum at the highest possible target upstream water level $h_U^{max} - h_U^{target} \rightarrow 0$. Surprisingly the plant's total energy production W_Σ also increases as h_U^{target} is raised, even though more water has to be drained over the weir. This is due to the fact that the increasing average head overcompensates the additional weir losses ΔW_{weir} .

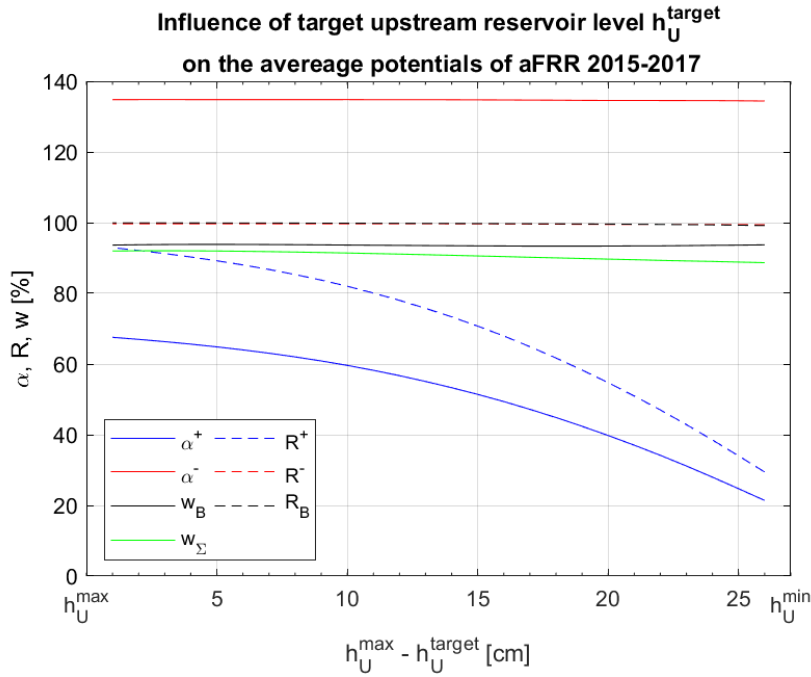


Figure 5: Delivered amounts and reliabilities of positive and negative automatic frequency restoration reserve, base power and total energy production, depending on the target upstream water level for a marketing factor of $\kappa = (1.5 ; 1.5)$ in the years 2015-2017.

The amount and reliability of the negative control energy and base power are largely indifferent to the target level of the upstream reservoir. Consequently, it can be summarized that a high reserve for lowering the water level largely increases the control energy potentials, whereas the possible range for raising the water level has no big effect.

In order to achieve maximum control energy-potentials, the target value for the upstream reservoir level should therefore be chosen as close as possible to the maximum water level. However, this does not necessarily lead to a maximum total energy production W_{Σ} . For two upstream water levels $h_{target}^2 > h_{target}^1$, this is only the case, when the condition

$$\left(\frac{h_{target}^2 - h_{target}^1}{H_{nom}} \right) > \frac{\int Q_W^2 - Q_W^1 dt}{\int Q dt} \Leftrightarrow W_{\Sigma}^2 > W_{\Sigma}^1 \quad (14)$$

with Q_W as the water drain over the weir, is fulfilled. This relation shows, that the energetic compensation of the increasing weir losses at h_{target}^2 by rising heads gets less, the higher the nominal head of the plant H_{nom} is. For the simulated plant with its nominal head of only 1.79 m this compensation effect was therefore particularly high.

4. Control energy potentials

Since the maximum control energy potentials can be achieved, when the upstream reservoir level is maintained as high as possible, for the further investigations a lead value $h_U^{max} - h_U^{target} = 2 \text{ cm}$ is used. This target allows a temporal lowering of the reservoir level of 25 cm, before the minimum value is reached.

Figure 6 shows the average achievable extrapolated delivery factor $\alpha(\kappa)$ and corresponding reliability $R(\kappa)$ of the frequency containment reserve over the marketing factor κ for the years 2015-2017. The dashed lines break these two values further down to

the positive and the negative power component. When extrapolating the potentials to the whole German ROR-capacity, a three-year average of more than 150% of the national demand can be covered. However, the coverage and reliability is generally higher for the negative power component than for the positive. Besides, especially for the positive power component higher coverages α^+ lead to lower reliabilities R^+ . In order to cover an average of 100% of the national demand for both power components, a marketing factor of $\kappa = 0.97$ is necessary. This leads to an overall reliability of 95%, meaning that 95% of the marketed control energy can actually be delivered when demanded. As a consequence, a remaining 5% gap has to be covered by backup capacities, of which around 91% are required for backing up the positive power component and only 9% are needed for the negative power component.

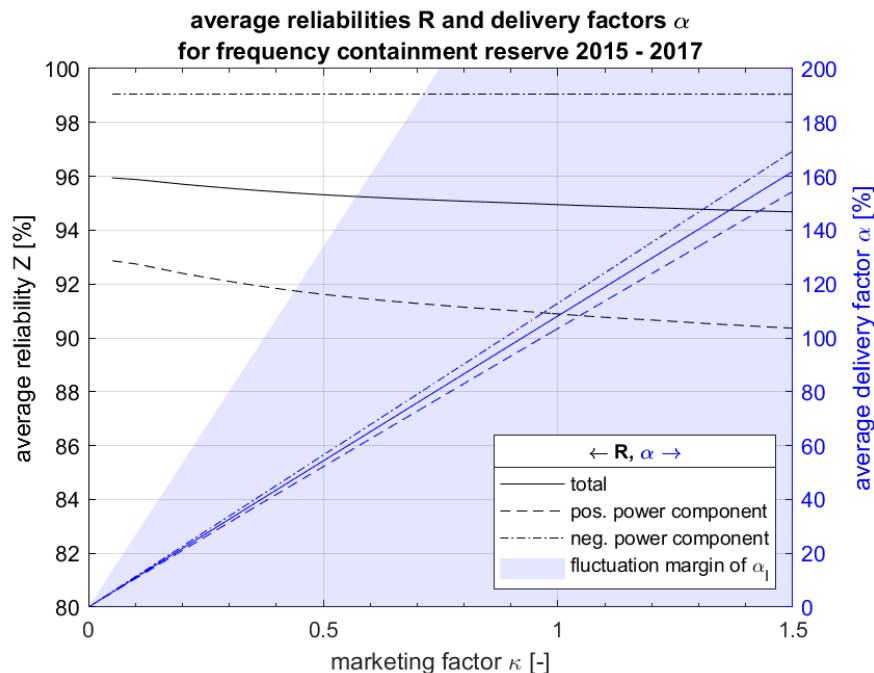


Figure 6: Average reliability $R(\kappa)$ and achievable shares of the national demand $\alpha(\kappa)$ of frequency containment reserve over the marketing factor κ during the years 2015-2017. The values are further broken down to the positive and negative component of the FCR-demand. The blue area shows the spread of $\alpha_j(\kappa)$ during the different one-week delivery intervals.

Due seasonal and climatic influences, the delivery factors $\alpha_j(\kappa)$ achieved during the 1-week delivery intervals j of the frequency containment reserve can strongly deviate from the three-year mean value $\alpha(\kappa)$. Therefore, in fig. 6 the range of $\alpha_j(\kappa)$ is highlighted in blue. At peak times, around 2.5 times of the average value can be supplied while no control power at all is delivered during flooding events. Thus, it can be summarized that the German ROR-hydropower can provide a considerable share of the national demand for frequency containment reserve in a climate-neutral manner. However, many rivers show similar seasonal flow characteristics in the course of one year. This bears a certain lump risk that FCR-potentials decrease on many plants at the same time due to flooding or general weather situations. Therefore supplementary technologies, such as pumped storage power are still required.

In the case of automatic and manual frequency restoration reserve the positive and negative balancing energy can be marketed and delivered independently. This leads to an additional degree of freedom reflected by the two independent marketing factors κ^+ and κ^- . Figure 7 shows the achievable reliabilities and extrapolated delivery factors for the positive and negative, automatic and manual frequency restoration reserve as two-

dimensional parameter fields over κ^+ and κ^- . The reliabilities $R^+(\kappa^+; \kappa^-)$ and $R^-(\kappa^+; \kappa^-)$ are shown as a color plot with solid isolines whereas the corresponding delivery factors $\alpha^+(\kappa^+; \kappa^-)$ and $\alpha^-(\kappa^+; \kappa^-)$ are printed as dashed isolines.

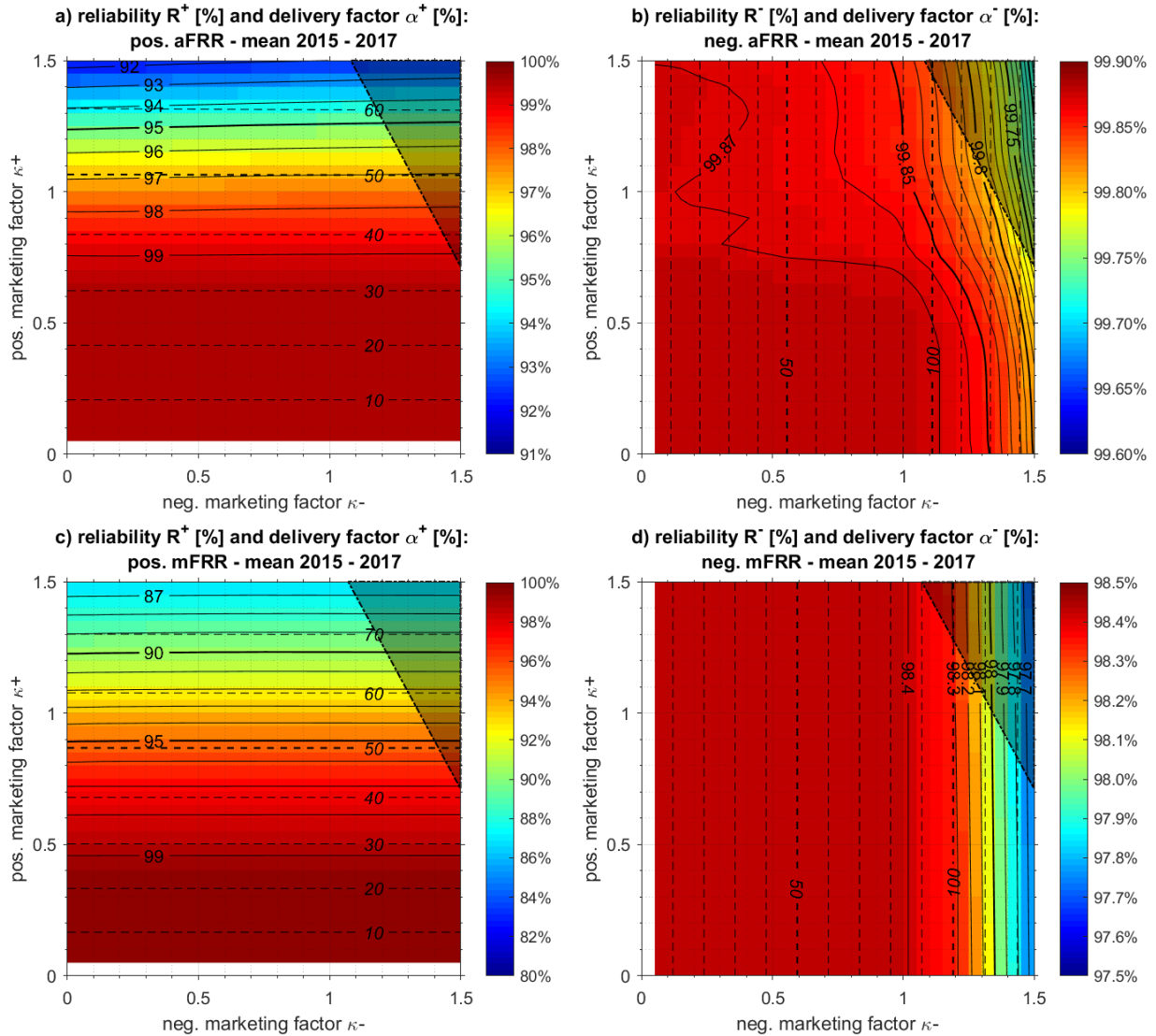


Figure 7: Average achieved reliabilities R (color plot and solid isolines) and corresponding shares of national demand α (dashed isolines) for the automatic frequency restoration reserve (top) and manual frequency restoration reserve (bottom) in the years 2015-2017.

With the exception of the reliability of the negative automatic frequency restoration reserve the isolines of both, the delivery factors α and the reliability R , can be considered horizontal for the positive control energy and vertical for the negative control energy in good approximation. This means that the control power potentials almost exclusively depend on the corresponding marketing factor κ whereas they are highly independent of the amount of control energy with the opposite sign. It can be stated

$$\begin{aligned} \alpha_C^+ &= \alpha^+(\kappa^+) & \alpha_C^- &= \alpha^-(\kappa^-) \\ R_C^+ &= R^+(\kappa^+) & R_{mFRR}^- &= R^-(\kappa^-) \\ & \text{for } C = \{aFRR; mFRR\}. \end{aligned} \quad (15)$$

Although the total demands of automatic and manual frequency restoration reserve widely differ over a year, the potentials of both types of control energy are generally similar.

According to the extrapolated delivery factor α^- , the national demands for negative automatic and manual frequency restoration reserve can be fully covered with high reliabilities R^- of around 99.8% for aFRR and around 98.3% for mFRR, respectively.

The achievable shares of the national demand α^+ and the corresponding reliabilities R^+ of the positive frequency restoration reserve are noticeably lower than for their negative counterparts. This is mainly due to two reasons. On the one hand, the positive control power is affected by system throttling occurring, when the upstream water level reaches the lower limit and at the same time enhances it by increasing plants' the water consumption. On the other hand, in order to keep the investment costs low, most ROR-hydroelectric plants have very limited reserves in terms of net power output and maximum flow rate. This narrows the potentials for providing positive control power, especially at times of high natural discharge.

When requesting a minimum average reliability of 95%, during the regarded three-year period 57% of the national demand of positive automatic and 51% of the national demand of positive manual frequency restoration reserve can theoretically be covered by the non-swelling ROR-hydropower in Germany. Since a reasonable increase of reliability can only be achieved when the amount of control energy is significantly decreased, backup capacities are generally necessary for positive control energy.

At marketing factors $\kappa > 1$, the peak control power offered in a tender is in fact higher than the power reserve estimated by the controller for this period. However, as these estimations have a limited accuracy, this does not necessarily mean that the maximum reserved control power cannot be delivered. What is more, it is very rare that the full amount of control energy auctioned in the tender is actually activated by the grid operators over a full 15-minute interval. For the investigated plant in Bannetze the average necessary positive and negative power reserves for frequency restoration reserve can be expressed for the as an empirical function of $\underline{\kappa}$:

$$\left(\frac{\bar{P}_c^+}{P_{max}} ; \frac{\bar{P}_c^-}{P_{max}} \right) = (\kappa^+ \cdot b^+ ; \kappa^- \cdot b^-) \quad (16)$$

with the factor b :

Table 3: Empirical factors for the calculation of average required power reserves from the marketing factors κ

Factors for calculation of necessary power reserves		
Type of control energy	b^+	b^-
Automatic frequency restoration reserve (aFRR)	28.4%	-53.2%
Manual frequency restoration reserve (mFRR)	28.9%	-52.0%

In case of $\underline{\kappa} = (1 ; 1)$ an average of 80% of the plant's maximum power output of 700 kW is required for providing control power. More precisely the plant is needs to retain around 200 kW for negative control power and around 370 kW for positive. Hence, in normal conditions, when the maximum plant output is not additionally limited by the maximum flow rate through the waterwheel, the simultaneous production of base power should be in the range of 200 kW to 700 kW - 370 kW = 330 kW. However, when choosing significantly higher marketing factors, the required power reserves can exceed the maximum power generation capacity of the plant. In this case a full delivery of the tendered amount of

control power is a priori impossible. In figure 7, these “forbidden” states of too high marketing factors are marked with a dash-dotted frame and a shadow.

According to these considerations, the maximum allowed marketing quantity of positive control energy depends is effected by the amount of negative control energy marketed and vice versa. If the national demand of negative automatic frequency restoration reserve shall be completely met by the ROR-hydropower, a maximum of 61.4% of positive aFRR could still be produced at an average reliability of 93.9% without reaching the forbidden κ -zone. In this scenario, a marketing factor of $\underline{\kappa} = (1.35 ; 1.15)$ is necessary. In case of the manual frequency restoration reserve, next to the coverage of the full negative demand 70.0% of the positive national demand can be covered at a reliability of 89.1%.

Even in the scenarios with the maximum investigated deliveries of control power the amount of simultaneously produced base energy P_B is still more than one magnitude higher. The base power reaches reliabilities of at least 99.8% in all the scenarios regarded, for all types of control energy and during every year considered.

5. Energy balance and economic efficiency

When the plant is operated in the illustrated operation mode providing control energy and constant base power, the amount of total energy produced is generally less than in conventional operation. Firstly, this is due to additional water losses over the weir ΔW_{weir} . Secondly, the average upstream reservoir levels reduce, decreasing the available head and thus the energy production. In comparison to the conventional operation, serving as a benchmark, these losses lead to an underproduction of total energy ΔW_Σ and an underproduction of base power ΔW_B . Both values are connected by the formula

$$\Delta W_B = \Delta W_\Sigma + W_C^+ + W_C^- \quad (17)$$

For an easier interpretation, the underproductions are related to the energy generation during conventional operation W_{conv} :

$$\Delta w_\Sigma = \frac{\Delta W_\Sigma}{W_{conv}} \quad (18)$$

$$\Delta w_B = \frac{\Delta W_B}{W_{conv}} \quad (19)$$

Δw_Σ and Δw_B are shown in figure 8 as a parameter field of $\underline{\kappa} = (\kappa^+ ; \kappa^-)$.

In the years 2015-2017, the relative underproduction of total energy Δw_Σ ranges between 1.4% and 8.0%, depending on the marketing factors. It is striking that the lowest gradients on the line $\Delta w_\Sigma(\kappa^+, \kappa^- = 0)$ point in the direction of κ^+ . Hence for any positive marketing factor the minimum total losses occur along the line $\kappa^- = 0$ where no negative control energy is produced. This is because the total energy losses are dominated by the additional weir losses. The latter are approximately proportional to the amount of negative control energy produced and thus become zero at $\kappa^- = 0$.

Compared to the additional weir losses the influence of a reduced head on the total underproduction of Δw_{Σ} is significantly lower. The head-losses increase the higher the amount of positive control power gets. In a smaller extent they also grow with a decreasing amount of negative control energy. In figure 8 this loss mechanism can be identified as the growing total underproduction Δw_{Σ} along the lines of constant negative marketing factors κ^{-} . These two loss mechanisms are the reason why the maximum total energy losses Δw_{Σ} occur at the point of the highest control power production at $\underline{\kappa} = (1.5 ; 1.5)$.

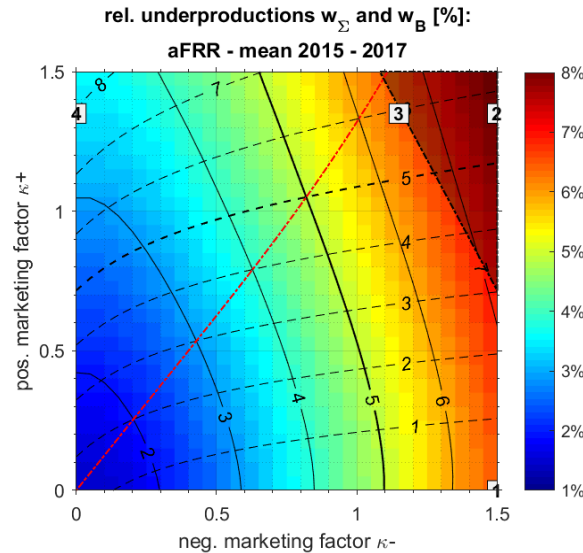


Figure 8: Average total underproduction Δw_{Σ} (color plot and solid isolines) and underproduction of base power Δw_B (dash-dotted isolines) in relation to the conventional energy production for the production of automatic frequency restoration reserve in the years 2015-2017

For the economic viability, the amounts of base power and control energy are more important than the sum of total energy produced. Due to the pay-as-bid auctions, the revenue generated from producing control energy strongly depends on the marketing strategy of each actor. For positive and negative frequency restoration reserve, revenues are generated from the total capacity reserved for production (power price) and from the amount of control energy actually delivered (energy price). For the base power, only an energy price is granted. This can be a fixed feed-in tariff or the fluctuating energy price on the electricity markets. Although the energy prices of both, base power sold directly on the markets and negative frequency restoration reserve can eventually become negative, their average prices remain positive [7].

When looking at the base power (dashed lines), figure 8 shows that the underproduction Δw_B is getting smaller than the total underproduction Δw_{Σ} for $W_c^+ < -W_c^-$. In a scenario of a maximum production of negative automatic frequency restoration reserve and no positive aFRR ($\underline{\kappa} = (0 ; 1.5)$), the underproduction of base power is even getting zero. Hence, the same amount of power can be marketed on the energy only market as in conventional operation. Additionally, the energy negative control energy, rewarded with an energy price, sums up to 6.6% of the conventional energy harvest. The corresponding power price is granted for 79.7% of the net output power, equivalent to 560 kW. Consequently, the total income in this scenario is higher than in the benchmarking conventional operation. The total energy, base energy and control energy for the scenarios, marked in figure 8, are listed in Table 4 as relative shares of the energy produced in conventional operation W_{conv} .

Table 4: Mean energy production 2015-2017 of total energy, base power and control energy as relative shares of the energy harvest during conventional operation (W_{conv}) for different automatic frequency response reserve scenarios

Energy balance for the delivery of aFRR						
Scenario	κ^+	κ^-	$\frac{W_{\Sigma}}{W_{conv}}$	$\frac{W_B}{W_{conv}}$	$\frac{W_C^+}{W_{conv}}$	$\frac{W_C^-}{W_{conv}}$
1	0.00	1.50	93.3%	100.0%	0.0%	-6.6%
2	1.35	1.50	92.2%	94.3%	4.5%	-6.6%
3	1.35	1.15	93.5%	94.0%	4.5%	-5.1%
4	1.35	0.00	96.6%	92.1%	4.5%	0.0%

In scenario 2, positive automatic frequency restoration reserve at a minimum reliability of $R^+ = 95\%$ is produced next to the maximum considered amount of negative aFRR. In this case of $\underline{\kappa} = (1.35; 1.50)$, the necessary power reserves for supplying 100% of the marketed control power are higher than the maximum plant power of 700 kW. Thus, when there are no backup capacities, the operation point is outside the allowed range. Compared to scenario 1, the total underproduction ΔW_{Σ} is further increased by 1.1 percentage points, mainly because of a decreasing average head. As more positive control energy is generated, the growing balance $W_C^+ + W_C^-$ raises the underproduction of base energy ΔW_B even more to 5.7%, whereas the amount of negative aFRR remains constant. On the other side, the positive automatic frequency restoration reserve amounts 4.5% of the conventional energy production with a refunded power reserve of 270 kW or 38.3% of the maximum output. An analysis of transparency data published in [7] revealed that the energy prices of positive automatic frequency restoration reserve were on average 1.7 times as high as the energy-only prices on the energy exchanges. On the other side the underproduction of base power only accounts to 1.3 times the positive control energy produced. What is more, power prices are granted in addition to the energy prices. Therefore plants receiving no or only low feed-in tariffs can be expected to generate even higher revenues in scenario 2 than in scenario 1 or conventional operation.

Compared to scenario 2, in scenario 3 the amount of negative automatic frequency restoration reserve is limited in a way that the same amount of positive aFRR is produced, but the total marketed power reserves do not exceed the maximum capacity of the plant. In this case, 61% of the national demand for positive and 100% of the national demand for negative automatic frequency restoration reserve can theoretically be covered by the ROR-hydropower. Compared to scenario 2, this reduction in negative control energy leads almost automatically to lower revenues. Firstly, because the growing control energy balance $W_C^+ + W_C^-$ leads to a lower base power production and secondly, because the revenues from the negative aFRR itself reduce. The underproduction of base energy compared to scenario 1 and conventional operation is 6.0%. At the same time, the energy incomes for the negative aFRR decrease by 1.5% and the refunded power reserve drops by 130 kW. In comparison to scenario 1, however, additional incomes from positive aFRR are generated for an energy amounting 4.5% of the conventional energy harvest and a power equivalent to 38.3% of the plant's maximum output. Whether the revenues in scenario 3 are still higher than in conventional operation therefore strongly depends on the price achieved in the power auctions.

In summary, when energy prices are positive the production of the maximum amount of negative automatic frequency restoration reserve with no positive aFRR can securely generate additional revenues, independent of a granted feed-in tariff. Producing positive and negative aFRR together is only economically feasible, when the additional incomes

from control energy can compensate the resulting underproduction of base energy. Since the control energy is auctioned in a pay-as-bid market, the incomes are individual for each market actor and during each tender period. The mean energy price of activated positive automatic frequency restoration reserve in the investigated three year period is approximately $52 \frac{\text{€}}{\text{MWh}}$, which is around 20 times higher than for negative aFRR with an average price of around $2.5 \frac{\text{€}}{\text{MWh}}$. The average positive power price in the same time period is around 4.1 € per MW and hour of reservation, which is around 3.5 times the power price for negative aFRR [7]. Therefore, when no higher feed-in tariff is granted for the base power, providing positive automatic frequency restoration reserve can be expected to generate additional revenues despite the higher potential costs for providing necessary backup capacities.

Summary

The simulations conducted on the projected ROR-hydroelectric plant in Bannetze-Hornbostel showed that a flexibilization of the upstream reservoir water level of less than 30 cm reveals significant short-term storage potentials. These potentials allow to schedule the power production one hour before the start of delivery and hold it constant for a period of three hours. Thus, the risks of direct marketing of ROR-hydropower can be reduced. More than that, the storage potentials can be used to produce high amounts of control energy along with the constant base power. These control energy potentials strongly depend on the maximum feasible temporal lowering of the upstream reservoir level. In change, the possibility to increase the water level reduces energy losses caused by water, spilled over the weir. In order to achieve high control energy potentials, the target upstream water level for the investigated plant in Bannetze-Hornbostel was chosen 2 cm below the maximum and 25 cm above the minimum acceptable limits. Even though the German ROR-hydropower approximately accounts for only 3% of the national energy mix, it can be expected to have considerable control energy potentials [8]. When upscaling the potentials of the investigated plant to the whole non-swelling ROR-hydropower capacity in Germany, the national demands of frequency containment reserve as well as negative automatic and manual frequency restoration reserve can be fully covered at average reliabilities of 95.0% for the FCR and 99.8% and 98.3% for the aFRR and mFRR, respectively only by hydropower.

For the production of automatic frequency restoration reserve additional energy balances were analyzed. In a first scenario with a maximum production of negative aFRR, 560 kW or 79.7% of the plant's net capacity need to be reserved for the production of control power. Due to various loss mechanisms, this mode of operation decreases the total plant energy production by 6.7%. However this loss is fully due to the production of negative control energy. Therefore, the same quantity of base power can still be sold. As the prices for both, the power of reserved negative aFRR and for the control energy actually delivered are usually positive, this scenario generates higher incomes than the conventional operation.

The developed operation mode also allows to produce significant amounts of positive automatic and manual frequency restoration reserve. However the potentials are lower than those of the corresponding negative control energy. When an average reliability of 95% shall be reached the German ROR-hydropower can theoretically cover 57% of the national demand for positive aFRR and 51% of the demand for positive mFRR, respectively. Higher amounts of control energy are generally possible, but cause a

decrease of reliability. This is why backup technologies are indispensable for the investigated peak-to-peak upstream reservoir amplitude of only 27 cm. Despite the need for backups, the production of positive and negative control energy can still be economically feasible. For the automatic frequency restoration reserve, this was investigated in scenario 3. Here, base load underproductions of 6.0% were faced by additional positive aFFR incomes composed of energy prices for 4.5% of the conventional energy production and power prices for 38.3% of the net output, equivalent to 270 kW. In addition to that, revenues for negative automatic frequency restoration reserve, corresponding to 5.1% of the energy harvest during conventional operation and 61.1% of the maximum power, equivalent to 430 kW are generated. Thus, for plants that do not receive high feed-in tariffs, the combined delivery of positive and negative aFRR can also be expected to yield higher incomes than conventional plant operation.

Acknowledgement

The authors thank the foundation Stiftung Nagelschneider for providing the funds for this research project.

Disclaimer

This conference article is based on the German publication in [9]. A similar version is currently in the publication process in Proceedings of the 14th International Renewable Energy Storage Conference 2020 (IRES 2020).

References

- [1] International Renewable Energy Agency, Renewable capacity statistics 2019. Abu Dhabi: IRENA, 2019.
- [2] L. Hirth, I. Ziegenhagen, and E. Tagesfragen, "Wind, Sonne und Regelleistung", *Energiewirtschaftliche Tagesfragen*, Bd. 63, Nr. 10, p. 2–4, 2013.
- [3] M. Brucker, "Wasserkraft als Netzdienstleister am Beispiel der E.ON Wasserkraft GmbH", in *Wasserkraftprojekte*, S. Heimerl, Hrsg. Wiesbaden: Springer Fachmedien Wiesbaden, 2013, p. 129–134.
- [4] P. Fischer, B. Stammel, P. Lang, A. Schwab, and B. Cyffka, „Hydrologische Dynamik als Motor für die Renaturierung von Auenhabitaten an der Donau zwischen Neuburg und Ingolstadt“, p. 13.
- [5] C. Seidel, „Regelleistung und Kurzzeitspeicherung bei Laufwasserkraftwerken“, *VGB PowerTech Journal*, Nr. 9/2015, p. 34–41, 2015.
- [6] WSA Verden, "Wehr Bannetze". [Online]. available on: <http://www.wsa-verden.wsv.de/wasserstrassen/bauwerke/wehre/bannetze/index.html>. [accessed: 24-Jan-2020].
- [7] Bundesnetzagentur, "SMARD Strommarktdaten". [Online]. available on: www.smard.de.
- [8] ENTSO-E, „Statistical Factsheet 2017“. May 04, 2018.
- [9] B. Hase and C. Seidel, „Laufwasserkraftwerke als Anbieter von Regelleistung? Potenziale einer dynamischen Stauhaltung am Beispiel der Forschungswasserkraftanlage Bannetze-Hornbostel“, *VGB PowerTech Journal*, Nr. 6/2020, S. 11, 2020.

G1104

Hydro Storage as Enabler of Energy Transition

Peter Bauhofer, Michael Zoglauer

Abt. Energiestrategie und Energieeffizienz

TIWAG-Tiroler Wasserkraft AG, Eduard-Wallnöfer Pl.2, A-6020 Innsbruck

++43 (0) 50607 – 0

peter.bauhofer@tiwag.at, michael.zoglauer@tiwag.at

www.tiwag.at

Abstract

Energy transition is speeding up. Europe's economy is about to be decarbonized until 2040. Carbonless electricity generation is expected to have large shares of energy procurement, while end energy consumption will be provided by electricity directly and sector coupling products as well. Thanks to hydropower, Austria starts from a 74 % RESE-share today and national energy policy claims a 100 % RESE target until 2030. Hydropower, windpower, PV and to a small extent biomass will have to match the game.

Extreme high shares of highly intermittent generation of windpower and PV will disproportionately increase Austria's flexibility needs in all timeframes up to seasonal dimensions, when system stability and security of supply shall be kept at today's level.

The given study analyses residual load parameters of Austria's electricity system up to 2050, estimates flexibility demand and discusses the central role of highly efficient hydropower to meet these challenges. Further on it discusses how reliable imported flexibility could be, when neighboring countries implement thermal drop off.

With its ambitious decarbonisation targets, Austria develops a field test for flexibility needs at times of highly intermittent RESE shares. Basic conclusions on residual load development as well as the role of hydropower to match ramping needs may be generalised for other regions. The ability of modern hydropower designs in the Alps to provide also seasonal flexibility is underlined.

Keywords: energy transition, hydropower, storage, decentralized storage, pumped hydro, flexibility, system stability, security of supply, residual load, ramping, sector coupling, intermittent renewables, windpower, photovoltaics.

Introduction

The strategic targets of the European Climate and Energy Package (CEP) aim to decarbonize the energy system until 2050, while the “Green Deal” shifts this target forward to 2040. Electricity is about to become the dominating energy source. In an overall context, the highly intermittent sources wind power and photovoltaics will substitute generation from coal and nuclear power plants to a significant extent, while gas generation capacities and CHP (fossil and biomass) remain an essential complement. The modification takes place at all stages of the value chain, at the same time, at high speed and in an increasingly uncoordinated manner.

The improvement of electricity infrastructure and system relevant stabilizing elements cannot keep up with the rest of the transition. The amount of reserves stepwise overrules the given physical reality. As long as calculable thermal units have dominated generation within the EU, system adequacy was determined by deterministic methodologies. This calculation was reliable. However, the high proportion of feature dependent power generation (e.g. wind power, PV, ...) together with an increasingly stimulated load profile made stochastic methodologies necessary (ENTSO-E 2015). The determination of security of supply therefore can no longer be done at the desired level of precision. Additionally, massive corrections and adjustments of energy policy targets of key players (e. g. German coal phase out ...) without any known fall back strategies at the time given are overruling previous planning assumptions fundamentally.

In Central Europe, during the first two quarters of 2019 there were at least four critical system situations observed. Finally, national energy regulators repeatedly give black out warnings. Energy transition is about to develop as a large-scale experiment with an uncertain outcome.

This mix of increasing uncertainties more than ever longs for reliable flexibility solutions. To reduce risk from imported flexibility, Art. 22 lit. d) of Reg. (EU) 2018/1999 requires, that every country has to increase the flexibility of the national system in particular by means of deploying domestic energy sources, demand response and energy storage, while critics of power plant projects claim for flexibility procurement mainly based on cross-border-exchange.

From the very beginning, Austria has decided upon generation preferably from renewables. Hydropower is the backbone. Today, with a RESE share of more than 72 %, Austria is top ranking within the EU28. Supporting EU's CEP targets, in 2018 Austria decided to have an electricity system based on 100 % renewable electricity (balanced p. a.) in 2030 meaning, that within the coming 10 years appr. 30 TWh⁴ of additional RESE has to be installed (#mission 2030). While biomass is lacking potential, hydropower (plus 5 – 8 TWh), wind power (plus 10 - 12 TWh) and PV (plus 10 - 12 TWh) are expected to match the game. In a longer run, Austria's full hydropower potential of in total 11 TWh is ready for use (Pöyry 2017). This ambitious target will result in an enormous dynamisation of the Austrian system and an increase of flexibility demand in all time frames.

⁴ Rem.: In 2018 first estimations suggested appr. 30 TWh of additional RESE, while the current policy program (2020) fixes this target to appr. 27 TWh.

The given analysis therefore responds to the following questions:

- How do Austria's residual load parameters develop under extreme shares of intermittent RESE?
- Can decentralized storage contribute to system stability?
- How does the system benefit from hydropower?

Key Findings

For the given Austrian energy strategy targets, already from 2025 on disproportionate growth is expected for all residual load parameters. Negative residual load will increase more than the positive. Peaks (PRLmax) come up to at least -6 GW and ramps/gradients (Δ PRL) of more than 3 GW/h with frequent changes of sign (+/-) are expected (Tab. 1). Large daily lifts of the residual load of more than 9 GW are likely. From 2030 on, the seasonal energy flexibility need of at least appr. 7 TWh in addition to existing storage capacities (appr. 4.3 TWh) is evident.

Choosing the proper generation portfolio, to a certain extent run-of-river plants damp intermittency effects of PV and wind power on the residual load. However, the most effective and efficient influence on increased flexibility in all time frames including seasonal flexibility is given by hydro storage and pumped hydro storage power plants. Additionally, they reduce the costly dynamic electricity generation and CO₂ emissions of thermal plants, avoid power reduction at wind- and PV-generation sites (dumped energy) and improve big scale RESE integration to the system. This also applies cross-border. Last, but not least, from the Austrian perspective, net imports and thus dependence on fossil and non-fossil energy imports can be reduced (TUW 2017).

#mission2030		2020	2025	2030	2040	2050
ERLpos	[TWh]	28,6	23,7	20,4	23,4	28,2
ERLneg	[TWh]	-1,1	-3,2	-6,8	-10,5	-12,4
of which seasonal shift	[TWh]	-1	-3	-6	-9	-10
PRLmax	[GW60]	10,3	10,6	11,0	12,9	15,4
PRLmin	[GW60]	-4,4	-6,1	-9,6	-14,3	-17,7
Jahresmax(PRLmax(d) - PRLmin(d))	[GW/d]	7,9	9,5	11,2	15,9	20,2
Δ PRLmax pos	[GW/Std]	2,4	2,8	3,1	4,1	5,3
Δ PRLmax neg	[GW/Std]	-2,4	-3,3	-4,1	-4,9	-6,5

Tab. 1: Changes of residual load characteristics caused by the nation energy strategy.

In order to guarantee policy success and in the sense of a sustainable Austrian long-term strategy it is suggested to consider and accept the role for the new construction and/or the extension of domestic hydropower and in particular alpine (pumped) hydro storage using the available potential. Appropriate operational framework (in particular for the surge/sunk question) should be provided for the optimized development of the flexibility effect of hydropower. System stability, security of supply as well as the large-scale integration of wind power and PV in Austria can be guaranteed also in future.

The enormous challenges are imminent. The speedy handling of permit proceedings is necessary.

The use of additional options (gas and biomass CHP, P2X, decentralized solutions such as battery storage and DSM, cross-border exchange, ...) will contribute to success. Decentralized solutions like batteries, DSM, P2H, etc. ... are expected to be preferably used by optimized, customer driven energy management solutions for buildings and/or industries as well as for distribution grids and will have a minor support for system needs. Moreover it may be assumed, that decentralized solutions – caused by these customer driven optimization – may also have negative system effects (peaks caused by price signals, etc. ...).

A polarizing discussion on the choice of solutions is not expedient. At the same time, the import of security of supply should be kept at a reasonable level. This is especially relevant for periods with lacking generation from windpower and PV („Dunkelflaute“).

Stability and Security of Supply

The energy transition of the coming years will be characterized by the following scare goods: acceptance, affordability as well as availability of energy for the individual and the economy at any time. The premise of the availability of basic services at any time, especially electricity, as a precondition for a prosperous European economy directly influences public acceptance of energy transition. So far, the energy transition has preferably succeeded in the electricity system. This success has mainly been enabled by reserves of grid infrastructure, thermal power plants and their flexibility as well as hydropower storage and pumped storage. The reserves of available capacities are used up or are rapidly fading in particular by the thermal phase-out in key regions.

A cardiological remote diagnosis for the future European system may find moderate to strong arrhythmias (grid frequency) or even standstills (blackout), if it is not possible- apart from the grid expansion – to replace timely fossil assets that have provided ancillary services and other flexibility measures at a large extent up to now. Hydro power plants with storage and/or pumped storage functions have fulfilled these tasks emission free, cost-effectively, reliably and, above all, predictably for decades, thus contributing today and even more in future as a substantial enabler for the system-wide large scale integration of intermittent RESE- generation - essentially wind power and photovoltaics.

Residual Load And Flexibility Needs

Compared to other grid-based energy systems (gas, oil, district heating), the electricity system is extremely sensitive. The balance between load and generation at any time is the necessary prerequisite for maintaining system stability and thus security of supply. Frequency and voltage are the key parameters for system stability. Therefore, the mechanisms for it's maintenance must already start in the seconds range and in the special case of the instantaneous reserve (inertia) even sub transient.

The mere focus on a balanced annual or at most seasonal energy balance by no means meets these requirements. The ability of a system to respond to changes in generation

and / or load is called system flexibility (ENTSO-E 2015). At the system level this is given by a performance (power-) -oriented short-term flexibility with a time range up to one hour and may differ from needs from distribution grids. To keep up security of supply, it is also necessary to ensure a balanced energy supply. Even more in future, long-term flexibilization based on energy storage is of key importance. In Austria, it is targeted for 2030 to cover the electricity supply by 100% from renewable sources (RESE). Additional generation by the highly intermitten and seasonally available wind power and PV sources (approx. 12 TWh each by 2030), supplemented by the seasonal fluctuating run of river power (approx. 5 - 8 TWh out of a total of 11 TWh potential) will be the backbone.

Controllable RESE, such as biomass, have a complementary effect but have only minimal growth potential. Gas-based CHP plants will continue to play an important role, not at least to cover the heat demand of large cities as well as industrial needs. Likewise, the trade-based cross border exchange of renewable energy, which, however, can only be limitedly available for wind power and PV generation due to simultaneously given wide area meteorological effects.

The residual load (PRL) is determined at system level in an hourly resolution as the power difference of the concurrent load of the public grid ($Last\ddot{O}N(t)$) and the variable infeed to the public grid $RESEvol(t)$:

$$PRL(t) = Last\ddot{O}N(t) - \sum RESEvol(t).$$

Residual load is - without further action - the random result of the multicausal relationship between the simultaneous occurrence of (intermittent) generation and load. It is an indicator for the effort given to maintain the balance respectively how much power has to be withdrawn from the system or fed into the system at any time. Within the course of an year, $PRL(t)$ can mean positive (the volatile generation is not able to cover the load at the same time, power or energy deficit) as well as negative values (temporary power or energy surplus). Intermittent generation and load only have limited predictable values or correlations in all timeframes.

The use and characteristics of flexibility tools are determined by the steady state characteristics but also significantly by the dynamic characteristics of the residual load, such as its gradient/ramp ΔPRL . Compensation must be given by proper flexibility solutions like hydro storage and pumped hydro storage systems, thermal generation, P2X applications, and to a certain extent also by decentralized solutions, such as DSM, battery storage, etc... .

Within the framework of the Integrated Climate and Energy Strategy (#mission2030), Austria aims to cover 100% of it's electricity demand by renewables (RESE) in 2030, while industrial consumption, reserve balancing and balance energy should be covered also by thermal generation in future. From 2025 on, the projected enormous increase of intermittent capacity will cause an enormous stress level for Austria's power system in the May to September period, that in relation may even exceed the respective figures of Germany. In particular, the summer surplus (seasonal flexibility) must be highly efficient shifted to winter time.

In the following, the effects of 100 % RESE with a high share of intermittent generation are estimated on Austria's residual load⁵. In order to minimize the need for flexibility a priori, a coordinated architecture of the generation mix of PV and wind together with run-of-river shall be pursued. The correlation of PV generation characteristic is slightly negative (-0.12) compared to wind. The annual simultaneity factor

$$\gamma_{inst} = \frac{\max(PWind(t) + PPV(t))}{PWind_{inst} + PPV_{inst}}$$

of the simultaneous infeed maximums related to the sum of installed capacities is approx. 50%. This causes temporarily moderate compensation effects. Starting at average load conditions, PV infeed significantly decreases and is negligible at times of peak load. This effect will also have to be mitigated by proper centralized and decentralized flexibility measures.

Under the given assumptions, the characteristics of the Austrian electricity system will change fundamentally within the coming 10 years (Fig. 10). In 2016, a seasonal characteristic is apparent for the total of generation from run-of-river power, wind and PV⁶, as well as for load, even if recognized in opposite directions. Generation tips are already typical for today, but they exceed load only in a few hours. Today, a seasonal energy shift is not required by this reason. The infeed tips are mainly determined by wind power. Residual load is overall positive, while already partially with high positive and negative gradients. The gradient of the simultaneous infeed of wind and PV related to the simultaneous load (how much does the intermittent infeed change per hour related to load at the same time?) is moderate.

In 2030 however, the seasonal characteristics of both, the total of infeed and the load of the public grid, will be increased (Fig. 5-7). While peak loads (load dynamics together with a general increase of annual consumption) increase significantly, the summer load of the public grid increases only moderately, because prosumers are assumed to have an increased self consumption at these times. However, the infeed peaks increase substantially throughout the year and are characterized by a high infeed of wind power and PV in their extremes. Overall, the picture is characterized by a pronounced roughness. Frequently, the infeed significantly exceeds the simultaneous load.

There is also a significant need for a seasonal energy shift (seasonal flexibility). The gradient of the simultaneous PV and wind infeed related to the simultaneous load achieves high values throughout the year. The distinctive morning and evening ramps of the residual load are supplemented during the late morning and early afternoon hours with partly steep ramps. Sign changes of the residual load ramps are given frequently.

In the following, the results for the most important parameters are summarized for the years of reference until 2050. Unless otherwise stated, the illustrations correspond to a

⁵ Note: The objective estimate serves to detect trends and the magnitudes of the relevant parameters. To illustrate the bandwidth, the analysis has to be rounded off on the basis of several weather years and scenarios for generation mix and load profile. According to the IKES convention, the gross electricity consumption is reduced by the industrial self-consumption and the control reserve call. The Austrian hydropower expansion potential amounts to a total of 11 TWh (Pöyry 2018).
All data - unless otherwise stated - apply to unaffected generation or load.

⁶ Note: PV infeed to the public grid (PVÖN) by PV directly coupled (PVnonHH(t)) and surplus infeed by prosumers (PVHHÜE(t)).

coordinated development of run-of-river, wind and PV and with equal generation shares extrapolated for the reference years 2040 and 2050 (solid lines). In order to test the limits, hypothetical scenarios based on wind only or PV only or the combination of both are shown as dashed lines. One of the usual benchmarks for residual load is the RES-Load-Penetration-Index RLPI,

$$RLPI = \max \left(\frac{P_{Wind}(t) + P_{PV}(t)}{Last\ddot{O}N(t)} \right)$$

as the annual maximum of the ratio of simultaneous total infeed from wind and PV related to the simultaneous load of the public grid (ENTSO-E 2015). This index provides information about the maximum hourly coverage of the load using wind and PV within one year. Already in 2025, for Austria this index is expected at least 130% with a rapid increase and reaching levels of up to 260% by 2050 (Fig. 1).

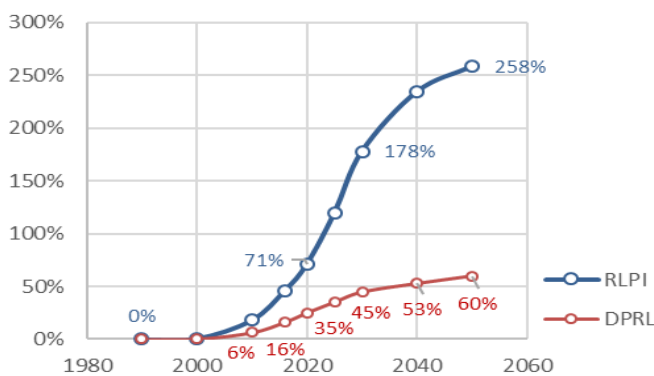


Fig. 1: RES-Load-Penetration Index RLPI and infeed ratio.

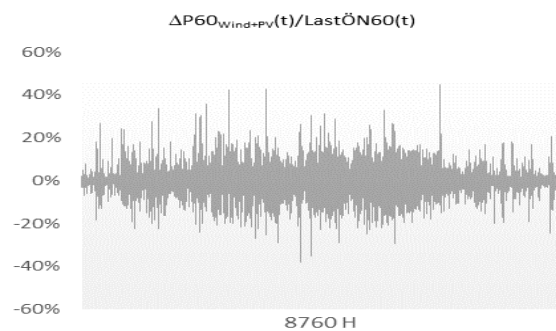


Fig. 2: Already in 2030, the hourly gradient of the simultaneous wind and PV infeed can exceed 40% of the net load in both energy directions for several times.

The phenomenon of a high infeed gradient to load ratio is evident throughout the year. In addition to the residual load ramp, it is an indicator of how quickly the flexibility assets have to control their infeed or outfeed in order to be able to balance the system at any time. In both energy directions, values of more than 20% and, in some cases, up to 40% are expected already by 2030 (Fig. 2).

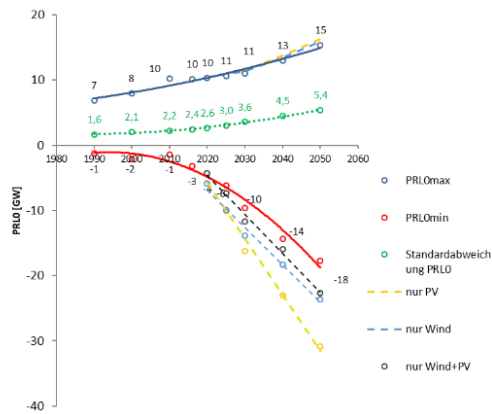


Fig. 3: Residual load peaks (GW60) together with standard deviation 1990 to 2050.

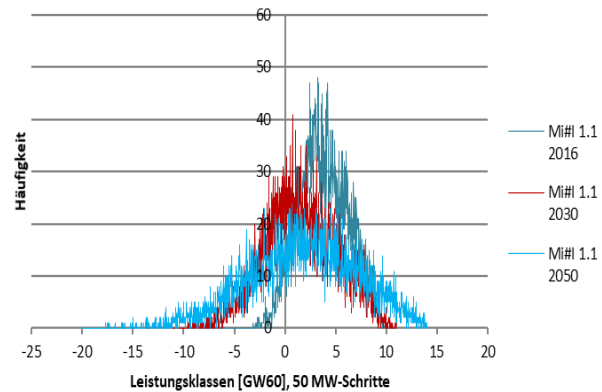


Fig. 4: PRL-Frequency distribution (GW60) for the reference years 2016, 2030 and 2050.

Under the given assumptions, the characteristics of the positive as well as the negative residual load increase disproportionate, while the increase of the negative residual load for both, the energy and the peak power, is much stronger. The cumulative energy content of all hours with a negative residual load may increase from currently approx. -0.4 TWh/a to at least -3 TWh/a by 2025 and to approx. -6.8 TWh/a by 2030. By 2050, -12 TWh/a are foreseeable. The negative peak PRLmin will double from -3 GW60 today to -6 GW60 by 2025 and reach up to -9 GW60 in 2030. Values around -17 GW60 are expected by 2050 (Fig. 3). Power peaks of the negative residual load can occur from May to September. From medium classes of its frequency on, an increase is expected (Fig. 4). If, from 2016 on, additional RESE generation would only be done by wind or PV or a combination of both, the residual load peaks will increase even more in both directions (Fig. 3, dashed lines). While for Austrian generation characteristics the combination of wind and PV may have moderate damping effects, the coordinated combination with run-of-river improves this damping effect significantly. The energy content of residual load and thus the storage (TWh) requirements for (seasonal) flexibility solutions will increase stronger than capacity requirements (GW) in a further perspective.

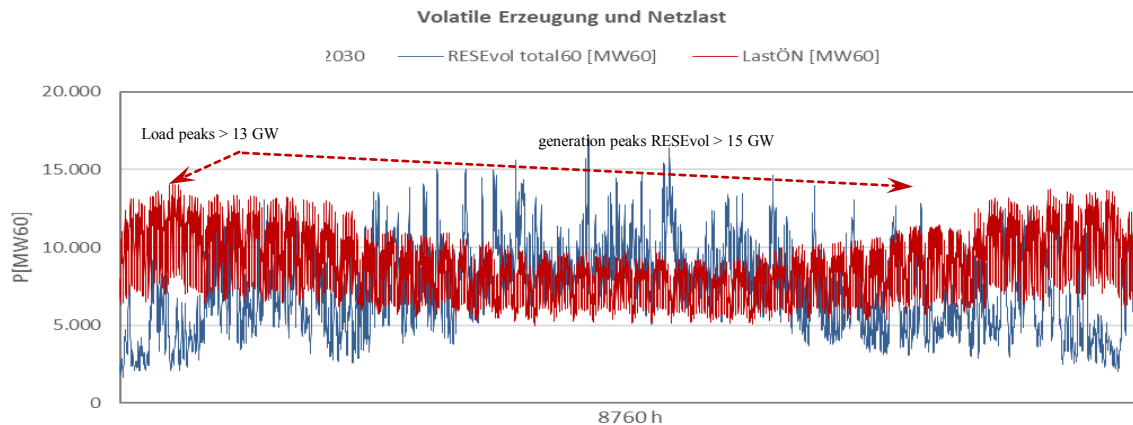


Fig. 5: Estimation of the load of the public grid (LastÖN) and generation from RESEvol (wind + PV + run off river). In the summer months there is a pronounced overlap, in the winter months a shortage of the load. Time series 2016 scaled for 2030.

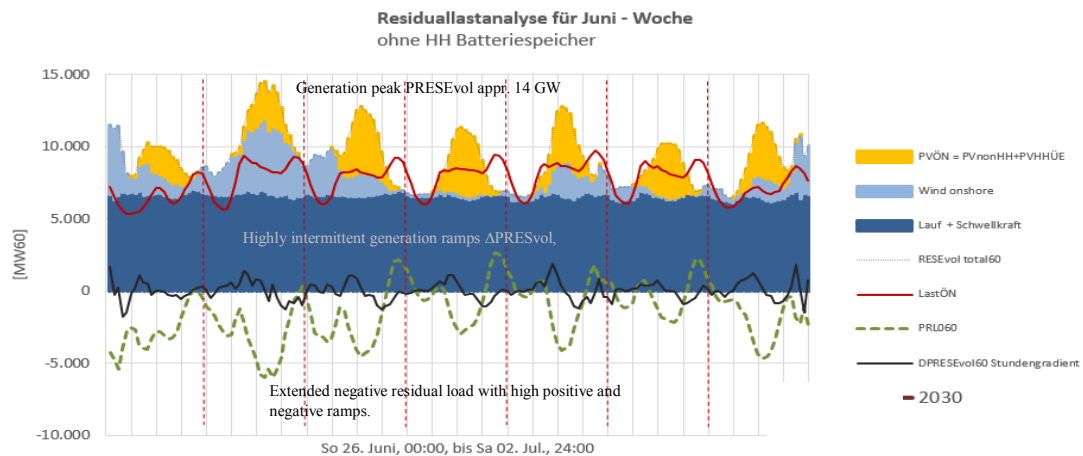


Fig. 6: Random sample for a week in June in 2030. Largely constant infeed from run of river combined with more or less strong daily infeed from wind power and PV with partially high infeed peaks, high intermittence and ramps in both directions. Essentially negative (energy surplus), strongly intermittent residual load with distinctive ramps and frequent sign changes.

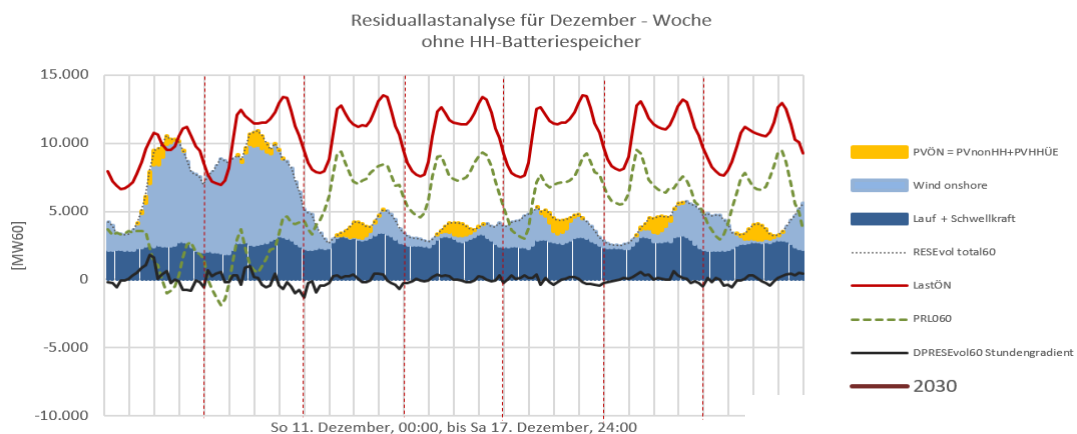


Fig. 7: Random sample for a week in December in 2030. Consistently strong wind infeed at the beginning of the week, temporarily supported by moderate PV infeed. High load with distinctive morning and evening peaks. Moderately to strongly intermittent infeed ramps. Strongly intermittent, essentially positive residual load (energy deficit) with high ramps in both directions.

The energy content of all hours with positive residual load (generation gap from intermittent sources) is appr. 20 TWh in 2030 and appr. 30 TWh by 2050. About 10 GW₆₀ peak remains roughly unchanged until 2030 and will increase to appr. 15 GW₆₀ by 2050 (Fig. 4).

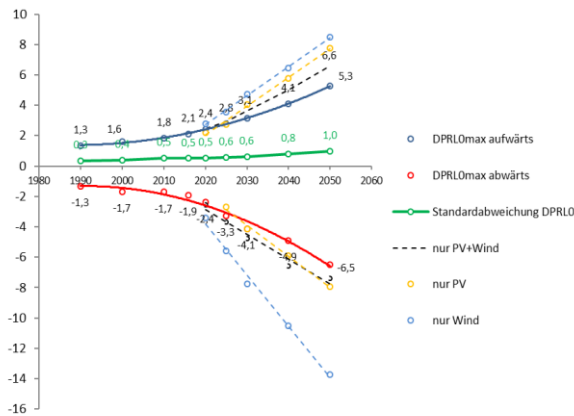


Fig. 8: Hourly residual load ramp ΔP_{RL60} (GW/h) together with standard deviation, 1990 to 2050.

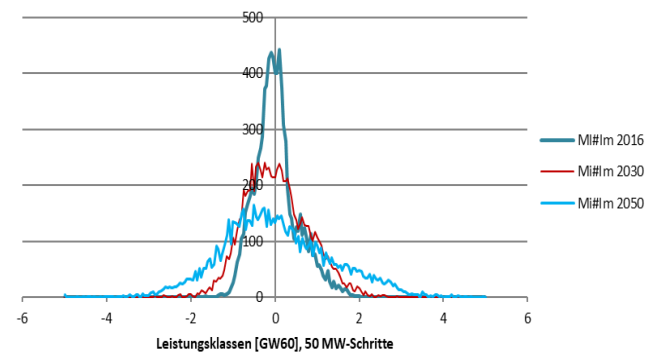


Fig. 9: Frequency distribution of the hourly residual load ramp $\Delta PRL60$ for reference years 2016, 2030, 2050.

The block duration of the negative residual load with maximum energy content increases from appr. 16 h (-0.02 TWh) to 117 h (-0.6 TWh) in 2030. It's counterpart for the positive residual load reduces from appr. 2.460 h (12 TWh) to 430 h (3 TWh) in 2030. The number of blocks with positive or negative residual load increases in each case from approx. 110 events/a in 2016 to approx. 340 events/a in 2030.

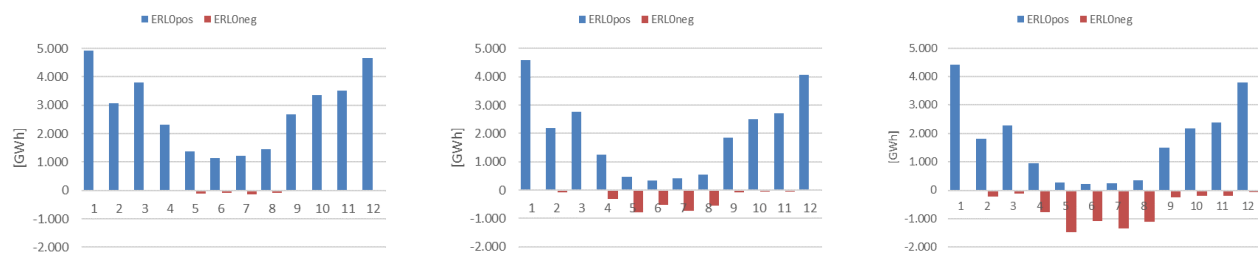


Fig. 10: Monthly accumulated energy content of the positive or negative residual load for 2016, 2025 and 2030.

A similar result emerges for the hourly residual load ramps ΔPRL (Fig. 8 and 9). The smoothing effect of run-of-river on the residual load ramps is even more evident than for the residual load peaks. In both directions, there is a disproportionate increase of the maximum values from approx. ± 2 GW/h today to approx. ± 4 GW/h in 2030 or ± 6 GW/h in 2050. The frequency of small ramps will decrease in the future, while it will increase for higher ranges in both directions.

The evolution of residual load peak power and ramps significantly increase the need for highly flexible short-term flexibility solutions. 2016 – as typical for the current generation mix – faced only minimal energy surpluses in the summer (Fig. 10). However, the planned

Austrian generation mix will cause an estimated seasonal flexibility need of approx. 2.8 TWh already in 2025 (11% of intermittent generation in summer) and at least 7 TWh in 2030 (appr. 18 % of the intermittent generation in summer). Compared to other countries, for Austria the issue of seasonal flexibility is of major concern from the mid-2020ies on. Hand in hand with the increase of residual load peaks, the annual maximum of daily residual load power increments

$$\vartheta = \max (PRL_{\max}(d) - PRL_{\min}(d))$$

experiences disproportionate growth as well, reaching at least 9 GW in 2025 and increasing to at least 20 GW by 2050. Forced PV and/or wind power expansion cause a considerable increase of these values. The dynamic sampling of the power system due to the emerging wind and PV generation shares has already caused a significantly increased interplay of (pump) storage use in the past. This increase will continue in future.

Correlations for the Alpine Region

- 1 In Europe, as well as in the alpine regions, RESE development will be determined by wind power, PV and hydro. In the summer months, the daily generation characteristics will be dominated by PV, underpinned by the temporary purchase of wind (Fig. 11), whereas in the winter months wind characteristics are decisive. Austria's load, intermittent generation and residual is highly correlated with those of other countries of the alpine region (Fig. 12). That means, that an area wide generation deficit (positive residual load) or a generation surplus (negative residual load) probably may occur at the same time. This fact is a basic precondition for the definition of a national flexibility strategy and the assessment of security of supply, if cross-border flexibility assistance should be taken into account.

2

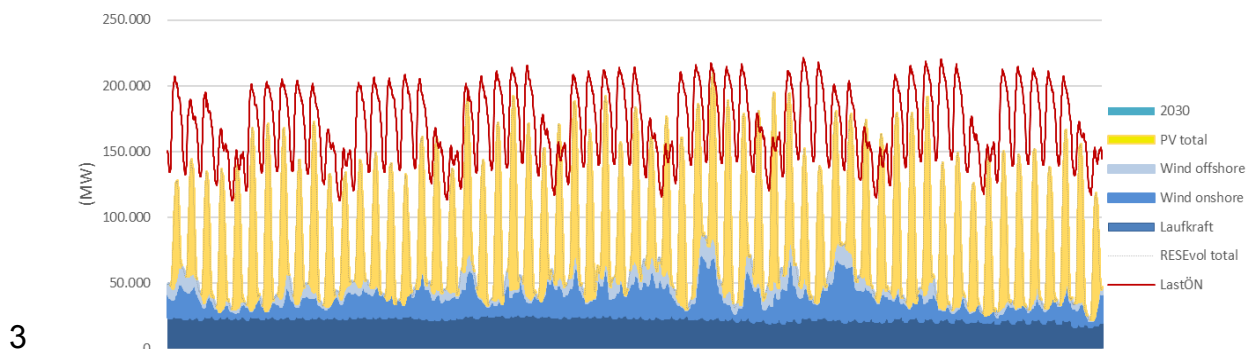


Fig. 11: Cumulative infeed from RESEvol and load in the alpine region (AT, CH, DE, FR, IT, Slo), sample Jun - Jul, 2030

A special phenomenon of concern is a period lacking generation from PV and wind ("Dunkelflaute") due to wide area meteorological situations. This phenomenon usually occurs in the winter months and has already been observed during the past years by statistics and price signals.

Meanwhile, several publications have analyzed this phenomenon, although it has remained unclear how to define “Dunkelflaute” (minimum intermittence of feed-in, etc.) in a standardised manner. A recent analysis by the TU Dresden (TUD 2019) concludes, that this phenomenon occurs in the medium time range up to 14 days in a significant frequency and is to be mastered especially with hydro storage, when thermal units are expected to be dropped off in future to a significant extent. Further in depth correlation studies for the alpine region remain necessary.

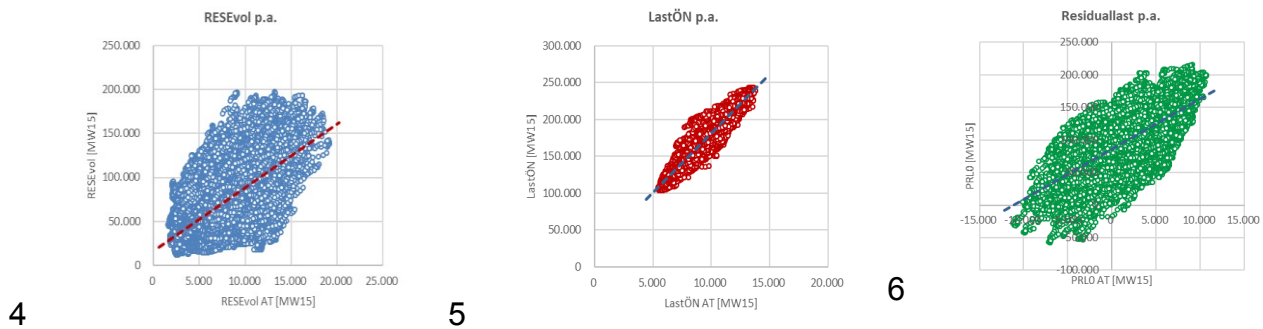


Fig. 12: For 2030 in the Alpine region (AT, CH, DE, FR, IT, Slo) there is a significant correlation of RESE generation (Pearson Coeff. = 0.60), load (Pearson Coeff. = 0.96) and residual load (Pearson Coeff. = 0.67) expected. Data without thermal must-run.

Flexibility Options

The overall goal of the energy and climate strategy is the decarbonisation of the energy system in general and of the electricity power system in particular. As a benchmark for success, the RESE generation is related to the gross electricity consumption. The efficiency-first principle (energy and costs) is, additionally to high availability and predictability, the essential precondition for achieving the RESE targets. As long as the RESE share does not exceed 100%, there will be no electricity surplus in the annual balance. Thus, temporary coverages (negative residual load) from (intermittent) renewable generation must be compensated at the lowest possible costs and losses and will be returned to the power system later on. The overall roundtrip efficiency factor of the flexibility process (electricity – electricity) has to be minimized.

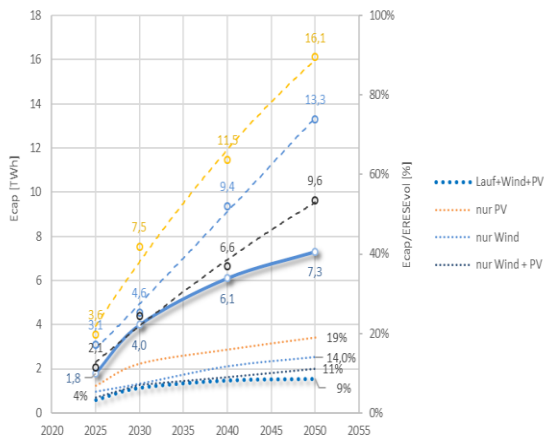


Fig. 13: Fictitious minimum storage capacity requirements for the AT-flex pool depending on RESE scenarios.

Existing storage capacities (appr. 4.3 TWh) are to be added.

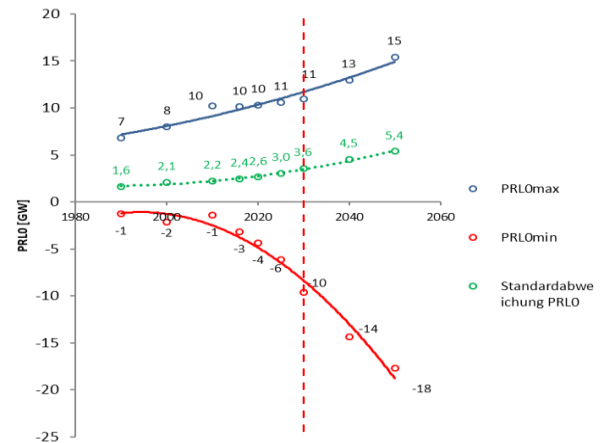


Fig. 14: Extrema of the residual load.

According to the architecture of the further renewable generation portfolio in addition to existing electricity hydro power storage capacity Austria needs a flexibility solution with an additional fictitious storage capacity in the amount of Fig. 13. To avoid dumped energy, this solution has to cover residual load peaks as given by Fig. 3 and ramps according to Fig. 8. If further RESE development is preferably based on wind and / or PV, this can cause a doubling of the fictitious storage requirement. Thus, a coordinated mix of suitable RESE technologies together with a moderate cross-border-flexibility exchange to cover short-, middle- and long-term needs should be chosen. For the overall strategic conception of the future Austrian flexibility system the following cornerstones are essential:

- non-discriminatory, market-oriented use of flexibility assets with full freedom of action with regard to their market use or application alternatives,
- consideration of development of energy policies in neighboring countries, preferably Germany (coal drop off) and availability of grid transfer capacity as well as flexibility capacity for Austrian needs,
- technical characteristics of flexibility assets including operational readiness, system compatibility and climate relevance,
- technical and operational availability and calculability for planning,
- planning period for the system concept versus technical lifetime of the options (capitalized production costs of the services as a basis for an objective comparison of options), level playing field for options,
- energy and cost efficiency.

Regarding these preconditions, the mere addition of statistically listed flexibility capacities of all categories is not useful. The assessment of national flexibility needs, including a moderate cross border exchange, will require a careful monitoring in the future. Wind and PV will continue to have similar characteristics system wide – in particular in the case of “Dunkelflaute”. While Germany’s further change to a net electricity importer was already fixed by the given national plan from 2030 onwards, today the extent, timing and type of replacement for decommissioned coal-fired power plants expands this import dependency

on electricity. Its dimension is unknown. Also in future, France and Belgium will be confronted with a high degree of planned non availability of nuclear generation caused by maintenance, even while cold periods. The generation-side assessment of security of supply (system adequacy) has so far been done deterministically on the basis of predictable assets: mainly thermal power stations and (pumped) hydro storage facilities. A significant intermittent renewable share goes hand in hand with a lack of calculable generation capacity. Meanwhile, it has been necessary to switch to probability-based methodologies (ENTSO-E SOAF). The upcoming challenges of residual load development will require to use all options of flexibility to safeguard system stability.

A polarizing debate in favor of a particular technology therefore is not a priori expedient. A level playing field is a key factor for further success.

3.1 Hydropower Storage and Pumped Hydro Storage

Today, hydropower plants represent 96% of world's operational electricity storage capacity. Also for Austria, the expansion of existing assets as well as new constructions are mandatory to maintain system stability and security of supply. Scale effects apply also here. Large, compact solutions provide energy- and cost-efficiency.

In a longer run, power to gas may be expected to act as a complementary solution in particular for seasonal flexibility. Presumed, that this technology proceeds commercially for large-scale use and its efficiency will be improved significantly.

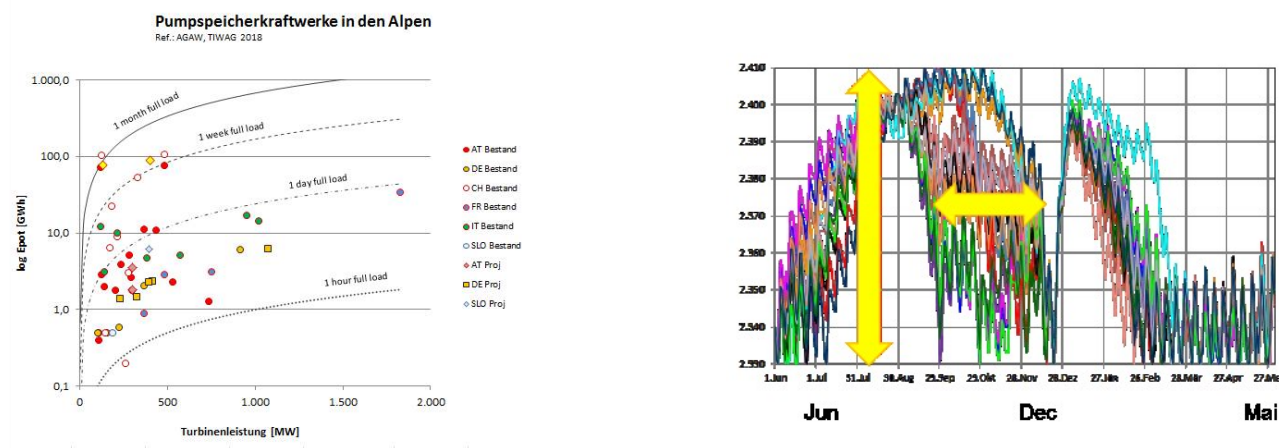
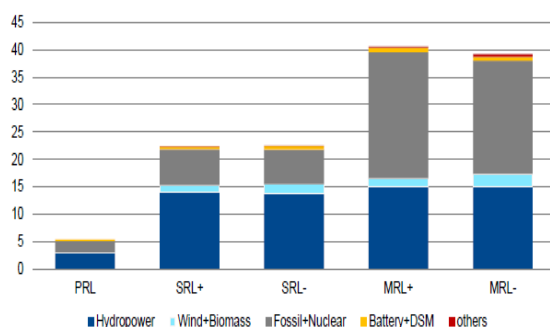


Fig. 15: Alpine (pump) storage is a multi-utility toolbox for the system requirements of the 21st century and differs from typical central European pumped storage solutions with medium drop height and small basins that are usually used for short term flexibility. Additionally, alpine storage solutions store energy from natural inflow from June to October, provide flex-products and ancillary services at all time scales characterized by maximum availability and flexibility (TIWAG 2018).

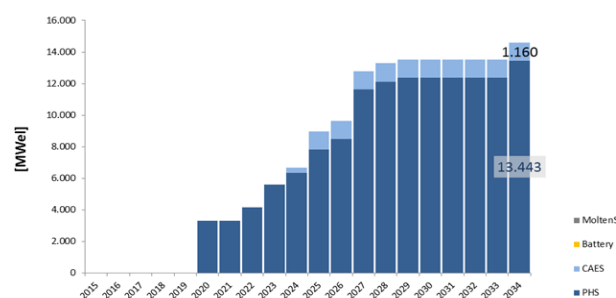
Compared to typical storage facilities in low mountain ranges, alpine (pumped) hydro storage power plants with their enormous storage volumes combined with large drop heights and huge machine capacities together with the use of natural inflow provides all

flexibility needs of the 21st century. New plant concepts also focus on seasonal storage requirements (Fig. 15 left).

The use of natural inflow is an integral part of the plant design and expands the range of flexibility applications (Fig. 15, right). This combination is a unique feature of alpine hydropower. During the period from June to October, melting snow and rainfall fill the reservoirs and thus ensure seasonal flexibility as well (Fig. 15 right, envelope curve).



8



Source: <https://www.regelleistung.net>, 2018

9 Fig. 16: Prequalified reserve capacities (GW) for Germany by generation type (left). Also in the long run, pumped storage technology remains a leading flexibility option for the Pan-European energy system (ENTSO-E, TYNDP 2018, Project Fact Sheet).

This seasonal storage of primary energy is unique. In this case, the potential energy of water is stored, and it avoids electricity generation at times not needed. Therefore, this form of seasonal storage is lossless. At the same time, also the need for short-term flexibility in both energy directions is met. The generation of renewable energy from the use of natural inflow is a by-product and inherent in the concept. The use of the natural inflow has always been common for pump storage concepts in the alps and may account for a significant share of green electricity production up to 8 % of a country's annual RESE generation.

Even in thermally dominated systems, such as Germany, hydropower storage and pumped storage safeguard a sizeable share of system reserves, where installations in the Alps are essential (Fig. 16). Efforts to strengthen Europe's energy infrastructure therefore not only include the expansion of transmission capacities, but also the integration of (pump) storage capacities in the Alps and their expansion (ENTSO-E (2017, 2018)). In terms of the Pan-European energy strategy, the cross-border relevance of such installations based on the Energy Infrastructure Regulation (EU) 347/2013 has an European dimension. Highly qualified, large (pumped) storage assets⁷ also can achieve the status of Projects of Common Interest (PCI). According to the planning for ENTSOE TYNDP 2018, more than 13 GW of additional pumped storage capacity have been planned for the maintenance of European system stability, security of supply and large scale renewable energy integration. Austrian projects share not less than 13%.

Thus, also in a longer run pumped storage technology will be the backbone for system wide stability and security of supply (Fig. 16). Additionally, the rotating mass (inertia) of

⁷ Note: The term "storage facilities" in this context refers to other storage technologies, such as battery or compressed air storage, etc.

directly grid connected machine sets of large hydropower units will play an increasingly important role for the transient stability, when thermal plants are successively dropped off, and wind power and PV are indirectly connected to the distribution grid by power electronics. The integration of the so-called "synchronous inertia", in particular of large hydropower at system level, will play an even more important role for grid stabilization by instantaneous reserve. Solutions with the help of power electronics for wind power, PV and decentralized battery storage systems (synthetic inertia) can be considered only a partially effective replacement for the rapid instantaneous reserve of thermal systems because it's delays by control procedures are relevant (dena 2015).

There is lacking public awareness on the role of alpine hydro storage and pumped storage power plants at all scales to avoid or overcome system instability resulting from anomalies of load and/or generation. Over the past 20 years, repeatedly there have been critical events that caused or were close to widespread major disruptions. The most well-known was the one in 2006 and most recently the one at the turn of the year 2018/2019. As a rule, where possible and being part of a well organized grid restoration concept, (pumped) hydro storage assets (black start and islanding operation capability) are a fixed solution to restore grids to islanding grids after black outs in a first step, keep the operation of islanded grids stable and finally help to reconnect islanded grids to a system. In such events, they significantly contribute to minimize or even avoid enormous economic damage.

Therefore, it has to be recommended that both, repowering and new construction of hydropower assets and in particular, all sorts of hydropower storages including all functional units with other hydropower assets are given the appropriate role in the upcoming years of energy transition. Moreover, regulatory conditions shall safeguard its full operational functionality and thus its full system benefit.

References

- AGORA (2019)**, Die Energiewende im Stromsektor: Stand der Dinge 2018.
- Burgholzer B., Schwabeneder D., Lettner G.**, HydroProfiles. TU Wien-EEG, 2017
- dena (2015)**, Der Beitrag von Pumpspeicherkraftwerken zur Netzstabilität und zur Versorgungssicherheit – die wachsende Bedeutung von Pumpspeicherkraftwerken in der Energiewende.
- ENTSO-E (2015)**, Scenario Outlook & Adequacy Forecast.
- ENTSO-E (2017)**, Regional Investment Plan 2017, Continental Central South, CCS.
- ENTSO-E (2018)**, Completing the Map 2018. System Needs Analysis.
- Energiewirtschaftliche Tagesfragen 69. Jg. (2019) H. 1 / 2.**
- EURELECTRIC, VGB (2018)**, Facts of Hydropower in The EU.
- IEA Hydropower, Annex IX**, Flexible hydropower providing value to renewable energy integration.
- Pöyry (2018)**, Wasserkraftpotenzialstudie Österreich, Aktualisierung 2018.
- stoRE (2013)**, The Role of Bulk Energy Storage in Facilitating Renewable Expansion.
- SuREmMa (2017)**, Technischer Bericht C. Die Rolle der Speicherwasserkraft im österreichischen und europäischen Stromversorgungssystem.
- TUD (2019)**, Dauer und Häufigkeit von Dunkelflauten in Deutschland.
- TUW (2017). Lettner G., Burgholzer B.**, Anforderungsprofile für die Wasserkraft in zukünftigen Energiemärkten. TU Wien-EEG, 2017.
- Wikipedia download 22.7.2018**, Stromausfall in Europa im November 2006.

The Authors

Dr. Peter Bauhofer graduated in electrical engineering at Technical University of Vienna, Austria, and joined TIWAG in 1988. He headed grid planning and operation as well as strategic planning of transmission grid and coordinated the project “Control Area Tyrol”.

He was member of the board of A&B Ausgleichsenergie & Bilanzgruppen-Management AG, coordinator of balance responsible parties for electricity and natural gas operating in Tirol and Vorarlberg. Since 2010; he has been heading the department of energy strategy and efficiency, TIWAG. He has been member or head of several expert groups at ENTSO-E, IEA Hydro Annex IX, VGB Hydro, E-Control and Oesterreichs Energie regarding market liberalisation, ancillary services, system balancing and imbalance settlement, renewable energy, climate and energy Policy. Peter Bauhofer is author of several papers and presentations.

e-mail: peter.bauhofer@tiwag.at

Michael Zoglauer graduated in electrical engineering at Technical University of Graz, Austria, and worked for Technical University Graz (Department of Energy Economy and Energy Innovation) before he joined TIWAG in 1994. He has been involved in several projects for the integration of renewable energies to the supply systems. He was involved to several working groups (BDEW, Oesterreichs-Energie, Eurelectric, ERGEG and ENTSO-E) regarding system and market design as well as infrastructural development for the electricity sector, by focusing to the issues regarding security of supply, ancillary services and integration of renewable energies.

e-mail: michael.zoglauer@tiwag.at